

MODELLING OF SAND FILTERS FOR RAINWATER HARVESTING

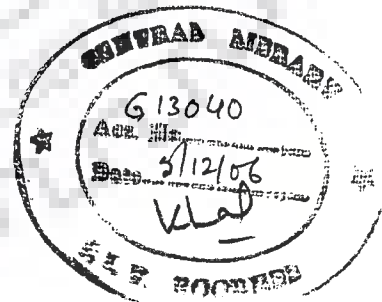
A THESIS

*Submitted in partial fulfilment of the
requirements for the award of the degree
of*

**DOCTOR OF PHILOSOPHY
in
WATER RESOURCES DEVELOPMENT**

By

RAMAKANT



**WATER RESOURCES DEVELOPMENT & MANAGEMENT
INDIAN INSTITUTE OF TECHNOLOGY ROORKEE
ROORKEE-247 667 (INDIA)**

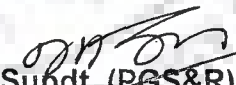
APRIL, 2006

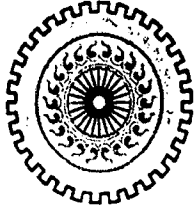


© INDIAN INSTITUTE OF TECHNOLOGY ROORKEE, ROORKEE, 2006

ALL RIGHTS RESERVED

6th Annual Convocation- 2006
Degree conferred on 11.11.2006


Supdt. (PGS&R)



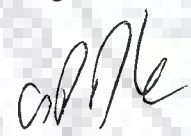
INDIAN INSTITUTE OF TECHNOLOGY ROORKEE
ROORKEE
CANDIDATE'S DECLARATION

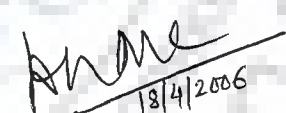
I hereby certify that the work which is being presented in the thesis entitled "MODELLING OF SAND FILTERS FOR RAINWATER HARVESTING" in partial fulfilment of the requirements for the award of the degree of DOCTOR OF PHILOSOPHY and submitted in the Department of Water Resources Development and Management of the Indian Institute of Technology Roorkee, Roorkee, is an authentic record of my own work carried out during the period from January 2003 to April 2006 under the supervision of Dr. Deepak Khare, Associate Professor, Department of Water Resources Development and Management and Dr. C.S.P. Ojha, Professor, Department of Civil Engineering, Indian Institute of Technology Roorkee, Roorkee. The matter presented in this thesis has not been submitted by me for the award of any other degree of this or any other institute.

Date: 18/4/2006


(RAMAKANT)

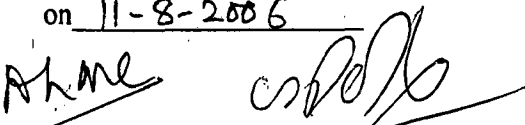
This is to certify that the above statement made by the candidate is correct to the best of our knowledge.

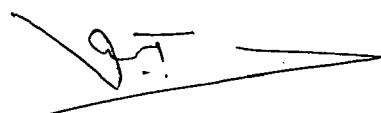

(Dr. C.S.P. OJHA)
Professor
Department of Civil Engineering


(Dr. DEEPAK KHARE)
Associate Professor
Department of Water Resources
Development and Management

Date: April 18, 2006

The Ph.D. viva-voce examination of Mr. Ramakant, Research Scholar, has been held on 11-8-2006


Signature of Supervisor(s)


Signature of External Examiner

ACKNOWLEDGEMENT

At the outset I wish to express my immense sense of gratitude to my supervisors Dr. Deepak Khare, Associate Professor, Department of Water Resources Development and Management and Dr. C.S.P. Ojha, Professor, Department of Civil Engineering, Indian Institute of Technology Roorkee, Roorkee, for their invaluable guidance, thought provoking discussions and untiring efforts throughout the tenure of this work. Their timely help, constructive criticism, and painstaking efforts made it possible to present the work contained in this thesis in its present form.

I am highly grateful to Dr. (Mrs.) Shanta Satyanarayan, Deputy Director (Retd.), National Environmental Engineering Research Institute, Nagpur for her constant encouragement and generous support during the course of my research work.

It is a pleasure to acknowledge the support extended by all my fellow research scholars in general and Er. Kishor A. Dhore, Er. Bhaskar R. Nikam, Er. Sonamani Singh, Dr. Rupesh Kumar Pati and Er. Sudhir Kumar in particular. I am also grateful to acknowledge Mr. Chamkaur Singh Addi, Mr. Beer Singh Chauhan and all technical staffs of the Department of Water Resources Development and Management for their constant support during my experimental work.

I also acknowledge my heartiest appreciation to my wife, Er. Savita Sharma, for the moral support and everlasting encouragement given to me during our stay at Roorkee. I can not close these prefatory remarks without expressing my deep sense of gratitude and reverence to my parents for their blessings and endeavour to keep my moral high throughout the period of my work.

Last but not the least I would like to express my sincere thanks to all those who directly or indirectly helped me at various stages of this work.

ABSTRACT

The research presented in this thesis has attempted to bridge some of the gaps in the rainwater harvesting filter systems. An extensive review of the literature was conducted to identify the gaps and relevant research issues in the area of rainwater harvesting. Based on the review of the literatures it was felt that the rooftop harvested rainwater often do not meet WHO and other national drinking water standards especially with respect to bacteriological water quality. Microbial growth in water is most extensive on the surfaces of particles (turbidity) because nutrients adsorb to surfaces, and adsorbed bacteria are thus able to grow more efficiently than when in free suspension.

A systematic field survey reveals that the design of sand filters for rainwater harvesting is on an ad-hoc since no design guidelines are available, particularly in India. Hence, the main objective of the research work is to develop new models to make the appropriate design of rainwater harvesting sand filters. Hsiung and Cleasby (1968) have suggested two models for water filtration based on effluent quality and critical head loss criteria. Testing the compatibility of statistical models of Hsiung and Cleasby (1968) with a variety of filtering conditions with & without harvested rainwater as an influent followed by formulation of new models have been investigated in the present work.

To support the study, different sand filter modules were operated in the laboratory with mean sand grain sizes of 3.647, 2.366, 1.673, 1.091, 0.714 and 0.505 mm and flow velocities of 1.65, 3.30, 4.95, 6.60 and 8.25 m³/hr/m². Total 110 experimental runs were operated in the laboratory and the time of each filter run was kept constant for 36 hours. Uniform sand and graded sand filters were used in operation for Fuller's earth suspension water solution and rainwater samples. Hsiung and Cleasby model has been tested for the influent concentrations of 17, 25, 30 and 40 mg/l for prediction of effluent quality. It is

observed that average percentage error (APE) is larger in case of experiments having lower sand grain sizes. For example, the APE reaches as high as 137.07% at flow velocity of 1.65 $\text{m}^3/\text{hr}/\text{m}^2$ and 0.714 mm sand grain size for rainwater and certainly, this type of model is not acceptable. High values of APE are also computed for other sand grain sizes although the magnitude of such errors are low in certain cases, particularly involving larger sand grain sizes.

Hsiung and Cleasby model has also been tested for the same influent concentrations for prediction of head loss. It is observed that APE is again larger in case of experiments having lower sand grain sizes. For example, corresponding to sand grain size of 0.714 mm and flow velocity of 8.25 $\text{m}^3/\text{hr}/\text{m}^2$, head loss APE reaches as high as 6381.62% for rainwater under vertically downward flow filter condition and certainly, this type of model is not acceptable. High values of APE have also been observed for other influent concentrations. With such a high APE, Hsiung and Cleasby model is not advocated for computation of effluent quality and head loss.

Based on flow velocity 'Q' ($\text{m}^3/\text{hr}/\text{m}^2$), media grain size 'd' (mm), filter run time 't' (Hr.), filter media depth 'L' (m), influent concentration 'C₀' (mg/l) and critical head loss (H_1-H_0) (m), certain models have been developed in the present work. The experimental data for influent concentration of 30 mg/l has been used to develop a unified relationship. This unified models were again tested against influent concentrations of 17 mg/l, 25 mg/l and 40 mg/l. Obviously, APE has gone upto less than 10% for effluent quality prediction and higher APE (>50%) for certain filter runs for head loss prediction shows the compatibility of the new developed regression models. Hence, the new regression models are advocated to use for performance prediction.

The views of Hsiung and Cleasby, that the top layer media grain size can be used as an effective media size in H-C model is not justified from the present work. It is shown that

effective size of graded filter lies somewhere in between the top two layers. In case of filters, impurities can penetrate to different depths depending on flow and media grain size and influent concentrations. The present research also supports the study made by Ojha and Graham (1992) that the topmost layer of the deep-bed filter is not representative of the behaviour of the entire media, as models based on the top-layer performance do not simulate very well the performance of the entire media bed. An insight into the dimensionless versus lumped approach for modelling of flow resistance is also provided to support the above view.



CONTENTS

Chapter	Descriptions	Page
	CANDIDATE'S DECLARATION	(i)
	ACKNOWLEDGEMENT	(ii)
	ABSTRACT	(iii)-(v)
	CONTENTS	(vi)-(x)
	LIST OF FIGURES	(xi)-(xiv)
	LIST OF PLATES	(xv)-(xvi)
	LIST OF TABLES	(xvii)-(xx)
	NOMENCLATURES	(xxi)-(xxii)
	MODEL ABBREVIATIONS	(xxiii)-(xxiv)
1	INTRODUCTION	1-12
	1.1 PREAMBLE	1
	1.2 IMPORTANCE OF RAINWATER HARVESTING	2
	1.3 PROBLEM STATEMENT	3
	1.3.1 Rainwater Quality Study	3
	1.3.2 Effect of Roofing Materials	6
	1.3.3 The Problem Description	7
	1.3.4 The Problem Identification	8
	1.4 OBJECTIVES AND METHODOLOGY	8
	1.5 ORGANIZATION OF THE THESIS	10
2	LITERATURE REVIEW	13-59
	2.1 GENERAL	13
	2.2 DEVELOPMENT OF RAINWATER HARVESTING CONCEPT	14

2.3	EVALUATION OF RAINFALL INTENSITIES IN INDIA	19
2.4	CONTAMINATION OF RAINWATER	22
2.4.1	Sources of Rainwater Contamination	22
2.4.1.1	Microbiological contamination	23
2.4.1.2	Chemical contamination	25
2.4.2	Selection of Study Parameter	26
2.5	RAINWATER QUALITY REVIEW	28
2.6	TREATMENT OF RAINWATER	40
2.6.1	Types of Treatment	40
2.6.2	Types of Filtration System	41
2.6.2.1	Sand-charcoal-stone	41
2.6.2.2	Reverse osmosis water purifier	41
2.6.2.3	UV-charcoal system	42
2.6.2.4	Solar disinfection	43
2.6.2.5	Electrochemical activation	43
2.6.2.6	Coarse leaf filter	43
2.6.2.7	Fine filters	44
2.7	OBJECTIVES OF FILTER USE	44
2.7.1	Filter Orientation	45
2.8	TECHNICAL EVALUATION OF RAINWATER HARVESTING SAND FILTERS	47
2.9	ASSESSMENT OF SAND FILTERS	57
2.9.1	Suitability of Sand Filters in Field Conditions	59
2.10	CONCLUDING REMARKS	59

3	EXPERIMENTAL PROGRAM	61-79
3.1	PREAMBLE	61
3.2	EXPERIMENTAL SET-UP	62
3.2.1	Selection of Filtration Velocities	69
3.2.2	Selection of Filter Properties	70
3.2.3	Selection of Filter Run Times	70
3.2.4	Selection of Influent Concentrations	71
3.3	EXPERIMENTATION WITH SAND FILTER MODULES	74
3.4	CONCLUDING REMARKS	79
4	EVALUATION OF SAND FILTER RUNS USING PROBABILISTIC APPROACH	80-114
4.1	GENERAL	80
4.2	CHI-SQUARE DISTRIBUTION APPLICATION	80
4.2.1	Criteria for Evaluation of Performance Models	82
4.2.1.1	Effluent quality performance	84
4.2.1.2	Head loss performance	84
4.3	EFFLUENT QUALITY MODEL TESTING	85
4.3.1	Model Testing for Vertically Downward Flow Filters	85
4.3.2	Model Testing for Horizontal Flow Filter	95
4.4	FLOW RESISTANCE MODEL TESTING	99
4.4.1	Model Testing for Vertically Downward Flow Filters	99
4.4.2	Model Testing for Horizontal Flow Filter	106
4.5	CONCLUDING REMARKS	114

5	MODELLING OF SAND FILTER PERFORMANCE	115-149
5.1	PREAMBLE	115
5.2	MODELLING FOR EFFLUENT QUALITY	115
5.2.1	Modelling for Vertically Downward Flow Filters	116
5.2.2	Modelling for Horizontal Flow Filter	129
5.3	MODELLING FOR FLOW RESISTANCE	132
5.3.1	Modelling for Vertically Downward Flow Filters	132
5.3.2	Modelling for Horizontal Flow Filter	141
5.4	ANALYSIS FOR THE LARGE ERRORS IN FLOW RESISTANCE MODELLING	144
5.5	CONCLUDING REMARKS	149
6	DIMENSIONLESS MODEL ANALYSIS	150-171
6.1	GENERAL	150
6.2	MODELLING FOR EFFLUENT QUALITY	150
6.3	GENERALIZED MODELLING FOR DIAMETER FUNCTION	158
6.4	MODELLING FOR FLOW RESISTANCE	160
6.5	NEW HEAD LOSS DIMENSIONLESS MODEL DEVELOPMENT	168
6.6	CONCLUDING REMARKS	171
7	APPLICABILITY OF DEVELOPED MODELS TO HARVESTED RAINWATER	172-183
7.1	PREAMBLE	172
7.2	VERIFICATION OF EFFLUENT QUALITY MODELS	172

7.3	VERIFICATION OF FLOW RESISTANCE MODELS	178
7.4	CONCLUDING REMARKS	183
8	RESULTS AND DISCUSSION	184-195
8.1	PREAMBLE	184
8.2	EFFLUENT QUALITY IN CASE OF VERTICALLY DOWNWARD FLOW FILTERS	184
8.3	HEAD LOSS IN CASE OF VERTICALLY DOWNWARD FLOW FILTERS	187
8.4	EFFLUENT QUALITY IN CASE OF HORIZONTAL FLOW FILTER	188
8.5	HEAD LOSS IN CASE OF HORIZONTAL FLOW FILTER	189
8.6	DIMENSIONLESS VERSUS DIMENSIONAL REPRESENTATIONS	189
8.7	USE OF GRADED SAND FILTERS	190
8.8	PERFORMANCE OF NEW REGRESSION MODELS USING HARVESTED RAINWATER	191
8.9	DISTRIBUTED VERSUS LUMPED MODEL ANALYSIS	193
8.10	CONCLUDING REMARKS	195
9	CONCLUSIONS AND FUTURE SCOPE OF WORK	196-199
9.1	CONCLUSIONS	196
9.2	FUTURE SCOPE OF WORK	199
	REFERENCES	200-214

LIST OF FIGURES

Figure	Descriptions	Page
1.1	Block diagram of the methodology adopted	10
4.1	Typical chi-square distribution curves	81
4.2	Plot of U versus cumulative probability at various degrees of freedom	83
4.3	Plot of C-observed versus C-computed using H-C model for influent concentration of 25 mg/l (run nos. 1 to 27)	89
4.4	Plot of C-observed versus C-computed using H-C model for influent concentration of 30 mg/l (run nos. 28 to 54)	89
4.5	Plot of C-observed versus C-computed using H-C model for influent concentration of 40 mg/l (run nos. 55 to 59)	91
4.6	Plot of C-observed versus C-computed using H-C model for influent concentration of 40 mg/l (run nos. 60 to 64)	91
4.7	Plot of C-observed versus C-computed using H-C model for influent concentration of 17 mg/l (run nos. 65 to 89)	94
4.8	Plot of C-observed versus C-computed using H-C model for influent concentration of 30 mg/l (run nos. 90 to 94)	97
4.9	Plot of C-observed versus C-computed using H-C model for influent concentration of 40 mg/l (run nos. 95 to 99)	97
4.10	Plot of C-observed versus C-computed using H-C model for influent concentration of 17 mg/l (run nos. 100 to 104)	98
4.11	Plot of head loss observed versus computed using H-C model for influent concentration of 25 mg/l (run nos. 1 to 27)	101
4.12	Plot of head loss observed versus computed using H-C model for influent concentration of 30 mg/l (run nos. 28 to 54)	103
4.13	Plot of head loss observed versus computed using H-C model for	

	influent concentration of 40 mg/l (run nos. 55 to 59)	105
4.14	Plot of head loss observed versus computed using H-C model for influent concentration of 40 mg/l (run nos. 60 to 64)	105
4.15	Plot of head loss observed versus computed using H-C model for influent concentration of 17 mg/l (run nos. 65 to 89)	108
4.16	Plot of head loss observed versus computed using H-C model for influent concentration of 30 mg/l (run nos. 90 to 94)	110
4.17	Plot of head loss observed versus computed using H-C model for influent concentration of 40 mg/l (run nos. 95 to 99)	112
4.18	Plot of head loss observed versus computed using H-C model for influent concentration of 17 mg/l (run nos. 100 to 104)	113
5.1	Plot of U versus t at constant grain size and flow velocity (run no. 48)	118
5.2	Plot of equiU curve for filter depth versus filter run time (run no. 48)	118
5.3	Plot of U versus filter run time for different flow rates at constant grain size (run nos. 48 to 52)	119
5.4	Plot of equiU for flow velocity versus filter run time (run nos. 48 to 52)	119
5.5	Plot of U versus filter run time at different grain sizes (run nos. 28 to 52)	120
5.6	Plot of equiU for flow velocity versus filter run time (run nos. 28 to 52)	120
5.7	Plot of C-observed versus C-computed using model (MOVEQ-30AL) for influent concentration of 30 mg/l (run nos. 28 to 54)	124
5.8	Plot of C-observed versus C-computed using model (MOVEQ-30AL) for influent concentration of 25 mg/l (run nos. 1 to 27)	126
5.9	Plot of C-observed versus C-computed using model (MOVEQ-30AL) for influent concentration of 40 mg/l (run nos. 55 to 59)	128
5.10	Plot of C-observed versus computed using model (MOVEQ-30AL) for influent concentration of 40 mg/l (run nos. 60 to 64)	128
5.11	Plot of C-observed versus C-computed using model (MOHEQ-30E) for influent concentration of 30 mg/l (run nos. 90 to 94)	131

5.12	Plot of C-observed versus C-computed using model (MOHEQ-30E) for influent concentration of 40 mg/l (run nos. 95 to 99)	131
5.13	Plot of head loss observed versus computed using model (MOVEHL-30AL) for influent concentration of 30 mg/l (run nos. 28 to 54)	136
5.14	Plot of head loss observed versus computed using model (MOVEHL-30AL) for influent concentration of 25 mg/l (run nos. 1 to 27)	138
5.15	Plot of head loss observed versus computed using model (MOVEHL-30AL) for influent concentration of 40 mg/l (run nos. 55 to 59)	140
5.16	Plot of head loss observed versus computed using model (MOVEHL-30AL) for influent concentration of 40 mg/l (run nos. 60 to 64)	140
5.17	Plot of head loss observed versus computed using model (MOHOHL-30E) for influent concentration of 30 mg/l (run nos. 90 to 94)	143
5.18	Plot of head loss observed versus computed using model (MOHOHL-30E) for influent concentration of 40 mg/l (run nos. 95 to 99)	143
6.1	Plot of C-predicted versus C-computed using dimensionless model (DIMOVEQ-30A) (run nos. 28 to 32)	153
6.2	Plot of C-predicted versus C-computed using dimensionless model (DIMOVEQ-30B) (run nos. 32 to 37)	153
6.3	Plot of C-predicted versus C-computed using dimensionless model (DIMOVEQ-30C) (run nos. 38 to 42)	154
6.4	Plot of C-predicted versus C-computed using dimensionless model (DIMOVEQ-30D) (run nos. 43 to 47)	154
6.5	Plot of C-predicted versus C-computed using dimensionless model (DIMOVEQ-30E) (run nos. 48 to 52)	155
6.6	Plot of C-predicted versus C-computed using dimensionless model (DIMOVEQ-30F) (run nos. 53 & 54)	155
6.7.	Plot of C-predicted versus C-computed using dimensionless model (DIMOHEQ-30E) (run nos. 90 to 94)	157
6.8	Plot of head loss observed versus computed using dimensionless model	

	(DIMOVEHL-30A) (run nos. 28 to 32)	162
6.9	Plot of head loss observed versus computed using dimensionless model (DIMOVEHL-30B) (run nos. 33 to 37)	162
6.10	Plot of head loss observed versus computed using dimensionless model (DIMOVEHL-30C) (run nos. 38 to 42)	163
6.11	Plot of head loss observed versus computed using dimensionless model (DIMOVEHL-30D) (run nos. 43 to 47)	163
6.12	Plot of head loss observed versus computed using dimensionless model (DIMOVEHL-30E) (run nos. 48 to 52)	164
6.13	Plot of head loss observed versus computed using dimensionless model (DIMOVEHL-30F) (run nos. 53 & 54)	164
6.14	Plot of head loss observed versus computed using dimensionless model (DIMOHHL-30E) (run nos. 90 to 94)	167
6.15	Plot of \hat{R}_d versus \hat{G} for new dimensionless model at 500 mm filter depth (run no. 28)	170
6.16	Plot of head loss computed versus observed for new dimensionless model at 500 mm filter depth (run no. 28)	170
7.1(a)- 7.1(c)	Plot of effluent quality observed versus computed using model (MOVEQ-30AL) for certain filter runs	175
7.2	Plot of C-observed versus C-computed using model (MOVEQ-30E) for rainwater samples (run nos. 100 to 104)	177
7.3	Plot of effluent quality observed versus computed using model (MOVEQ-30E) for certain filter run	177
7.4(a)- 7.4(c)	Plot of head loss observed versus computed using model (MOVEHL-30AL) for certain filter runs	180
7.5	Plot of head loss observed versus computed using model (MOHOHL-30E) for certain run	182

LIST OF PLATES

Plate	Descriptions	Page
2.1	Dual media rainwater harvesting filter system	48
2.2	Typical design of sand filter used for rainwater	48
2.3	Schematic of Dewas filter for rainwater harvesting	49
2.4	Horizontal sand filter called Dewas filter, Indore, India	49
2.5	Multi layers sand filter for rainwater harvesting	51
2.6	HDPE drum sand filter for rainwater harvesting	51
2.7	RainPC filter system using for rainwater harvesting	52
2.8	Mud pot filtration system used for drinking purpose	52
2.9	Vertically downward flow sand filter used for rooftop rainwater harvesting at Khandwa, India	54
2.10	Horizontal flow sand filter used for rooftop rainwater harvesting at Khandwa, India	54
2.11	Schematic of horizontal flow multi-media filter for rainwater harvesting at Khandwa, India	55
2.12	Schematic of tube well for surface runoff collection at Khandwa, India	55
2.13	Construction of tube well for surface run-off collection at Khandwa, India	56
2.14	Vertically downward flow sand filter for rooftop rainwater harvesting at I.I.T. Delhi, New Delhi, India	56
3.1	Overhead HDPE tank attached with stirring facility at I.I.T. Roorkee, Roorkee, India	63
3.2	Pictorial view of sand filter modules in the laboratory at I.I.T.	

	Roorkee, Roorkee, India	64
3.3	Pictorial view of various sand grain sizes used for filter in the laboratory at I.I.T. Roorkee, Roorkee, India	73
3.4	Close view of graded sand filter module (no. 1) in the laboratory at I.I.T. Roorkee, Roorkee, India	76
3.5	Close view of vertically downward flow sand filter modules (nos. 2 & 3) in the laboratory at I.I.T. Roorkee, Roorkee, India	77
3.6	Close view of horizontal flow sand filter module (no. 4) in the laboratory at I.I.T. Roorkee, Roorkee, India	78



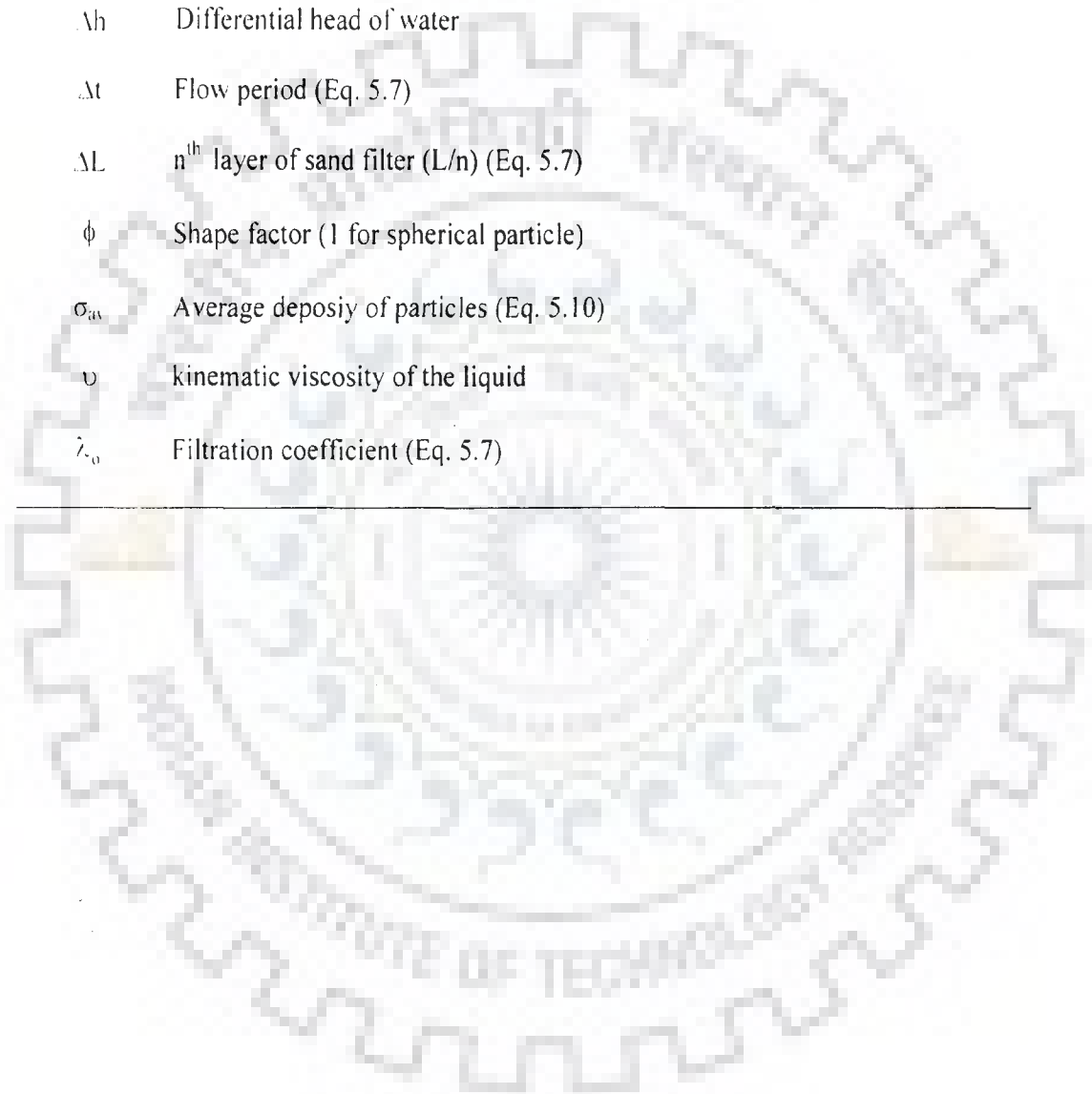
LIST OF TABLES

Table	Descriptions	Page
2.1	Suitability of rainwater harvesting structures in different zones of India	18
2.2	Rainfall intensity at various locations in India for return period of 30 years	20
2.3	Measuring rainfall flow rate at various rooftop for return period of 15 years	21
2.4	Studies of rainwater quality by various researchers	24
2.5	Concentration of pesticides in rainwater for various European sites, Europe	38
2.6	Correlation matrix for rainwater ion pairs at Agra city, India	39
2.7	Correlation coefficient of parameters in rainwater at Gopalpura city, India	39
2.8	Pros and cons of various filter positions on the conveyance path	46
2.9	Missing design parameters for rainwater harvesting sand filters	58
3.1	Details of experimental studies for sand filters in the laboratory	66
3.2	Details of experimental runs conducted in the laboratory	67
3.3	Comparative study of different filters used in water treatment	72
3.4	Details of various sand grain sizes used in the study of sand filters	72
4.1	Computed APE of U and C using H-C model for influent concentration of 25 mg/l (run nos. 1 to 27)	86
4.2	Computed APE of U and C using H-C model for influent concentration of 30 mg/l (run nos. 28 to 54)	88
4.3	Computed APE of U and C using H-C model for influent	

	concentration of 40 mg/l (run nos. 55 to 64)	90
4.4	Computed APE of U and C using H-C model for influent concentration of 17 mg/l (run nos. 65 to 89)	93
4.5	Computed APE of U and C using H-C model for Fuller's earth suspension samples (run nos. 90 to 94 and 95 to 99) and rainwater samples (run nos. 100 to 104)	96
4.6	Computed APE of head loss using H-C model for influent concentration of 25 mg/l (run nos. 1 to 27)	100
4.7	Computed APE of head loss using H-C model for influent concentration of 30 mg/l (run nos. 28 to 54)	102
4.8	Computed APE of head loss using H-C model for influent concentration of 40 mg/l (run nos. 55 to 64)	104
4.9	Computed APE of head loss using H-C model for influent concentration of 17 mg/l (run nos. 65 to 89)	107
4.10	Computed APE of head loss using H-C model for Fuller's earth suspension samples (run nos. 90 to 94 and 95 to 99) and rainwater samples (run nos. 100 to 104)	109
5.1	Computed APE of U and C using new developed individual regression model (run nos. 28 to 54)	121
5.2	Computed APE of U and C using new developed unified model (MOVEQ-30AL) (run nos. 28 to 54)	123
5.3	Computed APE of U and C using unified model (MOVEQ-30AL) for influent concentration of 25 mg/l (run nos. 1 to 27)	125
5.4	Computed APE of U and C using unified model (MOVEQ-30AL) for influent concentration of 40 mg/l (run nos. 55 to 64)	127
5.5	Computed APE of U and C using new developed unified model (MOHEQ-30E) (run nos. 90 to 94)	130
5.6	Computed APE of U and C using unified model (MOHEQ-30E) for influent concentration of 40 mg/l (run nos. 95 to 99)	130

5.7	Computed APE for head loss using new developed individual regression model (run nos. 28 to 54)	133
5.8	Computed APE for head loss using new developed unified model (MOVEHL-30AL) (run nos. 28 to 54)	135
5.9	Computed APE for head loss using unified model (MOVEHL-30AL) for influent concentration of 25 mg/l (run nos. 1 to 27)	137
5.10	Computed APE for head loss using unified model (MOVEHL-30AL) for influent concentration of 40 mg/l (run nos. 55 to 64)	139
5.11	Computed APE for head loss using new developed unified model (MOHOHL-30E) (run nos. 90 to 94)	142
5.12	Computed APE for head loss using unified model (MOHOHL-30E) for influent concentration of 40 mg/l (run nos. 95 to 99)	142
5.13	Comparison of head loss observed and computed at various assumed porosities of sand bed of 100 mm thickness	148
6.1	Computed APE for effluent quality using dimensionless models at an individual grain size (run nos. 28 to 54)	152
6.2	Computed APE for effluent quality using dimensionless model (DIMOHEQ-30E) (run nos. 90 to 94)	156
6.3	Computed APE using diameter function for different filter runs (nos. 28 to 54)	159
6.4	Computed APE for head loss using dimensionless models at an individual grain size (run nos. 28 to 54)	161
6.5	Computed APE for head loss using dimensionless model (DIMOHOHL-30E) (run nos. 90 to 94)	166
7.1	Computed APE of U and C using unified model (MOVEQ-30AL) against rainwater samples (run nos. 65 to 89)	174
7.2	Computed APE of U and C using unified model (MOHEQ-30E) against rainwater samples (run nos. 100 to 104)	176

t	Filtration run time
U	Random variables in the chi-square distribution (Eq. 4.1)
U	Variate (defined as ratio of C/C_0 ; Eq. 4.2)
V_s	Mean flow velocity (Eq. 5.19)
v	Degree of freedom
Δh	Differential head of water
Δt	Flow period (Eq. 5.7)
ΔL	n^{th} layer of sand filter (L/n) (Eq. 5.7)
ϕ	Shape factor (1 for spherical particle)
σ_{av}	Average density of particles (Eq. 5.10)
ν	Kinematic viscosity of the liquid
λ_0	Filtration coefficient (Eq. 5.7)



1.1 PREAMBLE

India still has an enormous amount of water, theoretically as much as 173 million hectare-metres, that could be captured as rain or as run-off from small catchments in and near villages or towns. Therefore, the theoretical potential of water harvesting for meeting household needs is enormous. Rain captured from 1-2 % of India's land could provide India's population of 950 million with as much as 100 litres of water per person per day (Agarwal, 1998). There is no village in India which could not meet its drinking water needs through rainwater harvesting. As there is a synergy between population density and rainfall levels, less land is required in more densely populated areas to capture the same amount of rainwater. And in such areas there are usually more non-porous surfaces like rooftops which have improved runoff efficiency. Water harvesting means capturing the rain where it falls. There are a variety of ways of harvesting water, such as capturing runoff from rooftops, local catchments, capturing seasonal flood waters from local streams and conserving water through watershed management.

Rainwater harvesting is often considered to be traditional method of water collection and storage. The practice of rainwater harvesting can be traced back many centuries, especially in country like India where rainwater harvesting is mentioned in ancient inscriptions as far back as 5th century before Christ (BC). However, types and methods of rainwater harvesting have changed over time and many different systems are now available all over the world. After a relatively long period in oblivion, domestic

rainwater harvesting is currently making an impact in many countries (especially in the developing world) as an alternative household water supply option. A number of reasons can be attributed to this resurgence, the more important of which are: (1) decrease in the quantity and quality of both groundwater and surface water, (2) failure of many piped water schemes due to poor operation and maintenance of infrastructure, (3) improvement in roofing material from thatched to more impervious materials like concrete, tiles, corrugated iron sheets and asbestos, (4) increased availability of low cost rainwater harvesting technology, (5) shift from more centralized to decentralized management and development of water resources, and (6) increase in competition between different water sectors and the global trend towards rural to urban migration.

During the past two decades significant development in rainwater harvesting has taken place both in the developed and developing countries. The growth in uptake of rainwater harvesting in the developing countries has been most significant in Thailand, Sri Lanka, Kenya, India, Ethiopia, Uganda and Brazil (Gould and Nissen-Petersen, 1999). In the arid regions of China, rainwater harvesting is seen as the only solution for providing domestic and productive water (Zhu and Liu, 1998). In all these countries, rainwater harvesting has been developed as a means of increased household water security, mostly for the rural communities. This is quite obvious as rural poor are the most vulnerable in water scarcity situations.

1.2 IMPORTANCE OF RAINWATER HARVESTING

By 2025, it is estimated that about two thirds of the world's population i.e. about 5.5 billion people will live in areas facing moderate to high water stress (UNPF, 2002). For fast growing urban areas, water requirements are expected to double from 25.0 billion cubic meters (BCM) in 1990 to 52.0 BCM in 2025. It has also been indicated that

industrial water demand would increase from 34.0 BCM of 1990 to 191.0 BCM by the year 2025. Agriculture, the largest consumer of water resources in India, will probably require 770.0 BCM by the year 2025 to support food demand in India. The total estimated demand of 1013.0 BCM by the year 2025 would be close to the current available annual utilizable water resource (1100.0 BCM) of India (Vasudevan and Pathak, 2000).

Water is the need of the hour and with failing monsoons year after year, there is a need to solve the crucial problem of water by conserving rainwater. There is no choice but to adopt better water management technique, such as rainwater harvesting to recharge the underground aquifers. The simple technique of rainwater harvesting is to save and store the water running off from a roof and using it for indoor needs. Artificial recharge is a process of augmenting the underground water table by artificial infiltration of rainwater and surface run off. In areas where water supply is problematic or water resources are scarce, rainwater harvesting is a good solution.

1.3 PROBLEM STATEMENT

1.3.1 Rainwater Quality Study

The quality of harvested rainwater depends on local circumstances and in particular, environmental factors, such as the degree of atmospheric pollution, the types of rainwater catchment surface materials and level of maintenance of the rainwater catchment systems (Haebler and Waller, 1987). Several studies indicated that rainwater supplies often do not meet WHO and other National Drinking Water Standards especially with respect to bacteriological water quality (Riddle and Speedy, 1984; Fujioka and Chinn, 1987; Haebler and Waller, 1987; Lye, 1987; Krishna, 1989; Wirojanagud and Hovichitr, 1989). A more direct source of evidence implicating a rainwater supply as a potential health risk comes from identifying the presence of specific pathogens. There are many

references to pathogens including *Salmonella* (Chareonsook, 1986; Fujioka *et al.*, 1991; Wirojanagud and Hovichitr, 1989), *Legionella-like spp.* (Lye, 1992b), *Clostridium perfringens* (Fujioka *et al.*, 1991), *Aeromonas*, *Vibrio parahaemolyticus* (Wirojanagud and Hovichitr, 1989), *Campylobacter* (Brodribb *et al.*, 1995), *Cryptosporidium* and *Giardia* (Crabtree *et al.*, 1996) having been isolated from rainwater samples.

A number of studies have investigated the prevalence of microbiological and chemical contaminants in roof-collected rainwater (Lye, 1987; Fujioka and Chinn, 1987; Fujioka *et al.*, 1991; Habler and Waller, 1987; Waller *et al.*, 1984; Gumbs and Dierberg, 1984; Olem and Berthouex, 1989; Sharpe and Young, 1982; Young and Sharpe, 1984). Lead is a cumulative poison which can cause serious damage to the central nervous system and infants, and foetuses are particularly vulnerable (NHMRC, 1996). Lead levels exceeding 3.5 times WHO drinking water standards have also been noted in Selangor, Malaysia (Yaziz *et al.*, 1989). Haebler and Waller (1987) monitored bacteriological, chemical and physical water quality of rainwater collection system in the Eastern Caribbean and found that bacteriological levels exceed Canadian drinking water standards.

Turbidity can affect or can be affected by the physical, microbiological, chemical and radiological characteristics of water. In general, the relationships between turbidity and other water quality parameters are due to the turbidity itself; the adsorptive and complexing capacity of the many types of particulates that contribute to turbidity; and the fact that particulate matter is a source of nutrients and protection for some microorganisms (Reilly and Kippin, 1983). The relationship between high turbidity, in both raw and filtered water, and taste and odour has long been recognized (Atkins and Tomlinson, 1963). Algal growths, Actinomycetes and their debris contribute to taste and odour problems in natural water (Mackenthun and Keup, 1970). The increase in turbidity in the raw water supply during an epidemic of infectious hepatitis in Delhi, India, was also

accompanied by objectionable taste and odour in the finished water (Dennis, 1959). Hudson (1962), using 1953 data on infectious hepatitis and raw water turbidity for 12 U.S. cities, observed that infectious hepatitis incidence was greater with increase in turbidity.

The presence of turbidity can have significant effects on both the microbiological quality of drinking water and the detection of bacteria and viruses in the water. Microbial growth in water is most extensive on the surfaces of particles. This occurs because nutrients adsorb to surfaces, and adsorbed bacteria are thus able to grow more efficiently than when in free suspension (Brock, 1966; Stotzky, 1966). Historically, filtration has been demonstrated to provide a substantial barrier to disease-causing organisms (AWWATGR, 1959). Studies reported indicate bacteriological count reductions with decreasing filtrate turbidity and practically complete removal of algae and coliform bacteria with 0.1 NTU effluents (Logsdon and Lippy, 1982).

Particulate matter (e.g., organic, inorganic, higher micro-organisms) can protect bacteria and viruses from the effects of disinfection or act as a source or vector for organisms. Distribution system studies have shown some conflicting findings with respect to turbidity. Haas *et al.*, (1983) noted that increasing values of pH, temperature and turbidity were associated with increasing concentrations of micro-organisms. Standard plate count increases with increasing turbidity have also been found at turbidity levels less than 2.0 NTU (Snead *et al.*, 1980). Goshko *et al.*, (1983) also found positive correlations between standard plate counts and turbidities in the range of 0.83 to 8.89 NTU. Sanderson and Kelly (1964) reported coliform organisms in water having turbidities ranging between 3.8 and 84.0 NTU even in the presence of free chlorine residuals of up to 0.5 mg/l and after a contact time in excess of 30 minutes. Neefe (1947) showed that chlorination alone would not protect human volunteers from infectious Hepatitis when water deliberately contaminated with faecal matter was ingested. Only by treating the water samples by

coagulation and filtration prior to chlorination could the water be rendered safe to drink.

Hence, turbidity, an indicative parameter has been considered in this study.

1.3.2 Effect of Roofing Materials

Vasudevan (2001) studied on rainwater flushes and found that the rainwater from brick tile roof always gave higher bacterial count as compared with water collected directly. Rainwater collected from plastic roof also had bacteria. Metallic roof rainwater samples generally gave lower bacterial count as compared with direct rainwater samples. Probably due to heating, the roof gets sterilized. In the case of asbestos also, there was some gradation between the three flushes. Initial 1st flush gave higher count than the sample from rain gauge although 2nd and 3rd flushes gave lower count. Thus quality of water samples was in the decreasing order of metallic, asbestos, plastic, tile roof. The volume of water to be rejected as first flush would depend on the roofing material and the amount of contamination. However, as a thumb rule the first 2.0 mm rain may have to be rejected.

Yaziz *et al.*, (1989) analysed the rainwater collected in open ground and from a galvanized iron roof in Malaysia. The values of faecal coliform and total coliform reported in rainwater were 0-3.20 CFU/100ml and 0-47 CFU/100ml, respectively. The turbidity in rainwater was in the range of 3.0-15.4 mg/l which is higher than the WHO drinking water standards. The concentration of turbidity and bacteriological quality of rooftop rainwater depend on the type of roof and quality & amount of dust deposited on it and presence of trees nearby as their leaves may fall on the roof and provide nutrients for bacterial growth.

1.3.3 The Problem Description

Many researchers have reported the physical, chemical and biological contamination of rainwater after harvesting but no one has suggested the treatment required for rainwater. Until now, only simple mechanical filtering devices have been available and these take out large particles but do not stop micro-organisms, organic and inorganic contaminants, such as heavy metals (Boelhouwer *et al.*, 2001). A systematic survey reveals that the different types of sand filter, such as single media, dual media and multi media, are in practice for rainwater harvesting for domestic purposes and for recharge of ground water. Wherever these filters are installed, the design of the filters is on an ad-hoc basis and no technical guidelines/specifications have been developed and followed for its designing. Infact, no design details are available for designing of sand filters, particularly in India, considering the different conditions, such as orientation of filter, rainwater quality variation for turbidity and microbiology, turbidity removal efficiency, filtration rate, depth of filter media and its grain size, flow resistance and clogging pattern with filter run.

Hsiung and Cleasby (1968) have suggested two models for water filtration, i.e. effluent quality and critical head loss models, based on sand filter experimental studies in the laboratory. The filter experiments were conducted by continuously adding ferrous sulfate in hard well water and the filter influent and effluent quality were evaluated by their iron contents. The depth of the filtration media was 21.5 inch and the influent iron concentrations for sand filter were 5.8 and 3.3 mg/l. The filters were operated at three different flow velocities of 3.0, 4.5 and 6.0 gpm/ft² for various sand grain sizes of 0.649, 0.545, 0.458 and 0.386 mm. The compatibility of these two filter models for rainwater harvesting followed by formulation of new models have been investigated in the present work.

1.3.4 The Problem Identification

Since the Hsiung and Cleasby (1968) models is developed for influent iron concentration in the manually prepared samples and hence the performance of these models should be checked for different type of samples. The application of these models has been extended for rainwater and Fuller's earth suspension water samples to check the compatibility for various influent concentrations and filtering conditions. The models are tested against various sand filter runs data generated for different sand filter modules in the laboratory. Verma (2004) also emphasized the need for further testing of Hsiung and Cleasby (1968) models against additional data on filter run for different influent concentrations. In view of this, present work focuses on a variety of lab-based experiments on a variety of filter beds. There were four sand filters installed in the laboratory and were operated under two different conditions at Fuller's earth suspension water samples and rooftop rainwater samples. Turbidity was the only parameter used to check the performance of sand filter because there is evidence in the literature that the removal of turbidity can be considered as a surrogate measure for removal of micro-organisms too. In fact, the process of filtration leads to deposition of impurities in the filter layers which also act as a site for attachment of the fine particles, and bacteria. Based on the laboratory study of sand filter, Hsiung and Cleasby (1968) models were checked for its compatibility with rooftop rainwater and different influent turbidity concentrations.

1.4 OBJECTIVES AND METHODOLOGY

The following objectives are considered for the present work

1. Detailed literature review in order to assess the characteristics of the rooftop rainwater collected from various roofs such as gravel roof, brick tile roof, metallic roof, thatch roof, asbestos roof, concrete roof and plastic roof and

their likely impact on the quality of the rainwater during its storage and to identify available methods of the treatment of rooftop rainwater.

2. Considering that a variety of filters are in use for rainwater harvesting systems in India and no information is available on their design details, technical evaluation of these filter units is considered as another objective.
3. Performing a variety of experiments on different filter modules with varying flow rates, sizes and depths of sand grain media, shapes of filter and its orientation for uniform sand grains. Graded sand filters are also considered in the experimental program.
4. Analysis of data on filter runs to identify the most efficient filters which lead to higher efficiency of particulate (turbidity) removal.
5. Testing the compatibility of statistical models of Hsiung and Cleasby (1968) for rainwater harvesting and other filtering conditions is another major objective of the work.
6. Development of new alternate models based on effluent quality and flow resistance for vertically downward flow and horizontal flow sand filters. The models are developed for different concentrations of Fuller's earth suspension water solution under vertically downward and horizontal flow filtering conditions.
7. Check the compatibility of new developed models in dimensionless form for various influent concentrations with respect to Hsiung and Cleasby models for sand filter performance prediction.
8. Testing of new developed model for compatibility to predict the performance of sand filter for rainwater harvesting in different conditions.

A block diagram, as shown in Fig.1.1, indicates the methodology adopted to achieve these objectives.

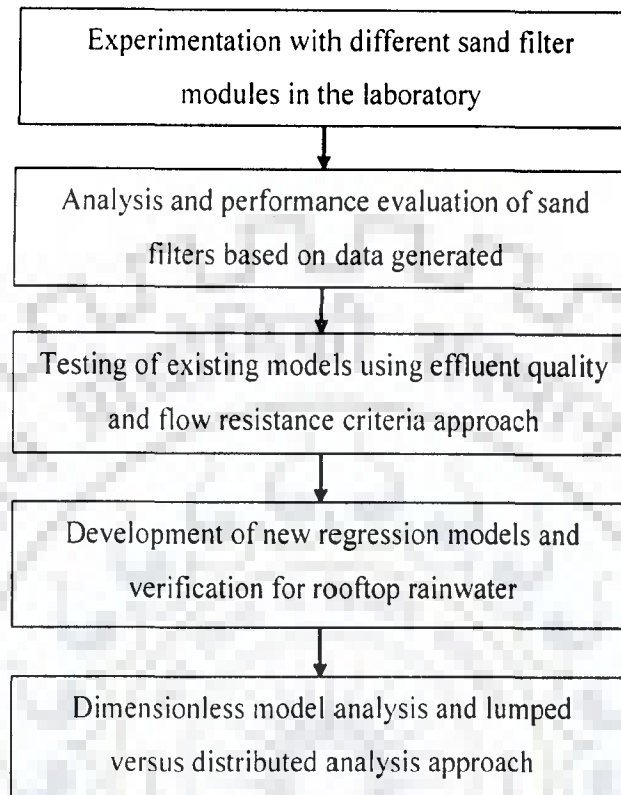


Fig. 1.1: Block diagram of the methodology adopted

1.5 ORGANIZATION OF THE THESIS

The chapter wise details of the thesis are as follows:

Chapter 1 introduces the importance of rainwater harvesting, its need and potential, the effect of roofing materials on rooftop rainwater harvesting and the variation in rainwater quality based on the available literature. Problem description and identification associated with rainwater harvesting filter system are also discussed. The objectives of the study are discussed in subsequent paragraphs. Then, the methodologies followed for the study is outlined. The organization of the thesis describes the details of each chapter of the thesis.

Chapter 2 presents literature review on the historical development of rainwater harvesting systems and general suitability of important rainwater harvesting systems/ structures in different zones of India. The second aspect is the precipitation study, need and the various practices of rainwater harvesting in India. Qualitative assessment of the rainwater in terms of physical, chemical and microbiology is covered in details. The requirement of treatment of rainwater before and after harvesting and the objective of filter use in rainwater harvesting is also covered. Technical evaluation of the conventional sand filters installed in the field for rainwater harvesting is discussed. The assessment of sand filter design parameters for rainwater harvesting is also described in the last paragraph.

Chapter 3 describes the details of experimental set-up in the laboratory for various sand filter modules. The experiments are operated in two set of observations, one for rainwater samples and second for Fuller's earth suspension water solution samples. The details of turbidity concentration in rainwater and Fuller's earth suspension water solution are illustrated in this section. The criteria for selection of filtration velocity, filter properties such as size and shape of filter, sand grain sizes, filtering media depths, filter run time, flow velocity, orientation of sand filter are discussed.

Chapter 4 presents the theory of probability and use of probabilistic approach for the development of models by Hsiung and Cleasby (1968). The compatibility of Hsiung and Cleasby models are tested against different concentrations of Fuller's earth suspension water solution and rainwater samples. The performance of sand filter is assessed in describing the removal of turbidity as well as flow resistance across the clogged bed. It also uses Hsiung and Cleasby (1968) approach to identify the most efficient filters and compare the results with those obtained in the laboratory. Filters having higher efficiency of particulate removal are also identified with respect to rainwater as well as Fuller's earth suspension water solution samples.

Chapter 5 describes the probabilistic approach for the development of new models of the data generated in the laboratory for the prediction of sand filter performance based on effluent quality and critical head loss with the help of regression analysis. The models are developed using Fuller's earth suspension water solution samples for certain filter runs at different conditions. The compatibility of new developed models is also tested against new experimental run data for rainwater samples. In the light of these new models, their influence on design of sand filter is discussed.

Chapter 6 illustrates the dimensionless model analysis of the new developed models. The new models developed are used in dimensionless form to check the performance of the models with respect to the Hsiung and Cleasby models. The compatibility of dimensionless model for effluent quality prediction has also been checked in this chapter.

Chapter 7 deals with the testing of new developed models of sand filter for rainwater harvesting and their interpretation to use in different filtering conditions. The compatibility of the models is tested on the basis of influent concentration removal efficiency and minimum head loss criteria under vertically downward and horizontal flow conditions. The recommendation of sand filter models for different grading of sand filter in different conditions is based on their performance of influent turbidity removal efficiency and minimum head loss criteria.

Chapter 8 contains the results and discussion of the research conducted for development and testing of new mathematical models for rainwater harvesting sand filter. The results of testing of dimensionless model performance are also illustrated. Major contributions and key findings of the research have also been highlighted in this chapter.

Chapter 9 presents the conclusions of the research work and future scope of work.

Towards the end, list of references including internet reference has been included.

2.1 GENERAL

Rooftop rainwater harvesting at household or community level is commonly used for domestic purposes including drinking water. Rainwater collected from roofs and stored in tanks is an essential source of drinking water in many countries throughout the world. The main constraints on using rainwater for domestic use have been the water quality aspects. The quality of rainwater collected depends on the atmosphere, materials used for the catchment surface, gutter and down pipe of the storage tank and water extraction devices. Numerous studies have shown that due to contamination following contact with the catchment surface, stored rainwater often does not meet WHO drinking water standards (WHO, 1993), especially with respect to microbiological quality criteria. Hence, this chapter briefly describes the study of physical, chemical and microbiological quality of rainwater, based on literature survey.

The simple technique of rainwater harvesting is to save and store the water running off from a roof for indoor needs. Artificial recharge is a process of augmenting the underground water table by artificial infiltration of rainwater and surface water. Riverbank filtration technique is another option to recharge the ground water from the lake or river surface water. The processes involved in riverbank filtration or conventional filtration systems are very much similar in nature. For example, Wett *et al.*, (2002) have developed the occurrence of clogging in case of riverbank filtration which is also observed in natural filters. Many substances present in surface water, such as natural organic matter or

biodegradable micro-pollutants, are largely and in most cases completely removed by bank filtration (Kuehn and Mueller, 2000). The riverbank filtration process has some similarity with the performance of slow sand filters. Organic mats, similar to the *schmutzdecke*, can develop at the river/aquifer interface, especially when the flow velocity is slow (Ray, 2002). Hiscock and Grischek (2002) stated that the pathogenic bacteria, viruses and *Cryptosporidium* can be effectively reduced or eliminated by bank filtration which is very similar in nature to the sand filter.

The presence of turbidity can have significant effects on both the microbiological quality of drinking water and the detection of bacteria & viruses in the rainwater. Hence, sand filter is required for the treatment of harvested rainwater before storage to tank. Various sand filter units are installed in the field for rainwater harvesting but presently, the design of sand filter is on adhoc basis especially in India. There is no design specification or mathematical models available for the design of sand filters. A review of various sand filters installed in the field for rainwater harvesting with details of their lack of technical parameters are presented in this chapter.

2.2 DEVELOPMENT OF RAINWATER HARVESTING CONCEPT

Rainwater harvesting and utilization systems have been used since ancient times and evidence of roof catchment systems dates back to early Roman times. Roman villas and even whole cities were designed to take advantage of rainwater as the principal water source for drinking and domestic purposes since at least 2000 B.C. The earliest evidence of the use of water harvesting is the well publicized systems used by the people of the Negev Desert in Israel perhaps 4000 years ago (Evenari, *et al.*, 1971). Hillsides were cleared of vegetation and smoothed in order to provide as much runoff as possible; the water was then channeled in contour ditches to agricultural fields and/or to cisterns. In the

Negev desert, tanks for storing runoff from hillsides for both domestic and agricultural purposes have allowed habitation and cultivation in areas with as little as 100mm of rain per year.

The earliest known evidence of the use of the technology in Africa comes from northern Egypt, where tanks ranging from 200 to 2000m³ have been used for at least 2000 years, many are still operational today (UNEP, 2002). The technology also has a long history in Asia, where rainwater collection practices have been traced back almost 2000 years in Thailand. The small-scale collection of rainwater from the eaves of roofs or via simple gutters into traditional jars and pots has been practiced in Africa and Asia for thousands of years. The world's largest rainwater tank is probably the Yerebatan Sarayi in Istanbul, Turkey. This was constructed during the rule of Caesar Justinian (AD 527-565). It measures 140x70m and has a capacity of 80,000 m³ (UNEP, 2002).

In the new world, about 400-700 years ago, people living in North America which is now the state of Colorado in the United States and those living in, is now Peru in South America employed relatively simple methods of water harvesting for irrigation (O'Bryan *et al.*, 1969). Although the practice of collecting water from rooftop is a very ancient type of water harvesting, the harvesting of rainwater for agriculture and ranching was pioneered in Australia during the 1920's. Galvanized roof like structures were built near the ground surface solely for the purpose of water harvesting (Kenyon, 1929).

A renewed interest in the technology of water harvesting occurred in 1950's in Israel, Australia and the United States. In Australia, "ROADED" catchments based on the concept of compacted earth were constructed over more than 2,000 hectares in order to collect water for agricultural purposes (Frith, 1975). In United States, at about the same time, catchments were constructed primarily of sheet metal for watering livestock. Also during this period, experimentation was undertaken with plastic and artificial rubber

membranes for the construction of both catchments and reservoirs (Lauritzen, 1960). Since 1950's, the technology of water harvesting has developed variety and sophistication through experimentation and demonstration projects. Not all have been successful but some have worked very well. The technology and experience gained have now reached the point where some form of water harvesting system can be designed to fit within the physical, climatological and economic constraints of almost any dry region of the world.

First definition of water harvesting came from Geddes, as quoted by Myers (1975): "the collection and storage of any farm waters, either runoff or creek flow, for irrigation use". Myers also quoted the definition: "The process of collecting natural precipitation from prepared watersheds for beneficial use". Myers himself used the definition: "The practice of collecting water from an area treated to increase runoff from rainfall or snowmelt." These definitions show that water harvesting encompasses methods to induce, collect and store runoff from various sources and for various purposes. The method applied depends strongly on local conditions and includes such widely differing practices as farming terraced wadi beds (Evensen *et al.*, 1971), growing trees on micro-catchments (NAS, 1974), catching runoff from sheet metal catchments (Chiarella and Beck, 1975; Mickelson, 1975), tapping surface runoff (Burdas, 1975; Agarwal, 1977; Smith, 1978) storing runoff behind a dam (Bowler and Turner, 1977; Myhrman *et al.*, 1978) and others (Evans *et al.*, 1975; Manges and Mao, 1978).

Hundreds of years before the birth of Christ, rainwater collection was already a common technique throughout the Mediterranean and Middle East, used by Egyptians, Palestinians, Iranians, Iraqis, Yemenis, Greeks and Romans (Movahed, 1997). Water was collected from roofs and other hard surfaces and stored in underground tanks, or excavated reservoirs (cisterns) with masonry domes (Movahed, 1997). In some parts of the Middle East, rainwater was collected from hard surface areas and channeled through vertical

shafts to horizontal tunnels (qanars), which in turn led the water to underground reservoirs (Smet and Moriarty, 2001).

In addition to the traditional rainwater harvesting techniques found in India, North Africa and the Western Mediterranean, there are also examples from Thailand, China, Bangladesh, Nepal, Sri Lanka, Indonesia and the small islands in the Pacific (Smet and Moriarty, 2001). In Africa, the collection of rainwater was (and is) practiced using small containers, in among others, most of Southern Africa, Ghana, Kenya and Tanzania (Smet and Moriarty, 2001). Even in Western Europe, historical records show that in many places rainwater was the primary drinking water source, the same applies to the America and Australia. In all three continents, rainwater continues to be an important source for isolated homesteads and farms (Smet and Moriarty, 2001). The general suitability of important rainwater harvesting systems/structures in different zones of India is summarized in Table 2.1 (Anonymous, 1990).

Table 2.1: Suitability of rainwater harvesting structures in different zones of India

(Anonymous, 1990)

Regions	State of the art	Remarks
Humid north-western Himalayas	Roof water harvesting, Diversion of perennial springs & streams in storage structures, Village ponds, Collection from hill slope	Improvement in roof structure and use of proper material and as corrugated sheets for generating higher runoff and with arrangement of foul slush diversion system and proper storage structure for checking water from contamination
Himalayan foot hills	Collection from hill slope, Village ponds, Roof water harvesting, Interflow harvesting	-do-
Humid high rainfall north-eastern	Roof water harvesting, Diversion of perennial springs & streams in a storage structure (tank)	-do-
Humid Assam Bengal plains	Tank, Anicut/check dam, Gully plugging, Contour bunding	Improved design of tank for minimizing evaporation and seepage losses, control of sediment load and water pollution
Sub-humid & humid Satluj Ganga alluvial zone	Pond, Check dam, Gully plugging, Contour bunding	-do-
North-western semi-arid & arid zone	Nadi, Tanka, Khadim, Percolation tank, Anicut, Gully plugging, Contour bunding, Roof harvesting	Adoption of improved design of Nadi and Tanka, Sand filled reservoir, Sub-surface barrier, Flat batter tank
Central semi-arid Vindhyan zone	Pond, Check dam, Contour bunding, Gully plugging, Sub-surface dykes	-do-
High rainfall, high runoff Chhotanagpur plateau	Tank, Anicut/check dam, Gully plugging, Contour bunding	-do-
Assured rainfall deep black soil Malwa plateau & Narmada basin	Ponds, Check dams, Sub-surface dams	Improvement of existing systems
Variable rainfall south central plateau zone Chhattisgarh plateau zone	Pond, Check dam, Percolation tank, Bandhara, Gully plugging, Subsurface dam, Contour bunding	Flat batter tank, Selection of suitable site, Improvement of existing system, better water management
Southern variable rainfall, mixed soil zone	Ponds/tanks, Nadi, Check dam, Percolation tank, Subsurface dam, Fully plugging	-do-
South eastern brown/red soil zone	Ponds/tanks, Percolation tanks, Subsurface dams	Improvement of existing systems
Southern bi-modal rainfall zone	Ponds/tanks, Percolation tanks, Gully plugging, Contour bunding, Checks dams	-do-
Western Coromandal	Pond/tank/kunta, Nadi, Check dam, Percolation tank, Gully plugging, Subsurface dam	Adoption of improved design of Nadi and tank, Selection of suitable sites and improvement of existing system for better water management
Western Malabar	Pond/tank/kunta, Nadi, Check dam, Percolation tank, Bandhara, Kolhapur type weirs, Subsurface dam, Contour bunding	Improvement in existing system, better water management, Construction of structures at suitable sites.

2.3 EVALUATION OF RAINFALL INTENSITIES IN INDIA

A key constraint to any filter in a rainwater harvesting system is that it should be capable of dealing with the high flows associated with high rainfall intensities and rooftop area. Rainfall intensity can be calculated using the general form of rainfall intensity-duration-return period relationship which is given in Eq. (2.1) (Ram Babu *et al.*, 1979)

$$I = \frac{KT^a}{(t+b)^n} \quad (2.1)$$

where, I is rainfall intensity (cm/hr.), T is return period (years), t = storm duration (hrs.). For finding out intensity of any particular place, one needs to select the values of the coefficients K, T, a, b and n against corresponding places, which are given by Singh *et al.*, (1990).

Using the Eq. (2.1), the rainfall intensity for return periods of 1, 5, 10, 15, 20, 25 and 30 years at various locations in India are presented in Table 2.2. The parameter, t, the time of concentration of a watershed which can be computed by using Eq. (2.2)

$$t = 0.01947K^{0.77} \quad (2.2)$$

where $K = \sqrt{\frac{L^3}{H}}$; t = time of concentration (min); L = maximum length of travel (m) and H = difference in elevation between most remote point and outlet (m) (Singh *et al.*, 1990).

Table 2.2 reveals that the maximum rainfall, in the proximity of I.I.T. Roorkee occurs at Dehradun city which is situated at only 70.0 km from the institute i.e. I.I.T. Roorkee, Roorkee, India. Considering the maximum rainfall intensity for 15 years from Table 2.2, rainwater runoff for various rooftop areas (LIG, MIG and HIG) have been computed, which can provide preliminary information for users interested to adopt rainwater harvesting. The rate of inflows for various categories of the buildings is also presented in Table 2.3.

Table 2.2: Rainfall intensity at various locations in India for return period of 30 years

Locations	Rainfall intensity (cm/hr.)						
	1 yr	5 yrs	10 yrs	15 yrs	20 yrs	25 yrs	30 yrs
Agartala	1.75	2.11	2.29	2.40	2.49	2.55	2.61
Agra	1.55	2.03	2.27	2.43	2.55	2.65	2.73
Allahabad	1.27	1.67	1.88	2.01	2.11	2.19	2.26
Amritsar	1.08	1.33	1.45	1.53	1.59	1.64	1.68
Aurangabad	0.79	0.99	1.10	1.17	1.22	1.26	1.29
Bangalore	0.58	0.93	1.01	1.07	1.11	1.14	1.17
Bhopal	1.34	1.82	2.08	2.24	2.37	2.47	2.55
Bhuj	0.62	0.85	0.97	1.05	1.11	1.15	1.20
Gaya	1.22	1.55	1.72	1.82	1.91	1.97	2.02
Chennai	1.36	1.78	2.00	2.14	2.24	2.33	2.40
Dehradun	1.34	1.91	2.23	2.43	2.59	2.72	2.84
Dumdum	1.10	1.33	1.45	1.51	1.56	1.60	1.64
Guwahati	1.19	1.54	1.71	1.82	1.91	1.97	2.03
Hyderabad	0.76	0.95	1.04	1.11	1.15	1.18	1.21
Indore	0.94	1.18	1.30	1.38	1.43	1.48	1.52
Imphal	0.81	0.99	1.09	1.15	1.20	1.23	1.26
Jabalpur	1.24	1.64	1.85	1.98	2.08	2.17	2.24
Jaipur	0.76	0.91	0.97	1.01	1.04	1.07	1.09
Jharsuguda	1.62	2.03	2.23	2.36	2.46	2.53	2.61
Jamshedpur	1.35	1.67	1.82	1.92	2.00	2.06	2.11
Jodhpur	0.59	0.77	0.86	0.93	0.97	1.01	1.04
Lucknow	0.88	1.17	1.33	1.43	1.51	1.57	1.63
Nagpur	1.48	1.90	2.12	2.26	2.36	2.45	2.52
New Delhi	0.66	0.84	0.94	1.00	1.05	1.09	1.12
Raipur	0.87	1.08	1.19	1.26	1.31	1.36	1.39
Shillong	1.08	1.38	1.53	1.62	1.69	1.75	1.80
Srinagar	0.21	0.33	0.40	0.45	0.48	0.51	0.54
Tiruvendrum	1.47	1.88	2.09	2.23	2.33	2.41	2.48
Visakhapatnam	1.02	1.35	1.52	1.63	1.71	1.78	1.83

Table 2.3: Measuring rainfall flow rate at various rooftop for return period of 15 years

Locations	Rainfall Intensity	LIG Rooftop (46 m ²)		MIG Rooftop (70 m ²)		HIG Rooftop (115 m ²)	
	(cm/hr.)	Flow rate (liter/min.)	Flow rate (liter/min.)	Flow rate (liter/min.)	Flow rate (liter/min.)	Flow rate (liter/min.)	Flow rate (liter/min.)
Agarhala	2.40	18.42	28.04	28.04	46.07	46.07	46.07
Agra	2.43	18.66	28.40	28.40	46.65	46.65	46.65
Allahabad	2.01	15.42	23.47	23.47	38.56	38.56	38.56
Amritsar	1.53	11.74	17.87	17.87	29.36	29.36	29.36
Aurangabad	1.16	8.95	13.63	13.63	22.39	22.39	22.39
Bangalore	1.06	8.19	12.47	12.47	20.49	20.49	20.49
Bhopal	2.24	17.18	26.15	26.15	42.96	42.96	42.96
Bhuj	1.04	8.02	12.21	12.21	20.07	20.07	20.07
Gaya	1.82	13.99	21.29	21.29	34.98	34.98	34.98
Chennai	2.13	16.40	24.96	24.96	41.01	41.01	41.01
Dehradun	2.43	18.67	28.41	28.41	46.67	46.67	46.67
Dumdum	1.51	11.60	17.65	17.65	29.01	29.01	29.01
Guwahati	1.82	13.98	21.28	21.28	34.97	34.97	34.97
Hyderabad	1.10	8.45	12.86	12.86	21.13	21.13	21.13
Indore	1.37	10.55	16.05	16.05	26.37	26.37	26.37
Imphal	1.15	8.82	13.43	13.43	22.06	22.06	22.06
Jabalpur	1.98	15.20	23.13	23.13	38.01	38.01	38.01
Jaipur	1.01	7.77	11.83	11.83	19.44	19.44	19.44
Jharsuguda	2.36	18.10	27.55	27.55	45.26	45.26	45.26
Jamshedpur	1.92	14.75	22.44	22.44	36.87	36.87	36.87
Jodhpur	0.92	7.10	10.81	10.81	17.75	17.75	17.75
Lucknow	1.43	11.00	16.74	16.74	27.50	27.50	27.50
Nagpur	2.25	17.32	26.36	26.36	43.31	43.31	43.31
New Delhi	1.01	7.69	11.71	11.71	19.24	19.24	19.24
Raipur	1.26	9.68	14.73	14.73	24.21	24.21	24.21
Shillong	1.62	12.44	18.94	18.94	31.11	31.11	31.11
Srinagar	0.44	3.43	5.22	5.22	8.591	8.591	8.591
Trivendrum	2.22	17.06	25.97	25.97	42.66	42.66	42.66
Visakhapatnam	1.62	12.48	18.99	18.99	31.20	31.20	31.20

*LIG: Low income group housing; MIG: Middle income group housing; HIG: High income group housing.

2.4 CONTAMINATION OF RAINWATER

The level of risk associated with drinking rainwater is a product of the concentration of pathogens/toxins present, the level of exposure and impact of the infective agent/toxin, and the vulnerability of the individual or population exposed (Gould and Nissen-Petersen, 1999). Local circumstances and in particular environmental factors are also critical, such as the degree of atmospheric pollution, the type of construction materials and level of maintenance of the rainwater catchment system (Haebler and Waller, 1987). In rural areas where atmospheric pollution is not generally a problem, several simple steps to reduce contamination of rainwater supplies can be taken. While, in the absence of serious atmospheric pollution it is possible to protect the quality of water in roof catchment tanks, for ground catchment systems serious contamination by the catchment surface is common and use of any water collected is not recommended for drinking unless first treated (Gould and McPherson, 1987). The water is, however, suitable for most non-consumptive purposes without treatment. Gould (1999) reviewed some of the rare rainwater related disease outbreaks and other potential health risks due to atmospheric pollution contaminating rainfall.

2.4.1 Sources of Rainwater Contamination

In most industrialized urban areas, the atmosphere has often been polluted to such a degree that the rainwater itself is considered unsafe to drink (Thomas and Greene, 1993). In U.S. the drinking water within 48 km of urban centres is not recommended unless no other source is available. Heavy metals such as lead are potential hazards especially in areas of high traffic density or in the vicinity of heavy industries (Yaziz *et al.*, 1989; Thomas and Greene, 1993). Organic chemicals such as organo-chlorines and organo-phosphates used in biocides can also contaminate rainwater. Although serious atmospheric

contamination of rainwater is normally limited to urban and industrial locations. studies in the northeastern United States revealing the presence of pesticides and herbicides in rainwater do give some cause for concern (Richards *et al.*, 1987). Despite the numerous sources of atmospheric pollution, in most parts of the world, especially in rural and island locations, levels of contamination of rainfall are low. Most contamination of rainwater occurs after contact with the catchment surface (roof or ground) and during subsequent delivery and storage (Waller, 1989).

2.4.1.1 Microbiological contamination

The quality of rainwater used for domestic supply is of particular importance because in most cases, it is used for drinking untreated. The issue of water quality is a complex and sometimes controversial one. In 1980's several studies indicated that rainwater supplies often do not meet WHO and other national drinking water standards especially with respect to bacteriological water quality (Riddle and Speedy, 1984; Fujioka and Chinn, 1987; Haebler and Waller, 1987; Lye, 1987; Krishna, 1989; Wirojanagud and Hovichitr, 1989). While these findings did not in themselves imply that the water is unsafe to drink, these did prompt further investigations which focused on determining both the sources and implications of any contamination (Fujioka *et al.*, 1991; Lye, 1992a).

Krishna (1993) and Fujioka (1993) also led to the development of less stringent bacteriological water quality standards for potable rainwater. In a parallel development, drinking water quality guidelines more appropriate for rural conditions in developing countries were proposed (Ockwell, 1986; Morgan, 1990). Both of these allowed less strict sets of guidelines water with mean *E. coli* counts of up to 10 per 100ml to be accepted for drinking as compared to the WHO recommended limit of zero per 100ml (WHO, 1993). When the quality of stored rainwater samples are judged according to this more realistic

criterion, the number of rainwater supplies with water deemed to be within acceptable limits for drinking is greatly increased. A more direct source of evidence implicating a rainwater supply as a potential health risk comes from identifying the presence of specific pathogens.

The health risks associated with tank rainwater consumption are not well defined. Simmons and Heyworth (1999) provided a schematic model for considering the health impacts of rainwater with microbial contamination using the epidemiological approach but encompassing risk assessment as a central theme. They discussed the merits of various epidemiological study designs as a tool to estimate the risk of illness from rainwater exposure. A number of pathogenic species have been identified in tank rainwater. Microbiological surveys have found *Clostridium perfringens*, *Salmonella*, spp. (Fujioka *et al.*, 1991), *Cryptosporidium* spp., *Giardia* spp. (Crabtree *et al.*, 1996), *Legionella* spp. (Broadhead and Negron-Alvira, 1988), *Aeromonas* sp. (Simmons and Smith, 1997), *Hepatitis A virus* (Luksamijarulkul *et al.*, 1994), *Pseudomonas* spp. (Waller *et al.*, 1984), *Shigella* spp. (Canoy and Knudsen, 1983) and *Vibro parahaemolyticus* (Wirojanagud and Hovichitr, 1989) as contaminations of rainwater. However, the degree of contamination and the implications for health have not been quantified.

The paucity of studies citing proven links between disease outbreaks and rainwater sources is perhaps not surprising, given this difficulty and the fact that many individual cases go unreported or result in no further investigation (Simmons and Heyworth, 1999). The probable cause for the outbreak was postulated as *Salmonella arechevalata* contained in animal or bird excrement on the camp roof and washed into the rainwater tank, from which water was used for drinking. Other studies that have established links between rainwater consumption and illness include outbreaks of;

- salmonellosis in New Zealand (Simmons and Smith, 1997)

- campylobacteriosis in Australia (Brodrigg *et al.*, 1995)
- giardiasis and cryptosporidiosis in Australia (Lester, 1992).

2.4.1.2 Chemical contamination

The constituents in rainwater are mostly derived from the atmosphere so its chemical composition depends on the atmosphere through which it falls, which in turn depends on various seasonal and local factors, such as the presence of industrial and agricultural activities and proximity to the sea. Various studies have been done to analyse the chemical composition of rainwater (Eriksson, 1957; Durfer and Baker, 1964; Gæmbell, 1966; Peirson, 1973; Dalal, 1979; Hofkes, 1981) and despite much variation, its general characteristic is the low content of minerals. Several studies, examining the chemical constituents of stored rainwater, have found that these generally meet WHO drinking water quality standards for a broad range of parameters (Haebler and Waller, 1987; Scott and Waller, 1987; Michealides, 1989).

In a few cases, slightly elevated levels of magnesium and zinc exceeding WHO guideline standards for drinking water have been detected but these do not pose any serious health concern (Wirojanagud and Hovichitr, 1989). Elevated levels of lead are the most common cause for concern. A recent pilot study of 25 potable household rainwater supplies around Auckland in New Zealand found lead exceeding national drinking water standards in 12% of the tanks surveyed (Simmons *et al.*, 1997). Potentially, the adverse health implications of the long term consumption of rainwater containing elevated levels of heavy metals such as lead pose a serious health threat. For roof catchment systems several potential sources of lead contamination exist. These include the use of lead flashing, lead headed nails, lead based paints/primers for roof construction and the deposition of lead particles on the catchment surface in regions subject to heavy industrial

or traffic pollution (especially in countries still using leaded petrol).

Where roof catchment systems are poorly maintained allowing for a build up of leaf litter in the tank, stored water can become more acidic. When the pH is depressed rainwater becomes more 'aggressive' and can leach out metals and other constituents from storage tanks, taps, fittings and sludge deposits on the tank floor. Evidence from Ohio, in an area with serious atmospheric pollution and acidic rainfall, suggested that elevated lead and cadmium levels in cistern sediment and water, posed a potentially serious health risk (Sharpe and Young, 1982). Investigations in Halifax, Nova Scotia also revealed high lead concentrations in runoff water collected from an old roof with considerable amounts of lead flashing from rainwater with pH 4 (Waller and Inman, 1982). The effect of acidic (pH 3) water and presence of leaf litter in the tank was also shown to increase the rate of dissolution of lead from tank sludge by up to 50 times. Evidence of the potential health dangers of excessive lead levels in stored rainwater also comes from a study in Port Pirie, a location of one of the world's biggest smelters in South Australia (Body, 1986).

From the above studies, it is clear that the rooftop rainwater is not safe to consume directly for drinking purposes. Hence, the methods to protect or improve rainwater quality include appropriate system design, sound operation and maintenance, the use of first flush devices and treatment. The use of sand filter is an essential in rooftop rainwater harvesting before the storage to avoid water born diseases while consumed by human being. The filtration system is also essential where rainwater has been used for artificial recharge of ground water by various processes.

2.4.2 Selection of Study Parameter

Turbidity can affect or can be affected by the physical, microbiological, chemical and radiological characteristics of water. In general, the relationships between turbidity

and other water quality parameters are due to the turbidity itself; the adsorptive and complexing capacity of the many types of particulates that contribute to turbidity; and the fact that particulate matter is a source of nutrients and protection for some microorganisms (Reilly and Kippin, 1983). The presence of turbidity can have significant effects on both the microbiological quality of drinking water and the detection of bacteria and viruses in the water. Hudson (1962), using 1953 data on infectious hepatitis and raw water turbidity for 12 U.S. cities, observed that infectious hepatitis incidence was greater with turbidity. Shaffer *et al.*, (1980) reported detection of polio virus in water with chlorine concentrations greater than 1.0 mg/l and turbidity less than 1.0 mg/l.

The relationship between high turbidity, in both raw and filtered water, and taste and odour has long been recognized (Atkins and Tomlinson, 1963). Algal growths, actinomycetes and their debris contribute to taste and odour problems in natural water (Mackenthun and Keup, 1970). The increase in turbidity in the raw water supply during an epidemic of infectious hepatitis in Delhi, India, was also accompanied by objectionable taste and odour in the finished water (Dennis, 1959). Microbial growth in water is most extensive on the surfaces of particles. This occurs because nutrients adsorb to surfaces, and adsorbed bacteria are thus able to grow more efficiently than when in free suspension (Brock, 1966; Stotzky, 1966). Historically, filtration has been demonstrated to provide a substantial barrier to disease-causing organisms (AWWATGR, 1959). Studies reported indicate bacteriological count reductions with decreasing filtrate turbidity and practically complete removal of algae and coliform bacteria with 0.1 mg/l effluent (Logsdon and Lippy, 1982).

Particulate matter (e.g., organic, inorganic, higher micro-organisms) can protect bacteria and viruses from the effects of disinfection or act as a source or vector for organisms. Distribution system studies have shown some conflicting findings with respect

to turbidity. Haas *et al.*, (1983) noted that increasing values of pH, temperature and turbidity were associated with increasing concentrations of micro-organisms. Standard plate count increases with increasing turbidity have also been found at turbidity levels less than 2.0 mg/l (Snead, *et al.*, 1980). Goshko *et al.*, (1983) also found positive correlations between standard plate counts and turbidities in the range of 0.83 to 8.89 mg/l. Sanderson and Kelly (1964) reported coliform organisms in water having turbidities ranging between 3.8 and 84.0 mg/l even in the presence of free chlorine residuals of up to 0.5 mg/l and after a contact time in excess of 30 minutes. Neefe *et al.*, (1947) showed that chlorination alone would not protect human volunteers from infectious Hepatitis when water deliberately contaminated with faecal matter was ingested. Only by treating the water samples by coagulation and filtration prior to chlorination could the water be rendered safe to drink. Hence, turbidity, an indicative parameter has been considered in this study.

2.5 RAINWATER QUALITY REVIEW

Table 2.4 summarizes the investigations of majority of investigators. In a study reported in Malaysia by Yaziz *et al.*, (1989), an average value of faecal coliform of 3.20 CFU/100ml was reported for galvanized iron roof and total coliform of 47.0 CFU/100ml was reported for galvanized iron roof (Table 2.4). The range of turbidity, lead and *F. coli* values exceeded the WHO drinking water guidelines. The turbidity of 3.0 NTU and 15.4 NTU were measured for rainwater collected in open ground and collected from galvanized iron roof respectively. Lead concentration remained consistently high in all samples and exceeded the WHO drinking water standards.

Table 2.4: Studies of rainwater quality by various researchers

Parameters	Researchers					
	Eriksson (1957)	Gambel (1966)	Dalal (1979)	Yaziz <i>et al.</i> , (1989)		Faisst and Fujioka (1993)
				Open ground	Galvanized iron roof	Storage tank
Aluminium (mg/l)	NR	NR	NR	NR	NR	NR
Ammonia (mg/l)	NR	NR	NR	NR	NR	NR
Arsenic (mg/l)	NR	NR	NR	NR	NR	NR
Barium (mg/l)	NR	NR	NR	NR	NR	NR
Boron (mg/l)	NR	NR	NR	NR	NR	NR
Cadmium (mg/l)	NR	NR	NR	NR	NR	NR
Calcium (mg/l)	0.12 - 2.64	0.65	1.88 - 4.32	NR	NR	NR
Chlorides (mg/l)	0.28 - 16.8	0.60	2.10 - 3.90	NR	NR	NR
Chromium (mg/l)	NR	NR	NR	NR	NR	NR
COD (mg/l)	NR	NR	NR	NR	NR	NR
Conductivity (μ S/cm)	NR	NR	NR	NR	NR	45.11
Copper (mg/l)	NR	NR	NR	NR	NR	NR
Cyanide (mg/l)	NR	NR	NR	NR	NR	NR
Dissolved solids (mg/l)	NR	NR	NR	7.00	20.20	NR
Faecal coliform (CFU/100 ml)	NR	NR	NR	0.00	3.20	17.10
Fluoride (mg/l)	NR	NR	NR	NR	NR	NR
Hardness as CaCO ₃ (mg/l)	NR	NR	NR	NR	NR	NR
Iron (mg/l)	NR	NR	NR	NR	NR	NR
Lead (mg/l)	NR	NR	NR	0.20	0.20	NR
Magnesium (mg/l)	NR	0.15	NR	NR	NR	NR
Manganese (mg/l)	0.15 - 3.04	NR	0.33 - 0.99	NR	NR	NR
Mercury (mg/l)	NR	NR	NR	NR	NR	NR
Nickel (mg/l)	NR	NR	NR	NR	NR	NR
Nitrate (mg/l)	0.00 - 0.09	0.60	0.41 - 1.24	NR	NR	NR
pH	NR	NR	NR	5.90	6.54	NR
Potassium (mg/l)	0.04 - 1.26	0.20	1.21 - 3.27	NR	NR	NR
Selenium (mg/l)	NR	NR	NR	NR	NR	NR
Sodium (mg/l)	0.19 - 9.80	0.60	1.92 - 2.54	NR	NR	NR
Sulphate (mg/l)	0.11 - 1.26	2.20	1.89 - 17.75	NR	NR	NR
Suspended solids (mg/l)	NR	NR	NR	17.0	72.0	NR
Temperature ($^{\circ}$ C)	NR	NR	NR	27.5	28.0	NR
Total coliform (CFU/100 ml)	NR	NR	NR	0.00	47.0	671.6
Turbidity (NTU)	NR	NR	NR	3.0	15.4	0.725
Zinc (mg/l)	NR	NR	NR	0.034	0.42	NR

NR: Not reported.

Table 2.4: Studies of rainwater quality by various researchers (contd...)

Parameters	Researchers						
	Appan (1995)	Nyika (1996)	Mansur (1999)	Coombes <i>et al.</i> , (1999)		Appan (1999)	Ariyananda (1999)
			Open tank	Open ground	Storage tank		Open tank
Aluminium (mg/l)	NR	NR	NR	NR	NR	NR	NR
Ammonia (mg/l)	NR	0.89	NR	0.295	0.10	NR	NR
Arsenic (mg/l)	NR	NR	NR	NR	NR	NR	NR
Barium (mg/l)	NR	NR	NR	NR	NR	NR	NR
Boron (mg/l)	NR	NR	NR	NR	NR	NR	NR
Cadmium (mg/l)	NR	NR	NR	<0.002	<0.002	NR	NR
Calcium (mg/l)	NR	8.56	NR	2.00	6.86	NR	NR
Chlorides (mg/l)	1.50	3.78	NR	7.53	7.10	NR	NR
Chromium (mg/l)	NR	NR	NR	NR	NR	NR	NR
COD (mg/l)	NR	NR	NR	NR	NR	NR	NR
Conductivity (μ S/cm)	NR	5.10	50-200	NR	NR	NR	50-200
Copper (mg/l)	NR	0.019	NR	NR	NR	NR	NR
Cyanide (mg/l)	NR	NR	NR	NR	NR	NR	NR
Dissolved solids (mg/l)	NR	NR	NR	21.0	98.23	NR	NR
Faecal coliform (CFU/100 ml)	4.0	NR	NR	0.00	119	6.70	NR
Fluoride (mg/l)	NR	NR	NR	NR	NR	NR	NR
Hardness as CaCO ₃ (mg/l)	NR	NR	NR	NR	NR	0.10	NR
Iron (mg/l)	NR	NR	NR	<0.01	<0.01	NR	NR
Lead (mg/l)	NR	NR	NR	<0.01	<0.01	NR	NR
Magnesium (mg/l)	NR	1.64	NR	NR	NR	NR	NR
Manganese (mg/l)	NR	NR	NR	NR	NR	NR	NR
Mercury (mg/l)	NR	NR	NR	NR	NR	NR	NR
Nickel (mg/l)	NR	NR	NR	NR	NR	NR	NR
Nitrate (mg/l)	0.45	0.97	NR	0.15	0.06	NR	NR
pH	4.3	6.78	6.0-7.5	5.95	6.19	4.10	6.0-7.5
Potassium (mg/l)	NR	0.71	NR	NR	NR	NR	NR
Selenium (mg/l)	NR	NR	NR	NR	NR	NR	NR
Sodium (mg/l)	NR	3.87	NR	9.90	4.85	NR	NR
Sulphate (mg/l)	6.50	2.89	NR	3.50	4.93	NR	NR
Suspended solids (mg/l)	NR	NR	NR	8.40	1.37	NR	NR
Temperature (°C)	NR	NR	NR	NR	NR	NR	NR
Total coliform (CFU/100 ml)	32	NR	4-180	0.00	834	92.0	4-1000
Turbidity (NTU)	2.50	NR	5.0-15.0	NR	NR	4.60	5.0-15.0
Zinc (mg/l)	NR	0.05	NR	NR	NR	NR	NR

NR: Not Reported.

Table 2.4: Studies of rainwater quality by various researchers (contd...)

Parameters	Researchers							
	Vasudevan <i>et al.</i> (2001)				Ariyananda (2001)		Bo and Guangen (2001)	
	Brick tile roof	Plastic roof	Metallic roof	Asbestos roof	Bandarawela	Welimada	Clay tank	Reinforced concrete tank
Aluminium (mg/l)	NR	NR	NR	NR	0.37	0.54	NR	NR
Ammonia (mg/l)	NR	NR	NR	NR	NR	NR	0.02-0.20	0.02-0.16
Arsenic (mg/l)	NR	NR	NR	NR	NR	NR	0.005-0.012	0.001-0.017
Barium (mg/l)	NR	NR	NR	NR	NR	NR	NR	NR
Boron (mg/l)	NR	NR	NR	NR	NR	NR	NR	NR
Cadmium (mg/l)	NR	NR	NR	NR	0.027	0.013	0-0.004	0.001-0.004
Calcium (mg/l)	NR	NR	NR	NR	NR	NR	NR	NR
Chlorides (mg/l)	NR	NR	NR	NR	NR	NR	5.4-25.8	5.4-27.0
Chromium (mg/l)	NR	NR	NR	NR	0.00	0.0078	0.004-0.015	0.005-0.021
COD (mg/l)	NR	NR	NR	NR	NR	NR	2.3-5.3	1.0-2.8
Conductivity (μ S/cm)	NR	NR	NR	NR	70.0	100.0	NR	NR
Copper (mg/l)	NR	NR	NR	NR	NR	NR	0.006-0.017	0.006-0.017
Cyanide (mg/l)	NR	NR	NR	NR	NR	NR	UD	UD
Dissolved solids (mg/l)	NR	NR	NR	NR	NR	NR	NR	NR
Faecal coliform (CFU/100 ml)	1100	1100	0.0	460	11.0	75.0	NR	NR
Fluoride (mg/l)	NR	NR	NR	NR	NR	NR	0.19-0.34	0.26-0.62
Hardness as CaCO ₃ (mg/l)	NR	NR	NR	NR	0.0-20.0	0.0-20.0	15.0-100.0	33-66
Iron (mg/l)	NR	NR	NR	NR	NR	NR	0.001-0.003	0.001-0.003
Lead (mg/l)	NR	NR	NR	NR	NR	NR	NR	NR
Magnesium (mg/l)	NR	NR	NR	NR	0.12	0.19	NR	NR
Manganese (mg/l)	NR	NR	NR	NR	0.0043	0.00	0.001-0.002	0.001-0.002
Mercury (mg/l)	NR	NR	NR	NR	NR	NR	UD	UD
Nickel (mg/l)	NR	NR	NR	NR	NR	NR	NR	NR
Nitrate (mg/l)	NR	NR	NR	NR	NR	NR	0.18-1.27	0.17-11.47
pH	NR	NR	NR	NR	7.80	8.40	7.5-7.6	7.7-9.6
Potassium (mg/l)	NR	NR	NR	NR	NR	NR	NR	NR
Selenium (mg/l)	NR	NR	NR	NR	NR	NR	NR	NR
Sodium (mg/l)	NR	NR	NR	NR	NR	NR	NR	NR
Sulphate (mg/l)	NR	NR	NR	NR	NR	NR	NR	NR
Suspended solids (mg/l)	NR	NR	NR	NR	NR	NR	NR	NR
Temperature (°C)	NR	NR	NR	NR	NR	NR	NR	NR
Total coliform (CFU/100 ml)	1100	1100	0.0	1100	NR	NR	2.3-238	0.52-238
Turbidity (NTU)	NR	NR	NR	NR	5.0	5.0	12-40	4.0-5.0
Zinc (mg/l)	NR	NR	NR	NR	0.556	0.045	UD	UD

NR: Not Reported; UD: Undetectable.

Table 2.4: Studies of rainwater quality by various researchers (contd...)

Parameters	Simmons <i>et al.</i> , (2001)	Researchers					WHO-DWS (1993)
		Zhu <i>et al.</i> , (2003)		Hu <i>et al.</i> , (2003)	Vazquez <i>et al.</i> , (2003)	Coombes <i>et al.</i> , (2003)	
		Roof & yard	Sloped land				
Aluminium (mg/l)	NR	0.093-0.336	0.377-1.256	NR	NR	NR	0.20
Ammonia (mg/l)	NR	NR	NR	0.19	NR	0.20-0.39	-
Arsenic (mg/l)	<0.005	UD	UD	NR	NR	NR	0.05
Barium (mg/l)	NR	0.0-0.0112	0.0-0.038	NR	NR	NR	-
Boron (mg/l)	NR	0.011-0.056	0.0-0.063	NR	NR	NR	-
Cadmium (mg/l)	NR	UD	UD	NR	NR	<0.002	0.005
Calcium (mg/l)	NR	11.2-31.15	12.56-16.68	0.16	0.85	2.0	-
Chlorides (mg/l)	NR	6.13-79.20	2.94-5.64	0.34	1.72	0.46-14.6	250
Chromium (mg/l)	NR	UD	0-0.004	NR	NR	NR	0.05
COD (mg/l)	NR	8.74-23.83	13.6-15.9	NR	NR	NR	-
Conductivity (µS/cm)	NR	NR	NR	NR	0.68	NR	-
Copper (mg/l)	0.06	0.0011-0.016	0-0.003	NR	NR	NR	1.0
Cyanide (mg/l)	NR	NR	NR	NR	NR	NR	0.10
Dissolved solids (mg/l)	NR	NR	NR	NR	NR	8.0-34.0	1000
Faecal coliform (CFU/100 ml)	2.0	300-1260	580-5120	NR	NR	0.00	0.0
Fluoride (mg/l)	NR	0.071-0.163	0.386-0.692	NR	NR	NR	1.5
Hardness as CaCO ₃ (mg/l)	NR	60.96-149.02	105.2-125.5	NR	NR	NR	500
Iron (mg/l)	NR	0.010-0.083	0.0-0.13	NR	NR	<0.01	0.10
Lead (mg/l)	<0.01	0.003-0.041	UD	NR	NR	<0.01-0.015	0.05
Magnesium (mg/l)	NR	0.930-1.143	0.0-3.77	0.06	0.44	NR	-
Manganese (mg/l)	NR	0.048-0.112	0.0-0.126	NR	NR	NR	0.10
Mercury (mg/l)	NR	UD	0.0-0.0021	NR	NR	NR	0.001
Nickel (mg/l)	NR	UD	0.003-0.013	NR	NR	NR	-
Nitrate (mg/l)	NR	NR	NR	0.22	0.25	0.1-0.2	10
pH	7.3	NR	NR	4.20	0.065	5.5-6.4	6.5-8.5
Potassium (mg/l)	NR	3.36-8.658	11.40-30.23	0.072	0.041	NR	-
Selenium (mg/l)	NR	0.004-0.009	UD	NR	NR	NR	0.01
Sodium (mg/l)	NR	3.02-11.20	3.77-12.56	0.33	1.46	9.9	200
Sulphate (mg/l)	NR	2.40-15.62	5.83-19.10	0.84	0.99	1.7-5.3	400
Suspended solids (mg/l)	NR	NR	NR	NR	NR	8.4	-
Temperature (°C)	NR	NR	NR	NR	27.0-28.50	NR	-
Total coliform (CFU/100 ml)	27	NR	NR	NR	NR	0.00	0.0
Turbidity (NTU)	0.56	2.0-3.5	3.0-6.5	NR	NR	NR	5.0
Zinc (mg/l)	0.40	NR	NR	NR	NR	NR	5.0

NR: Not Reported; UD: Undetectable.

The status of the composite precipitation samples collected in two consecutive years was assessed by Nyika (1996) in Bulawayo, Zimbabwe. The rainwater quality was assessed by analyzing various physical and chemical parameters. A typical single event precipitation sample on 10th January 1993 had pH 6.87 and conductivity 5.10 $\mu\text{S}/\text{cm}$. The overall quality of the atmospheric rainwater in Bulawayo, Zimbabwe is presented in Tables 2.4.

Ariyananda (1999) reviewed the quality of rainwater throughout Sri Lanka from different types of storage tanks and roofs. The review compared the traditional rainwater collecting methods with the present available technology of the Community Water Supply and Sanitation Project (CWSSP). The tank was constructed below ground and made of burnt brick & cement sand mortar. Total coliform and turbidity do not meet the WHO drinking water standards in both tanks particularly for open rectangular tank (Table 2.4).

In India, Agra city is known for one of the world's wonder monuments, Taj Mahal. There are various numbers of foundry and forging industries besides of large number of industries. The cupola, from foundry industry, emissions include CO, SO₂ and NO_x. The concentration of SO₂, NO_x and respirable dust were 47.1 $\mu\text{g}/\text{m}^3$, 60.2 $\mu\text{g}/\text{m}^3$ and 245 $\mu\text{g}/\text{m}^3$ respectively in the ambient air (PCRI, 1988). The high concentration of SO₂, NO_x and respirable dust are the main cause of concern for pollution in rainwater.

Rainwater samples directly collected from the atmosphere and through various roof catchments (aluminium, zinc, asbestos and thatch) in the Port Harcourt District, Rivers State, Nigeria, were analyzed and reported by Uba and Aghogho (2000). Results showed that the physico-chemical qualities of the rainwater, except for colour, were within the limits approved by the WHO. Asbestos and thatch materials caused an increase in colour of the rainwater. A near neutral pH (7.02-7.45) was obtained in all the samples. Higher levels of aluminium were obtained in the samples collected from the aluminium

roof while zinc was only detected in the rainwater collected from the zinc roof. Manganese and iron were present in all the samples. Microbiological analysis showed varying degrees of contamination in the different samples.

Rainwater samples from the roof catchments also contained high numbers of pathogenic bacteria, *Salmonella spp.*, *Shigella spp.* and *Vibrio spp.* Uba and Aghogho (2000) suggested that the microbiological analysis of all rainwater should be undertaken and appropriate treatment measures adopted before rainwater can be declared potable. Zinc appears to be a better material for rainwater collection than aluminium, asbestos and thatch.

Ariyananda (2001) reported the quality of collected rainwater in relation to household water security at Sri Lanka. Rainwater was collected and stored in cement tanks from a badly managed roof and after few days, it creates a bad smell in the collected rainwater due to anaerobic action or open tank breed mosquitoes making the water unacceptable for drinking. The rainwater collected meets the WHO drinking water standards for physico-chemical quality except in few tanks, the pH was little high due to cement dissolving. However bacteriological quality (faecal coliform) of rainwater does not meet the WHO drinking water standards except at Siyabaladuwa, where all the tanks are fitted with filters. The quality of rainwater collected from two locations is presented in Table 2.4.

Vasudevan *et al.*, (2001) tested samples regularly for bacteriological quality of the water immediately after the rain. These were examined both by H₂S strip test and most probable number (MPN) for faecal coliform (FC) and faecal *Streptococcus* (FS) and the results are presented in Table 2.4. H₂S strip developed by Manja (1982), is a rapid test available for field level applications, it is based on production of H₂S by sulphur producing bacteria such as *Clostridium perfringens*.

Bo and Guangen (2001) collected rainwater samples from storage tanks made of clay and reinforced concrete in Beijing, China and reported that the water quality may deteriorate through the putrefaction of organic materials in the water or through growth of bacteria and other micro-organisms. Turbidity, total coliform and total bacteria are much higher than WHO drinking water standards (Table 2.4).

Simmons *et al.*, (2001) performed a cross-sectional survey of domestic roof-collected rainwater supplies from four rural Auckland Districts, New Zealand. Samples of cold faucet water were analyzed for physico-chemical and microbiological determinants, including metals (lead, copper, zinc and arsenic), total coliform (TC) and faecal coliform (FC). results are given in Table 2.4. Twenty-two supplies (17.6%) exceeded one or more of the maximum guideline values for New Zealand drinking water standards (NZDWS) and 70 supplies (56.0%) exceeded the microbiological criteria of less than one FC/100ml. Eighteen supplies (14.4%) exceeded the NZDWS for lead of 0.01 mg/l and three (2.4%) exceeded for copper of 2.0 mg/l. This study demonstrates that roof-collected rainwater systems provide potable supplies of relatively poor physico-chemical and microbiological quality in the Auckland area, New Zealand.

Hu *et al.*, (2003) carried out a short-term study for one year of the chemical composition of rainwater at Singapore. The rainwater was typically acidic with a mean pH of 4.2. Sulfate was the most abundant ion and comparable to the results reported for other industrialized regions. The concentrations of major ions (NH_4^+ , Ca^{2+} , K^+ , Na^+ , Mg^{2+} , SO_4^{2-} , NO_3^- , Cl^- , HCOO^- , CH_3COO^-) varied monthly. Results presented in Table 2.4, show that local meteorological conditions influence the chemical compositions to a significant extent. Sulfate and nitrate account for the most of acidity and their relative contributions were about 80% and 20% respectively.

Vazquez *et al.*, (2003) presented the preliminary results on the ionic rainfall composition at different sampling locations in Galicia, NW Spain and the results are presented in Table 2.4. The differences were detected in chemical composition of collected rainwater depending on the location of sampling points, weather conditions and industrial, urban or agricultural activities. Rainwater samples collected in open areas at Figtree Place, Hamilton, Australia, were tested for two years and reported by Coombes *et al.*, (2003). The results are presented in Table 2.4. All values of the parameters are well within the WHO drinking water standards.

Contamination of rainwater by pesticides has also been investigated by Olav *et al.*, (1995), from three locations in Norway: Lista, Ås and Tromsø. The samples were analyzed for nine different pesticides including five herbicides MCPA, dichlorprop, atrazine, simazine and ioxynil, the fungicide propiconazole and the insecticides lindane, dimethoate and cypermethrin. The samples from Tromsø, however, showed no residues of pesticides. The highest concentrations measured for MCPA, dichlorprop, atrazine and lindane were 320 ng/l, 250 ng/l, 86 ng/l and 84 ng/l respectively. The level of pesticides stated in the EEC-directive 80/778 for the quality of water intended for human consumption is 100 ng/l. This level was exceeded twice for the herbicides MCPA and dichlorprop. On an average, total deposition of pesticides in 1992-1993 was 2.4 times higher at Ås than at Lista. Atrazine and lindane were often found in precipitation when the wind was blowing from the east.

van Maanen *et al.*, (2001) investigated the occurrence of high levels of pesticides in groundwater and rainwater in "The Province of Limburg in The Netherlands". A number of pesticides were found in high concentrations; e.g. atrazine (>200 ng/l). Two pesticides detected in rainwater (β + γ -HCH and atrazine) were found to exceed the groundwater standard of 100 ng/l.

Manabu (2003) has conducted studies on pesticides in rainwater at Isogo Ward of Yokohama, Japan and 51 kinds of pesticides were investigated. Although sampling point was not located in the agricultural area, dichlorvos (0.33-0.05 $\mu\text{g/l}$), chlorothalonil (0.27-0.05 $\mu\text{g/l}$), fenitrothion (0.24-0.05 $\mu\text{g/l}$), molinate (0.12-0.05 $\mu\text{g/l}$), diazinon (0.07-0.05 $\mu\text{g/l}$) and malathion (0.05 $\mu\text{g/l}$) were detected. Dichlorvos was the most frequently detected (65% of samples) and its highest concentration (0.33 $\mu\text{g/l}$) in rainwater was found. Chlorothalonil was the second most frequently detected (33% of samples) and its highest concentration (0.27 $\mu\text{g/l}$) in rainwater was observed.

Dubus *et al.*, (2000) has also investigated the presence of pesticides in rainfall in Europe where 28 pesticides were analyzed in rainwater between 1990 and 1997. Of these 28 pesticides, 23 have been actually detected in rainwater and larger concentrations up to a few thousand ng/l, were detected occasionally at most monitoring sites. The most frequently detected compounds were lindane (γ -HCH) and its isomer (α -HCH), which were detected on 90 to 100% of sampling occasions at most of the sites where they were monitored. Some of detected pesticides are presented in Table 2.5.

Saxena *et al.*, (1996) collected rainwater (wet-only) samples on the roof of the academic building about 8.0 m from ground level and 1.0 m from the floor of the roof, in the monsoon season of 1991 at Dayalbagh, India. The results are presented in Table 2.6. The highest correlations appear for the ion pair NO_3 and SO_4 ($r = 0.96$), followed by Na and NO_3 ($r = 0.83$), Ca and Cl ($r = 0.75$), Mg and SO_4 ($r = 0.73$); Cl and SO_4 ($r = 0.71$); Ca and Mg ($r = 0.70$) and Na and SO_4 ($r = 0.65$). The study reveals that rainwater is alkaline, its acidity being neutralized by soil components Ca, Mg, and Ammonia.

Satsangi *et al.*, (1998) mentioned the composition of rainwater at a semi-arid rural site, Gopalpura, India in the monsoon of 1996. There are no major cities or towns within a radial distance of 35 km from Gopalpura. The cations (Ca, Mg, Na, K and NH_4) and

anions (F, Cl, NO₃, SO₄, acetate and formate) along with pH and conductance were measured and presented in Table 2.7. Volume weighted mean pH of rainwater was 6.93. The percentage distribution of Ca, Mg, Na, K and NH₄ were observed to be higher.

Table 2.5: Concentration of pesticides in rainwater for various European sites, Europe

[Dubus *et al.*, (2000)]

Parameters	Minimum	25 th percentile	Median	75 th percentile	95 th percentile
Atrazine (ng/l)	10	83	135	408	5000
DDD (ng/l)	66	70.5	93	2651	3500
DDE (ng/l)	1	1.7	14.5	95.3	96
DDT (ng/l)	2	9.5	72	3044	6000
Diazinon (ng/l)	80	89.3	153	289	322
Hexachlorobenzene (ng/l)	1	1.5	4.5	183.5	350
Lindane (ng/l)	6	73	270	550	833
Parathion-ethyl (ng/l)	50	140	200	382	569
Simazine (ng/l)	40	66.5	140	435	8100
Carbaryl (ng/l)	-	-	110	-	-
Chlorothalonil (ng/l)	-	-	1100	-	-
Dichlobenil (ng/l)	-	-	3120	-	-
Parathion-methyl (ng/l)	-	-	3400	-	-
Propoxur (ng/l)	27	-	29	-	31
Vinclozolin (ng/l)	11	-	11	-	16

The dashed line separates compounds that were reported on ≥ 4 sites (enabling calculation of distribution characteristics) from compounds that were reported on < 4 sites.

Table 2.6: Correlation matrix for rainwater ion pairs at Agra city, India

[Saxena *et al.*, (1996)]

Parameters	Cl	NO ₃	SO ₄	HCO ₃	H	Na	K	Ca	Mg	NH ₄	F
Cl	1.00										
NO ₃	0.55*	1.00									
SO ₄	0.71*	0.96*	1.00								
HCO ₃	0.27	0.40	0.40	1.00							
H	0.21	0.24	0.20	-0.11	1.00						
Na	0.46	0.83*	0.65*	0.41	0.35	1.00					
K	0.13	0.24	0.23	0.09	0.08	0.50*	1.00				
Ca	0.75*	0.57*	0.71*	0.43	0.16	0.67*	0.19	1.00			
Mg	0.58*	0.71*	0.73*	0.22	0.08	0.42*	0.29	0.70*	1.00		
NH ₄	-0.01	0.59*	0.43	0.51	0.13	0.66*	0.29	0.08	0.30	1.00	
F	0.0007	0.23	0.08	0.06	-0.10	0.01	-0.14	0.06	-0.01	-0.20	1.00

Note. tailed signal: +p = 0.01; *p = 0.001

Table 2.7: Correlation coefficient of parameters in rainwater at Gopalpura city, India

[Satsangi *et al.*, (1998)]

Parameters	HCO ₃	F	Cl	NO ₃	SO ₄	NH ₄	Ca	Mg	Na	K	HCOOH	CH ₃ COOH
HCO ₃	1.00											
F	0.67*	1.00										
Cl	0.53*	0.61*	1.00									
NO ₃	0.60*	0.59*	0.71*	1.00								
SO ₄	0.56*	0.50*	0.66*	0.78*	1.00							
NH ₄	0.71*	0.66*	0.54*	0.56*	0.33	1.00						
Ca	0.64*	0.39	0.45*	0.52*	0.65*	0.60*	1.00					
Mg	0.76*	0.62*	0.57*	0.62*	0.66*	0.64*	0.89*	1.00				
Na	0.61*	0.67*	0.67*	0.64*	0.51*	0.57*	0.63*	0.76*	1.00			
K	0.64*	0.61*	0.55*	0.52*	0.53*	0.58*	0.61*	0.73*	0.67*	1.00		
HCOOH	0.20	0.37	0.01	0.12	-0.14	0.21	-0.01	0.07	0.08	-0.23	1.00	
CH ₃ COOH	0.14	0.25	0.11	0.03	0.11	0.11	0.09	0.19	0.12	0.02	0.64*	1.00

Note. tailed signal: +p = 0.01; *p = 0.001

2.6 TREATMENT OF RAINWATER

The review of literature reveals that the rainwater is not free from contaminants and it is polluted because of surface of collection of rainwater. Since rainwater is used for drinking purpose and domestic use, it should be properly treated before the storage and use. Treatment of harvested rainwater is practically non-existent, and at the best, first flush diversion systems have been attempted. Even simple unit processes like filtration and disinfection are found only in isolation (Appan, 1995). The water quality in cisterns will be affected by a number of factors like quantity of rainfall, roofing material, type and condition of gutters, type and location of storage containers, method of collection and usage and host of other reasons.

The intake of contaminating components occurs while rainwater droplets are in the air (mainly organic and inorganic compounds, heavy metals). Contact with the catchment surface, heavy metals, microbiological contamination, organic and inorganic compounds, add yet more pollutants, originating from industry, transport and agriculture, or is naturally present. There are a wide variety of systems available for treating water before, during and after storage. The level of sophistication also varies, from extremely high-tech to very rudimentary.

2.6.1 Types of Treatment

Treatment of stored rainwater only makes sense if it is done properly and if hygienic collection and use of the water will ensure that it does not suffer from re-contamination. There are several types of treatment possible the most common being: chlorination, boiling, filtration and exposure to ultra-violet or natural sunlight.

Boiling water thoroughly for at least one minute normally ensures that it is free from harmful bacteria and pathogens (WHO, 1993). Since it is not practical to treat water

regularly in this way, it is again only usually appropriate as an emergency measure.

A solar powered ultraviolet unit is able to process 1.5 litres of water per minute developed by Joklik (1995) was evaluated on rainwater cistern water in Hawaii, USA and found to be 99.9% effective in removing indicator bacteria (Fujioka *et al.*, 1995). Effective ultra-violet sterilization may be too expensive for widespread use.

Chlorination is most appropriately used to treat rainwater if contamination is suspected due to the rainwater being coloured or smelling bad. It should only be done if the rainwater is the sole source of supply and the tank should first be thoroughly inspected to try to ascertain the cause of any contamination (Cunliffe, 1998). Direct sunlight can also be used to kill many of the harmful bacteria in water by exposing it in clear glass or plastic bottles for several hours (Wegelin and Sommer, 1998).

2.6.2 Types of Filtration System

Filtration can be used both to prevent material from entering the storage tank, during extraction of water from the tank or prior to consumption. Potentially, properly maintained filters will improve the water quality (Morgan, 1990).

2.6.2.1 Sand-charcoal-stone

The sand-charcoal-stone filter is often used for filtering rainwater entering a tank. This type of filter is only suitable, however, where the inflow is slow, and will soon overflow if the inflow exceeds the rate at which the water can percolate through the sand.

2.6.2.2 Reverse osmosis water purifier

Several types of filtration methods have been used worldwide, one of which is the **Portable Reverse Osmosis Water Purifier**. It involves a process whereby aqueous solution,

under pressure, is passed through an appropriate membrane and withdrawing the membrane permeates at atmospheric pressure and temperature, in this case water was used as the solution (Kahdim *et al.*, 2003). This device is able to produce 7.0 lit/hr. from any type of water. The problem of this system is that it will not be able to function properly if its reverse osmosis membrane is fouled due to the organic, biological and colloidal matter in the feed water (Isaias, 2001). The reverse osmosis system would thus require a filter membrane to aid in the removal of suspended particles before the water can go through to be purified, by the reverse osmosis process. This system would also experience problems due to the start-stop cycles and partial load operations during periods of oscillating power supply (Tzen and Morris, 2003). The system is expensive which might prove to be a stumbling block.

2.6.2.3 UV-charcoal system

Another type of filtration system used is the UV-protected granulated activated charcoal bed method, which uses charcoal and UV lights to sterilize the water. Serpien *et al.*, (2000) states charcoal attracts the bacteria onto its surface while the UV light kills the bacteria. The UV light also extends the life span of the charcoal. Unlike other disinfectants, UV light does not leave any byproducts, which reduces the number of processes need to finally clean the water. This method is relatively inexpensive and suitable for the treatment of rainwater but the process is not suitable for bulk volume of liquid treatment. Hence, the suitability of UV-charcoal systems in rainwater harvesting is suspicious. However, sunlight should be considered as the source of UV light as sunlight is more cost effective.

2.6.2.4 Solar disinfection

Solar disinfection (SODIS) is another relatively cheap method (Wegelin and Sommer, 1998). This technology uses UV radiation to kill microorganisms in the water collected in either fully transparent or half-black containers. Studies carried out in two villages in Thailand show significant decrease in gastrointestinal disorder cases. Another test in November 2002 in Nepal showed that in high altitude areas, half black containers serve better in removing microorganisms than fully transparent ones. This method is relatively cheap, but will only remove the microorganisms from the water. Additional steps have to be taken to remove the impurities in the water.

2.6.2.5 Electrochemical activation

In this method, electrical means instead of light is used for purification. When current is passed into the system, all organic and biological substances in the water are oxidized thus decontaminating the water. Besides purifying the water, this system is able to produce chemicals like hydrogen peroxide, a powerful oxidizing agent capable of preventing bacterial growth in the water during storage (Grimm *et al.*, 1998). Water purification by electrical means is expensive and furthermore the quality of the filtrate is not satisfactory.

2.6.2.6 Coarse leaf filter

The coarse leaf filter can be installed anywhere from the gutter to the entrance to the tank. It need not be especially fine (a 5mm grid is sufficient) and so no problems should be encountered with flow rate through the filter and the filter itself can be removable for cleaning (Martinson and Thomas, 2003).

2.6.2.7 Fine filters

Most of the fine filters used in developing countries are based on sand or gravel. These filters can be used for rooftop rainwater harvesting systems, however there can be problems with upkeep as householders often dispose of the filter media when it blocks, replacing it with coarser media or nothing at all (Ranatunga, 1999). In developed countries, self-cleaning filters are available with a fine mesh screen (typically 0.4mm). These screens use the first flow of water from a storm to flush the filter of debris or have a continual washing action using about 10% of the water (Martinson and Thomas, 2003).

2.7 OBJECTIVES OF FILTER USE

Rott and Mayer (2001) examined a number of filter designs available in Germany and reported the results according to hydraulic efficiency and efficiency in material removal. In recent years, more and more countries such as Thailand, Nepal, Philippines, Germany and Japan are beginning to carry out rainwater harvesting for different uses such as domestic and industrial usage. Different collection systems, filtration system and storage systems have been used in the different processes (UNEP, 2002). Several countries have started to collect rainwater for different uses. Japan, who had adopted a rainwater collection system called the "ROJISON" to collect rainwater for non-potable usages. In Berlin, Germany, a project was undertaken in October 1998 to collect rainwater at 19 large buildings, also for non-potable usage (UNEP, 2002).

Since 1989, Philippines have started rainwater harvesting with the assistance of Canadian International Development Research Centre (UNEP, 2002). Now a day, almost every country is emphasizing on rainwater harvesting but detailed guidelines and design criteria for treatment of the rainwater are not available. The objective is to treat rainwater for safe use in domestic purpose or in drinking purpose. The study reveals that the sand

filter system is more effective for rainwater treatment. After reviewing the above filtration systems, it is clear that the appropriate methods of treatment of rainwater in doubtful.

2.7.1 Filter Orientation

As the rainwater must pass from the roof to the tank inlet, the conveyance is a prime location for placing a filter to block any contamination from entering the tank. The vast majority of contaminants will be stuck to debris from the roof so removing the debris will also remove the contaminant. Removing debris also reduces the level of nutrient reaching the tank and thereby impedes mosquito larvae development and long-term survival of bacteria. Hence, the placement of the filters in rainwater harvesting is also important to remove the pollutants. Table 2.8 shows the pros and cons of various positions on the conveyance path (Martinson and Thomas, 2003).

Table 2.8: Pros and cons of various filter positions on the conveyance path

(Martinson and Thomas, 2003)

Type	Pros	Cons
In gutter	<ul style="list-style-type: none"> • Prevents leaf build-up in gutter thus <ul style="list-style-type: none"> ◦ removes fire hazard ◦ reduces mosquito breeding ◦ avoids cleaning chore 	<ul style="list-style-type: none"> • Can be expensive due to large areas to be covered • Poor installation can <ul style="list-style-type: none"> ◦ increase leaf build-up due to leaves catching on filter ◦ make cleaning what isn't filtered more difficult
At down pipe	<ul style="list-style-type: none"> • Central location minimizes filter area • Can be combined with a drop to increase efficiency • Can replace down pipe connection as gutter box • Can be self cleaning (to an extent) 	<ul style="list-style-type: none"> • Difficult to clean due to height • If simply placed into gutter-level down pipe connection can block entire gutter
In down pipe	<ul style="list-style-type: none"> • Increase in filter area due to length of down pipe available • Low space use • Wetting requirement means first flush is dumped 	<ul style="list-style-type: none"> • Uses more than 10% of water for self cleaning action • Requires more complex design • Poor design can lead to excessive water loss • Difficult to access for cleaning • Blockages not obvious
In-line (underground)	<ul style="list-style-type: none"> • Removes mounting problems • Easily accessed for cleaning 	<ul style="list-style-type: none"> • Only useful for underground tanks • Poor design can lead to ingress of storm water into the tank
At tank entrance	<ul style="list-style-type: none"> • Simple and inexpensive installation • Can be as simple as a cloth over the tank inlet • Very visible 	<ul style="list-style-type: none"> • Entrance to tank is available to accidental (or deliberate) contamination • Reduces possibility of any further filtration

2.8 TECHNICAL EVALUATION OF RAINWATER HARVESTING SAND FILTERS

Various types of sand filter, such as single media, dual media and multi media, are in practices for rainwater harvesting in India. Wherever it is installed, the technical specification for filter has not been followed. Infact, no design details are available for designing sand filters. Hence, technical evaluation of installed sand filters for rainwater harvesting at various locations in India is needed. The filter is used to remove suspended pollutants from rainwater collected from rooftop. A filter unit is a chamber filled with filtering media such as fibre, gravel and coarse sand layers to remove debris and dirt from water before it enters the storage tank. Charcoal can be added for additional filtration. A typical design of multi layer sand filter with one of charcoal layer, which has been used in the field for rainwater harvesting, is shown in Plate 2.1 (RWH manual, 2003).

Sand filters have been made with commonly available sand as filtering material. Sand filters are easy and inexpensive to construct. These filters can be employed for effective removal of turbidity, colour and microorganisms from bulk liquid. In a simple sand filter that can be constructed domestically, the top layer comprises coarse sand followed by a 5-10 cm layer of gravel followed by another 5-25 cm layer of gravel and boulders. Typical design of sand filter used for domestic purpose is shown in Plate 2.2 (RWH manual, 2003).

A typical horizontal sand filter designed by Rao (1999), called Dewas filter has been used for rainwater harvesting for recharge of ground water through service tube well in Dewas District, India and shown in Plate 2.3. Khare (2001) also developed new horizontal sand filters for rooftop rainwater harvesting. The installation of filter with rooftop is shown in Plates 2.4. Both filters (Plates 2.3 & 2.4) were made of HDPE pipe and various grading of sand was used as filtering media.

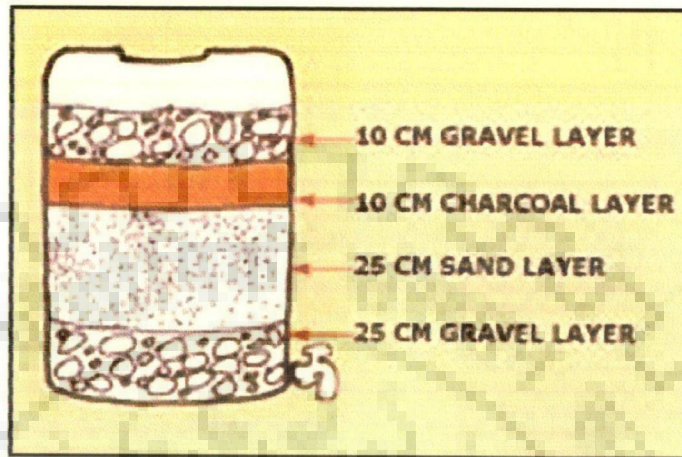


Plate 2.1: Dual media rainwater harvesting filter system (RWH manual, 2003)

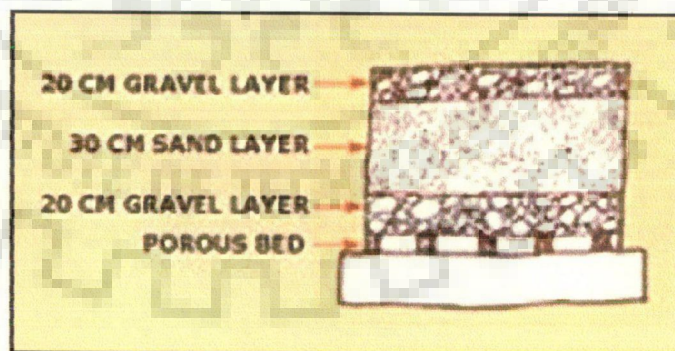


Plate 2.2: Typical design of sand filter used for rainwater (RWH manual, 2003)

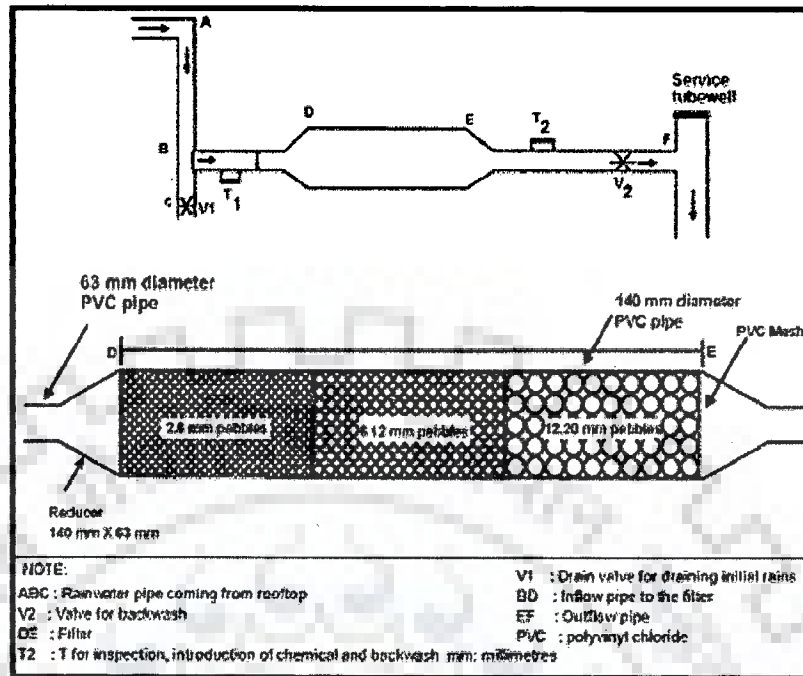


Plate 2.3: Schematic of Dewas filter for rainwater harvesting (Rao, 1999)

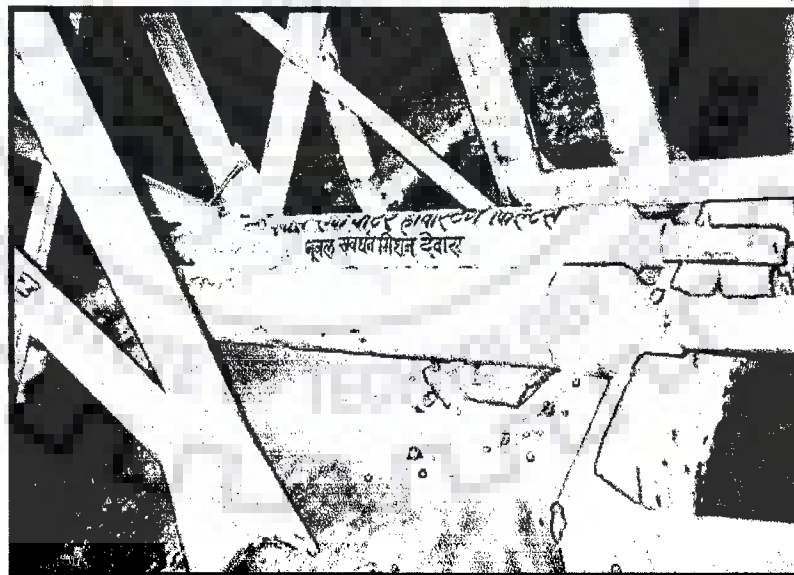


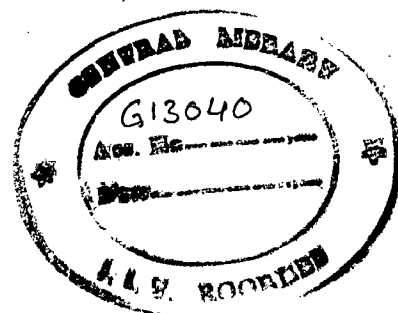
Plate 2.4: Horizontal sand filter called Dewas filter, Indore, India (Khare, 2001)

When rainwater is harvested in a large rooftop area, the filtering system should accommodate the excess flow. A filter system is designed by Jeyakumar (2001) for Chennai Metro City, India, with three concentric circular chambers in which the outer chamber is filled with sand, the middle one with coarse aggregate and the inner-most layer with pebbles, as shown in Plate 2.5. Rainwater reaches the centre core and is collected in the sump where it is treated with few tablets of chlorine.

Another sand filter called Varun, designed by Vishwanath (2001) for Bangalore city, India. It is made of 90 litre High Density Poly Ethylene (HDPE) drum, as shown in Plate 2.6. The lid is turned over and holes are punched in it. This is the first sieve which keeps out large leaves, twigs etc. Rainwater coming out of the lid sieve then passes through three layers of sponge and a 150 mm thick layer of coarse sand. Presence of sponge in the filter makes the cleaning process very easy but there may be a chance of frequent clogging.

AcquaSure, a consortium of three specialist Netherlands-based companies, has developed a system for the conversion of rainwater to drinking water in the form of a Rainwater Purification Centre (RainPC), as shown in Plate 2.7 (Website). Xenotex-A and activated carbon cartridges along with ultra membrane filtration or micro-membrane filtration modules incorporated in the RainPC has the capacity to deal with *E-coli* and the potential of meeting World Health Organizations (WHO) water regulation standards.

Mud-pot filtration system has been used in South-Asia countries for drinking purpose (Plate 2.8). This filtration consists of a three layer system requiring no electrical power. This kind of filtration is cheap and produce relatively clean water, the collection rate is slow and the substances used in the filtration needs to be changed frequently. As such, it can be seen that it is quite troublesome to maintain the setup, and that it may take too long for the water to be filtered for use (Kiran *et al.*, 2004)



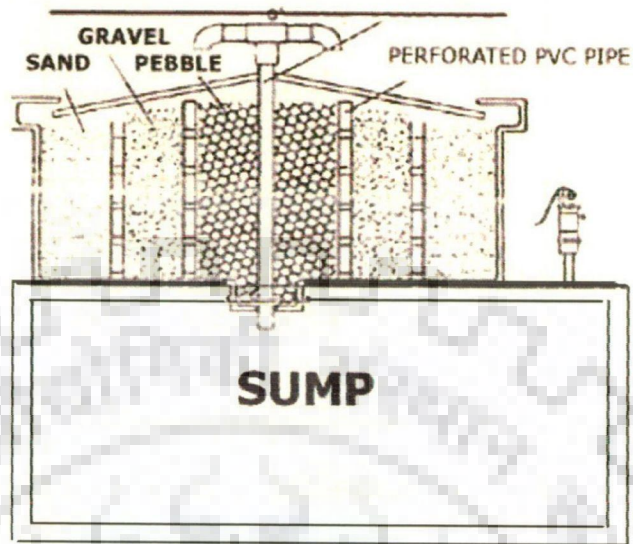


Plate 2.5: Multi layers sand filter for rainwater harvesting (Jeyakumar, 2001)

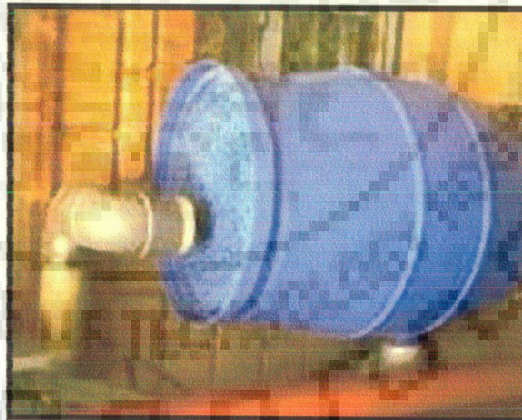


Plate 2.6: HDPE drum sand filter for rainwater harvesting (Vishwanath, 2001)

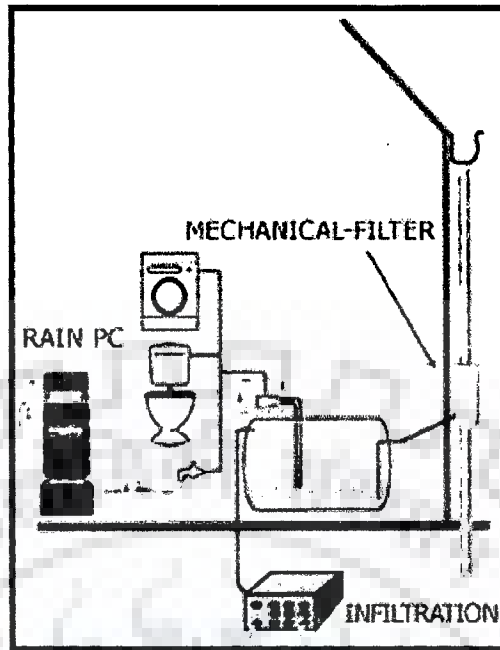


Plate 2.7: RainPC filter system using for rainwater harvesting
 (Source: <http://www.rainwaterharvesting.org>)

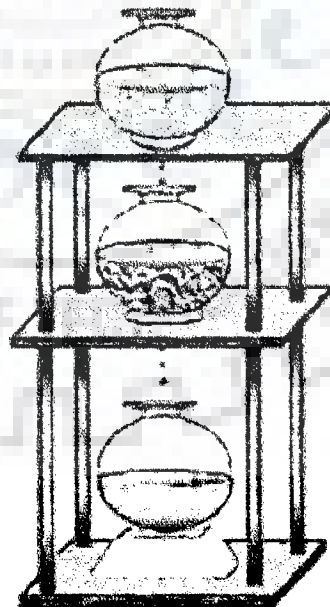


Plate 2.8: Mud pot filtration system used for drinking purpose (Kiran *et al.*, 2004)

During the field visit of Khandwa district, India, it was observed that the two types of filter fitted with residential and commercial buildings, one is vertically downward flow filter (as shown in Plate 2.9) and another is horizontal flow filter (as shown in Plate 2.10). A simple 6-inch diameter HDPE pipe has been used as filter system for rooftop rainwater harvesting. The another type of horizontal flow multi-media filter has also been used for recharging of ground water using rooftop rainwater and shown in Plate 2.11 (Anonymous, 2002). These filters were normally working in rainy season but for other seasons, it is not mentioned about their maintenance and there was no information available for selection of filter properties.

In the rainy season, surface run-off was also collected by the people of Khandwa region, India for recharging of ground water at various locations. The schematic of the tube well prepared for collection of surface run-off is shown in Plates 2.12 (Anonymous, 2002) and the construction structure of the tube well used for ground water recharge is shown in Plate 2.13 (field visit). Rainwater harvesting at various locations in New Delhi, the capital of India, is a normal practice. Most of the rainwater harvesting practices has been used for ground water recharge. Plate 2:14 shows a critical example of rainwater harvesting filter system attached with rooftop at Indian Institute of Technology Delhi, New Delhi, India (field visit). This is vertically downward flow sand filter which is not yet in operation because of poor maintenance.



Plate 2.9: Vertically downward flow sand filter used for rooftop rainwater harvesting at Khandwa, India (Field visit)

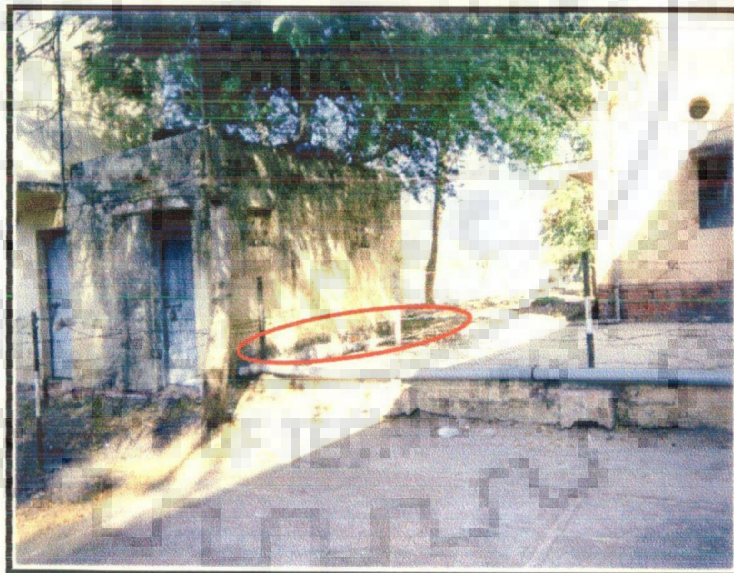


Plate 2.10: Horizontal flow sand filter used for rooftop rainwater harvesting at Khandwa, India (Field visit)

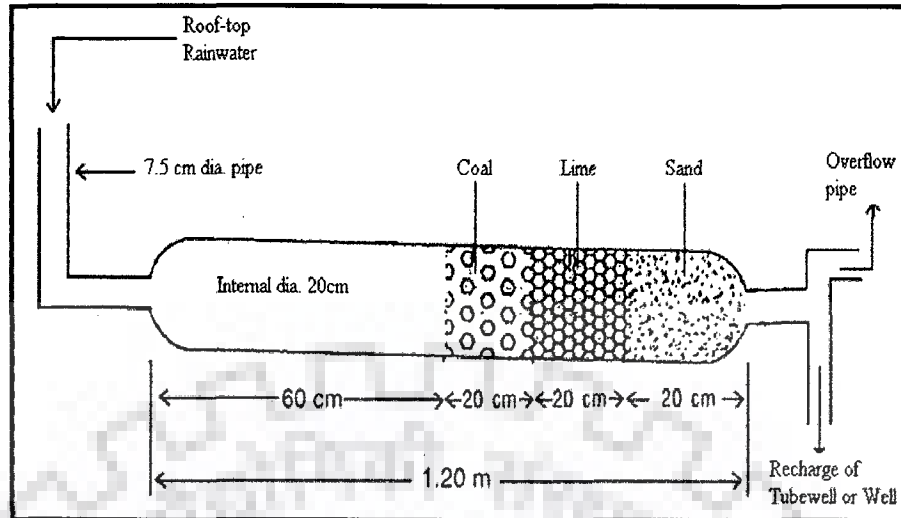


Plate 2.11: Schematic of horizontal flow multi-media filter for rainwater harvesting at Khandwa, India. (Anonymous, 2002)

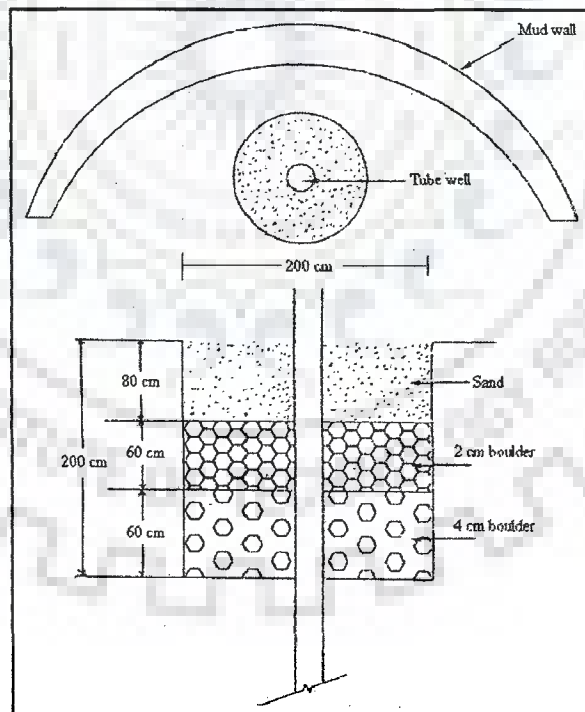


Plate 2.12: Schematic of tube well for surface runoff collection at Khandwa, India (Anonymous, 2002)



2.9 ASSESSMENT OF SAND FILTERS

The type of sand filters for rainwater harvesting discussed above reveal that there is no technical specification available for designing of sand filters. If the water is to be used for drinking purposes, filtration and chlorination or disinfection by other means (e.g., boiling) is necessary. Filtration is a process for separating solids, as suspended and colloidal impurities from water by passing it through a porous media. Filtration mechanisms are affected by such physical characteristics as size of the filter grain, characteristics of filter media, filtration rate, fluid temperature and the density and size of the suspended particles. The points which should be considered for design of above mentioned sand filters are summarized in Table 2.9.

Sand filter for rainwater harvesting should be designed in such a way that the total amount of rainwater entering to filter should pass within a stipulated time period. The discharge through a filter may be calculated by using Darcy's equation (Punmia, 1991)

$$Q = k.i.A \quad (2.3)$$

where, Q is discharge per unit time (cm^3/s), k is Darcy's coefficient [1×10^{-2} – 5×10^{-2} cm/sec for sand (mixture)], i is the hydraulic gradient and A is cross sectional area (cm^2) of the filter perpendicular to the direction of flow.

If the depth of sand media is L and cross section area of the filter is A and it is subjected to differential head of water, Δh , then the discharge will be

$$Q = k \cdot \frac{\Delta h}{L} \cdot A \quad (2.4)$$

Textural classification of sand, cross sectional area of the filters, amount of rainwater filtered in a specific time, clogging of sand filter media, removal efficiency of turbidity and coliform and effect of grain size of filtrate quality should be defined for all the above mentioned sand filters.

Table 2.9: Missing design parameters for rainwater harvesting sand filters

Plate No.	Missing design parameters	Remarks
2.1 & 2.2	Cross sectional area of filter, head loss during filter run, rate of filtration, time of full clogging, effective size and uniformity coefficient of sand and gravel, sand treatment before use in filter	Filtration rate and filtrate quality not mentioned, clogging of filter bed and charcoal layer not defined, application of the filter in high rain is suspicious
2.3 & 2.4	Head loss during filter run, rate of filtration, suitability for large family or community, uniformity coefficient of pebbles, variation in rainwater quality with turbidity and coliform, time of clogging, sediment build in the filter, available void space	Chances of negative pressure, passing of small suspended particles, unpredicted filtrate quality, gravity or pressure flow of water, rate control pattern unknown, developed for ground water recharge not for domestic purpose
2.5	Vertical depth and horizontal length of sand media, chances of flush out of sand to other media, media particle size diameter, clogging of media as well as perforated PVC pipe, rate of filtration, coverage of roof area during full rain, space required	Rainwater and filtrate quality undefined, proper treatment required for sump water before use
2.6	Sponge layer prevent high rate of filtration, textural classification of sand media, particle size analysis	Not suitable for large roof area in high rain, filtrate quality suspected
2.7	Clogging rate of filter, head loss, suitability in high rainfall, space required	Installation and maintenance costly, filtrate quality good
2.8	Suspended particle size and its removal, inflow rate, clogging of the filters, turbidity analysis	Only large debris can remove, frequently clogging occurs, not suitable for high filtration rate, filter media size not defined
2.9, 2.10 & 2.11	Sand media size, clogging pattern, filtration rate, removal efficiency, head loss, rainfall frequency & intensity, influent turbidity concentration in rainwater	Economical, filtrate quality not reported, developed for ground water recharge, no installation guidelines available
2.12 & 2.13	Effective size of the filter grain, depth of filter media, filtration rate, filtrate quality, clogging of filter media	Arbitrary selection of filter grain, filtrate quality not reported, effective size not defined for single media, rainfall frequency & intensity not considered
2.14	Filtration rate, overflow design, clogging rate, pollution removal efficiency	Not in operation because of ill-maintenance

The selection criteria of sand filters, based on location and orientation, should also be defined for all existing filters. Some more existing sand filters are suitable for removal of pollution load on rainwater before use but are uneconomical. Hence, the above mentioned sand filters are not technically and economically suitable for rainwater harvesting for domestic purposes. Most of the filters, which have been used for rainwater harvesting in the field, lack details of cross sectional area, head loss and rate of filtration during its run time and many more parameters. The rate of filtration, based on amount of rainfall and catchment area of rainwater harvesting, can be calculated using Eqs. (2.3) & (2.4) but the required parameters should be available. Hence, the lack of design parameters makes it extremely difficult to explain the performance of the existing sand filters for rainwater harvesting.

2.9.1 Suitability of Sand Filters in Field Conditions

Review indicates that the filters installed in the field are not designed according to the technical guidelines. Orientation of filters has much more impact on the performance of sand filters. This is a factor, which depends on the availability of space in the field for rainwater harvesting. Hence, the suitability of the sand filter should be considered based on the turbidity removal during high rainfall hour and catchment area of rainwater harvesting.

2.10 CONCLUDING REMARKS

Most of the information on rainwater quality appears to be carried out on an ad-hoc basis. Consequently, the technical information on design of sand filter for rainwater harvesting is scanty. Various sand filters, as treatment option, have been installed and used for rainwater harvesting all over the India but the reliability of their design and pollutants

removal efficiencies are not yet studied. The design of sand filters should be based on the degree of pollution in rainwater, frequency and intensity of rainwater, availability of filter media, etc. Non availability of technical guidelines for design of sand filters for rainwater harvesting leads to questions about its performance in terms of pollution removals such as coliform and turbidity. No details have been provided regarding the maintenance of all the sand filters installed in the field for rainwater harvesting.

A systematic study should be undertaken considering rainfall pattern, types of roofing materials, rainwater and rooftop rainwater qualities, guttering systems, materials used for storage tanks, maintenance practices, sequence and frequency of collection of rainwater, testing schedules and any other salient features specific to the country or region. Rate of filtration based on amount of rainfall for a defined harvesting area, sand particle size analysis, textural classification such as uniformity coefficient and effective size, depth of sand filter media, clogging period and behaviour of filter with respect to pollution level should be considered while designing and installation of sand filters for rainwater harvesting.

EXPERIMENTAL PROGRAM

3.1 PREAMBLE

Rainwater is contaminated with various pollutants and only turbidity has been considered in this study as pollution indicator parameter to know the performance of the sand filters. Rainwater is required to remove the turbidity and bacteria associated with suspended solids using sand filter. Hence, an extensive experimental work for the present study was planned and carried out with various sand filter modules installed in the laboratory of Department of Water Resources Development and Management, Indian Institute of Technology Roorkee (I.I.T. Roorkee), Roorkee, India to collect the data on turbidity removal and flow resistance. The filtration experiments were first started with rainwater and the same sand filter modules were again operated at various influent turbidity concentrations to know their performance at different filtering conditions. The influent concentrations were prepared by mixing fixed amount of Fuller's earth (China clay) suspension in tap water.

A total of 110 experimental runs were operated under both the cases of Fuller's earth suspension water solution and rainwater samples. Out of them, 64 runs (nos. 1 to 64) were operated at uniform sand grains, 02 runs (nos. 105 to 106) at graded sand of vertically downward flow filters and 10 runs (nos. 90 to 99) at uniform sand grains of horizontal flow filter using Fuller's earth suspension water solution samples. Out of remaining 34 runs, 25 runs (nos. 65 to 89) were operated at uniform sand grains, 04 runs (nos. 107 to 110) at graded sand of vertically downward flow filters and 05 runs (nos. 100

to 104) at uniform sand grains of horizontal flow filters using rainwater samples. The uniform sand grains filters were operated for 36 hours for each and every set of observation assuming that there is no continuous rainfall beyond this time limit and graded sand filters were operated for 120 hours to check the performance of the filters at different time intervals.

3.2 EXPERIMENTAL SET-UP

Experiments were started in the laboratory with four sand filter modules of different shapes and sizes. Out of these four modules, three were made of high density polyethylene (HDPE) pipe, circular in cross section and one was made of perspex sheet, square in cross section to know the variability of the performance of the filters. These modules were connected with an overhead tank of Indian Standard Organization (ISO) certified having capacity of 500 litres. The tank was connected with rooftop of the Institute's laboratory building through HDPE pipe of sufficient diameter to convey the rooftop rainwater. The rainwater collected from rooftop was stored in plastic tank which was provided with facility to discard first flush in the first rain of the season. The tank was also connected with various sand filter modules through galvanized iron pipe of sufficient diameter to get the desired flow velocities. Plate 3.1 shows overhead HDPE tank with stirring facility. This tank was used to store the rainwater and Fuller's earth suspension water solution samples. Plate 3.2 shows various sand filter modules installed in the laboratory at I.I.T. Roorkee, Roorkee, India for the experimentation.



Plate 3.1: Overhead HDPE tank attached with stirring facility
at I.I.T. Roorkee, Roorkee, India

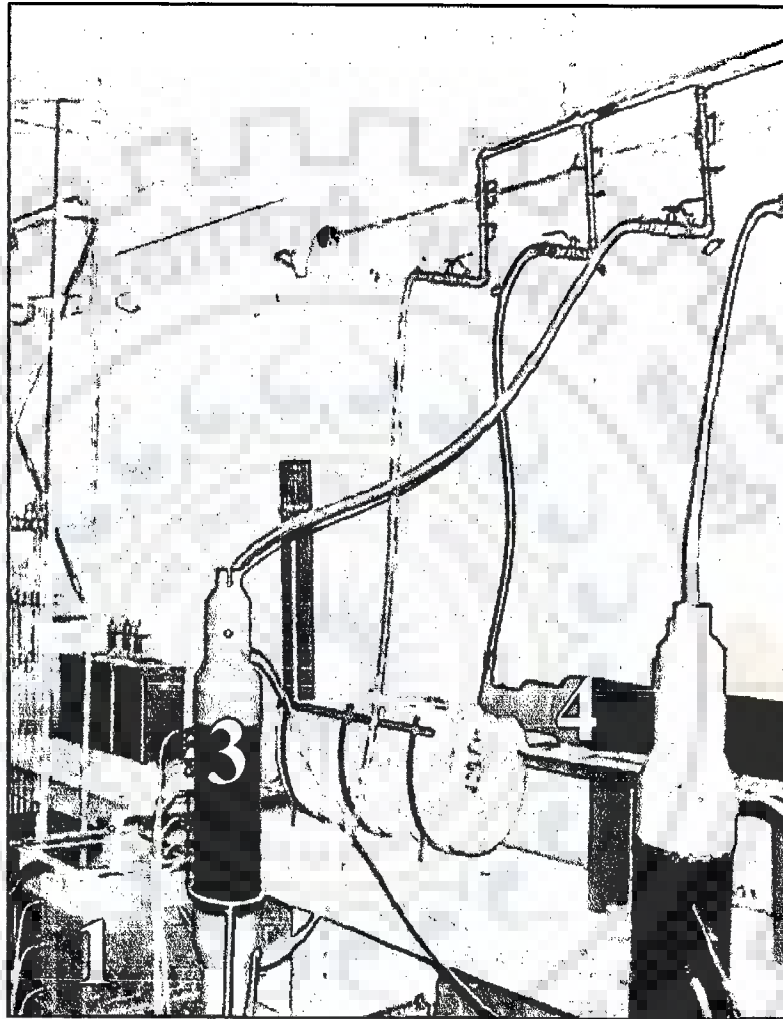


Plate 3.2: Pictorial view of sand filter modules in the laboratory at I.I.T. Roorkee, Roorkee, India.

The experiments were run in two different cases, one with natural rooftop rainwater and another with Fuller's earth (China clay) suspension water solution. Stirrer was used in the case of Fuller's earth suspension water solution to stir the liquid so that there should not be settlement of Fuller's earth at the bottom of the overhead tank. Out of these four sand filter modules (nos. 1, 2, 3 & 4), three filters (nos. 1, 2 & 3) were fed vertically downward flow and one filter (no. 4) was fed horizontal flow. The three sand filter modules (nos. 2, 3 & 4) were having same cross sectional area. A circular perforated perspex sheet was placed at the top and bottom of each circular filter to prevent the dispersion of topmost sand layer particles and flushing out the filter media in the outlet. The diameter of the circular perspex sheet was same as diameter of sand filter modules. In the graded sand filter, each layer of different sand grading was separated out by thin plastic mat which could protect the intermixing of the layers.

The top most portion of the three vertically downward flow filters (nos. 1, 2 & 3) were kept open at atmospheric pressure during experimentation and it was closed for the horizontal flow filter (no. 4). Effluent port of the filters was conical in shape which was attached with outlet pipe. Sand was thoroughly washed with tap water to make it clean from dirt and suspended particles and made it dried before use in the filter. Selection of filtration rate, filter media grain size, sizes of filters and filter run time were kept constant at each and every set of observation in both the cases of filtration systems. Details of experimental studies for sand filters are presented in Table 3.1. Details of experimental runs for different filtering conditions are presented in Table 3.2.

Table 3.1: Details of experimental studies for sand filters in the laboratory

Filter no.	Filter (%S area (m ²))	Total filter runs	Effective depth (mm)	Filter media grain size (mm)	Experimentation with	Influent turbidity (mg/l)	Filter run (Hrs.)	Filtration rate (m ³ /hr/m ²)	Mode of operation
2	0.0182	15	500	3.647	Rainwater	17	36	1.65, 3.30, 4.95, 6.60 and 8.25	Vertically downward flow
			500	2.366					
3	0.0182	30	360	1.673	Fuller's earth	25 and 30	36	1.65, 3.30, 4.95, 6.60 and 8.25	- do -
2	0.0182	30	500	2.366					
2	0.0182	10	360	1.673	Rainwater	17	36	1.65, 3.30, 4.95, 6.60 and 8.25	- do -
3	0.0182	10	500	1.091					
2	0.0182	30	500	1.091	Fuller's earth	25, 30 and 40	36	1.65, 3.30, 4.95, 6.60 and 8.25	- do -
3	0.0182	30	360	0.714					
3	0.0182	4	360	0.505	Fuller's earth	25 and 30	36	1.65 and 3.30	- do -
4	0.0182	5	600	0.714	Rainwater	17	36	1.65, 3.30, 4.95, 6.60 and 8.25	Horizontal flow
4	0.0182	10	600	0.714	Fuller's earth	30 and 40	36	1.65, 3.30, 4.95, 6.60 and 8.25	- do -
2	0.0182	2	500	2.366 and 3.647 (250 mm each)	Rainwater	17	36	1.65	Vertically downward flow
				1.091 and 2.366 (250 mm each)					
1	0.145	2	500	1.673, 3.647, 4.899, 8.485 and 17.888 (100 mm each)	Rainwater	17	120	0.21 and 0.41	- do -
				1.673, 3.647, 4.899, 8.485 and 17.888 (100 mm each)					
1	0.145	2	500	1.673, 3.647, 4.899, 8.485 and 17.888 (100 mm each)	Fuller's earth	25	120	0.21 and 0.41	- do -

Total 110 experimental runs (76 runs with Fuller's earth suspension water solution samples and 34 runs with rainwater samples).

Table 3.2: Details of experimental runs conducted in the laboratory

Influent turbidity (mg/l)	Samples	Mode of operation	Mean grain size (mm)	Filtration velocity (m ³ /hr/m ²)	Filter run no.
25	Fuller's earth solution	Vertically downward flow	3.647	1.65	1
				3.30	2
				4.95	3
				6.60	4
				8.25	5
			2.366	1.65	6
				3.30	7
				4.95	8
				6.60	9
				8.25	10
			1.673	1.65	11
				3.30	12
				4.95	13
				6.60	14
				8.25	15
			1.091	1.65	16
				3.30	17
				4.95	18
				6.60	19
				8.25	20
			0.714	1.65	21
				3.30	22
				4.95	23
				6.60	24
				8.25	25
			0.505	1.65	26
				3.30	27
1.65	28				
3.30	29				
4.95	30				
30	Fuller's earth Solution	Vertically downward flow	3.647	6.60	31
				8.25	32
				1.65	33
				3.30	34
				4.95	35
			2.366	6.60	36
				8.25	37
				1.65	38
				3.30	39
				4.95	40
			1.673	6.60	41
				8.25	42
				1.65	43
				3.30	44
				4.95	45
			1.091	6.60	46
				8.25	47
				1.65	48
				3.30	49
				4.95	50
			0.714	6.60	51
				8.25	52
				1.65	53
				3.30	54

Table 3.2: Details of experimental runs conducted in the laboratory (contd...)

Influent turbidity (mg/l)	Samples	Mode of operation	Mean grain size (mm)	Filtration velocity (m ³ /hr/m ²)	Filter run no.
40	Fuller's earth solution	Vertically downward flow	1.091	1.65	55
				3.30	56
				4.95	57
				6.60	58
				8.25	59
			0.714	1.65	60
				3.30	61
				4.95	62
				6.60	63
				8.25	64
17	Rainwater	Vertically downward flow	3.647	1.65	65
				3.30	66
				4.95	67
				6.60	68
				8.25	69
			2.366	1.65	70
				3.30	71
				4.95	72
				6.60	73
				8.25	74
			1.673	1.65	75
				3.30	76
				4.95	77
				6.60	78
				8.25	79
			1.091	1.65	80
				3.30	81
				4.95	82
				6.60	83
				8.25	84
0.714	1.65	85			
	3.30	86			
	4.95	87			
	6.60	88			
	8.25	89			
30	Fuller's earth solution	Horizontal flow	0.714	1.65	90
				3.30	91
				4.95	92
				6.60	93
				8.25	94
40	Fuller's earth solution	Horizontal flow	0.714	1.65	95
				3.30	96
				4.95	97
				6.60	98
				8.25	99
17	Rainwater	Horizontal flow	0.714	1.65	100
				3.30	101
				4.95	102
				6.60	103
				8.25	104

Table 3.2: Details of experimental runs conducted in the laboratory (contd...)

Influent turbidity (mg/l)	Samples	Mode of operation	Mean grain size (mm)	Filtration velocity ($\text{m}^3/\text{hr}/\text{m}^2$)	Filter run no.
25	Fuller's earth solution	Vertically downward flow	1.673, 3.647,	0.21	105
			4.899, 8.485 and 17.888	0.41	106
17	Rainwater		1.673, 3.647,	0.21	107
			4.899, 8.485 and 17.888	0.41	108
17	Rainwater		2.366 and 3.647	1.65	109
			1.091 and 2.366	1.65	110

3.2.1 Selection of Filtration Velocities

The different flow velocities between 1.65 and $8.25 \text{ m}^3/\text{hr}/\text{m}^2$ at an equal interval of $1.65 \text{ m}^3/\text{hr}/\text{m}^2$ were maintained in the laboratory for rainwater and Fuller's earth suspension water solution samples. A constant rate of filtration was maintained throughout the run by controlling the inlet and outlet valves for a particular set of observation. The flow velocity was selected on the basis of average rainfall intensity and rooftop area in India, as described in chapter 2. The rainfall intensities were also computed at various locations in India and the maximum rainfall intensity was observed at Dehradun, India which is very near to the experiment station. For roof area of 115.0 m^2 and return period of 15 years (design period), the rate of rainfall was observed as $46.67 \text{ lit}/\text{min}$ ($2.80 \text{ m}^3/\text{hr}$) and hence the flow velocities for the experiment were selected on higher side in consideration of this input. The flow velocities may depend upon the placement of the sand filters with the rainwater harvesting buildings. The filters which have been placed nearby the rooftop, will receive the lower velocity but the filters placed at the bottom of the rooftop will receive higher rate of velocity. Hence, the placement of filters is also an important aspect.

3.2.2 Selection of Filter Properties

Camp (1964) has computed the hydraulic gradient at various depths versus time during the filter runs and the corresponding values of the deposit ratio and rate of removal for sand filter. Diaper and Ives (1965) made filtration study using Dicalite L-10 and Microsepiolite from a perspex (lucite) tube 6.0 ft high and 5.5 inch internal diameter, fitted with end pieces of conical shape to allow distribution of suspension at the inlet and to prevent settlement as far as possible. Fox and Cleasby (1966) made filtration experiment using hydrous ferric oxide floc formed by addition of ferrous sulfate solution to University tap water. The sand column was contained in a 6.0 inch ID plexiglass tube of 53.0 inch deep. Effluent samples were collected at various depths periodically during the filter runs and the performance of sand filter was assessed by iron concentration in water solution samples. Hsiung and Cleasby (1968) again made an extensive filtration study on suspension water solution prepared by continuously adding ferrous sulfate solution to aerated tap water. The filter influent and effluent quality were evaluated by their iron contents. Deb (1969) made an experiment by allowing turbid water of known Fuller's earth suspension concentration in water through a deep bed of uniform size.

3.2.3 Selection of Filter Run Times

Filter run times were selected on the basis of maximum probable rainfall duration and intensity in a single event in India. It has been considered that the rainfall will not last for more than 36 hours in normal case. The intensity of rainfall may vary from higher range to lower range during one rainfall event and hence, the filter has been designed to accommodate the rainfall for 36 hours. The performance of the sand filters was predicted at 36 hours filter run time in both the cases of rainwater as well as Fuller's earth suspension water solution samples. The details are given in section 2.3.

3.2.4 Selection of Influent Concentrations

Analysis of a set of data related to influent concentration in mg/l & NTU revealed that $1.0 \text{ mg/l} \cong 0.45 \text{ NTU}$. In the present study, four turbidity values of 40 mg/l, 30 mg/l, 25 mg/l and 17 mg/l have been considered. The values of 40 mg/l and 17 mg/l reported extreme conditions encountered in the field. Average of 40 mg/l & 17 mg/l worked out to be nearly 30 mg/l. For this reason, experiments have been planned at 30 mg/l as well as 25 mg/l influent concentrations. Calibration of runs based on such influent concentration has been used to develop models, which are further tested at extreme conditions. The details of experimental studies are presented in Table 3.1. The details of different sand filter studies made by various researchers are presented in Table 3.3.

The sand which was used as filter media throughout the runs in the present study, brought from local River at Roorkee, India. It has specific gravity of 2.65 and porosity of about 40.0%. The sand was graded into various sizes using IS sieves (IS: 460-1962) to use in the filters as uniform media & graded media and is presented in Table 3.4. Mean grain size refers as the square root of the product of the sizes of opening of adjacent sieves. Plate 3.3 shows various sand grading used in the laboratory.

Table 3.3: Comparative study of different filters used in water treatment

Details	Type of solids	Depth of filter media	Sand grains size	Filtration velocity	Initial concentration
Diaper and Ives (1965)	Dicalite L-10 and Microsepiolite	47.5 inch	14-25 sand sieve	4.0 gpm/ft ²	100 mg/l
Fox and Cleasby (1966)	Hydrous ferric oxide floc	53.0 inch	0.704 mm	3.0, 4.0 and 6.0 gpm/ft ²	5.0 & 7.0 mg/l
Hsiung & Cleasby (1968)	Ferrous sulfate	21.5 inch	0.649, 0.545, 0.458 & 0.386 mm	3.0, 4.5 & 6.0 gpm/ft ²	5.8 & 3.3 mg/l
Deb (1969)	Fuller's earth	24.0 inch	0.772 & 0.647 mm	4.72, 5.88 and 7.04 m/hr.	100 mg/l (45 ppm)
Laboratory study at I.I.T. Roorkee, Roorkee, India (2004 - 05)	Fuller's earth & rainwater	14.2, 19.7 & 23.64 inch	3.647, 2.366, 1.091, 1.091, 0.714 & 0.505 mm	1.65, 3.30, 4.95, 6.60 and 8.25 m/hr.	17, 25, 30 & 40 mg/l

Table 3.4: Details of various sand grain sizes used in the study of sand filters

Sr. No.	Sand passing opening Size (mm)	Sand retaining opening size (mm)	Mean size (mm)
1	20.0	16.0	17.888
2	12.0	6.00	8.485
3	6.00	4.00	4.899
4	4.75	2.80	3.647
5	2.80	2.00	2.366
6	2.00	1.40	1.673
7	1.40	0.850	1.091
8	0.850	0.600	0.714
9	0.600	0.425	0.505

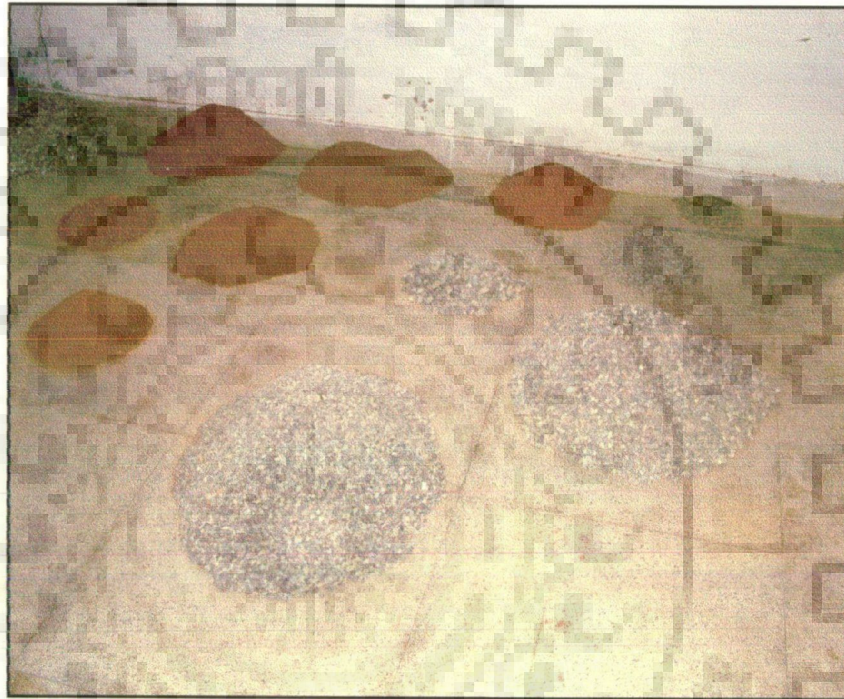


Plate 3.3: Pictorial view of various sand grain sizes used for filter in the laboratory at I.I.T. Roorkee, Roorkee, India



500 mm was effective depth of filter media and 100 mm below of lowermost sampling port was provided for support of effective filter media. A total of five sampling ports were placed at an equal interval of 100 mm from top to bottom of the filter. An overflow system was also provided to maintain a constant head over filter bed. Close view of the sand filter (no. 2) is shown in Plate 3.5.

Vertically downward flow filter (no. 3) was also made of HDPE having 6.0 inch internal diameter. The total depth of the filter was 460 mm out of which 360 mm was effective depth of filter media and 100 mm below the lowermost sampling port was provided for support of effective filter media. A total of six sampling ports were placed at an equal interval of 60 mm from top to bottom of the filter. Close view of the sand filter (no. 3) is also shown in Plate 3.5. All other arrangements for the vertical filter no. 3 were same as for vertical filter no. 2.

Horizontal flow filter (no. 4) was again made of same HDPE having 6.0 inch internal diameter. The system was completely air tight. The total effective depth of filter media was 600 mm. A total of six sampling ports were placed at an equal interval of 100 mm from inlet to outlet points. Close view of the filter (no. 4) is shown in Plate 3.6. The sand filter media was protected from both the sides by perforated perspex sheet to control the washing out the filter media. No overflow system was provided with this system. A constant pressure head was maintained by controlling the control valve at the inlet point. All other arrangements for horizontal filter (no. 4) were same as for vertical filters (nos. 2 & 3). Filters (nos. 2, 3 & 4) were continuously run for 36 hours and samples from all sampling points were collected simultaneously at one hour interval during each filter run. Samples collected from each sampling port were analyzed for turbidity. Head losses were also measured at all sampling ports at an equal time interval of one hour.

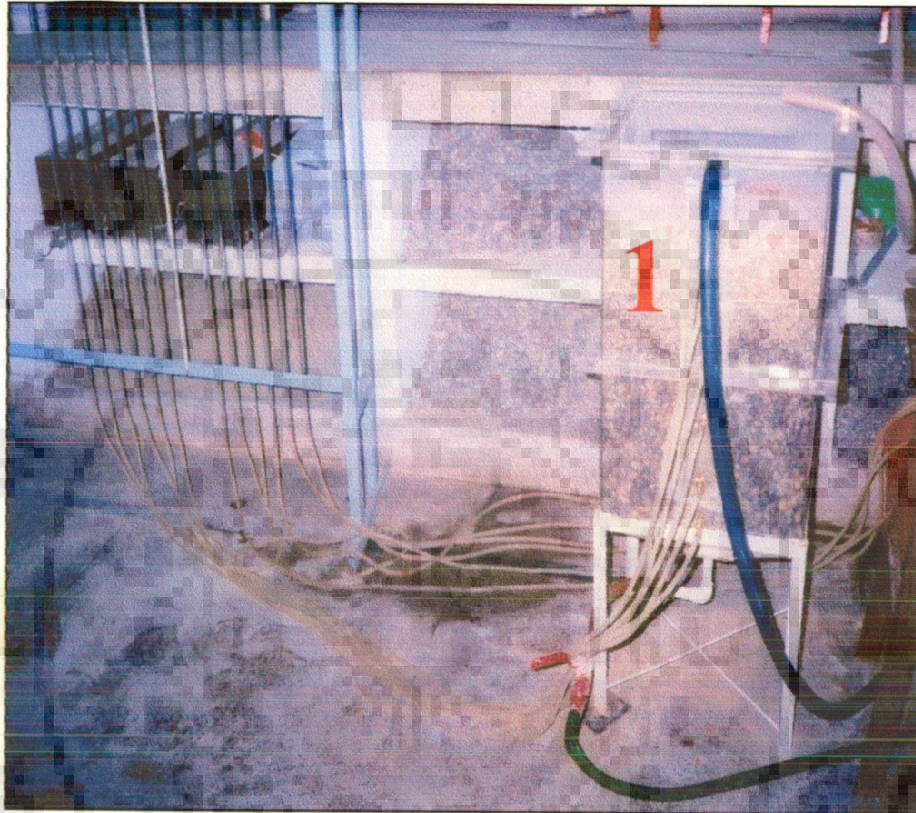


Plate 3.4: Close view of graded sand filter module (no. 1) in the laboratory at I.I.T. Roorkee, Roorkee, India



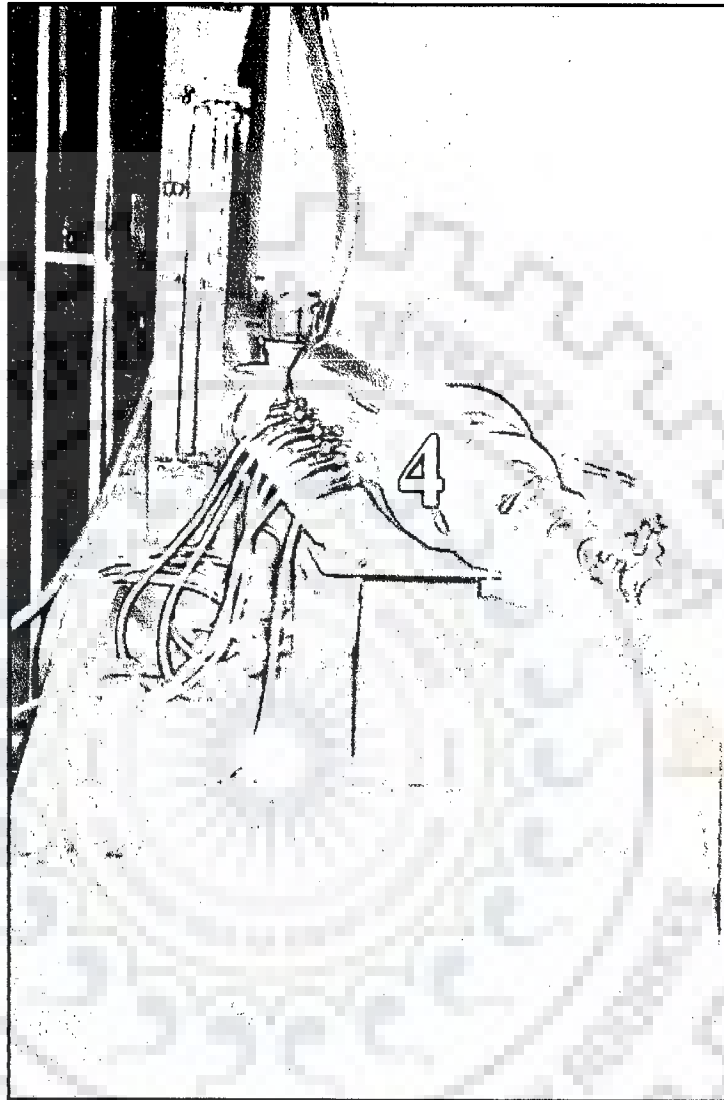


Plate 3.6: Close view of horizontal flow sand filter module (no. 4) in the laboratory at I.I.T. Roorkee, Roorkee, India

3.4 CONCLUDING REMARKS

Experiments on different sand modules were conducted with vertically downward flow and horizontal flow sand filters in the laboratory. Different sand grains and flow velocities were covered within the range of experimental study. The range of experimental variables was selected based on the literature review and field visit at rainwater harvesting sites in India. A total of 110 experimental runs (76 runs with Fuller's earth suspension water solution samples and 34 runs with rainwater samples) were operated under different filtering conditions. Out of them, 95 runs were operated for vertically downward flow filters and remaining 15 runs were operated for horizontal flow filters. The flow velocities were maintained between 1.65 and 8.25 m³/hr/m² at an equal interval of 1.65 m³/hr/m². The mean sand grain sizes were selected as 3.647 mm, 2.366 mm, 1.673 mm, 1.091mm, 0.714 mm and 0.505 mm and each set of experimentation was run for 36 hours. Different grain sizes and filtration velocities were selected for graded sand filter.

EVALUATION OF SAND FILTER RUNS USING PROBABILISTIC APPROACH

4.1 GENERAL

Hsiung and Cleasby (1968) developed models based on probabilistic approach for prediction of sand filter performance in terms of effluent quality and critical head loss. The data generated in the laboratory for vertically downward flow and horizontal flow sand filters are tested using Hsiung and Cleasby (H-C) model. The compatibility of the models has been checked for different data sets for varying influent concentration of turbidity of Fuller's earth suspension water solution and rainwater samples. But the models do not seem compatible for performance prediction of sand filter in different conditions than developed.

4.2 CHI-SQUARE DISTRIBUTION APPLICATION

Hsiung and Cleasby (1968) gave a model to predict the performance of sand filter on probabilistic approach. Many probability distributions in statistical problems, such as normal distribution, poisson distribution, gamma distribution, chi-square distribution, etc., can approximate the binomial distribution and also can be generalized to satisfy a single differential equation (Kenny and Keeping, 1951). Therefore, any one of these distribution may describe the filtration process to some extent. Among these, the chi-square distribution occurs so often in statistical problems (shown in Fig. 4.1).

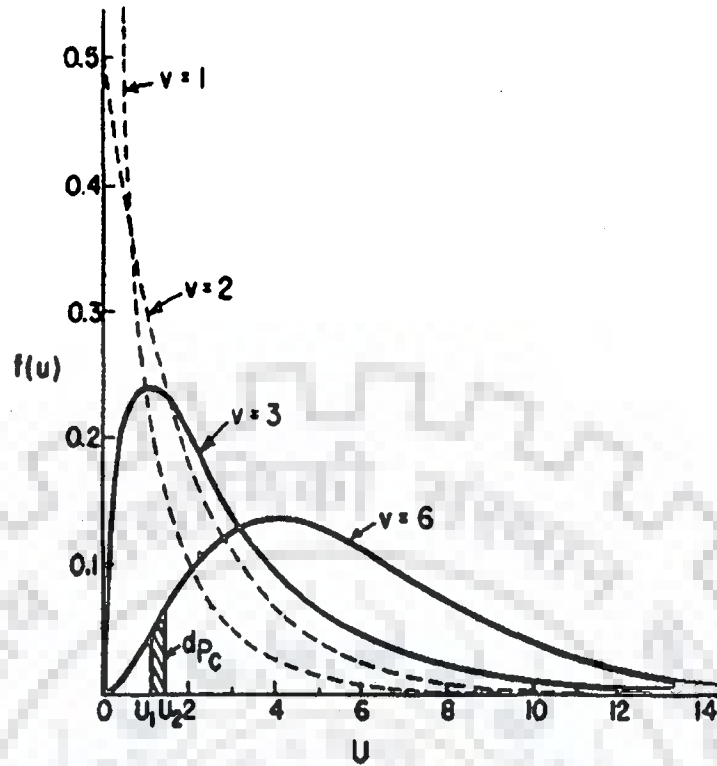


Fig. 4.1: Typical chi-square distribution curves (Hsiung and Cleasby, 1968)

Each curve in the Fig. 4.1 represents a typical chi-square distribution for a specific degree of freedom. The area under each curve between U and $U + dU$ equals $f(U)du$. By definition, the cumulative probability $P_c = \int f(U)dU$ for a continuous random variable; therefore, the area under each curve between U and $U + dU$ equals dP_c . The functional form of chi-square distribution is expressed as

$$f(U) = \frac{U^{(v/2-1)} \exp(-U/2)}{2^{v/2} \Gamma(v/2)} \quad (4.1)$$

in which U is random variable in the chi-square distribution, v is the degree of freedom, Γ is the symbol of gamma function, defined by $\Gamma(v/2)$ is $\int y^{(v/2-1)} e^{-y} dy$ as it appears in the chi-square distribution. If $v/2 =$ a positive integer, $\Gamma(v/2) = (v/2 - 1)!$, and

$f(U)$ is chi-square probability function $\int_0^{+\infty} f(U)dU = 1$ for the chi-square distribution curve since U is a continuous variable. The values of U are restricted to positive values and the values of ' v ' are restricted to positive integers.

Hsiung and Cleasby (1968) related the variate U in the chi-square distribution to filtration data as:

1. Let $C/C_0 = P_c$ where C is the effluent turbidity concentration in mg/l, C_0 is the influent turbidity concentration in mg/l and P_c is the cumulative probability and t is filtration time in hour = v , i.e., 1 hour = 1 degree of freedom.
2. Using observed values of C/C_0 at various depths and times, U was found readily by the tabulated cumulative probability curves (Ostle, 1964), as given in Fig. 4.2.
3. When relating t to v , any convenient unit may be used. In this study all values are derived on the basis of 1 hour = 1 degree of freedom. For example, $U_{1/2}$ represents that it is derived on the basis of 1/2 hour = 1 degree of freedom.

4.2.1 Criteria for Evaluation of Performance Models

Using the superposition techniques, two single models, called "Performance Models" have been obtained by Hsiung and Cleasby (1968). Two different criteria, one for effluent quality and the other one for terminal head loss increase have been distinguished in evaluating the effects of filtration variables on filter performance. In the filtration system where the depth of sand and available terminal head loss are fixed, the filtration rate, grain size and filter run length may be selected so that the effluent turbidity just reaches its acceptable limit when the full terminal head loss occurs.

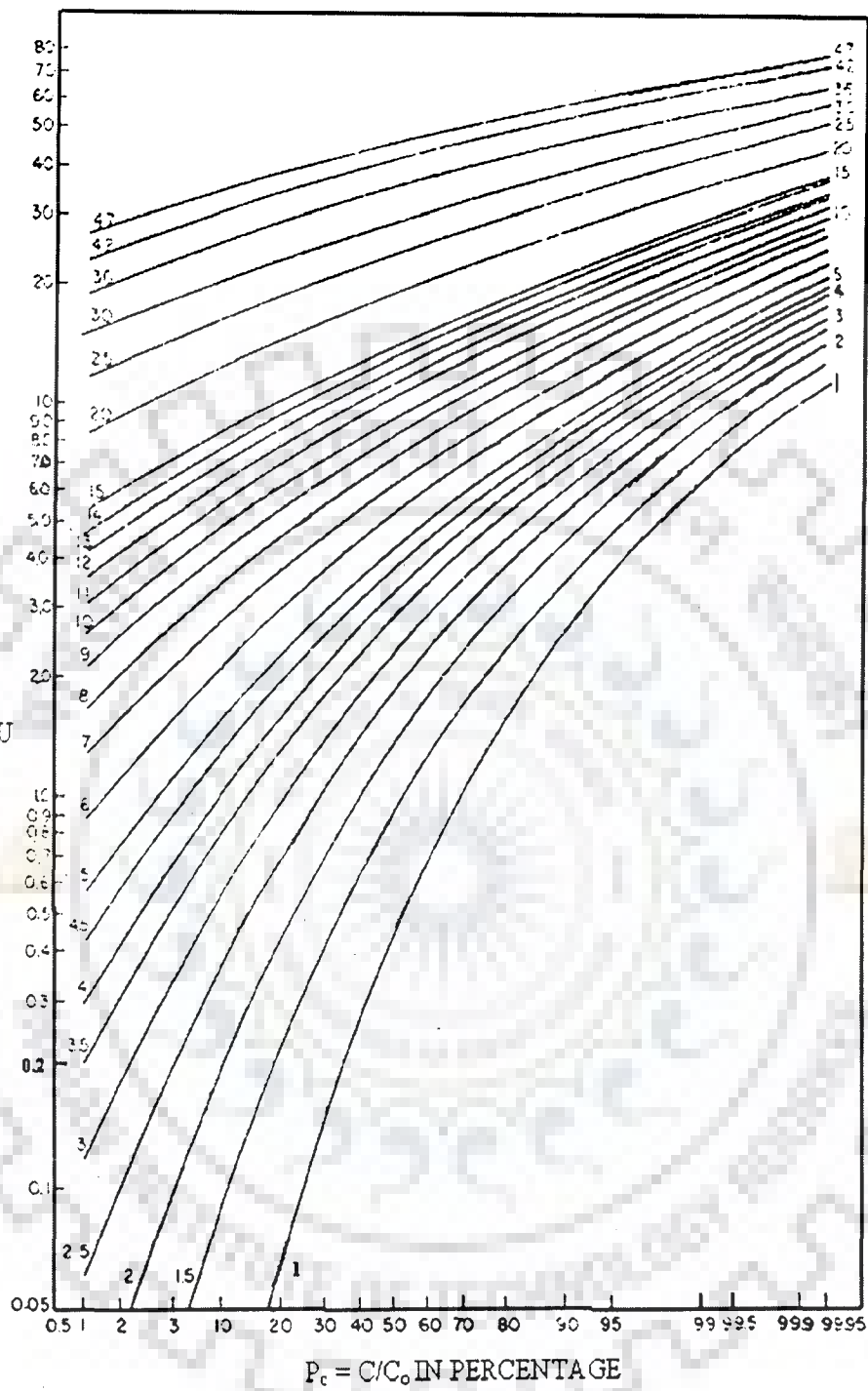


Fig. 4.2: Plot of U versus cumulative probability (P_c) at various degrees of freedom (Ostle, 1964)

In designing a new filtration system, however, many combinations of the five variables (Q , d , t , C_0 and L) could be selected to achieve an optimum design, where Q is flow rate in gpm/ft^2 , d is diameter of grain size in mm, t is time of filter run in hours called degree of freedom in case of probabilistic approach, C_0 is the influent concentration in mg/l and L is the depth of filter media in inch.

4.2.1.1 Effluent quality performance

An equiU plot for Q versus t was drawn by Hsiung and Cleasby (1968) with a slope approximately equal to $-1/0.29$ for the experimental runs using the same grain size and filter depth but different flow rates. Therefore, $\log Q \propto (-1/0.29) \log t$ or $t \propto 1/Q^{0.29}$. This indicates that for a given value of $Q^{0.29}t$, the U value was constant for the given filter depth. In a similar manner it was found that for given value of $d^{0.62}t$, the U value was constant. Hence, they obtained G is a function of $Q^{0.29}d^{0.62}t$.

When U/L was plotted against $G/L^{1.2}$ for the lumped data of various grain size, flow rate, influent concentration, depth of bed and time of filtration, a single model to best fit the plotted data was obtained by the method of multiple regression analysis and expressed mathematically as

$$\log\left(\frac{U}{L}\right) = -0.208 + 1.950 \log\left(\frac{G}{L^{1.2}}\right) - 0.645 \left[\log\left(\frac{G}{L^{1.2}}\right) \right]^2 \quad (4.2)$$

4.2.1.2 Head loss performance

To describe head loss performance, Hsiung and Cleasby (1968) grouped the four variables ($H_t - H_0$), Q , d and C_0 into another term, R , which is defined as

$$R = d^{2.5} (H_t - H_0) / Q^{1.2} C_0^{1.4} \quad (4.3)$$

When $R/L^{1.6}$ was plotted against $G/L^{1.2}$, for the lumped data of various grain size, flow rate and influent concentration, a single model to best fit the plotted data was obtained by the method of multiple regression analysis and expressed mathematically as

$$\log\left(\frac{R}{L^{1.6}}\right) = -3.250 + 1.013 \log\left(\frac{G}{L^{1.2}}\right) - 0.036 \left[\log\left(\frac{G}{L^{1.2}}\right)\right]^2 \quad (4.4)$$

4.3 EFFLUENT QUALITY MODEL TESTING

4.3.1 Model Testing for Vertically Downward Flow Filters

The performance of the sand filters operated under 25 mg/l influent turbidity concentration was evaluated using H-C model (Eq. 4.2). The results at different sand grain sizes with different flow velocities are presented in Tables 4.1. For each of the runs, effluent concentration (C) has been computed at different times and percentage errors

$\left| \left(\frac{\text{observed} - \text{computed}}{\text{observed}} \right) \times 100 \right|$ are computed at these times using observed values.

Subsequently, an average percentage error (APE) is obtained using these errors. The data of experimental runs (nos. 1 to 27) were used for the computation of errors and the average of such errors for each of the runs is presented in Table 4.1. From the Table 4.1, APE of U and C using H-C model is computed as 62.51% and 92.73% respectively at 0.505 mm grain size and flow velocity of $1.65 \text{ m}^3/\text{hr}/\text{m}^2$ (run no. 26). To provide an insight into the effectiveness of each filter run, removal efficiency at the end of filter run (at 36 hours) is also presented in Table 4.1. It is observed that the filter run (no. 26) at 0.505 mm sand grain and $1.65 \text{ m}^3/\text{hr}/\text{m}^2$ flow velocity has the highest removal efficiency of 96.0%. It is also observed that the filter run (no. 21) at 0.714 mm sand grain and $1.65 \text{ m}^3/\text{hr}/\text{m}^2$ flow velocity has the same removal efficiency of 96.0%.

Table 4.1: Computed APE of U and C using H-C model for influent concentration

of 25 mg/l (run nos. 1 to 27)

Sand grain size (mm)	Flow velocity (m ³ /hr/m ²)	Influent turbidity (mg/l)	% Removal (observed at the end of filter run time)	Computed APE	
				U	C
3.647	1.65	25	40.00	28.10	32.06
	3.30		40.00	30.24	31.62
	4.95		36.00	21.79	27.93
	6.60		32.00	21.12	25.51
	8.25		32.00	21.75	24.00
2.366	1.65	25	60.00	38.94	52.41
	3.30		56.00	48.80	52.53
	4.95		52.00	44.40	46.26
	6.60		52.00	42.20	46.80
	8.25		48.00	39.11	44.10
1.647	1.65	25	63.00	34.75	52.47
	3.30		60.00	36.48	52.03
	4.95		56.00	43.97	60.14
	6.60		56.00	48.84	60.18
	8.25		56.00	52.81	57.86
1.091	1.65	25	83.00	54.59	78.22*
	3.30		77.00	43.84	59.58
	4.95		75.00	38.28	49.47
	6.60		73.00	36.86	45.98
	8.25		70.00	38.99	48.71
0.714	1.65	25	96.00	54.35	85.04
	3.30		92.00	39.10	63.08
	4.95		92.00	35.16	55.90
	6.60		92.00	34.05	57.70
	8.25		88.00	33.59	57.95
0.505	1.65	25	96.00	62.51	92.73
	3.30		96.00	51.84	83.24

An analysis of experimental runs (nos. 28 to 54) pertaining to 30 mg/l influent turbidity concentration was done using H-C model (Eq. 4.2). The results of observed removal efficiency and computed average errors at various grain sizes and flow rates are presented in Table 4.2. From the Table 4.2, APE of U and C using H-C model is computed as 68.08% and 95.20% respectively at 0.505 mm grain size and flow velocity of $1.65 \text{ m}^3/\text{hr}/\text{m}^2$ (run no. 53). To provide an insight into the effectiveness of each filter run, removal efficiency at the end of filter run (at 36 hours) is also given in Table 4.2. It is observed that the filter runs (nos. 53 & 54) at 0.505 mm sand grain and $1.65 \text{ m}^3/\text{hr}/\text{m}^2$ flow velocity have highest removal efficiency of 97.0%. Figures 4.3 & 4.4 show much deviation of the values with the line of perfect agreement for lumped data of influent concentrations of 25 mg/l (run nos. 1 to 27) and 30 mg/l (run nos. 28 to 54), respectively. Hence, H-C model is incompatible for effluent quality prediction at these influent turbidity concentrations.

An analysis of experimental runs (nos. 55 to 64) pertaining to 40 mg/l influent turbidity concentration was done using H-C model (Eq. 4.2). The results of observed removal efficiency and computed average errors at two sand grain sizes (1.091 mm and 0.714 mm) and different flow rates are presented in Table 4.3. From the Table 4.3, APE of U and C using H-C model is computed as 57.82% and 84.81% respectively at 0.714 mm grain size and flow velocity of $1.65 \text{ m}^3/\text{hr}/\text{m}^2$ (run no. 60). This reveals the wide difference between the computed values and the observed values. To provide an insight into the effectiveness of each filter run, removal efficiency at the end of filter run (at 36 hours) is also given in Table 4.3. It is observed that the filter run (no. 60) at 0.714 mm sand grain and $1.65 \text{ m}^3/\text{hr}/\text{m}^2$ flow velocity has highest removal efficiency of 89.50%.

Table 4.2: Computed APE of U and C using H-C model for influent concentration of 30 mg/l (run nos. 28 to 54)

Sand grain size (mm)	Flow velocity (m ³ /hr/m ²)	Influent turbidity (mg/l)	% Removal (observed at the end of filter run time)	Computed APE	
				U	C
3.647	1.65	30	47.0	37.64	39.49
	3.30		47.0	39.31	40.57
	4.95		43.0	26.86	33.35
	6.60		43.0	32.83	35.61
	8.25		43.0	29.07	33.82
2.366	1.65	30	57.0	38.87	51.69
	3.30		53.0	47.91	50.77
	4.95		53.0	46.46	49.78
	6.60		47.0	41.69	45.06
	8.25		43.0	38.51	41.95
1.647	1.65	30	63.0	34.67	51.02
	3.30		60.0	37.17	51.52
	4.95		60.0	41.14	52.65
	6.60		57.0	47.03	52.22
	8.25		53.0	41.15	49.09
1.091	1.65	30	85.0	52.14	75.85
	3.30		77.0	40.84	58.84
	4.95		75.0	37.88	52.06
	6.60		75.0	37.08	48.36
	8.25		72.0	38.76	51.49
0.714	1.65	30	90.0	59.69	88.80
	3.30		90.0	46.85	73.79
	4.95		90.0	38.89	60.13
	6.60		87.0	35.41	52.57
	8.25		83.0	33.03	48.96
0.505	1.65	30	97.0	68.08	95.20
	3.30		97.0	57.69	87.77

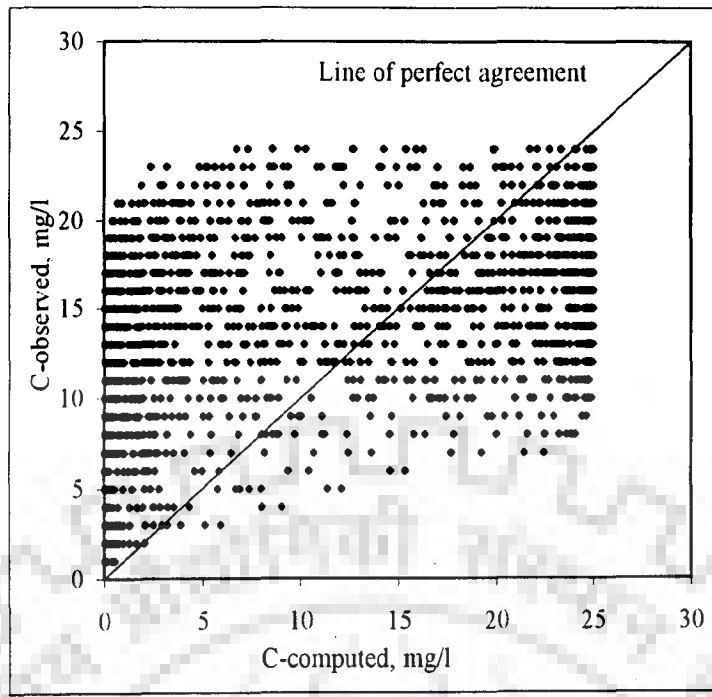


Fig. 4.3: Plot of C-observed versus C-computed using H-C model for influent concentration of 25 mg/l (run nos. 1 to 27)

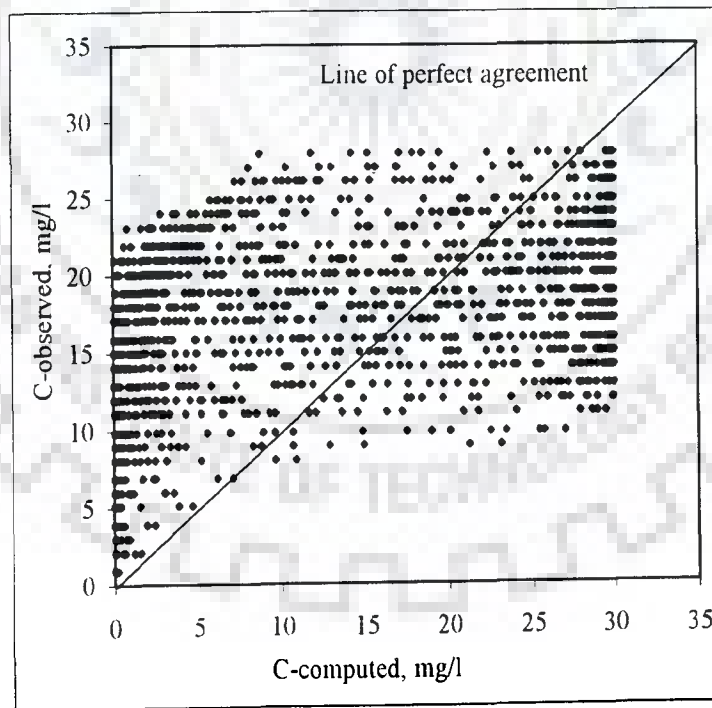


Fig. 4.4: Plot of C-observed versus C-computed using H-C model for influent concentration of 30 mg/l (run nos. 28 to 54)

Table 4.3: Computed APE of U and C using H-C model for influent concentration of 40 mg/l (run nos. 55 to 64)

Sand grain size (mm)	Flow velocity (m ³ /hr/m ²)	Influent turbidity (mg/l)	% Removal (observed at the end of filter run time)	Computed APE	
				U	C
1.091	1.65	40	82.00	43.89	69.70
	3.30		74.00	40.50	61.19
	4.95		73.00	39.11	55.22
	6.60		69.00	38.38	56.36
	8.25		66.00	38.47	54.73
0.714	1.65	40	89.50	57.82	84.81
	3.30		89.50	54.43	80.84
	4.95		87.50	51.51	76.81
	6.60		87.50	49.35	74.17
	8.25		80.00	49.12	72.91

Figure 4.5 shows much deviation of the values with the line of perfect agreement at 1.091 mm sand grain size for 40 mg/l influent concentration (run nos. 55 to 59). Figure 4.6 also shows much deviation of the values with the line of perfect agreement for at 0.714 mm sand grain size for 40 mg/l influent concentration (run nos. 60 to 64). Hence, H-C model is also incompatible to predict the performance of sand filter in terms of effluent quality at influent turbidity concentration of 40 mg/l.

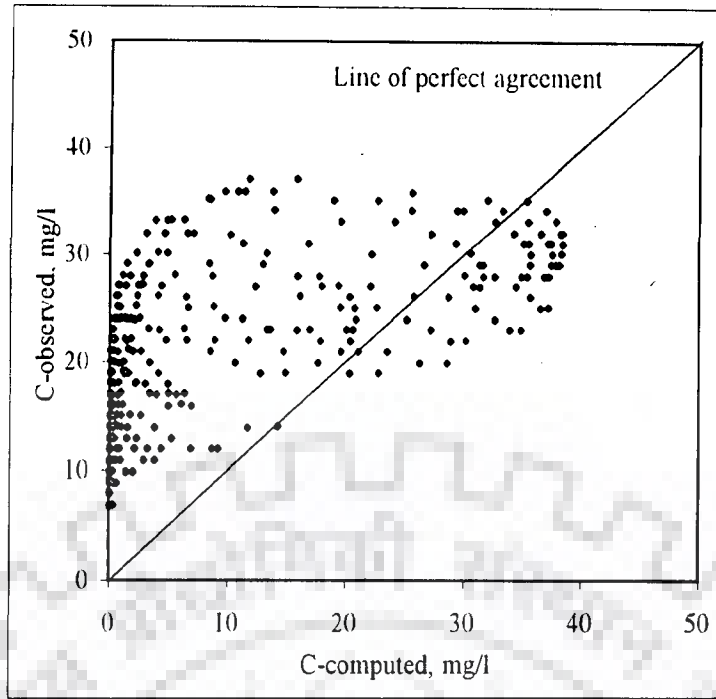


Fig. 4.5: Plot of C-observed versus C-computed using H-C model for influent concentration of 40 mg/l (run nos. 55 to 59)

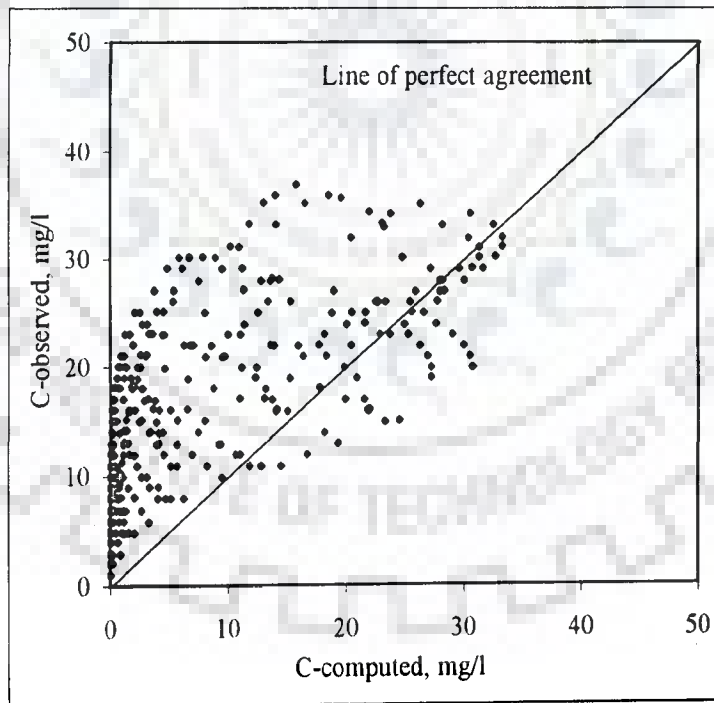


Fig. 4.6: Plot of C-observed versus C-computed using H-C model for influent concentration of 40 mg/l (run nos. 60 to 64)

Now, H-C model is used to predict the performance of sand filter for harvested rainwater. An analysis of experimental runs (nos. 65 to 89) was done using H-C model (Eq. 4.2). The results of observed removal efficiency and computed average errors at different grain sizes and flow velocities are presented in Table 4.4. From the Table 4.4, APE of U and C using H-C model is computed as 92.44% and 137.07% respectively at 0.714 mm grain size and flow velocity of $1.65 \text{ m}^3/\text{hr}/\text{m}^2$ (run no. 85). To provide an insight into the effectiveness of each filter run, removal efficiency at the end of filter run (at 36 hours) is also given in Table 4.4. It is observed that the filter run at 0.714 mm sand grain and $1.65 \text{ m}^3/\text{hr}/\text{m}^2$ flow velocity has highest removal efficiency of 94.12% (run no. 85). Figure 4.7 shows much deviation of the values with the line of perfect agreement and hence, H-C model is incompatible for prediction of sand filter effluent quality for harvested rainwater samples.

Table 4.4: Computed APE of U and C using H-C model for influent concentration of 17 mg/l (run nos. 65 to 89)

Sand grain size (mm)	Flow velocity (m ³ /hr/m ²)	Influent turbidity (mg/l)	% Removal (observed at the end of filter run time)	Computed APE	
				U	C
3.647	1.65	17	47.05	37.44	39.68
	3.30		35.29	29.22	29.48
	4.95		29.41	19.99	25.38
	6.60		29.41	13.01	19.96
	8.25		17.65	14.15	16.68
2.366	1.65	17	52.94	39.04	47.53
	3.30		49.41	34.85	42.68
	4.95		41.18	26.19	33.14
	6.60		33.53	22.05	27.08
	8.25		23.53	23.28	24.53
1.673	1.65	17	64.71	60.96	85.27
	3.30		58.82	60.64	80.26
	4.95		52.94	62.12	67.67
	6.60		52.94	59.14	68.32
	8.25		47.06	52.68	61.19
1.091	1.65	17	82.35	76.72	82.73
	3.30		64.71	77.96	83.09
	4.95		64.71	82.42	83.87
	6.60		64.71	84.05	84.20
	8.25		64.71	84.07	84.42
0.714	1.65	17	94.12	92.44	137.07
	3.30		88.24	74.49	114.09
	4.95		88.24	63.77	104.04
	6.60		82.35	59.76	93.94
	8.25		82.35	59.74	98.95

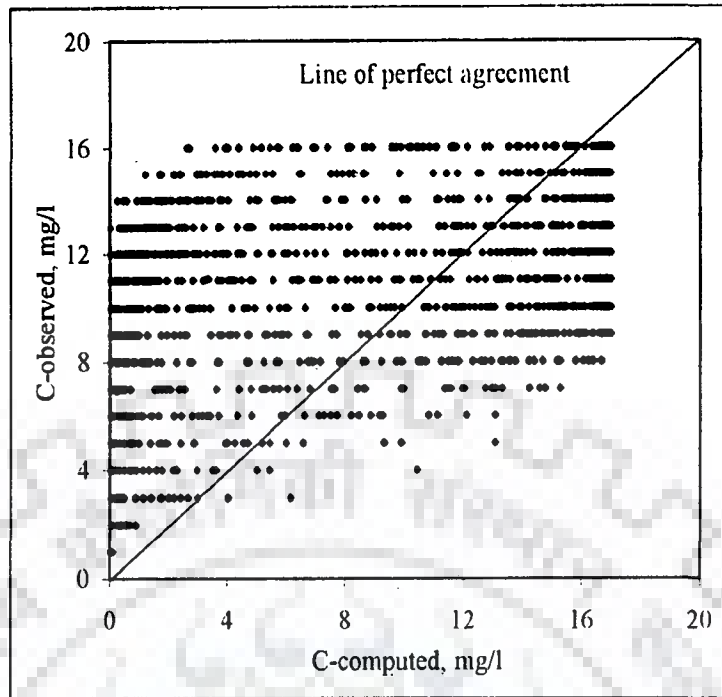


Fig. 4.7: Plot of C-observed versus C-computed using H-C model for influent concentration of 17 mg/l (run nos. 65 to 89)

4.3.2 Model Testing for Horizontal Flow Filter

From the above study of vertically downward flow filters (section 4.3.1), it is clear that H-C model is incompatible to predict the filter performance for effluent quality and hence, the behaviour of the model (Eq. 4.2) is again evaluated under horizontal flow condition. An analysis of experimental runs (nos. 90 to 94) was done using H-C model (Eq. 4.2). The results of observed removal efficiency and computed average errors at 0.714 mm sand grain size and different flow velocities at 30 mg/l influent turbidity concentration are given in Table 4.5. From the Table 4.5, APE of U and C using H-C model is computed as 75.24% and 95.65% respectively (run no. 90). Table 4.5 reveals high average errors between the computed and the observed values. To provide an insight into the effectiveness of each filter run, removal efficiency at the end of filter run (at 36 hours) is also given in Table 4.5. It is observed that the filter runs (nos. 90 to 93) at 0.714 mm sand grain have highest removal efficiency of 97.12%. Figure 4.8 shows much deviation of the values with the line of perfect agreement.

An analysis of experimental runs (nos. 95 to 99) pertaining to 40 mg/l influent turbidity concentration was done using H-C model (Eq. 4.2). The results of observed removal efficiency and computed average errors at 0.714 mm grain size and different flow velocities at 40 mg/l influent concentration are presented in Table 4.5. From the Table 4.5, APE of U and C using H-C model is computed as 79.61% and 96.92% respectively at 0.714 mm grain size and flow velocity of $1.65 \text{ m}^3/\text{hr}/\text{m}^2$. To provide an insight into the effectiveness of each filter run, removal efficiency at the end of filter run (at 36 hours) is also given in Table 4.5. It is observed that the filter run at 0.714 mm sand grain and $1.65 \text{ m}^3/\text{hr}/\text{m}^2$ flow velocity has highest removal efficiency of 90.11% (run no. 95). Figure 4.9 shows much deviation of the values with the line of perfect agreement.

Horizontal filter was also operated for rainwater at 0.714 mm sand grains. The analysis of filter runs (nos. 100 to 104) was done using H-C model. The results of observed removal efficiency and computed average errors at 0.714 mm grain size and different flow velocities are presented in Table 4.5. From the Table 4.5, APE of U and C using H-C model is computed as 75.86% and 94.23% respectively at 0.714 mm grain size and flow velocity of 1.65 m³/hr/m². It is also observed that the filter run (no. 100) at 0.714 mm sand grain and 1.65 m³/hr/m² flow velocity has highest removal efficiency of 94.12%. Figure 4.10 shows wide deviation of the values with the line of perfect agreement and also shows incompatible of H-C model for effluent quality prediction for sand filter.

Table 4.5: Computed APE of U and C using H-C model for Fuller's earth suspension samples (run nos. 90 to 94 and 95 to 99) and rainwater samples (run nos. 100 to 104)

Sand grain size (mm)	Flow velocity (m ³ /hr/m ²)	Initial turbidity (mg/l)	% Removal (Observed at the end of filter run time)	Computed APE	
				U	C
0.714	1.65	30 (Fuller's earth)	97.12	75.24	95.65
	3.30		97.12	66.12	89.20
	4.95		97.12	61.69	84.65
	6.60		97.12	57.96	81.07
	8.25		94.78	56.52	78.76
0.714	1.65	40 (Fuller's earth)	90.11	79.61	96.92
	3.30		88.00	72.04	92.01
	4.95		85.61	67.27	87.20
	6.60		80.13	63.08	82.87
	8.25		75.31	60.75	80.09
0.714	1.65	17 (Rainwater)	94.12	75.86	94.23
	3.30		94.12	68.92	90.00
	4.95		94.12	63.52	86.29
	6.60		94.12	59.47	82.96
	8.25		94.12	56.30	79.78

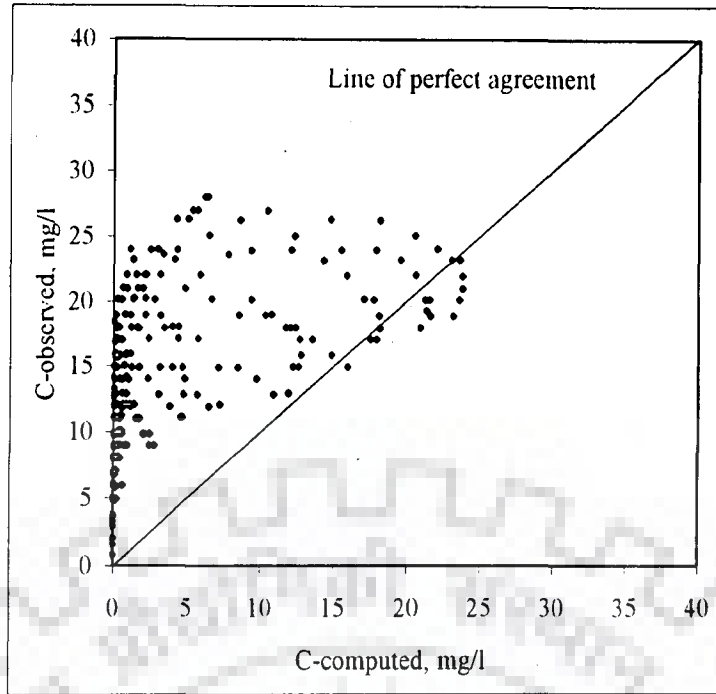


Fig. 4.8: Plot of C-observed versus C-computed using H-C model for influent concentration of 30 mg/l (run nos. 90 to 94)

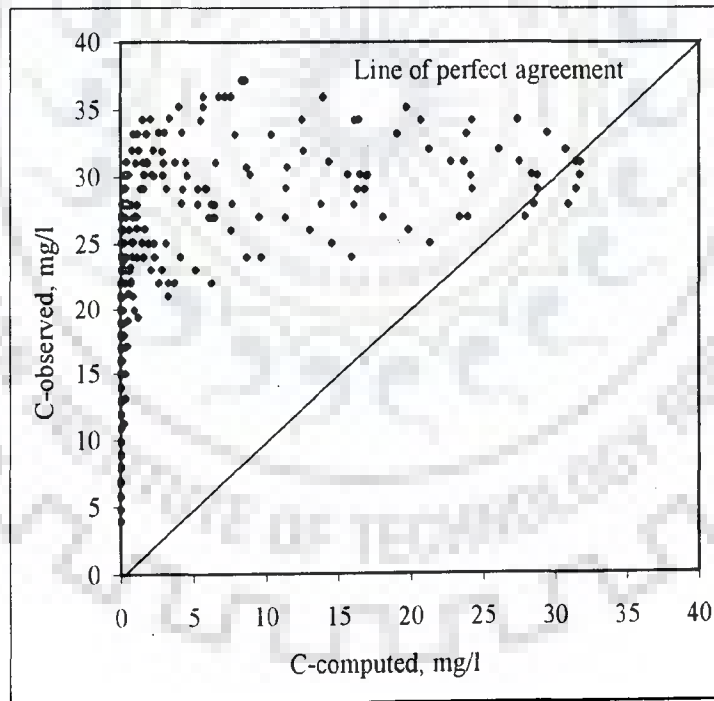


Fig. 4.9: Plot of C-observed versus C-computed using H-C model for influent concentration of 40 mg/l (run nos. 95 to 99)

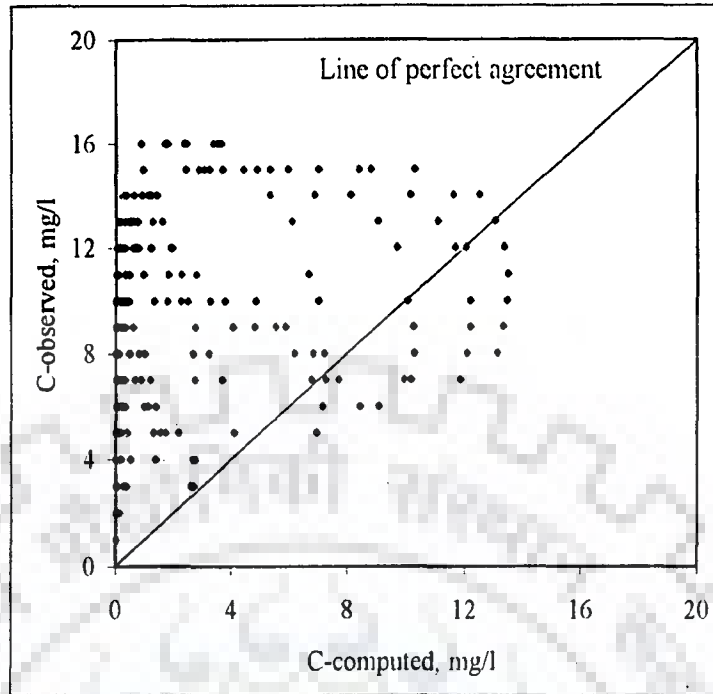


Fig. 4.10: Plot of C-observed versus C-computed using H-C model for influent concentration of 17 mg/l (run nos. 100 to 104)

4.4 FLOW RESISTANCE MODEL TESTING

4.4.1 Model Testing for Vertically Downward Flow Filters

The performance of sand filters for head loss prediction operated under 25 mg/l influent turbidity concentration was evaluated using H-C model (Eq. 4.4). H-C model was tested against different data sets of Fuller's earth suspension water solution and rainwater samples. Here, the average error of head loss is computed using all the observations obtained at different filter depths and filter runs (nos. 1 to 27) for 25 mg/l influent turbidity concentration. The average of such errors for each of the runs is presented in Table 4.6. From the Table 4.6, maximum APE of 7296.88% (run no. 25) is computed at 0.714 mm grain size and flow velocity of $8.25 \text{ m}^3/\text{hr}/\text{m}^2$. This reveals that the computed head loss has much deviation with observed head loss values. Figure 4.11 shows deviation of computed head loss values with observed head loss values.

An analysis of experimental runs (nos. 28 to 54) pertaining to 30 mg/l influent turbidity concentration was done using H-C model (Eq. 4.4). The average error of head loss is computed using all the observations obtained at different filter depths and filter runs (nos. 28 to 54) for 30 mg/l influent turbidity concentration. The average of such errors for each of the runs is presented in Table 4.7. From the Table 4.7, maximum APE of 6643.53% (run no. 52) is computed at 0.714 mm grain size and flow velocity of $8.25 \text{ m}^3/\text{hr}/\text{m}^2$. This reveals that the computed head loss has much deviation with observed head loss values. Figure 4.12 shows deviation of computed head loss values with observed head loss values. Hence, the above study reveals that H-C model is incompatible to predict the performance of sand filters in terms of head loss at influent turbidity concentration of 30 mg/l.

Table 4.6: Computed APE of head loss using H-C model for influent concentration of 25 mg/l (run nos. 1 to 27)

Sand grain size (mm)	Flow velocity (m ³ /hr/m ²)	Influent turbidity (mg/l)	Computed APE
3.647	1.65	25	184.57
	3.30		505.51
	4.95		841.22
	6.60		1184.08
	8.25		1446.98
2.366	1.65	25	379.84
	3.30		1113.47
	4.95		1795.58
	6.60		2719.34
	8.25		3447.78
1.673	1.65	25	450.79
	3.30		1163.36
	4.95		2069.59
	6.60		3038.24
	8.25		3993.24
1.091	1.65	25	800.66
	3.30		2030.25
	4.95		3553.68
	6.60		5095.02
	8.25		6115.77
0.714	1.65	25	1033.94
	3.30		2877.62
	4.95		4785.31
	6.60		6756.89
	8.25		7296.88
0.505	1.65	25	1880.73
	3.30		5025.89

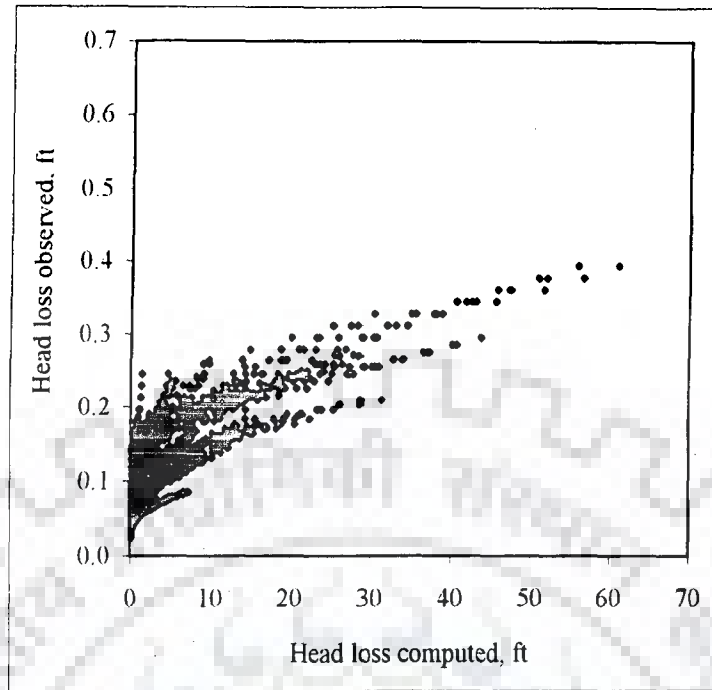


Fig. 4.11: Plot of head loss observed versus computed using H-C model for influent concentration of 25 mg/l (run nos. 1 to 27)

Table 4.7: Computed APE of head loss using H-C model for influent concentration of 30 mg/l (run nos. 28 to 54)

Sand grain size (mm)	Flow velocity (m ³ /hr/m ²)	Influent turbidity (mg/l)	Computed APE
3.647	1.65	30	172.49
	3.30		533.52
	4.95		928.12
	6.60		1228.00
	8.25		1643.94
2.366	1.65	30	413.21
	3.30		1233.38
	4.95		2088.92
	6.60		3046.83
	8.25		3906.45
1.673	1.65	30	460.23
	3.30		1359.16
	4.95		2378.77
	6.60		3473.15
	8.25		4351.43
1.091	1.65	30	804.34
	3.30		2310.65
	4.95		3940.26
	6.60		5339.81
	8.25		6637.78
0.714	1.65	30	866.15
	3.30		2216.18
	4.95		3672.58
	6.60		5346.75
	8.25		6643.53
0.505	1.65	30	1634.76
	3.30		4506.49

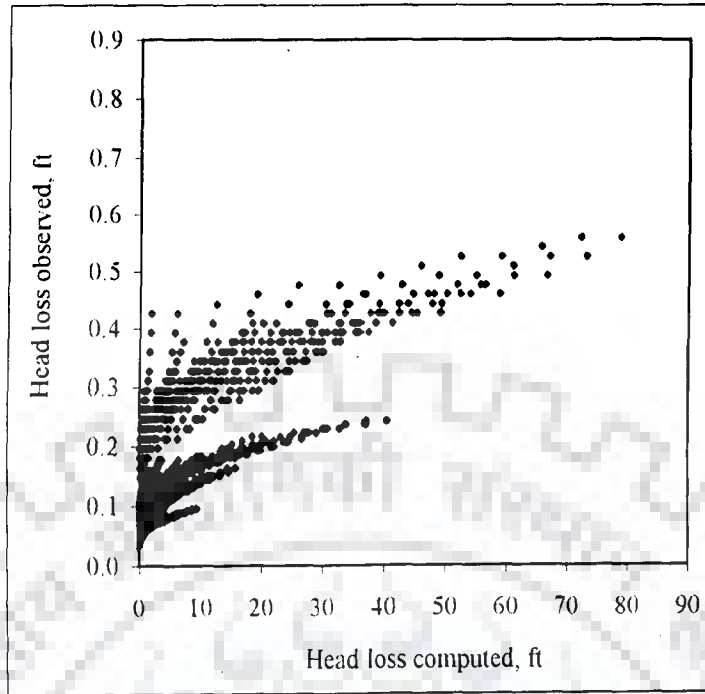


Fig. 4.12: Plot of head loss observed versus computed using H-C model for influent concentration of 30 mg/l (run nos. 28 to 54)

An analysis of experimental runs (nos. 55 to 64) pertaining to 40 mg/l influent turbidity concentration was also done using H-C model (Eq. 4.4). The average percentage error at different filter depths for each of the filter runs is presented in Table 4.8. From the Table 4.8, maximum APE of 11428.80% (run no. 64) is computed at 0.714 mm grain size and flow velocity of 8.25 m³/hr/m². This reveals that the computed head loss has much deviation with observed head loss values. Figures 4.13 & 4.14 show deviation of computed head loss values with observed head loss values. Hence, it is clear that the H-C model is incompatible to predict the performance of sand filters in terms of head loss at influent turbidity concentration of 40 mg/l.

Table 4.8: Computed APE of head loss using H-C model for influent concentration of 40 mg/l (run nos. 55 to 64)

Sand grain size (mm)	Flow velocity (m ³ /hr/m ²)	Influent turbidity (mg/l)	Computed APE
1.091	1.65	40	696.80
	3.30		1969.06
	4.95		3443.22
	6.60		5012.87
	8.25		6589.96
0.714	1.65	40	1327.51
	3.30		3706.69
	4.95		6354.51
	6.60		9044.24
	8.25		11428.8

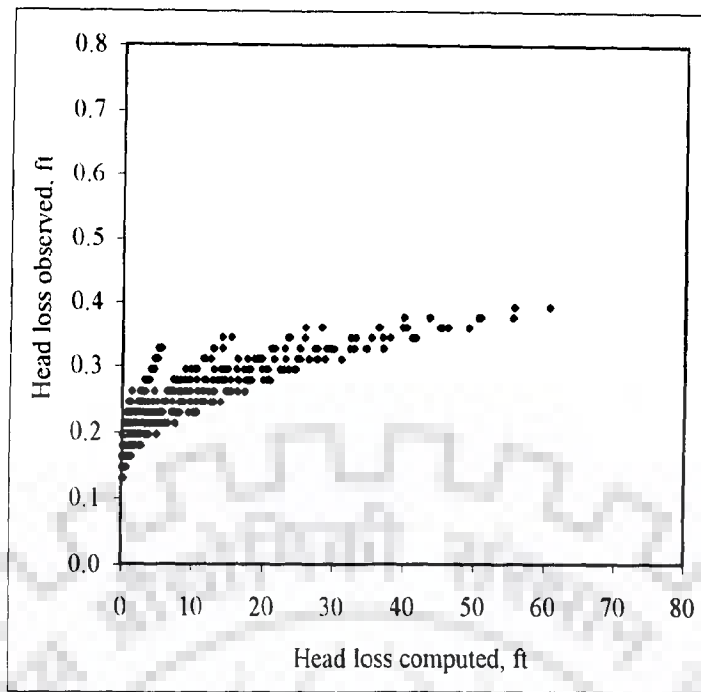


Fig. 4.13: Plot of head loss observed versus computed using H-C model for influent concentration of 40 mg/l (run nos. 55 to 59)

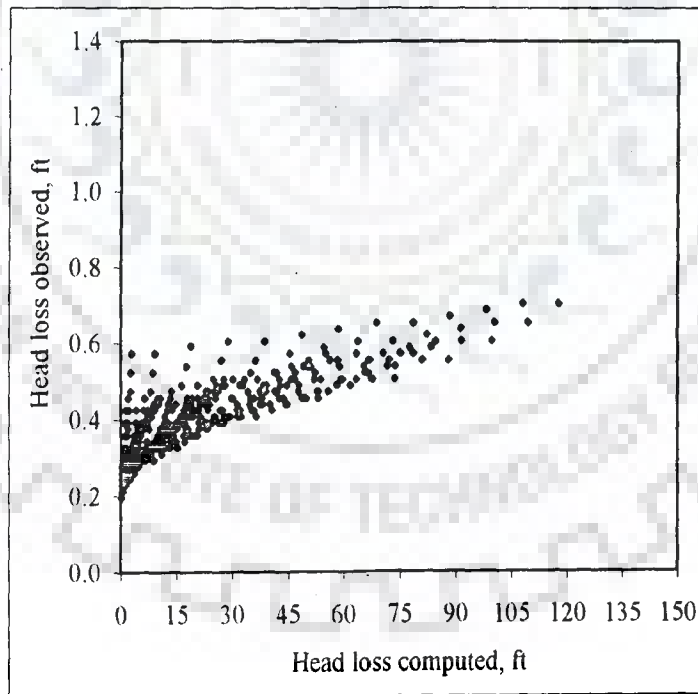


Fig. 4.14: Plot of head loss observed versus computed using H-C model for influent concentration of 40 mg/l (run nos. 60 to 64)

H-C model (Eq. 4.4) was also tested for the experimental runs data (nos. 65 to 89) for rainwater of 17 mg/l influent turbidity concentration. The average percentage error at different filter depths for each of the filter runs is presented in Table 4.9. From the Table 4.9, maximum APE of 6381.62% (run no. 89) is computed. This indicates the much deviation between observed head loss and computed head loss values. Figure 4.15 shows deviation of computed head loss values with observed head loss values. Hence, it is clear that H-C model is incompatible to predict the performance of sand filters in terms of head loss for rainwater samples.

4.4.2 Model Testing for Horizontal Flow Filter

From the above study of vertically downward flow filters (section 4.4.1), it is clear that H-C model is incompatible to predict the filter performance in terms of head loss and hence, the behaviour of the model is again evaluated under horizontal flow filtering condition. An analysis of experimental runs (nos. 90 to 94) was done using H-C model (Eq. 4.4) for influent concentration of 30 mg/l. The average error of head loss is computed using all the observations obtained at different filter depths and filter runs. The average of such errors for each of the runs is presented in Table 4.10. From the Table 4.10, maximum APE of 1991.14% (run no. 90) is computed at 0.714 mm grain size and flow velocity of $1.65 \text{ m}^3/\text{hr}/\text{m}^2$. Figure 4.16 shows deviation of computed head loss values with observed head loss values.

Table 4.9: Computed APE of head loss using H-C model for influent concentration of 17 mg/l (run nos. 65 to 89)

Sand grain size (mm)	Flow velocity (m ³ /hr/m ²)	Influent turbidity (mg/l)	Computed APE
3.647	1.65	17	111.39
	3.30		390.45
	4.95		668.52
	6.60		966.43
	8.25		1432.29
2.366	1.65	17	257.00
	3.30		739.40
	4.95		1216.04
	6.60		1709.11
	8.25		2249.71
1.673	1.65	17	435.78
	3.30		1237.60
	4.95		1783.76
	6.60		2615.78
	8.25		3272.76
1.091	1.65	17	512.69
	3.30		1557.91
	4.95		2606.88
	6.60		3908.78
	8.25		5892.71
0.714	1.65	17	639.01
	3.30		1992.90
	4.95		3007.41
	6.60		4886.88
	8.25		6381.62

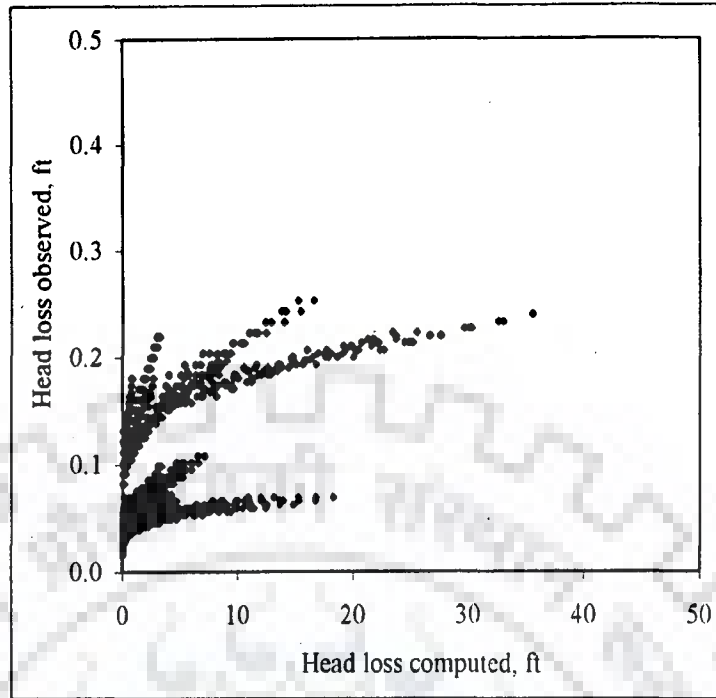


Fig. 4.15: Plot of head loss observed versus computed using H-C model for influent concentration of 17 mg/l (run nos. 65 to 89)

Table 4.10: Computed APE of head loss using H-C model for Fuller's earth suspension samples (run nos. 90 to 94 and 95 to 99) and rainwater samples (run nos. 100 to 104)

Sand grain size (mm)	Flow velocity (m ³ /hr/m ²)	Influent turbidity (mg/l)	Computed APE
0.714	1.65	30 (Fuller's earth)	1991.14
	3.30		1616.44
	4.95		1376.46
	6.60		1170.68
	8.25		1066.06
0.714	1.65	40 (Fuller's earth)	1745.74
	3.30		1404.76
	4.95		1249.89
	6.60		1171.34
	8.25		1065.98
0.714	1.65	17 (Rainwater)	14144.16
	3.30		36058.27
	4.95		58912.10
	6.60		77566.48
	8.25		101243.04

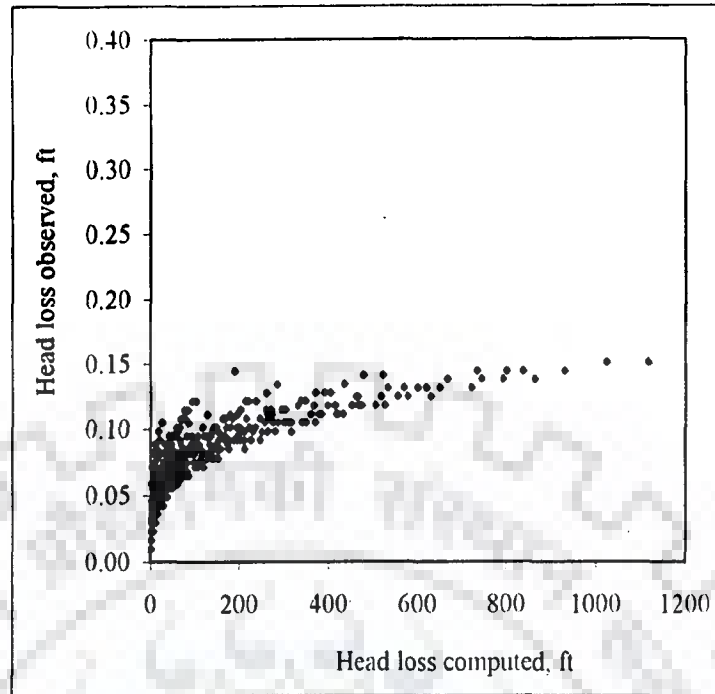


Fig. 4.16: Plot of head loss observed versus computed using H-C model for influent concentration of 30 mg/l (run nos. 90 to 94)

An analysis of experimental runs (nos. 95 to 99) was also done using H-C model (Eq. 4.4) for influent concentration of 40 mg/l. The average error of head loss is computed using all the observations obtained at different filter depths and filter runs. The average of such errors for each of the runs is presented in Table 4.10. From the Table 4.10, maximum APE of 1745.74% (run no. 95) is computed at 0.714 mm grain size and flow velocity of $1.65 \text{ m}^3/\text{hr}/\text{m}^2$. Figure 4.17 shows deviation of computed head loss values with observed head loss values.

An analysis of experimental runs (nos. 100 to 104) for rainwater samples of 17 mg/l influent turbidity concentration was also done using H-C model (Eq. 4.4). The average of such errors for each of the runs is presented in Table 4.10. From the Table 4.10, maximum APE of 101243.04% (run no. 104) is computed at 0.714 mm grain size and flow velocity of $8.25 \text{ m}^3/\text{hr}/\text{m}^2$. Figure 4.18 shows deviation of computed head loss values with observed head loss values. Hence, the above study reveals that the H-C model is incompatible for sand filter head loss performance prediction.

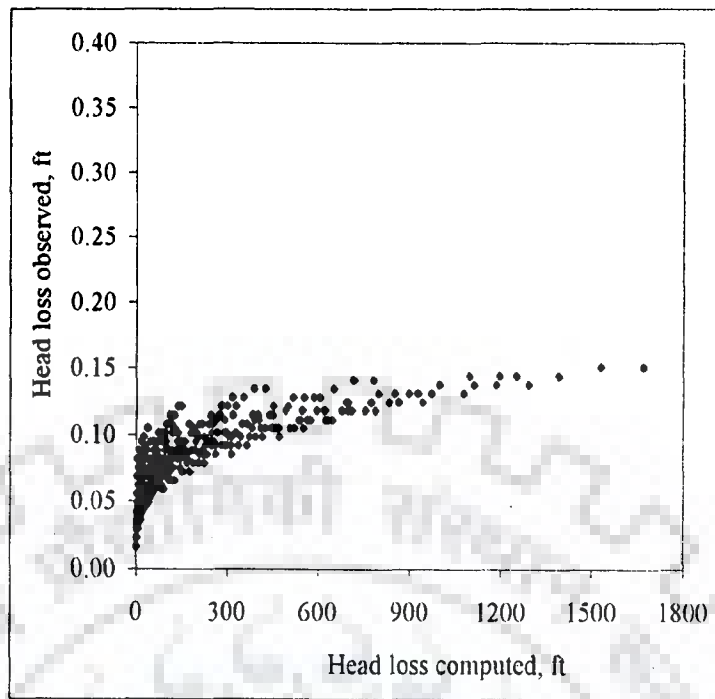


Fig. 4.17: Plot of head loss observed versus computed using H-C model for influent concentration of 40 mg/l (run nos. 95 to 99)

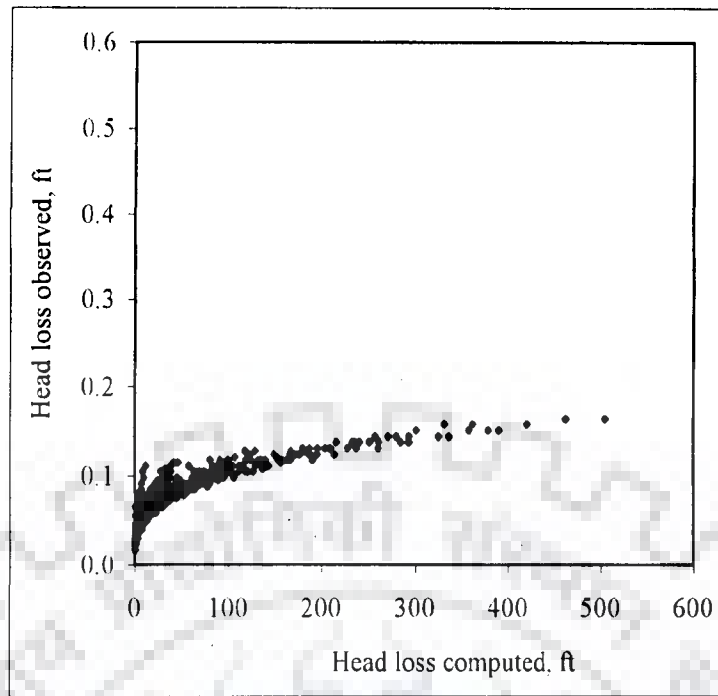


Fig. 4.18: Plot of head loss observed versus computed using H-C model for influent concentration of 17 mg/l (run nos. 100 to 104)

4.5 CONCLUDING REMARKS

Average percentage errors between observed and computed values of effluent quality and head loss for the cases of influent turbidity concentrations of 17 mg/l, 25 mg/l, 30 mg/l and 40 mg/l have been found in the range approximately from 50% to 100% for effluent concentration and from 50% to several thousands for head loss. This strongly reveals the incompatibility of H-C models for the prediction of sand filter performance. It seems that H-C models are very specific for a particular grain size, flow rate, depth of filter and concentration of suspended materials in the liquid. Based on the sand filter module studied in the laboratory, there is a need to develop new models using different experimental runs based on effluent quality criteria and head loss criteria approach.



MODELLING OF SAND FILTER PERFORMANCE

5.1 PREAMBLE

Previous chapter indicates that the models developed by Hsiung and Cleasby (1968) based on effluent quality and critical head loss are incompatible to predict the performance of sand filters under different experimental conditions. With this in view, alternate mathematical models are developed for vertically downward flow and horizontal flow sand filters for performance prediction. In this section, regression models are developed for each grain size and with lumped data for influent concentration of 30 mg/l under vertically downward flow (run nos. 28 to 54) and horizontal flow (run nos. 90 to 94) conditions. The behavior of these models is also tested at higher and lower influent concentrations. The models developed under vertically downward flow condition are tested against influent concentrations of 25 mg/l run data (run nos. 1 to 27) and 40 mg/l run data (run nos. 55 to 64). In the similar fashion, the model developed under horizontal flow condition is also tested against influent concentration of 40 mg/l run data (run nos. 95 to 99).

5.2 MODELLING FOR EFFLUENT QUALITY

As a basis for the new model development, G has been modified. Here, G' and G'' are introduced for vertically downward flow and horizontal flow filters. G' and G'' are considered as a function of flow velocity, Q ($\text{m}^3/\text{hr}/\text{m}^2$), sand grain size, d (mm) and time of filter run, t (hr.).

5.2.1 Modelling for Vertically Downward Flow Filters

To obtain G' , approach suggested by Hsiung and Cleasby (1968) is followed. When plotting the U values against filter run time obtained from experimental data (run no. 48), curves show a slightly definite converging trend and approach nearly constant slopes as shown in Fig. 5.1. An equi U curve (Fig. 5.2) has been obtained from Fig. 5.1 using filter depth and filter run time as coordinate by taking values of L and t at arbitrarily selected U levels ($U = 1, 2, 5, 10, 15, 20$). The U value for a given filter depth increases significantly with filter runtime, t , even if the filtrate quality does not change significantly. The curves in Fig. 5.1 do not show only a definite trend but also a typical shape regardless of the flow rate, grain size and influent concentration being used.

The selected run values at different flow velocities and times for experimental run data (run nos. 48 to 52) are shown in Fig. 5.3. An equi U plot for flow velocity and filter runtime has been obtained from Fig. 5.3 and shown in Fig. 5.4. The curves of Fig. 5.4 reveal that the nature of slope of each curve is slightly different and varying between (-8.33) and (-2.78) . Therefore, $\log Q \alpha (-1/0.12) \log t$ or $t \alpha 1/Q^{0.12}$ and $\log Q \alpha (-1/0.36) \log t$ or $t \alpha 1/Q^{0.36}$ were achieved. If the slope of the curves would have been same then a single coefficient value might have been considered. But in this case, a graph was plotted between observed and computed influent concentration in combination with each and every coefficient of Q to get the minimum average percentage error (APE). The minimum APE was obtained at $1/Q^{0.12}$. This indicates that for a given value of $Q^{0.12} t$, the U value is constant for a given filter depth.

A similar approach has been applied to evaluate the effect of grain size on filtrate quality while the flow rate was kept constant in different runs. The results of experimental data (run nos. 28 to 52) obtained for different grain sizes and times at particular flow

velocity of $1.65 \text{ m}^3/\text{hr}/\text{m}^2$ are presented in Fig. 5.5. An equiU plot for grain sizes and filter runtime has been obtained from Fig. 5.5 and shown in Fig. 5.6. The curves of Fig. 5.6 reveal that the nature of slope of each curve is slightly different and varying between (-4.35) and (-2.56). Therefore, $\log \alpha(-1/0.23) \log t$ or $\alpha 1/d^{0.23}$ and $\log \alpha(-1/0.39) \log t$ or $\alpha 1/d^{0.39}$ were achieved. If the slope of the curves would have been same then a single coefficient value might have been considered. But in this case, a graph was plotted between observed and computed influent concentration in combination with each and every coefficient of d to get the minimum average percentage error (APE). The minimum APE was obtained at $d^{0.35} \cdot t$. This indicates that for a given value of $d^{0.35} \cdot t$, the U value is constant for a given filter depth.

After combining these two terms at constant value of U, a new grouped term called G' is formulated and is given as;

$$G' = Q^{0.12} d^{0.35} t \quad (5.1)$$

Using G', U and L, a series of regression equations for each grain size are developed, as given in Table 5.1. For each of the runs (nos. 28 to 54), C has been computed at different times and errors are computed at these times using observed values. The experimental runs data (run nos. 28 to 54) were used for development of new regression models for effluent quality.

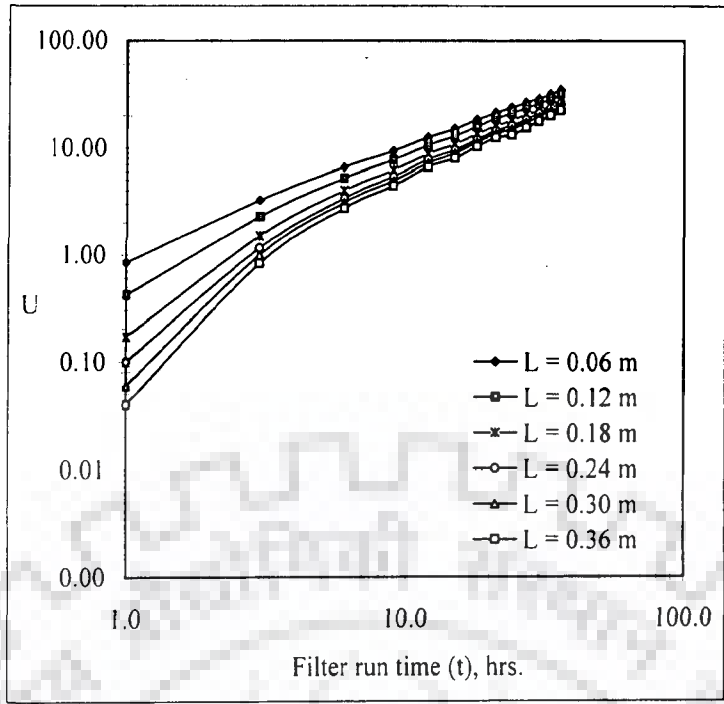


Fig. 5.1: Plot of U versus t at constant grain size and flow velocity (run no. 48)

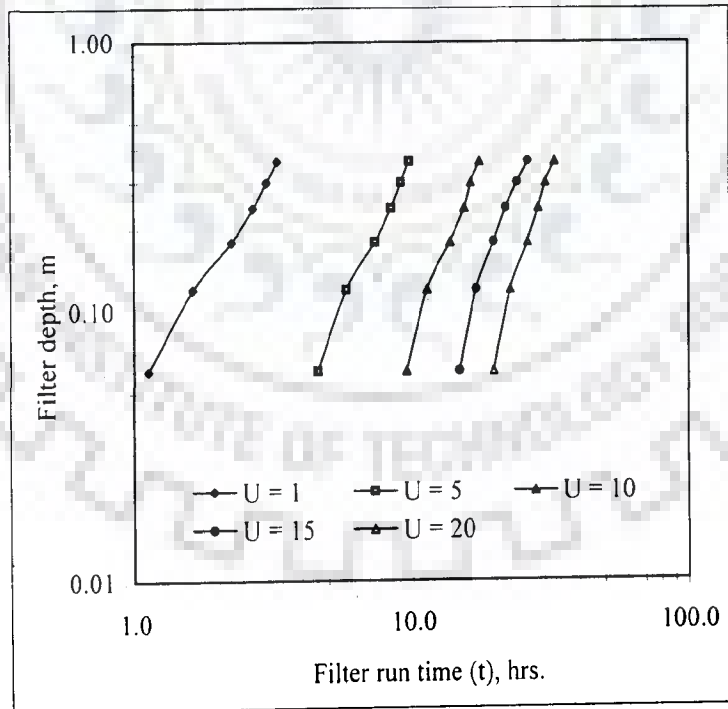


Fig. 5.2: Plot of equi U curve for filter depth versus filter run time (run no. 48)

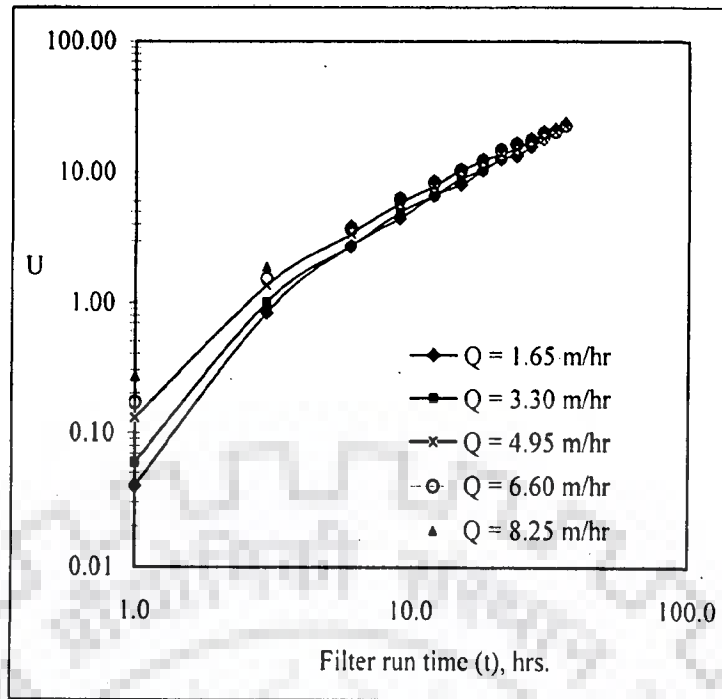


Fig. 5.3: Plot of U versus filter run time for different flow rates at constant grain size (run nos. 48 to 52)

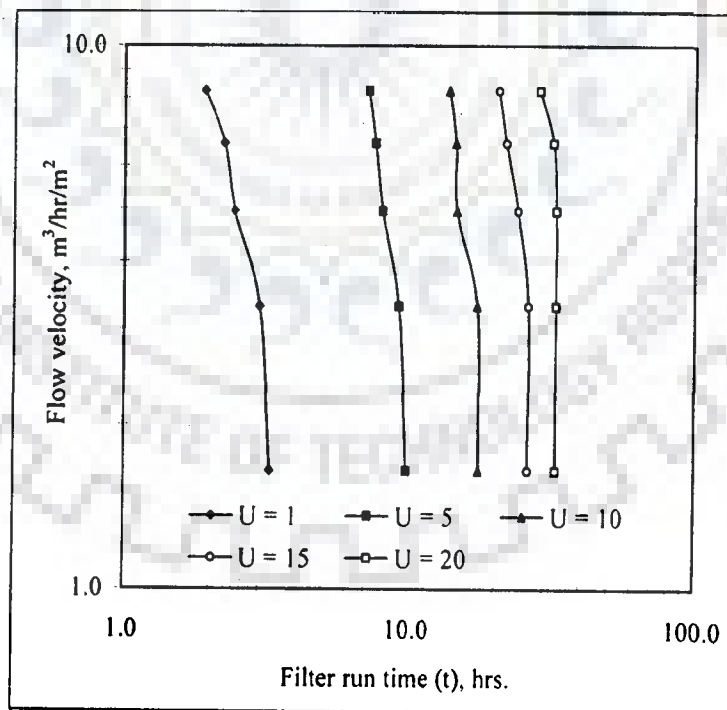


Fig. 5.4: Plot of $equU$ for flow velocity versus filter run time (run nos. 48 to 52)

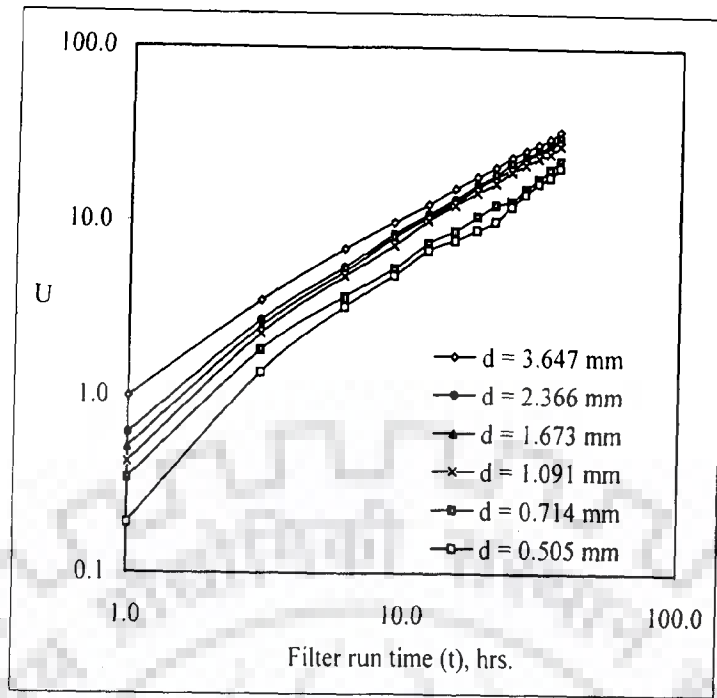


Fig. 5.5: Plot of U versus filter run time at different grain sizes (run nos. 28 to 52)

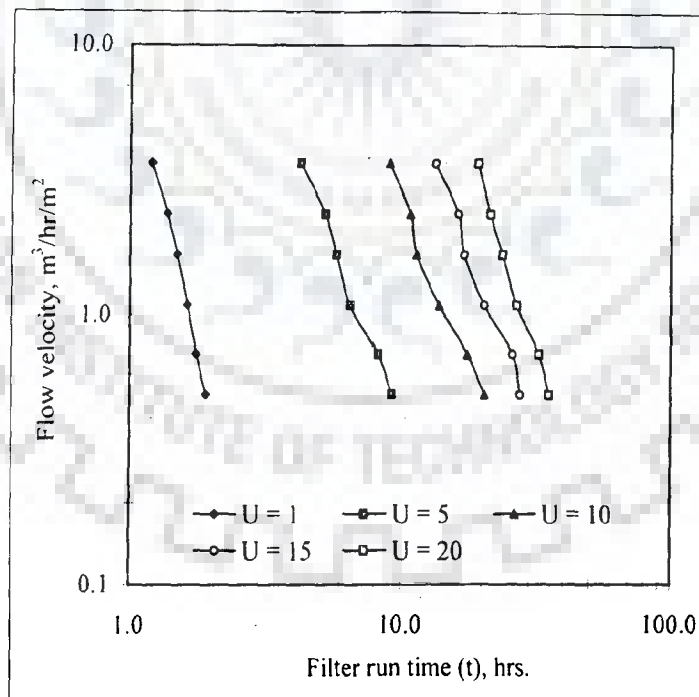


Fig. 5.6: Plot of equi U for flow velocity versus filter run time (run nos. 28 to 52)

Table 5.1: Computed APE of U and C using new developed individual regression model (run nos. 28 to 54)

Grain size (mm)	Models name	New models	Flow velocity (m ³ /hr/m ²)		Computed APE	
			U	C	U	C
3.647	MOVEQ-30A	$\log\left(\frac{U}{L}\right) = -0.494 + 1.196 \log\left(\frac{G'}{L^{1.5}}\right) - 0.081 \left[\log\left(\frac{G'}{L^{1.5}}\right)\right]^2$ $G' = Q^{0.12} d^{0.35} t; R^2 = 0.996$	1.65	7.30	9.53	
			3.30	3.68	3.84	
			4.95	2.91	3.52	
			6.60	5.93	6.96	
			8.25	6.51	7.36	
				4.76	7.74	
2.366	MOVEQ-30B	$\log\left(\frac{U}{L}\right) = -0.635 + 1.351 \log\left(\frac{G'}{L^{1.5}}\right) - 0.115 \left[\log\left(\frac{G'}{L^{1.5}}\right)\right]^2$ $G' = Q^{0.12} d^{0.35} t; R^2 = 0.995$	1.65	5.12	7.63	
			3.30	5.33	7.87	
			4.95	5.68	5.79	
			6.60	5.43	5.71	
			8.25	5.52	12.25	
				4.67	7.85	
1.673	MOVEQ-30C	$\log\left(\frac{U}{L}\right) = -0.396 + 1.376 \log\left(\frac{G'}{L^{1.5}}\right) - 0.110 \left[\log\left(\frac{G'}{L^{1.5}}\right)\right]^2$ $G' = Q^{0.12} d^{0.35} t; R^2 = 0.995$	1.65	4.65	7.00	
			3.30	5.09	6.64	
			4.95	5.90	6.20	
			6.60	5.02	10.92	
			8.25	4.33	6.57	
				5.13	6.31	
1.091	MOVEQ-30D	$\log\left(\frac{U}{L}\right) = -0.679 + 1.452 \log\left(\frac{G'}{L^{1.5}}\right) - 0.137 \left[\log\left(\frac{G'}{L^{1.5}}\right)\right]^2$ $G' = Q^{0.12} d^{0.35} t; R^2 = 0.986$	1.65	5.48	7.37	
			3.30	10.22	13.63	
			4.95	5.62	11.96	
			6.60	5.38	9.87	
			8.25	6.77	15.44	
				7.19	15.29	
0.714	MOVEQ-30E	$\log\left(\frac{U}{L}\right) = -1.579 + 2.017 \log\left(\frac{G'}{L^{1.5}}\right) - 0.221 \left[\log\left(\frac{G'}{L^{1.5}}\right)\right]^2$ $G' = Q^{0.12} d^{0.35} t; R^2 = 0.995$	1.65	7.16	13.47	
			3.30	6.62	15.92	
			4.95	8.40	28.64	
			6.60	8.40	28.64	
			8.25	8.40	28.64	
				8.40	28.64	
0.505	MOVEQ-30F	$\log\left(\frac{U}{L}\right) = -0.840 + 1.497 \log\left(\frac{G'}{L^{1.5}}\right) - 0.137 \left[\log\left(\frac{G'}{L^{1.5}}\right)\right]^2$ $G' = Q^{0.12} d^{0.35} t; R^2 = 0.995$	1.65	6.62	15.92	
			3.30	8.40	28.64	

From the Table 5.1, it can be seen that the calibration errors are much reduced and are as low as 3.52% (run no. 30) and as high as 28.64% (run no. 54) using an individual model. Attempts were also made to develop unified regression relationships (MOVEQ-30AL) using lumped data for all grain sizes at 30 mg/l influent concentration, as given in Table 5.2. It can be seen from Table 5.2 that the errors are increased due to unification of data pertaining to different grain sizes. An agreement between observed and computed effluent concentrations using the unified regression model (MOVEQ-30AL) for influent concentration of 30 mg/l (run nos. 28 to 54) is shown in Fig. 5.7.

Now, the new unified regression model (MOVEQ-30AL) has been tested for the lumped data of experimental run (nos. 1 to 27) for the computation of average errors of effluent quality for influent concentration of 25 mg/l. The errors of the unified model are given in Table 5.3. From the Table 5.3, it can be seen that the calibration errors are as low as 6.70% (run no. 33) and as high as 29.74% (run no. 45) using the unified regression model. An agreement between observed and computed concentrations using the unified regression model for influent concentration of 25 mg/l (run nos. 1 to 27) is shown in Fig. 5.8. From the Fig. 5.8, it can be seen that the behaviour of the model with influent concentration of 25 mg/l is similar to the behaviour with influent concentration of 30 mg/l.

The unified model is again tested against influent concentration of 40 mg/l (run nos. 55 to 64). The errors for individual grain size are presented in Table 5.4. It can be seen from the Table 5.4 that the errors are within the acceptable range. An agreement between observed and computed concentrations for filter run nos. 55 to 59 and filter run nos. 60 to 64 is shown in Figs. 5.9 & 5.10, respectively. Hence, the new unified regression model is compatible to predict the performance of sand filters in terms of effluent quality.

Table 5.2: Computed APE of U and C using new developed unified model (MOVEQ-30AL) (run nos. 28 to 54)

Grain size (mm)	Model name	New model	Flow velocity (m ³ /hr/m ²)	Computed APE	
				U	C
3.647	MOVEQ-30AL	$\log\left(\frac{U}{L}\right) = -0.907 + 1.549 \log\left(\frac{G'}{L^{1.5}}\right) - 0.147 \left[\log\left(\frac{G'}{L^{1.5}}\right)\right]^2$ $G' = Q^{0.12} d^{10.35} t; R^2 = 0.978$	1.65	6.41	7.59
			3.30	12.40	14.72
			4.95	12.08	12.43
			6.60	16.69	17.12
			8.25	16.92	17.18
			1.65	5.92	6.99
2.366	MOVEQ-30AL	$\log\left(\frac{U}{L}\right) = -0.907 + 1.549 \log\left(\frac{G'}{L^{1.5}}\right) - 0.147 \left[\log\left(\frac{G'}{L^{1.5}}\right)\right]^2$ $G' = Q^{0.12} d^{10.35} t; R^2 = 0.978$	3.30	8.90	12.07
			4.95	10.22	13.28
			6.60	10.07	10.79
			8.25	10.59	11.16
			1.65	5.28	9.33
			3.30	6.75	10.11
1.673	MOVEQ-30AL	$\log\left(\frac{U}{L}\right) = -0.907 + 1.549 \log\left(\frac{G'}{L^{1.5}}\right) - 0.147 \left[\log\left(\frac{G'}{L^{1.5}}\right)\right]^2$ $G' = Q^{0.12} d^{10.35} t; R^2 = 0.978$	4.95	7.84	12.59
			6.60	8.20	12.25
			8.25	8.66	11.03
			1.65	14.74	29.34
			3.30	11.73	21.09
			4.95	11.51	17.86
1.091	MOVEQ-30AL	$\log\left(\frac{U}{L}\right) = -0.907 + 1.549 \log\left(\frac{G'}{L^{1.5}}\right) - 0.147 \left[\log\left(\frac{G'}{L^{1.5}}\right)\right]^2$ $G' = Q^{0.12} d^{10.35} t; R^2 = 0.978$	6.60	12.23	16.51
			8.25	9.71	10.81
			1.65	13.89	23.05
			3.30	13.30	18.95
			4.95	12.82	18.96
			6.60	11.36	16.63
0.714	MOVEQ-30AL	$\log\left(\frac{U}{L}\right) = -0.907 + 1.549 \log\left(\frac{G'}{L^{1.5}}\right) - 0.147 \left[\log\left(\frac{G'}{L^{1.5}}\right)\right]^2$ $G' = Q^{0.12} d^{10.35} t; R^2 = 0.978$	8.25	9.18	13.98
			1.65	18.26	27.45
			3.30	17.29	25.61

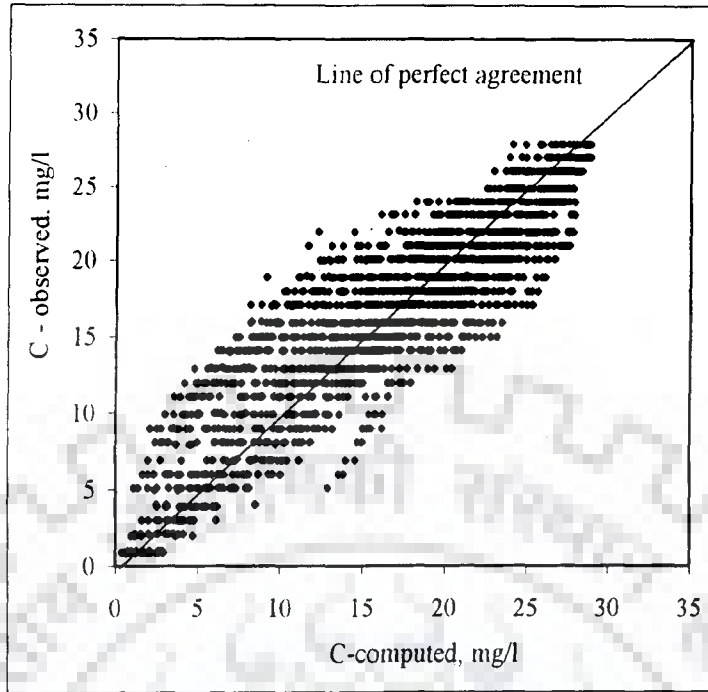


Fig. 5.7: Plot of C-observed versus C-computed using model (MOVEQ-30AL) for influent concentration of 30 mg/l (run nos. 28 to 54)

Table 5.3: Computed APE of U and C using unified model (MOVEQ-30AL) for influent concentration of 25 mg/l (run nos. 1 to 27)

Grain size (mm)	Model name	New model	Flow velocity (m ³ /hr/m ²)		Computed APE	
			U	C	U	C
3.647			1.65	7.49	7.55	7.55
			3.30	7.17	8.56	8.56
			4.95	7.02	8.57	8.57
2.366			6.60	7.06	9.10	9.10
			8.25	7.42	8.86	8.86
			1.65	5.33	6.70	6.70
1.673			3.30	8.79	11.74	11.74
			4.95	9.32	10.53	10.53
			6.60	10.57	12.85	12.85
1.091			8.25	10.44	12.71	12.71
			1.65	6.02	10.14	10.14
			3.30	8.70	13.32	13.32
0.714			4.95	10.23	17.98	17.98
			6.60	9.29	17.47	17.47
			8.25	9.82	17.87	17.87
0.505			1.65	22.15	25.90	25.90
			3.30	20.01	20.74	20.74
			4.95	22.01	29.74	29.74
			6.60	20.61	27.23	27.23
			8.25	17.74	18.28	18.28
			1.65	20.69	24.97	24.97
			3.30	27.04	29.57	29.57
			4.95	21.90	26.37	26.37
			6.60	18.01	24.02	24.02
			8.25	13.67	25.12	25.12
			1.65	4.07	14.33	14.33
			3.30	5.25	19.38	19.38

$$\log\left(\frac{U}{L}\right) = -0.907 + 1.549 \log\left(\frac{G'}{L^{1.5}}\right) - 0.147 \left[\log\left(\frac{G'}{L^{1.5}}\right)\right]^2$$

$$G' = Q^{0.12} d^{0.35} t; R^2 = 0.978$$

MOVEQ-30AL.

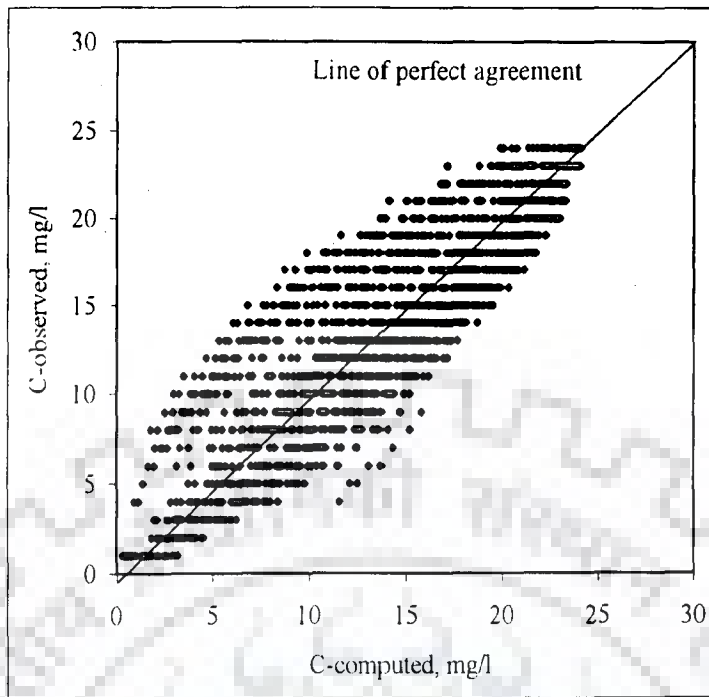


Fig. 5.8: Plot of C-observed versus C-computed using model (MOVEQ-30AL) for influent concentration of 25 mg/l (run nos. 1 to 27)

Table 5.4: Computed APE of U and C using unified model (MOVEQ-30AL) for influent concentration of 40 mg/l (run nos. 55 to 64)

Grain size (mm)	Model name	New model	Flow velocity (m ³ /hr/m ²)		Computed APE	
			U	C	U	C
1.091	MOVEQ-30AL	$\log\left(\frac{U}{L}\right) = -0.907 + 1.549 \log\left(\frac{G'}{L^{1.5}}\right) - 0.147 \left[\log\left(\frac{G'}{L^{1.5}}\right) \right]^2$ $G' = Q^{0.12} d^{0.35} t; R^2 = 0.978$	1.65	11.30	6.73	11.30
			3.30	10.56	7.02	10.56
			4.95	13.11	9.34	13.11
			6.60	5.10	4.10	5.10
			8.25	8.65	7.84	8.65
0.714	MOVEQ-30AL	$\log\left(\frac{U}{L}\right) = -0.907 + 1.549 \log\left(\frac{G'}{L^{1.5}}\right) - 0.147 \left[\log\left(\frac{G'}{L^{1.5}}\right) \right]^2$ $G' = Q^{0.12} d^{0.35} t; R^2 = 0.978$	1.65	7.59	4.28	7.59
			3.30	6.36	3.19	6.36
			4.95	5.41	2.55	5.41
			6.60	8.60	3.19	8.60
			8.25	9.56	5.45	9.56

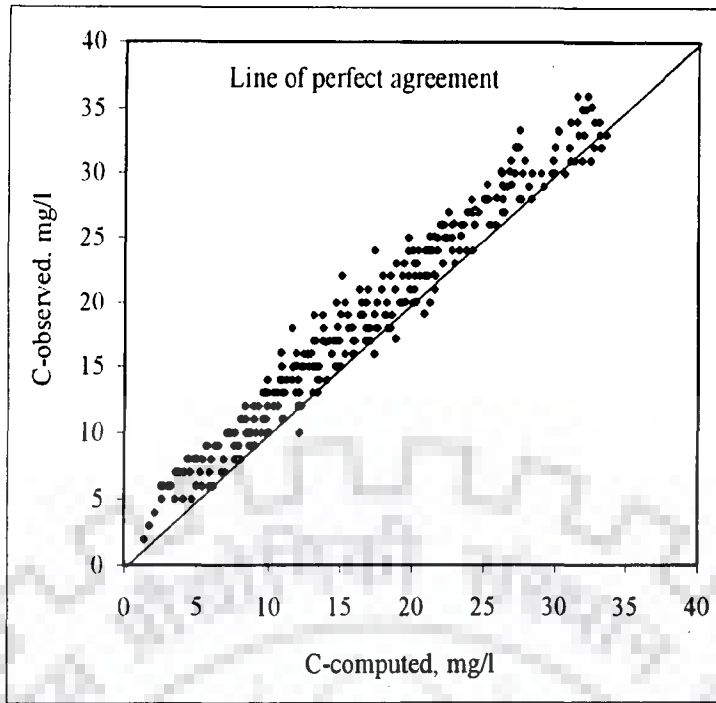


Fig.5.9: Plot of C-observed versus C-computed using model (MOVEQ-30AL) for influent concentration of 40 mg/l (run nos. 55 to 59)

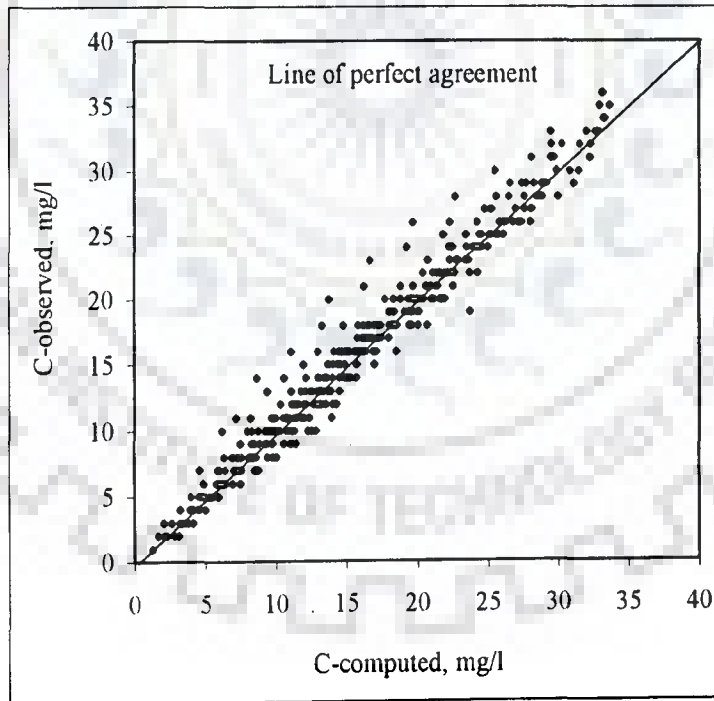


Fig.5.10: Plot of C-observed versus computed using model (MOVEQ-30AL) for influent concentration of 40 mg/l (run nos. 60 to 64)

5.2.2 Modelling for Horizontal Flow Filter

The above defined (section 5.2.1) grouped term G' does not seem compatible in case of horizontal flow filter. The assessment was done on the basis of APE and it was found very high. Hence, new G'' has been developed in a similar fashion as described in section 5.2.1 and defined as;

$$G'' = Q^{0.19} d^{0.50} t \quad (5.2)$$

The unified model (MOHEQ-30E) was developed using the experimental run data (nos. 90 to 94) for influent concentration of 30 mg/l. Average percentage errors between observed and computed effluent concentrations using the unified model are given in Tables 5.5. From the Table 5.5 it can be seen that the errors are as low as 13.96% (run no. 90) and as high as 16.82% (run no. 91). An agreement between observed and computed values is shown in Fig. 5.11 and it also shows scattering of the values around the line of perfect agreement.

The performance of the unified model (MOHEQ-30E) is again tested for influent concentration of 40 mg/l (run nos. 95 to 99). The errors for effluent concentration are given in Table 5.6. It is clear from the Table 5.6 that the performance of the unified model is similar to the performance for influent concentration of 30 mg/l. The errors are found as low as 14.54% (run no. 96) and as high as 18.86% (run no. 99) which is very close to the errors given in Table 5.5. An agreement of between observed and computed values for influent concentrations of 40 mg/l is shown in Fig. 5.12 and it also shows scattering of the values about the line of perfect agreement. Hence, the unified model (MOHEQ-30E) has wide application for performance prediction of horizontal flow sand filter.

Table 5.5: Computed APE of U and C using new developed unified model (MOHEQ-30E) (run nos. 90 to 94)

Grain size (mm)	Model name	New model	Flow velocity (m ³ /hr/m ²)	Computed APE	
				U	C
0.714	MOHEQ-30E	$\log\left(\frac{U}{L}\right) = -1.091 + 1.684 \log\left(\frac{G''}{L^{1.9}}\right) - 0.192 \left[\log\left(\frac{G''}{L^{1.9}}\right) \right]^2$ $G'' = Q^{0.19} d^{0.50} t; R^2 = 0.994$	1.65	6.68	13.96
			3.3	7.12	16.82
			4.95	9.60	14.70
			6.6	10.34	16.12
			8.25	6.62	11.46

Table 5.6: Computed APE of U and C using unified model (MOHEQ-30E) for influent concentration of 40 mg/l (run nos. 95 to 99)

Grain size (mm)	Model name	New model	Flow velocity (m ³ /hr/m ²)	Computed APE	
				U	C
0.714	MOHEQ-30E	$\log\left(\frac{U}{L}\right) = -1.091 + 1.684 \log\left(\frac{G''}{L^{1.9}}\right) - 0.192 \left[\log\left(\frac{G''}{L^{1.9}}\right) \right]^2$ $G'' = Q^{0.19} d^{0.50} t; R^2 = 0.994$	1.65	6.97	16.97
			3.3	6.88	14.54
			4.95	8.52	16.75
			6.6	10.17	18.54
			8.25	10.37	18.86

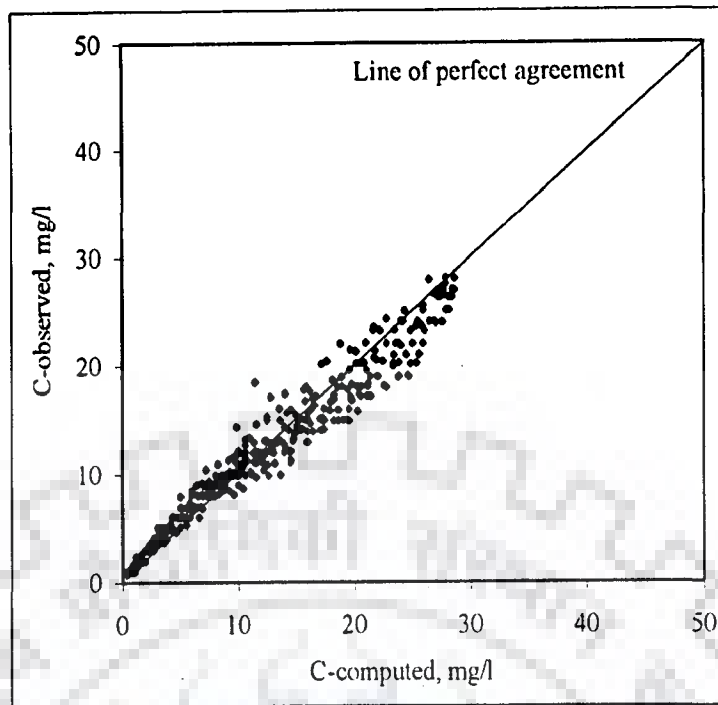


Fig. 5.11: Plot of C-observed versus C-computed using model (MOHEQ-30E) for influent concentration of 30 mg/l (run nos. 90 to 94)

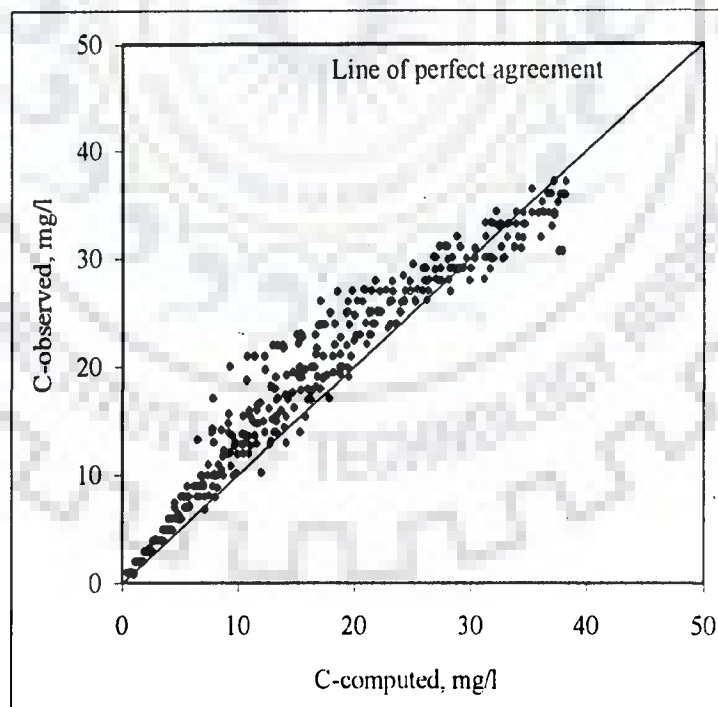


Fig. 5.12: Plot of C-observed versus C-computed using model (MOHEQ-30E) for influent concentration of 40 mg/l (run nos. 95 to 99)

5.3 MODELLING FOR FLOW RESISTANCE

5.3.1 Modelling for Vertically Downward Flow Filters

The parameter R is modified as R' for vertically downward flow sand filters. The new coefficients of R' are developed on the basis of the experimental run data (run nos. 48 to 52). For computation of R' , the procedure laid down by the Hsiung and Cleasby (1968) is followed. For any selected flow velocity, influent concentration, L and t , the values of U were plotted against the corresponding observed head loss for different grain sizes. It has been found that in an equi- U curve for d versus $(H_1 - H_0)$, the slopes were different for each curve. With the help of multiple regression analysis, the minimum APE was found at $(H_1 - H_0)d^{1.20}$, the U value was constant for the given depth (similar description is given in section 4.2.1.2). In a similar manner, it has also been found that for a given value of $(H_1 - H_0)Q^{0.19}$ or $(H_1 - H_0)C_0^{1.30}$, the U value was constant for a given depth. Then the four variables $(H_1 - H_0)$, Q , d , and C_0 have grouped into another term, R' . The resulting expression is given as;

$$R' = \left(\frac{d^{1.20} (H_1 - H_0)}{Q^{0.19} C_0^{1.30}} \right) \quad (5.3)$$

The experimental runs data (run nos. 28 to 54) were used for development of new regression models of head loss. The average errors for each grain size using new models are given in Table 5.7. Here, the average error of head loss is computed using all observations obtained at different filter depths and filter runs (nos. 28 to 54) for 30 mg/l influent turbidity concentration. From the Table 5.7, it can be seen that the maximum error of 25.23% (run no. 37) is computed.

Table 5.7: Computed APE for head loss using new developed individual regression model (run nos. 28 to 54)

Grain size (mm)	Models name	New models	Flow velocity (m ³ /hr/m ²)	Computed APE
3.647	MOVEHL-30A	$\log\left(\frac{R'}{L^{1.3}}\right) = -2.238 - 0.587 \log\left(\frac{G'}{L^{1.5}}\right) + 0.227 \left[\log\left(\frac{G'}{L^{1.5}}\right)\right]^2$ $R' = \left[\left(d^{1.20} (H_t - H_o) \right) / \left(Q^{0.19} C_o^{1.30} \right) \right]; R^2 = 0.695$	1.65	19.43
			3.30	21.26
			4.95	23.70
			6.60	23.49
			8.25	24.04
2.366	MOVEHL-30B	$\log\left(\frac{R'}{L^{1.3}}\right) = -2.505 - 0.551 \log\left(\frac{G'}{L^{1.5}}\right) + 0.228 \left[\log\left(\frac{G'}{L^{1.5}}\right)\right]^2$ $R' = \left[\left(d^{1.20} (H_t - H_o) \right) / \left(Q^{0.19} C_o^{1.30} \right) \right]; R^2 = 0.709$	1.65	20.43
			3.30	20.40
			4.95	22.48
			6.60	24.32
			8.25	25.23
1.673	MOVEHL-30C	$\log\left(\frac{R'}{L^{1.3}}\right) = -2.285 - 0.554 \log\left(\frac{G'}{L^{1.5}}\right) + 0.213 \left[\log\left(\frac{G'}{L^{1.5}}\right)\right]^2$ $R' = \left[\left(d^{1.20} (H_t - H_o) \right) / \left(Q^{0.19} C_o^{1.30} \right) \right]; R^2 = 0.788$	1.65	15.77
			3.30	18.01
			4.95	20.45
			6.60	21.82
			8.25	20.79
1.091	MOVEHL-30D	$\log\left(\frac{R'}{L^{1.3}}\right) = -2.617 - 0.481 \log\left(\frac{G'}{L^{1.5}}\right) + 0.227 \left[\log\left(\frac{G'}{L^{1.5}}\right)\right]^2$ $R' = \left[\left(d^{1.20} (H_t - H_o) \right) / \left(Q^{0.19} C_o^{1.30} \right) \right]; R^2 = 0.720$	1.65	20.27
			3.30	21.31
			4.95	23.31
			6.60	23.23
			8.25	22.86
0.714	MOVEHL-30E	$\log\left(\frac{R'}{L^{1.3}}\right) = -2.275 - 0.510 \log\left(\frac{G'}{L^{1.5}}\right) + 0.215 \left[\log\left(\frac{G'}{L^{1.5}}\right)\right]^2$ $R' = \left[\left(d^{1.20} (H_t - H_o) \right) / \left(Q^{0.19} C_o^{1.30} \right) \right]; R^2 = 0.763$	1.65	18.49
			3.30	20.61
			4.95	21.61
			6.60	21.51
			8.25	21.23
0.505	MOVEHL-30F	$\log\left(\frac{R'}{L^{1.3}}\right) = -2.507 - 0.483 \log\left(\frac{G'}{L^{1.5}}\right) + 0.218 \left[\log\left(\frac{G'}{L^{1.5}}\right)\right]^2$ $R' = \left[\left(d^{1.20} (H_t - H_o) \right) / \left(Q^{0.19} C_o^{1.30} \right) \right]; R^2 = 0.771$	1.65	17.70
			3.30	22.60

Now, the new unified regression relationship (MOVEHL-30AL) is developed with the experimental runs data (nos. 28 to 54) for influent concentration of 30 mg/l. The performance of the model for each grain size is presented in Table 5.8. It can be seen from Table 5.8 that the errors are increased due to unification of data pertaining to different grain sizes. Using the unified regression model from Table 5.8, Fig. 5.13 shows scattering of the values around the line of perfect agreement.

Now, the new unified regression model (MOVEHL-30AL) has been tested for the computation of average errors for head loss for influent concentration of 25 mg/l (nos. 1 to 27). The errors for individual run are given in Table 5.9. From the Table 5.9, it can be seen that the calibration errors are as low as 14.01% (run no. 11) and as high as 34.22% (run no. 27) using the unified model. An agreement between observed and computed head for influent concentration of 25 mg/l (run nos. 1 to 27) is shown in Fig. 5.14. From the Fig. 5.14, it can be seen that the behaviour of the model with influent concentration of 25 mg/l is similar to the behaviour with influent concentration of 30 mg/l.

The unified model (MOVEHL-30AL) is again tested for head loss against influent concentration of 40 mg/l (run nos. 55 to 64). The errors for individual grain size are presented in Table 5.10. It can be seen from the Table 5.10 that the errors are even in the lower ranges than the errors computed at influent concentration of 30 mg/l and hence, it is clear that the unified regression model (MOVEHL-30AL) has some potential for application of head loss prediction provided these APE values are accepted. An agreement between observed and computed head loss for run nos. 55 to 59 and run nos. 60 to 64 is shown in Figs. 5.15 & 5.16, respectively. Although the head loss values are not very high, scattering of the data around the line of perfect agreement is noticeable.

Table 5.8: Computed APE for head loss using new developed unified model (MOVEHL-30AL) (run nos. 28 to 54)

Grain size (mm)	Model name	New model	Flow velocity (m ³ /hr/m ²)	Computed APE
3.647	MOVEHL-30AL	$\log\left(\frac{R'}{L^{1.3}}\right) = -2.453 - 0.483 \log\left(\frac{G'}{L^{1.5}}\right) + 0.212 \left[\log\left(\frac{G'}{L^{1.5}}\right)\right]^2$ $R' = [(d^{1.20}(H_i - H_o)) / (Q^{0.19} C_o^{1.30})]; R^2 = 0.694$	1.65	23.01
			3.30	22.40
4.95			24.64	
6.60			26.53	
8.25			26.99	
1.65			23.06	
3.30			34.84	
4.95			35.65	
6.60			37.91	
8.25			36.36	
1.673	MOVEHL-30AL	$\log\left(\frac{R'}{L^{1.3}}\right) = -2.453 - 0.483 \log\left(\frac{G'}{L^{1.5}}\right) + 0.212 \left[\log\left(\frac{G'}{L^{1.5}}\right)\right]^2$ $R' = [(d^{1.20}(H_i - H_o)) / (Q^{0.19} C_o^{1.30})]; R^2 = 0.694$	1.65	15.48
			3.30	20.37
4.95			22.82	
6.60			24.62	
8.25			23.95	
1.65			19.62	
3.30			27.03	
4.95			28.79	
6.60			26.21	
8.25			23.18	
0.714	MOVEHL-30AL	$\log\left(\frac{R'}{L^{1.3}}\right) = -2.453 - 0.483 \log\left(\frac{G'}{L^{1.5}}\right) + 0.212 \left[\log\left(\frac{G'}{L^{1.5}}\right)\right]^2$ $R' = [(d^{1.20}(H_i - H_o)) / (Q^{0.19} C_o^{1.30})]; R^2 = 0.694$	1.65	26.35
			3.30	25.17
4.95			26.69	
6.60			25.58	
8.25			30.82	
1.65			19.14	
3.30			25.77	

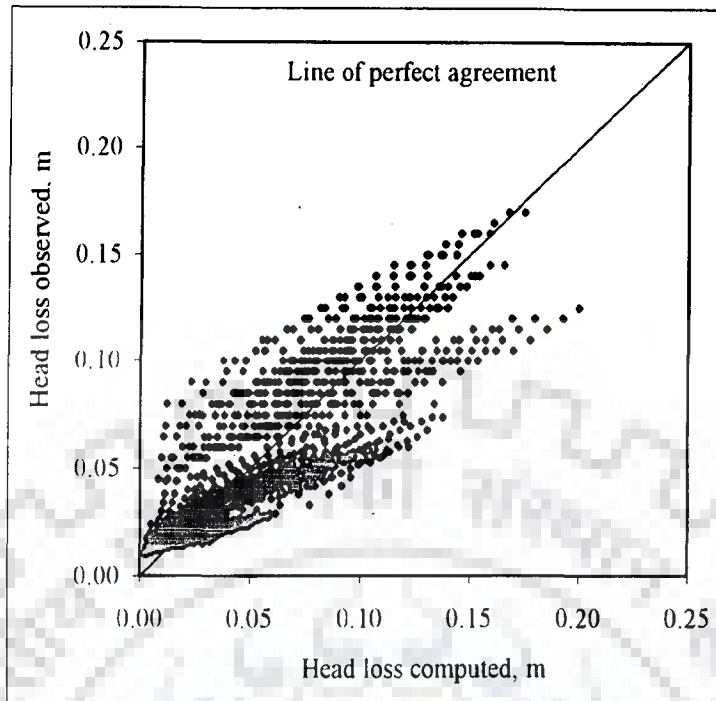


Fig. 5.13: Plot of head loss observed versus computed using model (MOVEHL-30AL) for influent concentration of 30 mg/l (run nos. 28 to 54)

Table 5.9: Computed APE for head loss using unified model (MOVEHL-30AL) for influent concentration of 25 mg/l (run nos. 1 to 27)

Grain size (mm)	Model name	New model	Flow velocity (m ³ /hr/m ²)	Computed APE
3.647			1.65	19.50
			3.30	21.53
			4.95	28.45
2.366			6.60	26.89
			8.25	31.50
			1.65	19.99
1.673	MOVEHL-30AL	$\log\left(\frac{R'}{L^{1.3}}\right) = -2.453 - 0.483 \log\left(\frac{G'}{L^{1.5}}\right) + 0.212 \left[\log\left(\frac{G'}{L^{1.5}}\right) \right]^2$ $R' = [(d^{1.20}(H_t - H_o)) / (Q^{0.19} C_o^{1.30})]; R^2 = 0.694$	3.30	15.79
			4.95	17.34
			6.60	18.89
1.091			8.25	19.99
			1.65	19.16
			3.30	20.30
0.714			4.95	22.52
			6.60	22.99
			8.25	20.41
0.505			1.65	17.87
			3.30	20.56
			4.95	20.57
			6.60	20.95
			8.25	22.06
			1.65	25.72
			3.30	34.22

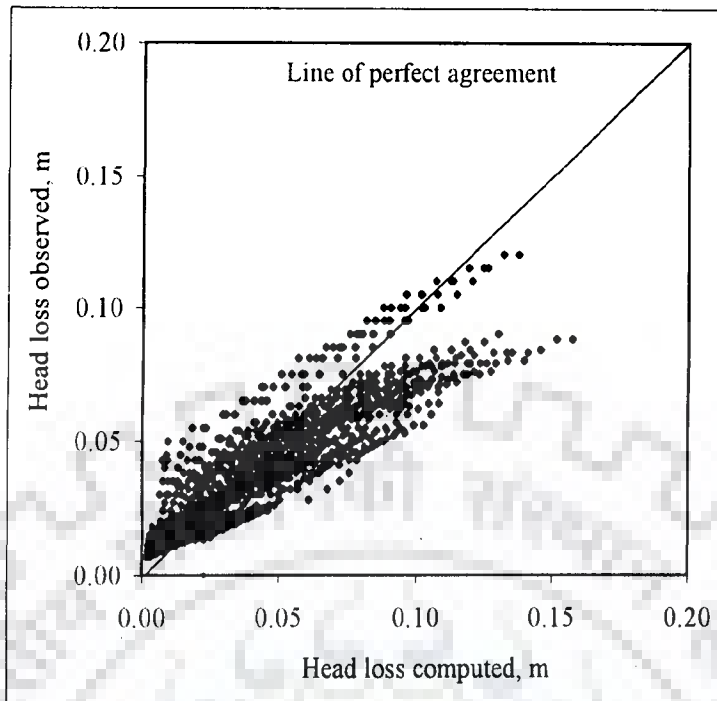


Fig. 5.14: Plot of head loss observed versus computed using model (MOVEHL-30AL) for influent concentration of 25 mg/l (run nos. 1 to 27)

Table 5.10: Computed APE for head loss using unified model (MOVEHL-30AL) for influent concentration of 40 mg/l (run nos. 55 to 64)

Grain size (mm)	Model name	New model	Flow velocity (m ² /hr/m ²)	Computed APE
1.091	MOVEHL-30AL	$\log\left(\frac{R'}{L^{1.5}}\right) = -2.453 - 0.483 \log\left(\frac{G'}{L^{1.5}}\right) + 0.212 \left[\log\left(\frac{G'}{L^{1.5}}\right)\right]^2$ $R' = \left[(d^{1.20} (H_1 - H_0)) / (Q^{0.19} C_0^{1.30}) \right]; R^2 = 0.694$	1.65	19.84
			3.30	17.50
			4.95	18.37
			6.60	19.02
			8.25	19.87
0.714	MOVEHL-30AL	$\log\left(\frac{R'}{L^{1.5}}\right) = -2.453 - 0.483 \log\left(\frac{G'}{L^{1.5}}\right) + 0.212 \left[\log\left(\frac{G'}{L^{1.5}}\right)\right]^2$ $R' = \left[(d^{1.20} (H_1 - H_0)) / (Q^{0.19} C_0^{1.30}) \right]; R^2 = 0.694$	1.65	22.84
			3.30	18.87
			4.95	20.31
			6.60	21.76
			8.25	24.04

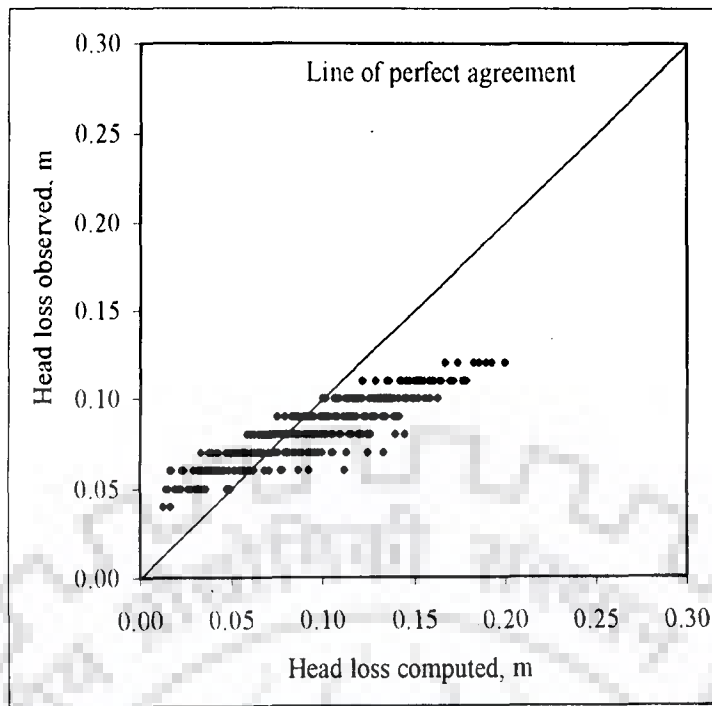


Fig.5.15: Plot of head loss observed versus computed using model (MOVEHL-30AL) for influent concentration of 40 mg/l (run nos. 55 to 59)

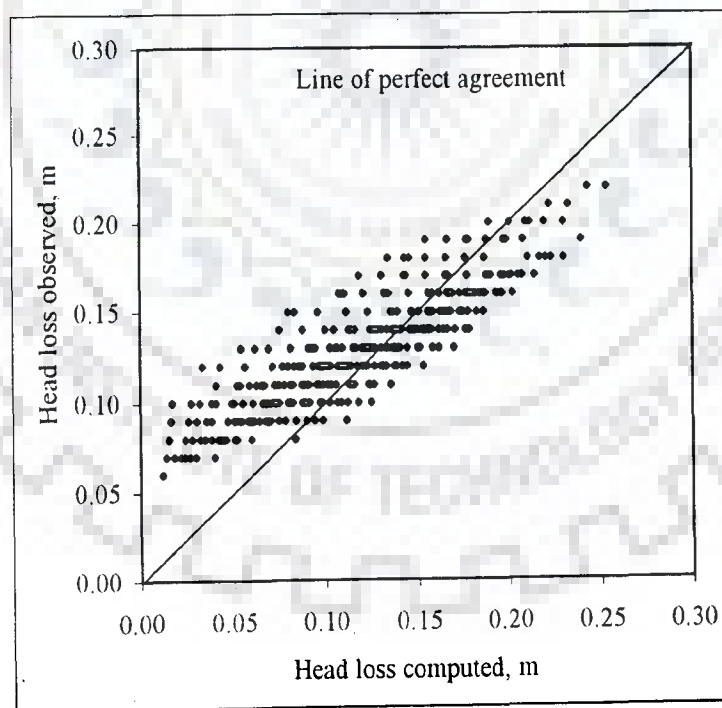


Fig.5.16: Plot of head loss observed versus computed using model (MOVEHL-30AL) for influent concentration of 40 mg/l (run nos. 60 to 64)

5.3.2 Modelling for Horizontal Flow Filter

The regression relationships developed for vertically downward flow filters seem incompatible to predict the performance of horizontal flow filter. Hence, new regression relationships have been developed for horizontal flow filter. For computation of R'' , the procedure laid down by the Hsiung and Cleasby (1968) is followed. The parameter R' of head loss model for vertically downward flow is incompatible for horizontal flow filter. Hence, new R'' has been developed (as similar in section 4.2.1.2) and given by Eq. (5.4).

$$R'' = \left(\frac{d^{1.60} (H_1 - H_0)}{Q^{0.80} C_o^{1.40}} \right) \quad (5.4)$$

A unified regression relationship (MOHOHL-30E) is developed with experimental run data (run nos. 90 to 94) for influent concentration of 30 mg/l. The average errors for different flow velocities are given in Table 5.11. The maximum error of 73.13% (run no. 92) and minimum of 17.12% (run no. 90) is computed. Table 5.11 reveals that the errors are much lower than the errors computed using H-C model (Table 4.10). Using the unified regression model from Table 5.11, Fig. 5.17 shows scattering of the values around the line of perfect agreement.

Now, the unified model (MOHOHL-30E) is tested against influent concentration of 40 mg/l (run nos. 95 to 99). The average errors for the unified relationship are given in Table 5.12. The errors are ofcourse not acceptable but it is certainly better than errors by using of H-C model (Table 4.10). Figure 5.18 shows scattering of the values around the line of perfect agreement.

Table 5.11: Computed APE for head loss using new developed unified model (MOHOHL-30E) (run nos. 90 to 94)

Grain size (mm)	Model name	New Model	Flow velocity	Computed APE
			(m ³ /hr/m ²)	
0.714	MOHOHL-30E	$R'' = \left[\left(d_i^{1.60} (H_i - H_o) \right) / \left(Q^{0.80} C_o^{1.40} \right) \right]; R^2 = 0.819$	1.65	17.12
			3.3	43.14
			4.95	73.13
			6.6	56.89
			8.25	53.69

Table 5.12: Computed APE for head loss using unified model (MOHOHL-30E) for influent concentration of 40 mg/l (run nos. 95 to 99)

Grain size (mm)	Model name	New Model	Flow velocity	Computed APE
			(m ³ /hr/m ²)	
0.714	MOHOHL-30E	$R'' = \left[\left(d_i^{1.60} (H_i - H_o) \right) / \left(Q^{0.80} C_o^{1.40} \right) \right]; R^2 = 0.819$	1.65	27.12
			3.3	80.09
			4.95	58.09
			6.6	77.84
			8.25	65.79

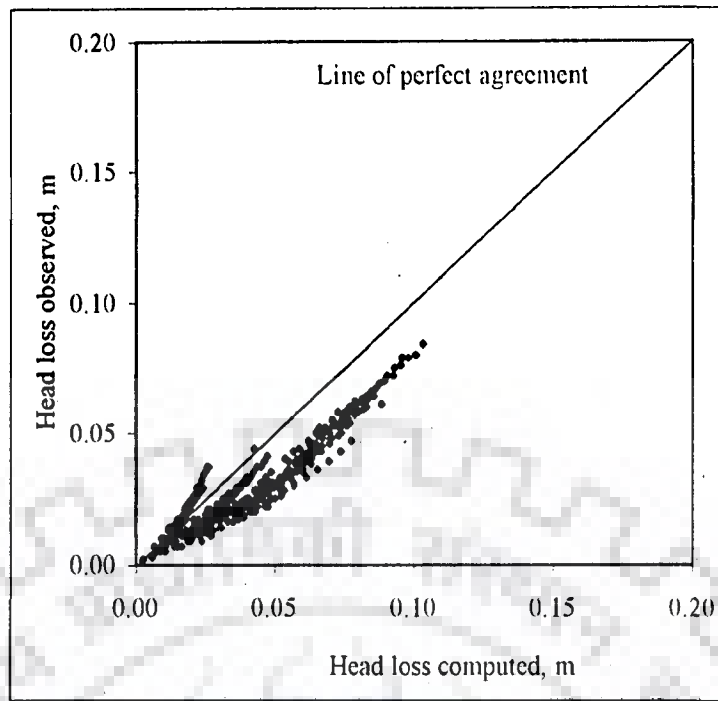


Fig. 5.17: Plot of head loss observed versus computed using model (MOHOHL-30E) for influent concentration of 30 mg/l (run nos. 90 to 94)

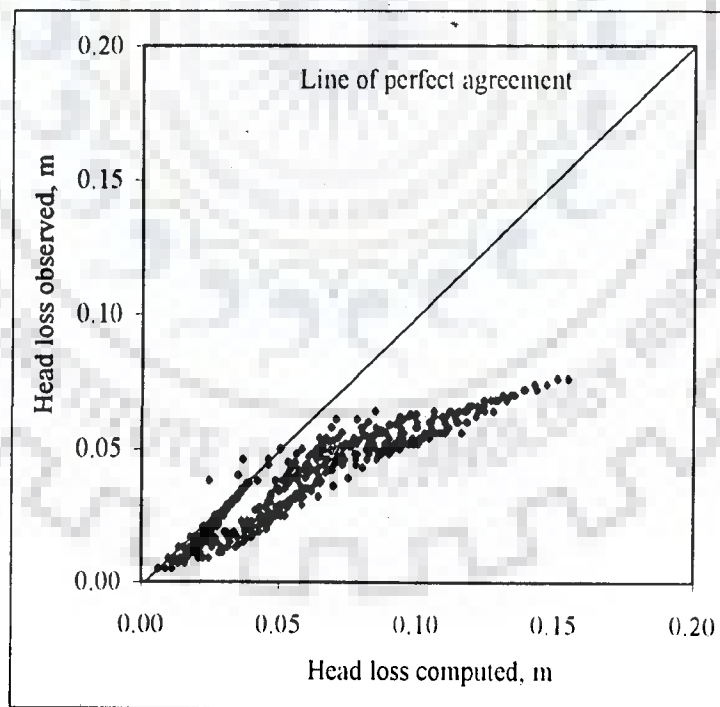


Fig. 5.18: Plot of head loss observed versus computed using model (MOHOHL-30E) for influent concentration of 40 mg/l (run nos. 95 to 99)

5.4 ANALYSIS FOR THE LARGE ERRORS IN FLOW RESISTANCE MODELLING

The head loss observed during experimentation is in the lower range and the errors computed using the new unified model are still on higher side. To explain the larger errors in modelling of flow resistance, an attempt is made to develop a power law type relationship using flow resistance data for certain experimental runs (nos. 90 to 94) and this yields the following relationship

$$\frac{R}{L^{1.6}} = 5 \times 10^{-5} \left(\frac{G}{L^{1.9}} \right)^{0.31} \quad (5.5)$$

Rearranging Eq. (5.5) leads to

$$H_t = H_o + \left[\frac{5 \times 10^{-5} \left(\frac{Q^{0.30} \cdot d^{1.20} \cdot t}{L^{1.90}} \right)^{0.31} L^{1.60} Q^{0.40} C_o^{1.60}}{d^{1.60}} \right] \quad (5.6)$$

where, H_o is the initial head loss (m), H_t is the head loss at any time t (m), Q is flow velocity (m/hr.), d is grain size of filtering media (m), t is the time of filter run (hrs.) and L is the depth of filter media (m)

Equation (5.6) indicates that H_t increases with increase in Q , t and C_o . It is obvious that in this approach, the effect of head loss computation by individual layers is lumped and therefore, flow resistance modelling contains larger errors.

To explain it further, let Q be the flow velocity with influent concentration C_o . Let the filter bed of length L be divided into n layers so that each layer is of thickness $\Delta L = \frac{L}{n}$. Let the filter cross-sectional area be A and let the initial filtration coefficient be λ_o with the absolute specific deposits $\sigma_1, \sigma_2, \dots, \sigma_n$ in layers 1, 2, ..., n , respectively. For a flow period of Δt , one can write the following expressions for

$$\sigma_1 = \frac{Q \Delta t}{A \Delta L} \{C_o - C_o \exp(-\lambda_o \Delta L)\} \quad (5.7)$$

$$\sigma_2 = \frac{Q \Delta t}{A \Delta L} \{C_o \exp(-\lambda_o \Delta L) - C_o \{\exp(-\lambda_o \Delta L)\}^2\} \quad (5.8)$$

$$\sigma_n = \frac{Q \Delta t}{A \Delta L} \{C_o \{\exp(-\lambda_o \Delta L)\}^{n-1} - C_o \{\exp(-\lambda_o \Delta L)\}^n\} \quad (5.9)$$

Using Eqs. (5.7 to 5.9), average deposit σ_{av} in the entire bed can be obtained as

$$\sigma_{av} = \frac{\sigma_1 + \sigma_2 + \dots + \sigma_n}{n} \quad (5.10)$$

or

$$\sigma_{av} = \frac{Q \Delta t C_o}{A \Delta L n} \{1 - \{\exp(-\lambda_o \Delta L)\}^n\} \quad (5.11)$$

One can approximate $\{\exp(-\lambda_o \Delta L)\}$ if the argument is less than 1. Thus,

$$\exp(-\lambda_o \Delta L) = 1 - \lambda_o \Delta L + \dots \quad (5.12)$$

This leads to

$$1 - \{\exp(-\lambda_o \Delta L)\}^n = 1 - (1 - \lambda_o \Delta L)^n \quad (5.13)$$

Using binomial expansion of $(1 - \lambda_o \Delta L)^n$ for the assumption that $\lambda_o \Delta L$ is < 1 , leads to the following approximation

$$\{1 - \exp(-\lambda_o \Delta L)\}^n = 1 - 1 + \lambda_o n \Delta L \quad (5.14)$$

Thus, with $(\lambda_o \Delta L)$ being less than unity, one can have the following expression for σ_{av} ;

$$\sigma_{av} = \frac{Q \Delta t C_o \lambda_o}{A} \quad (5.15)$$

Instead of dividing the layers into n parts, if one considers the entire filter bed of thickness L as one layer, the specific deposit computed will turn out to be

$$\sigma_L = \frac{Q \Delta t C_o}{A L} \{1 - \exp(-\lambda_o L)\} \quad (5.16)$$

With the assumption that $(\lambda_o L)$ is still less than 1, Eq. (5.16) will lead to

$$\sigma_L = \frac{Q \Delta t C_o}{A L} (\lambda_o L) = \frac{Q \Delta t C_o}{A} \lambda_o \quad (5.17)$$

Thus, under the assumption of $\lambda_o L$ and $\lambda_o \Delta L$ being less than one, it can be seen that $\sigma_L = \sigma_{av}$. It means that the lumping can be done under such conditions. However, in many situations and particularly with the progress of filter run, it is possible that the assumption of $\lambda_o L$ being very low (less than unity) may be violated & under these circumstances, errors will be introduced. Specifically, the approach based on individual layers is more appropriate for the modelling of flow resistance or the effluent quality. However, such an approach is more complicated and this is the reason why the approach of the H-C model has been considered in the present study.

Coming back to Eq. (5.6) and its consequent simplification, one obtains

$$H_t = H_o + \left\{ \frac{5 \times 10^{-5} Q^{0.50} t^{0.31} L C_o^{1.60}}{d^{1.23}} \right\} \quad (5.18)$$

Assuming that initial head loss H_o is described by Karman-kozeny relationship, one can write the following expression of H_o (Ojha *et al.*, 2003)

$$H_o = f \left(\frac{L}{\phi d} \right) \left(\frac{1-n}{n^3} \right) \left(\frac{v_s^2}{g} \right) \quad (5.19)$$

where, H_o is initial head loss (m), L is depth of filter media (m), ϕ is shape factor (1 for spherical particle), n is porosity of filter bed, v_s is mean flow velocity is equivalent to Q (m/hr.), g is acceleration due to gravity (m/sec^2) and f is coefficient of

friction = $150 \left(\frac{1-n}{R_e} \right)$ and R_e is Reynold's number, $R_e = \left(\frac{\phi d v_s}{\nu} \right)$, ν is kinematic viscosity of the liquid (Kg.sec/m²).

It can be seen that H_o is proportional to L (Eq. 5.19). Substituting expression for H_o from Eq. (5.19) to Eq. (5.18), one gets

$$H_t = \left\{ f \left(\frac{L}{\phi d} \right) \left(\frac{1-n}{n^3} \right) \left(\frac{v_s^2}{g} \right) \right\} + \left\{ \frac{5 \times 10^{-5} Q^{0.50} t^{0.31} L C_0^{1.60}}{d^{1.23}} \right\} \quad (5.20)$$

From Eq. (5.20), H_t is again proportional to L . However, in reality it is not obtained as head loss is more in upper layers because of higher deposition of impurities in these layers (Ojha & Graham, 1992). Thus, lumped approach is an approximation only for modelling of flow resistance. It is not surprising that larger errors apparent in the development of flow resistance relationship are most likely a consequence of such an approach and this relationship is also true for H-C model.

To achieve better calibration results, the power law type relationship has been replaced by logarithmic with nonlinear relationship (Tables 5.7 & 5.8). Thus, the relationships are better than the power law type relationship. Table 5.13 indicates that initial head loss values computed using Eq. (5.19) for certain assumed values of porosities are still very low. Thus, very high head loss values, say of few meters, as typically encountered in deep bed filters, have not been encountered in the present experimental study.

Table 5.13: Comparison of head loss observed and computed at various assumed porosities of sand bed of 100 mm thickness

Run no.	Flow velocity (m/sec)	Grain size (m)	Head loss (n=0.4) observed (m)	Head loss (n=0.4) computed (m)	Head loss (n=0.3) computed (m)	Head loss (n=0.2) computed (m)
1	0.00046	0.003647	0.010	0.0003	0.0008	0.0032
2	0.00092	0.003647	0.012	0.0006	0.0016	0.0063
3	0.00138	0.003647	0.014	0.0009	0.0025	0.0095
4	0.00183	0.003647	0.017	0.0012	0.0033	0.0127
5	0.00229	0.003647	0.018	0.0015	0.0041	0.0159
6	0.00046	0.002366	0.011	0.0007	0.0020	0.0075
7	0.00092	0.002366	0.012	0.0014	0.0039	0.0151
8	0.00138	0.002366	0.014	0.0021	0.0059	0.0226
9	0.00183	0.002366	0.016	0.0028	0.0078	0.0301
10	0.00229	0.002366	0.018	0.0035	0.0098	0.0377
11	0.00046	0.001673	0.014	0.0009	0.0023	0.0090
12	0.00092	0.001673	0.016	0.0017	0.0047	0.0181
13	0.00138	0.001673	0.018	0.0026	0.0070	0.0271
14	0.00183	0.001673	0.020	0.0034	0.0094	0.0362
15	0.00229	0.001673	0.024	0.0042	0.0117	0.0452
16	0.00046	0.001091	0.025	0.0033	0.0092	0.0354
17	0.00092	0.001091	0.030	0.0066	0.0184	0.0709
18	0.00138	0.001091	0.034	0.0100	0.0276	0.1063
19	0.00183	0.001091	0.038	0.0133	0.0367	0.1417
20	0.00229	0.001091	0.044	0.0166	0.0459	0.1772
21	0.00046	0.000714	0.045	0.0047	0.0129	0.0496
22	0.00092	0.000714	0.055	0.0093	0.0257	0.0993
23	0.00138	0.000714	0.065	0.0140	0.0386	0.1489
24	0.00183	0.000714	0.070	0.0186	0.0515	0.1985
25	0.00229	0.000714	0.080	0.0233	0.0644	0.2482
26	0.00046	0.000505	0.050	0.0093	0.0257	0.0992
27	0.00092	0.000505	0.055	0.0186	0.0515	0.1985

5.5 CONCLUDING REMARKS

For the flow rate & influent quality variation typically encountered in rainwater harvesting situation, it appears that head loss is not a critical parameter and the effluent quality is the most important parameter. As the errors inherent in the computation of filter quality is reasonably good, it is reasonable to state that regression relationship developed in this chapter have merit of being used in filters for harvested rainwater. To improve upon H-C models, new regression models are developed using different experimental runs data (run nos. 28 to 54) for influent concentrations of 30 mg/l for effluent quality and head loss prediction under vertically downward flow and horizontal flow conditions.

The effluent quality errors are observed as low as 6.99% (run no. 33, Table 5.2) and as high as 29.34% (run no. 43, Table 5.2) with majority of lower values for the unified model under vertically downward flow condition. The head loss errors are observed as low as 15.48% (run no. 38, Table 5.8) and as high as 37.91% (run no. 36, Table 5.8) for vertically downward flow filter. Hence, the performance of new unified regression models is more compatible than H-C models for wider range of experimental studies. The performance of the new unified regression model is also tested with harvested rainwater samples for different experimental runs data (run nos. 65 to 89 and 100 to 104) in the next chapter.

DIMENSIONLESS MODEL ANALYSIS

6.1 GENERAL

The new regression models developed for effluent quality and critical head loss prediction are much more compatible than the Hsiung and Cleasby (1968) models (as discussed in the previous chapter). However, the developed models for effluent quality and head loss prediction are not truly dimensionless in nature, hence an attempt has been made to develop an alternate dimensionless models which involves only dimensionless parameter. The objective is to test whether these models can lead to a better performance or behave in the similar fashion as the H-C model.

6.2 MODELLING FOR EFFLUENT QUALITY

For a given d , G' is a function of Q and t only. Thus, if G' is defined equal to Qt , G'/L will become Qt/L , which is a dimensionless quantity and U is also a dimensionless quantity. Thus, relationship between U & Qt/L will be a dimensionally balanced relationship. In this dimensionless model, G' is not a function of sand grain size, d , and hence, the lumped model consideration in the dimensionless form is not justifiable. The regression relationships for each sand grain size are given in Table 6.1 for influent concentrations of 30 mg/l for vertically downward flow filters. The data of experimental runs (nos. 28 to 54) were used for the computation of percentage errors and the average of such errors for each of the runs is presented in Table 6.1. The highest error of 71.97% was

computed at 0.714 mm grain size and flow velocity of $1.65 \text{ m}^3/\text{hr}/\text{m}^2$ (run no. 48). Similarly, using regression relationships of Table 6.1, Figs. 6.1 to 6.6 show the agreement between observed and computed effluent turbidity concentrations. From these Figs. 6.1 to 6.6, it is clear that the values of effluent concentrations are significantly deviated from the line of perfect agreement. This means that the observed values and computed values have wide differences in their magnitude. Hence, the dimensionless models are incompatible to predict the performance of sand filter in terms of effluent quality and behave in the similar manner as the H-C model.

The behaviour of the new developed models for horizontal flow filter was again tested in dimensionless form to check the improvement in their performance. Horizontal filter was operated for two different influent turbidity concentrations of 30 mg/l and 40 mg/l. Maximum turbidity removal efficiency was observed at grain size of 0.714 mm, and hence this grain size has been selected for horizontal flow filter study.

The regression relationships for each grain size are given in Table 6.2 for influent concentrations of 30 mg/l. The data of experimental runs (nos. 90 to 94) were used for the computation of errors and the average of such errors for each of the runs is presented in Table 6.2. It can be seen from the Table 6.2, the highest computed error is 70.07% (run no. 90) at 30 mg/l influent concentration using dimensionless model (DIMOHEQ-30E). Using regression relationship of Table 6.2, Fig. 6.7 shows the agreement between observed and computed effluent concentration. Figure 6.7 shows significant deviation of the values from the line of perfect agreement. Hence, the dimensionless model is also incompatible to predict the performance of horizontal flow sand filter in terms of effluent quality and again behave in the similar manner as the H-C model.

Table 6.1: Computed APE for effluent quality using dimensionless models at an individual grain size (run nos. 28 to 54)

Grain size (mm)	Models name	New models	Flow velocity (m ³ /hr/m ²)	
			U	C
3.647	DIMOVEQ-30A	$\log(U) = -1.132 + 1.537 \log\left(\frac{Q_t}{L}\right) - 0.219 \left[\log\left(\frac{Q_t}{L}\right)\right]^2$ $R^2 = 0.785$	1.65	30.63
			3.30	22.56
			4.95	19.57
			6.60	14.83
			8.25	14.25
2.366	DIMOVEQ-30B	$\log(U) = -1.702 + 1.702 \log\left(\frac{Q_t}{L}\right) - 0.251 \left[\log\left(\frac{Q_t}{L}\right)\right]^2$ $R^2 = 0.802$	1.65	28.44
			3.30	25.86
			4.95	22.60
			6.60	21.46
			8.25	21.15
1.673	DIMOVEQ-30C	$\log(U) = -1.661 + 1.789 \log\left(\frac{Q_t}{L}\right) - 0.253 \left[\log\left(\frac{Q_t}{L}\right)\right]^2$ $R^2 = 0.791$	1.65	37.11
			3.30	26.65
			4.95	23.58
			6.60	22.88
			8.25	22.66
1.091	DIMOVEQ-30D	$\log(U) = -1.546 + 1.809 \log\left(\frac{Q_t}{L}\right) - 0.269 \left[\log\left(\frac{Q_t}{L}\right)\right]^2$ $R^2 = 0.803$	1.65	31.10
			3.30	26.16
			4.95	26.81
			6.60	25.84
			8.25	26.34
0.714	DIMOVEQ-30E	$\log(U) = -2.760 + 2.461 \log\left(\frac{Q_t}{L}\right) - 0.360 \left[\log\left(\frac{Q_t}{L}\right)\right]^2$ $R^2 = 0.832$	1.65	42.91
			3.30	21.08
			4.95	32.53
			6.60	36.82
			8.25	38.51
0.505	DIMOVEQ-30F	$\log(U) = -3.146 + 3.010 \log\left(\frac{Q_t}{L}\right) - 0.499 \left[\log\left(\frac{Q_t}{L}\right)\right]^2$ $R^2 = 0.917$	1.65	25.83
			3.30	41.59

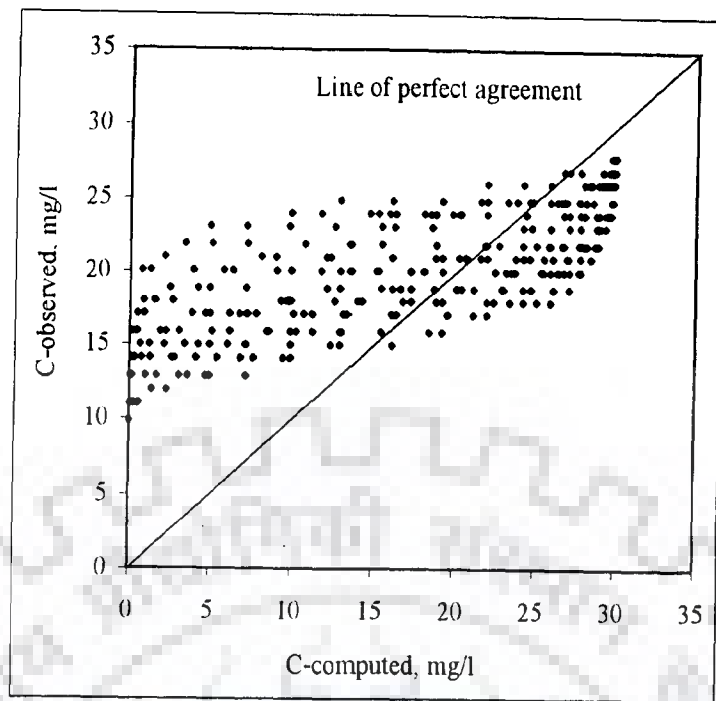


Fig. 6.1: Plot of C-predicted versus C-computed using dimensionless model (DIMOVEQ-30A) (run nos. 28 to 32)

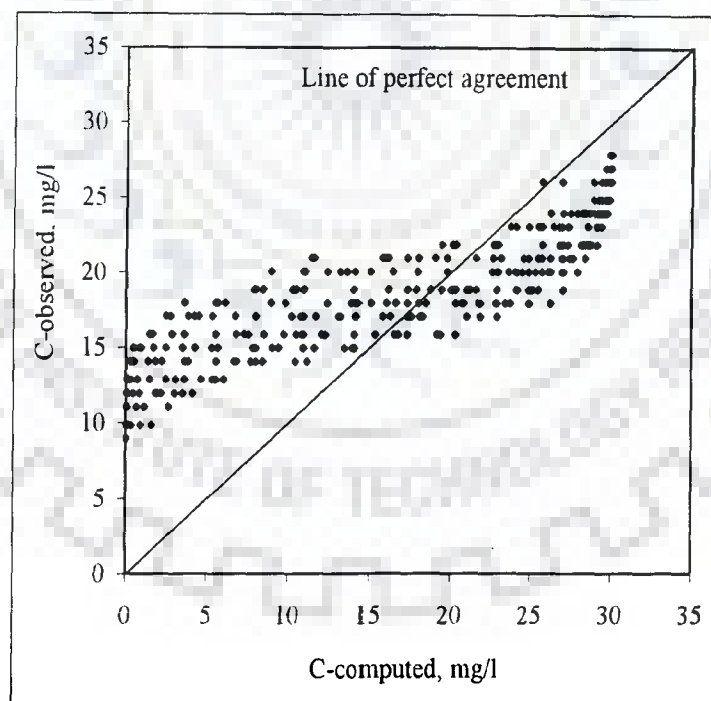


Fig. 6.2: Plot of C-predicted versus C-computed using dimensionless model (DIMOVEQ-30B) (run nos. 32 to 37)

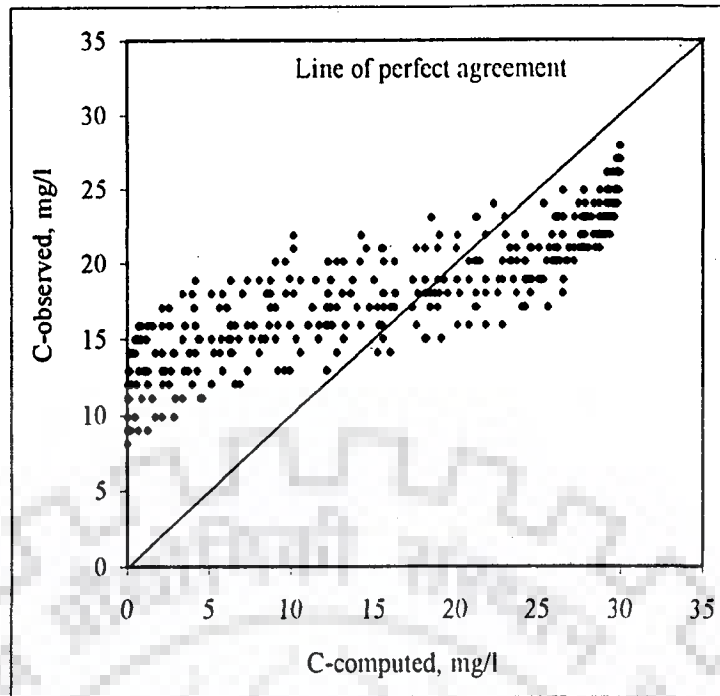


Fig. 6.3: Plot of C-predicted versus C-computed using dimensionless model (DIMOVEQ-30C) (run nos. 38 to 42)

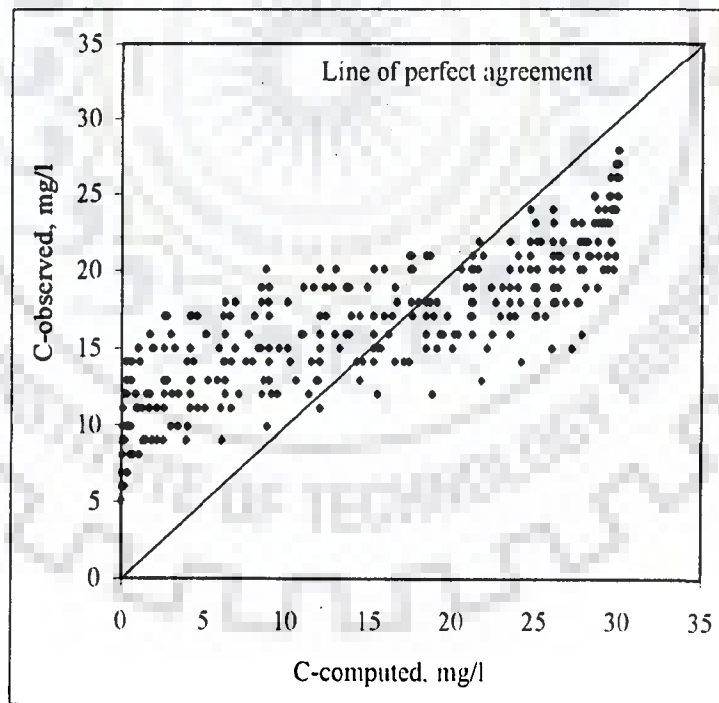


Fig. 6.4: Plot of C-predicted versus C-computed using dimensionless model (DIMOVEQ-30D) (run nos. 43 to 47)

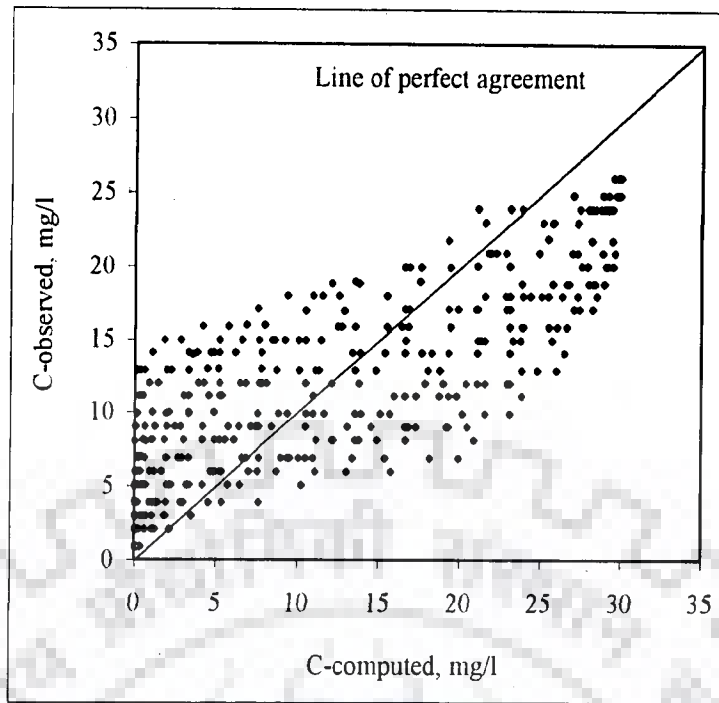


Fig. 6.5: Plot of C-predicted versus C-computed using dimensionless model (DIMOVEQ-30E) (run nos. 48 to 52)

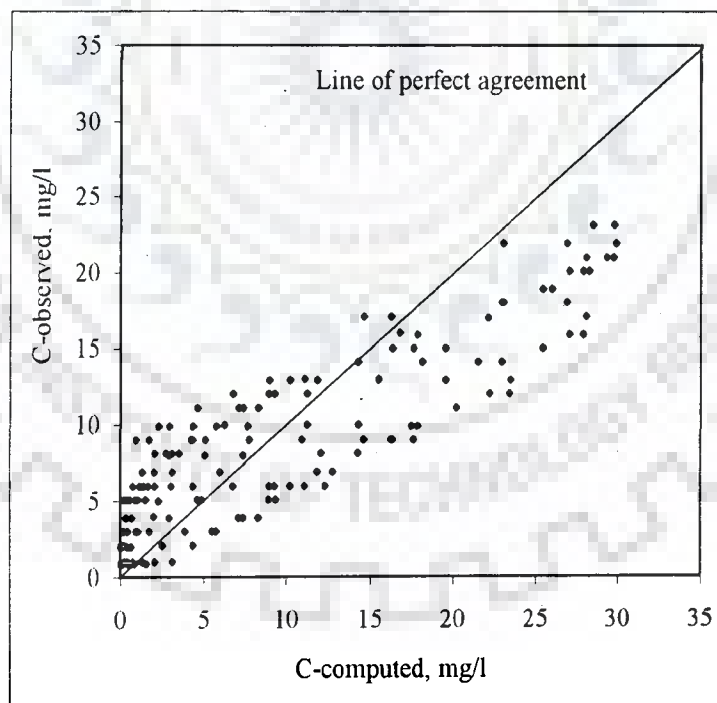


Fig. 6.6: Plot of C-predicted versus C-computed using dimensionless model (DIMOVEQ-30F) (run nos. 53 & 54)

Table 6.2: Computed APE for effluent quality using dimensionless model (DIMOHEQ-30E) (run nos. 90 to 94)

Grain size (mm)	Model name	New model	Flow velocity (m ³ /hr/m ²)		Computed APE	
			U	C	U	C
0.714	DIMOHEQ-30E	$\log(U) = -1.730 + 1.893 \log\left(\frac{Q_t}{L}\right) - 0.280 \left[\log\left(\frac{Q_t}{L}\right) \right]^2$ $R^2 = 0.826$	1.65		42.62	70.07
			3.30		18.66	43.59
			4.95		32.74	40.50
			6.60		46.83	49.04
			8.25		39.58	44.73

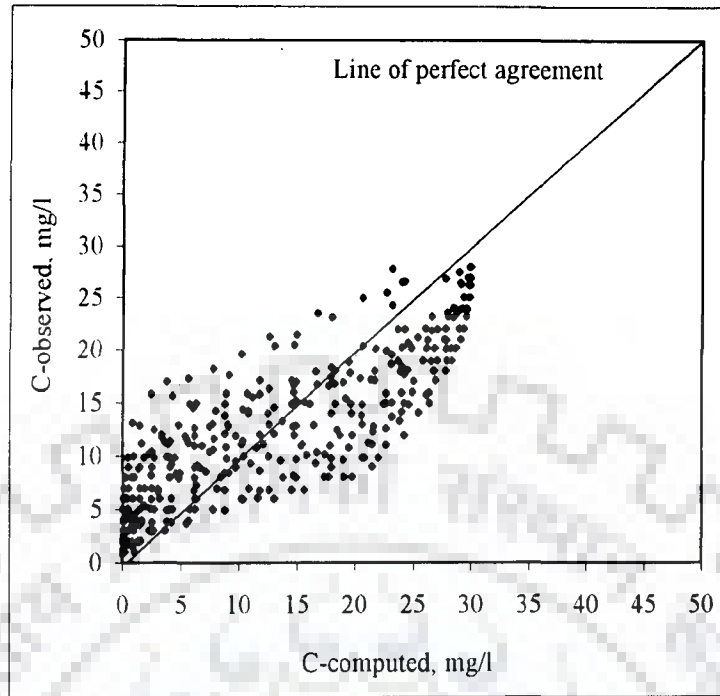


Fig. 6.7: Plot of C-predicted versus C-computed using dimensionless model (DIMOHEQ-30E) (run nos. 90 to 94)

6.3 GENERALIZED MODELLING FOR DIAMETER FUNCTION

The use of dimensionless model for 30 mg/l influent concentration (run nos. 28 to 54) shows higher range of average percentage errors (nearly 50%, Table 6.1). However, the values are also in lower ranges for individual grain size but certainly not in acceptable range (about 10%). In the section 6.2, G' has been made dimensionless without the function of diameter of sand grain. To maintain the similar form of the function as in the H-C model, G' has been made again dimensionless with the function of Q , d , t and L and it is defined as dimensionless parameter, $G' = \left(\frac{Q^a t^b}{d^b L^{a-b}} \right)$, where a is the coefficient of Q & L and b is the coefficient of t , d & L .

This dimensionless parameter, G' , has been again used in the dimensionless model developed. A regression analysis between observed $\log(G')$ and observed $\log(U)$, shows high average percentage errors for observed and computed effluent quality. An individual model developed for each sand grain at influent turbidity concentration of 30 mg/l was used. The average errors were computed at certain combinations of 30 mg/l influent turbidity concentration for sand grain sizes of 3.647 mm, 2.366 mm, 1.673 mm, 1.091 mm, 0.714 mm and 0.505 mm and flow velocities of 1.65 m³/hr/m², 3.30 m³/hr/m², 4.95 m³/hr/m², 6.60 m³/hr/m² and 8.25 m³/hr/m². With the different combinations of various values of coefficients, a and b , the value of errors at certain runs is presented in Table 6.3.

Table 6.3: Computed APE using diameter function for different filter runs (nos. 28 to 54)

Coefficients of a	Coefficients of b	Computed APE
0.50	0.00	74.38
1.00		74.38
1.50		74.37
2.00		74.36
3.00		74.36
4.00		74.31
0.50	0.25	84.13
1.00		81.58
1.50		76.36
2.00		71.45
0.50	0.50	85.15
2.00		68.98
3.00	-1.00	77.27
	-2.00	77.69
	-3.00	78.21
4.00	-1.00	77.27
	-2.00	77.45
	-3.00	77.66
5.00	-1.00	77.32
	-2.00	77.89
	-3.00	78.04
6.00	-1.00	76.97
	-2.00	77.16
	-3.00	77.37
-1.00	1.00	76.11
	1.00	91.86
-2.00	2.00	88.59
0.12	0.35	96.64

6.4 MODELLING FOR FLOW RESISTANCE

To maintain the similar form of the Hsiung and Cleasby (1968) model, the new developed head loss regression models for vertical filters are tested in dimensionless form for improvement of performance. From the previous chapter, $\left(\frac{R'}{L^{1.3}}\right)$ is written as

$$\left(\frac{R'}{L^{1.3}}\right) = \frac{d^{1.2}(H_t - H_o)}{Q^{0.19} C_o^{1.3} L^{1.3}} \quad (6.1)$$

After adding the new parameters, γ and g in Eq. (6.1), Eq. (6.1) becomes dimensionless and written as

$$R'_d = \left\{ \frac{\left(\frac{R'}{L^{1.3}}\right) \gamma^{1.3}}{g Q \left(\frac{L}{g}\right)^{0.295}} \right\} \quad (6.2)$$

where, R'_d is the dimensionless function, γ is unit weight of water ($\text{kg/m}^2 \cdot \text{sec}^2$), g is acceleration due to gravity (m/sec^2), L is depth of filter (m) and Q is flow velocity (m/hr.).

Equation (6.2) is one way of obtaining R'_d . Infact, in place of $\left(\frac{L}{g}\right)$, one can also use $\left(\frac{d}{g}\right)$. With the use of $\left(\frac{d}{g}\right)$, the percentage errors for head loss were found in unacceptable range ($>20\%$). The following section is based on Eq. (6.2).

The data of experimental runs (nos. 28 to 54) were used for the computation of errors and the comparison of average of errors for each of the runs is presented in Table 6.4. From the Table 6.4, it can be seen that the errors using dimensionless model are computed as low as 38.02% (run no. 30) and as high as 132.17% (run no. 42). Such ranges of high errors are not acceptable in any case. The deviation of the head loss computed and observed values from the line of perfect agreement shows incompatibility of the dimensionless model, as shown in Figs. 6.8 to 6.13.

Table 6.4: Computed APE for head loss using dimensionless models at an individual grain size (run nos. 28 to 54)

Grain size (mm)	Models name	New models	Flow velocity (m ³ /hr/m ²)	Computed APE
3.647	DIMOVEHL-30A	$\log(R'_d) = 2.090 - 0.623 \log\left(\frac{Q_t}{L}\right) + 0.185 \left[\log\left(\frac{Q_t}{L}\right) \right]^2$ $R^2 = 0.086$	1.65	74.82
			3.30	44.43
			4.95	38.02
			6.60	49.70
			8.25	74.44
2.366	DIMOVEHL-30B	$\log(R'_d) = 1.866 - 0.602 \log\left(\frac{Q_t}{L}\right) + 0.178 \left[\log\left(\frac{Q_t}{L}\right) \right]^2$ $R^2 = 0.074$	1.65	74.55
			3.30	46.03
			4.95	40.02
			6.60	56.54
			8.25	80.57
1.673	DIMOVEHL-30C	$\log(R'_d) = 2.236 - 0.712 \log\left(\frac{Q_t}{L}\right) + 0.198 \left[\log\left(\frac{Q_t}{L}\right) \right]^2$ $R^2 = 0.11$	1.65	68.36
			3.30	39.71
			4.95	55.95
			6.60	94.02
			8.25	132.17
1.091	DIMOVEHL-30D	$\log(R'_d) = 1.819 - 0.598 \log\left(\frac{Q_t}{L}\right) + 0.181 \left[\log\left(\frac{Q_t}{L}\right) \right]^2$ $R^2 = 0.085$	1.65	76.71
			3.30	45.20
			4.95	38.46
			6.60	53.96
			8.25	74.45
0.714	DIMOVEHL-30E	$\log(R'_d) = 2.277 - 0.705 \log\left(\frac{Q_t}{L}\right) + 0.199 \left[\log\left(\frac{Q_t}{L}\right) \right]^2$ $R^2 = 0.12$	1.65	65.55
			3.30	40.05
			4.95	54.91
			6.60	92.88
			8.25	120.54
0.505	DIMOVEHL-30F	$\log(R'_d) = 2.194 - 0.805 \log\left(\frac{Q_t}{L}\right) + 0.284 \left[\log\left(\frac{Q_t}{L}\right) \right]^2$ $R^2 = 0.285$	1.65	42.36
			3.30	86.52

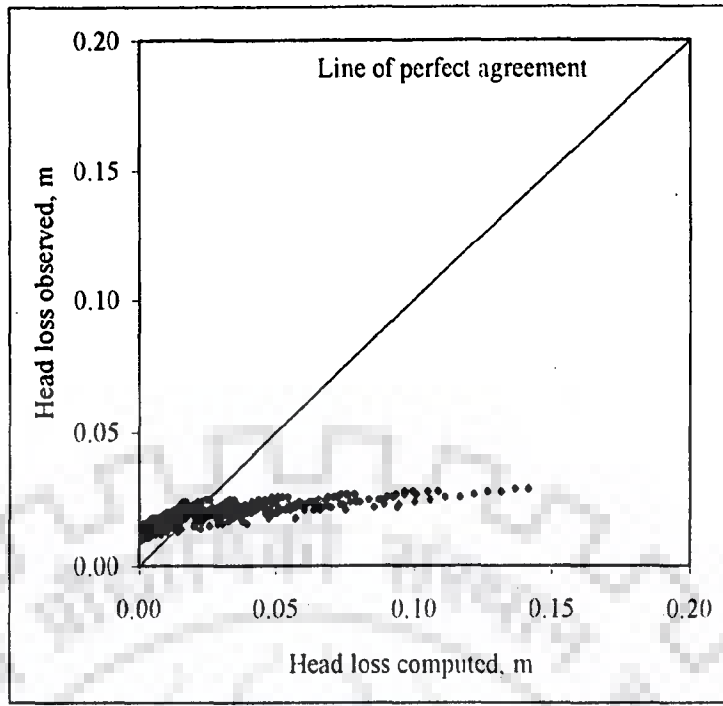


Fig. 6.8: Plot of head loss observed versus computed using dimensionless model (DIMOVEHL-30A) (run nos. 28 to 32)

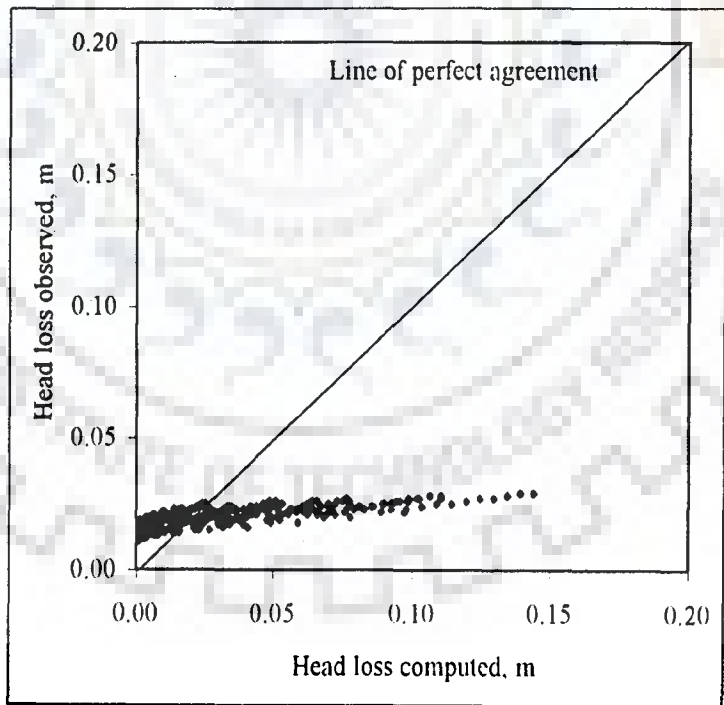


Fig. 6.9: Plot of head loss observed versus computed using dimensionless model (DIMOVEHL-30B) (run nos. 33 to 37)

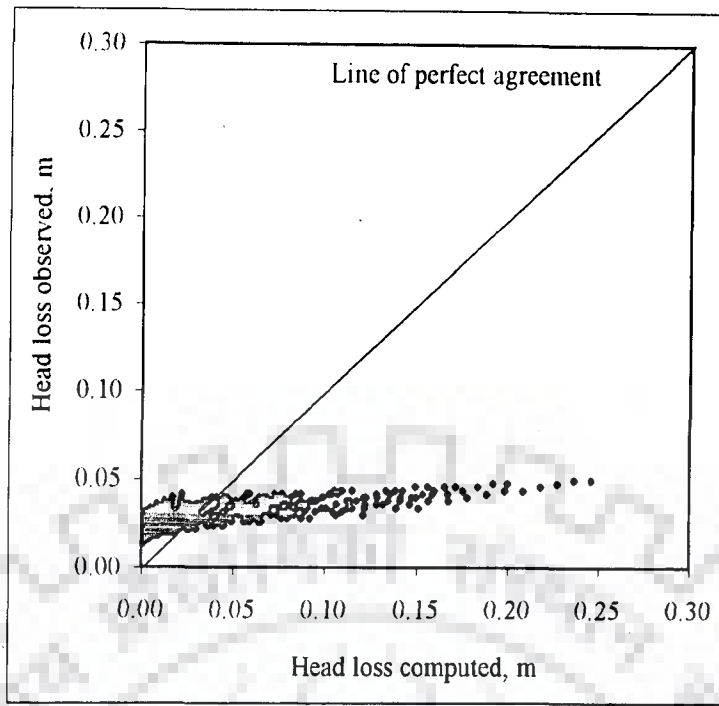


Fig. 6.10: Plot of head loss observed versus computed using dimensionless model (DIMOVEHL-30C) (run nos. 38 to 42)

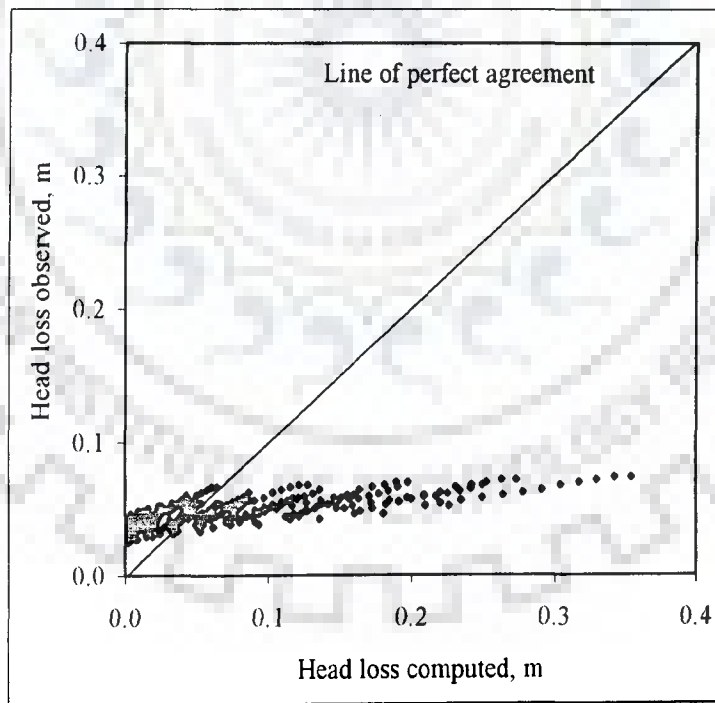


Fig. 6.11: Plot of head loss observed versus computed using dimensionless model (DIMOVEHL-30D) (run nos. 43 to 47)

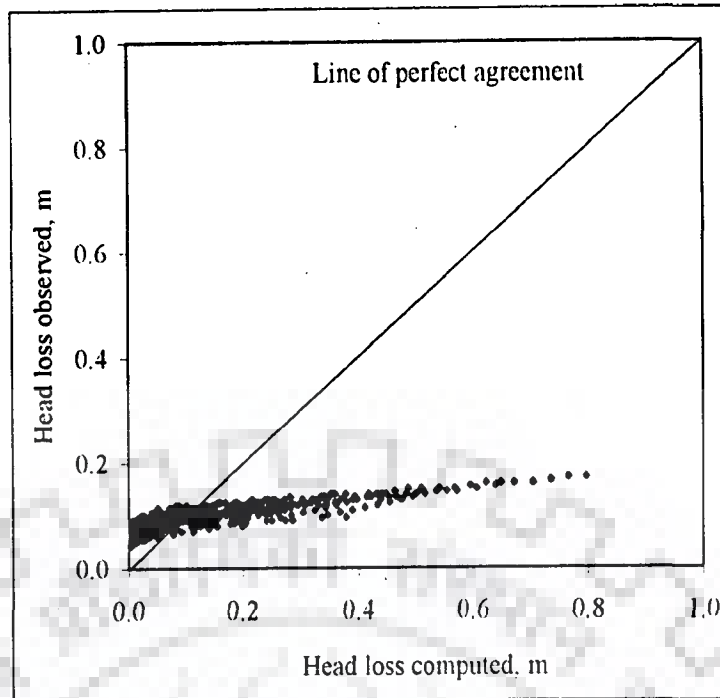


Fig. 6.12: Plot of head loss observed versus computed using dimensionless model (DIMOVEHL-30E) (run nos. 48 to 52)

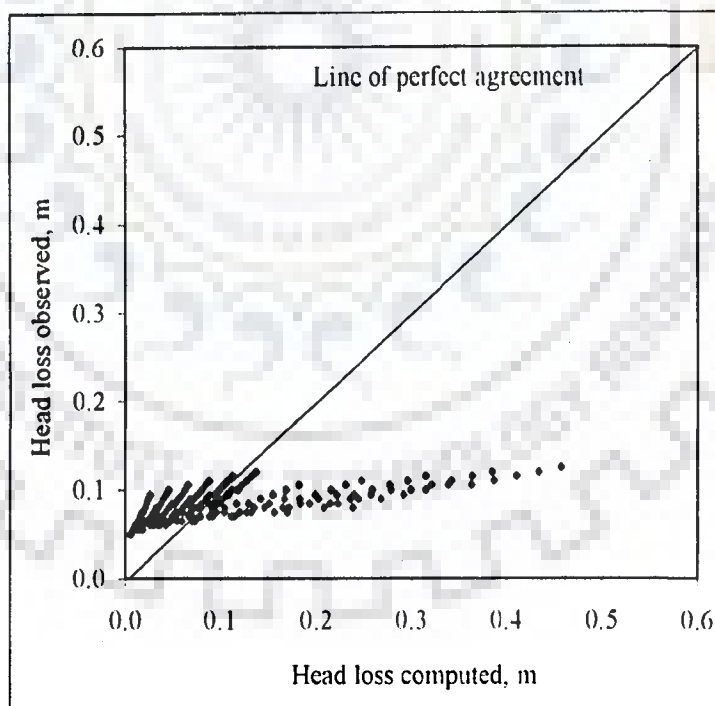


Fig. 6.13: Plot of head loss observed versus computed using dimensionless model (DIMOVEHL-30F) (run nos. 53 & 54)

In the same fashion, the model for horizontal filter has also been checked in dimensionless form. The function $\left(\frac{R''}{L^{1.2}}\right)$ in dimensionless form is followed as:

$$\left(\frac{R''}{L^{1.2}}\right) = \frac{d^{1.6} (H_t - H_o)}{Q^{0.8} C_o^{1.4} L^{1.2}} \quad (6.3)$$

After adding γ and g in Eq. (6.3), Eq. (6.3) becomes dimensionless and written as

$$R''_d = \left\{ \frac{\left(\frac{R''}{L^{1.2}}\right) \gamma^{1.4}}{g L^{0.4}} \right\} \quad (6.4)$$

In Eq. (6.4), the change of d can be made in place of L . With the use of d , the percentage errors for head loss were found in unacceptable range ($>30\%$). However, the next section deals with use of Eq. (6.4). The experimental runs data (nos. 90 to 94) were used for the computation of errors and the comparison of average of errors for each of the runs is presented in Table 6.5. From the Table 6.5, it can be seen that the errors using dimensionless model are computed as low as 26.15% (run no. 91) and as high as 51.06% (run no. 94). Such high ranges of errors are not acceptable in any case. The deviation of computed and observed head loss from the line of perfect agreement, as shown in Fig. 6.14, shows incompatibility of the dimensionless model. The dimensionless model in the similar form of the H-C model is not compatible to predict the performance of sand filters in terms of head loss and hence, there is a need to develop new dimensionless form.

This shows that the head loss model developed by the Hsiung and Cleasby (1968) with lumping of data was not a correct approach and it has been explained in the subsequent paragraph. The consideration of distributed data for individual filter depth for head loss model development is more appropriate than the lumping of data since the head loss depends on the filter media depth. Hence, new dimensionless model has been developed to overcome the dimensionless model errors.

Table 6.5: Computed APE for head loss using dimensionless model (DIMOHHL-30E) (run nos. 90 to 94)

Grain size (mm)	Model name	New model	Flow velocity (m ³ /hr/m ²)	Computed APE
0.714	DIMOHHL-30E	$\log(R_d'') = 1.694 - 0.718 \log\left(\frac{Qt}{L}\right) + 0.227 \left[\log\left(\frac{Qt}{L}\right) \right]^2$ $R^2 = 0.473$	1.65	45.83
			3.3	26.15
			4.95	50.42
			6.6	45.12
			8.25	51.06

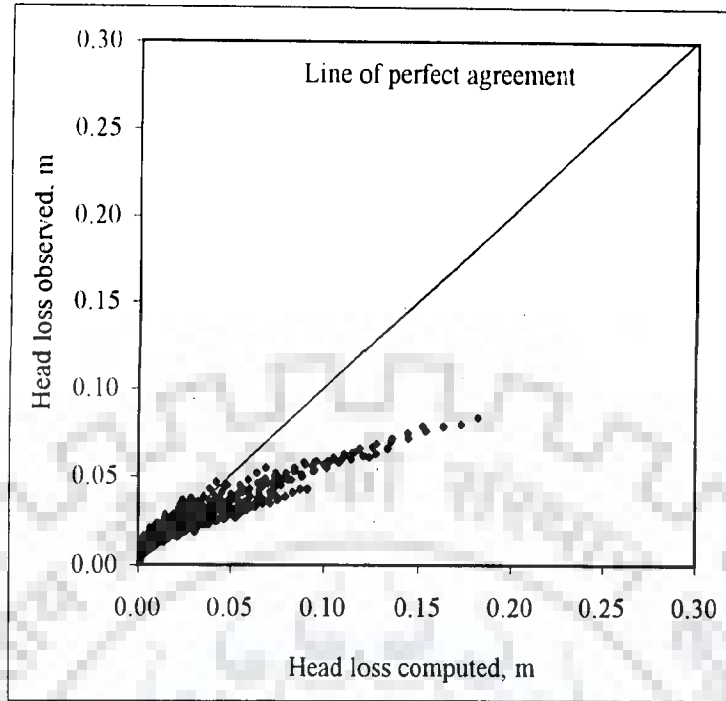


Fig. 6.14: Plot of head loss observed versus computed using dimensionless model (DIMOHHL-30E) (run nos. 90 to 94)

6.5 NEW HEAD LOSS DIMENSIONLESS MODEL DEVELOPMENT

The performance of the dimensionless model with lumping of data is incompatible to predict the performance and hence, new dimensionless model has been developed. Since head loss is also a function of filter media depth, so lumping of data for the model development is not appreciated. The data of vertically downward flow filter (run nos. 28 to 54) have been taken for the dimensionless model analysis. Since, R' is a function of Q , d , C_o and $(H_t - H_o)$, as given in Eq. (6.1), the new form of R' , designated now as \hat{R}_d is as

$$\hat{R}_d = L^a L \left(\frac{L}{T} \right)^b \left(\frac{M}{L^3} \right)^c (ML^{-2}T^{-2})^e \quad (6.5)$$

$$\hat{R}_d = (L^{a+1+b-3c-2e}) (T^{-b-2e}) (M^{c+e}) \quad (6.6)$$

where, a , b , c and e are coefficients of diameter and filter depth (d & L), flow velocity (Q), influent concentration (C_o) and unit weight of water (γ), respectively and \hat{R}_d is the new dimension factor;

Assuming the coefficient $c = -e$ in Eq. (6.6), then

$$-b+2c = 0; \text{ or } b = 2c \text{ and} \quad (6.7)$$

$$a+1+2c-3c+2c = 0; \text{ or } a+1+c = 0; \text{ or } a = -1-c \quad (6.8)$$

After putting the values of a , b and e in Eq. (6.6), one can get

$$\hat{R}_d = L^{-1-c} L \left(\frac{L}{T} \right)^{2c} \left(\frac{M}{L^3} \right)^c (ML^{-2}T^{-2})^{-c} \quad (6.9)$$

And hence, the final dimension of \hat{R}_d is as follows

$$\hat{R}_d = \left\{ \frac{(H_t - H_o) Q^{2c} C_o^c}{\gamma^c d^{1+c}} \right\} \quad (6.10)$$

In the similar fashion, G' has been made dimensionless by rearranging the coefficients as

$$G' = \left(\frac{Qt}{L} \right) \quad (6.11)$$

or,

$$\hat{G} = \left(\frac{gt^2}{L} \right) \quad (6.12)$$

Plot of \hat{R}_d versus \hat{G} shows constant values of regression coefficient at different assumed values of c and hence, $c=1$ has been selected in Eq. (6.10) for convenience. Hence, Eq. (6.10) becomes

$$\hat{R}_d = \left\{ \frac{(H_t - H_o) Q^2 C_o}{\gamma d^2} \right\} \quad (6.13)$$

A regression relationship between \hat{R}_d and \hat{G} is obtained as

$$\hat{R}_d = -5E - 23(\hat{G})^2 + 2E - 14(\hat{G}) + 8E - 06; R^2 = 0.27 \quad (6.14)$$

The use of Eq. (6.14) for entire filter media depth of 500 mm (from top) for certain filter run (no. 28), shows an average error of 37.88% which indicates the incompatibility of lumped data model for head loss prediction. Plot between \hat{R}_d and \hat{G} also shows very poor regression coefficient ($R^2 = 0.2735$), as shown in Fig. 6.15 and the observed and the corresponding computed head loss values is also shown in Fig. 6.16.

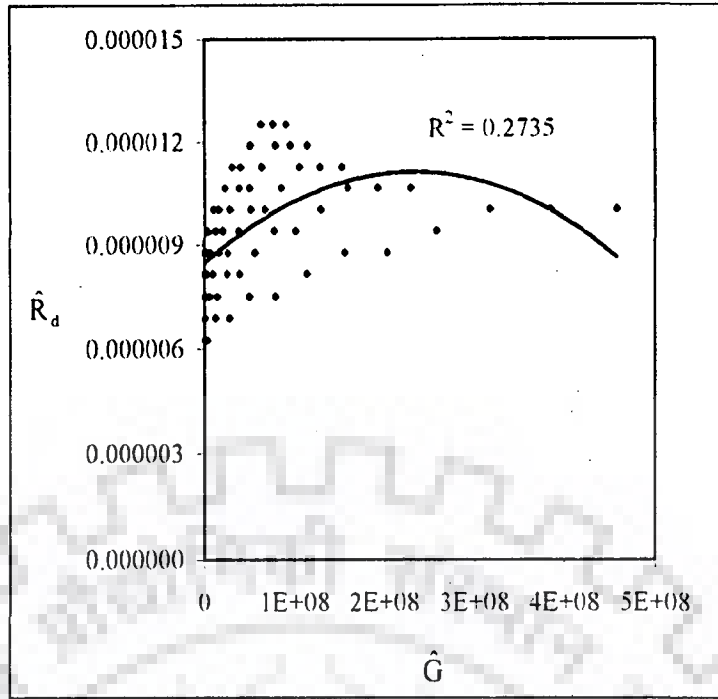


Fig. 6.15: Plot of \hat{R}_d versus \hat{G} for new dimensionless model at 500 mm filter depth (run no. 28)

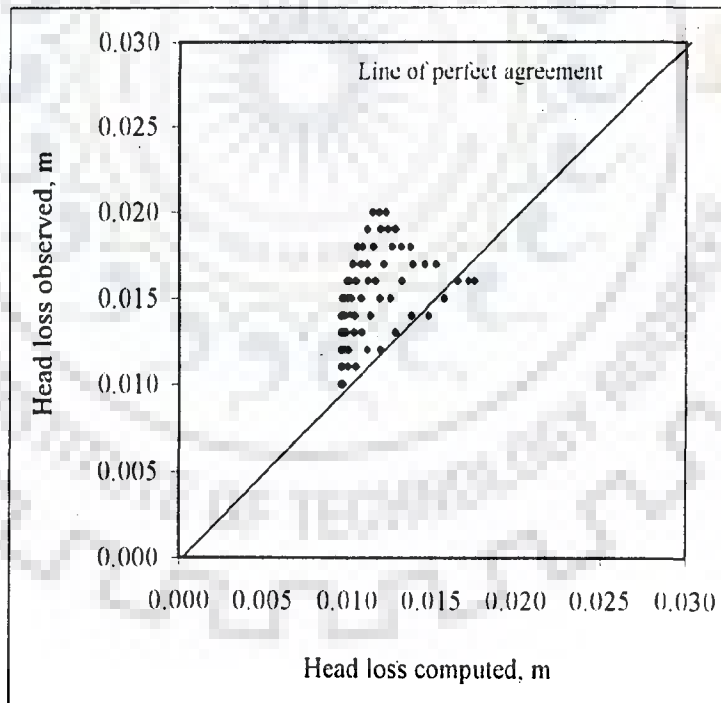


Fig. 6.16: Plot of head loss computed versus observed for new dimensionless model at 500 mm filter depth from top (run no. 28)

6.6 CONCLUDING REMARKS

In the present chapter, the performance of the new developed models has been studied in dimensionless form. The higher range of APE reveals that the behaviour of the dimensionless model is incompatible with respect to the new developed models but certainly it is better than the H-C model. To maintain the similar pattern of new developed dimensionless model, the testing of new formulation of generalized dimensionless model for diameter function is again found incompatible because of high APE between the observed and computed values of effluent concentrations. Considering the non-superior performance of dimensionless equations, the models developed for effluent quality and head loss prediction, as given in the previous chapter, are considered for testing against rainwater samples for different filter runs, as discussed in the next chapter.

APPLICABILITY OF DEVELOPED MODELS TO HARVESTED RAINWATER

7.1 PREAMBLE

An attempt to develop dimensionless models was also not rewarding. In the previous chapter, the performance of the unified regression models developed at influent concentrations of 30 mg/l (run nos. 28 to 54) is tested under different conditions for influent concentrations of 25 mg/l and 40 mg/l. Thus, in this section, new unified regression model is tested for effluent quality and head loss prediction against rainwater samples (run nos. 65 to 89) which were not used in the calibration of the models for vertically downward flow filters. Also, the new unified model developed for lumped data of influent concentrations of 30 mg/l is tested against rainwater samples (run nos. 100 to 104) for horizontal flow filter. It is worth mentioning that all these experiments are based on harvested rainwater.

7.2 VERIFICATION OF EFFLUENT QUALITY MODELS

The new unified regression models (MOVEQ-30AL and MOHEQ-30E) developed in chapter 5, are tested against rainwater fed vertically downward flow (run nos. 65 to 89) and horizontal flow (run nos. 100 to 104) sand filters, respectively. The performance of the unified regression models for effluent quality prediction is discussed in details in subsequent sections.

The selection of particular grain size, as considered in the study, for the sand filter is impractical in the field condition. Hence, the new unified models are used to predict the performance of vertically downward flow sand filters against rainwater samples having influent concentration of 17 mg/l. The data of experimental runs (nos. 65 to 89) were used for the computation of errors and the average of such errors for each of the runs is presented in Table 7.1 for unified model (MOVEQ-30AL). From the Table 7.1, it can be seen that the errors are found as low as 4.71% (run no. 84) and as high as 14.01% (run no. 87). Figures 7.1(a)-7.1(c) show the agreement between the observed and the computed effluent concentrations for certain filter runs. Hence, the new regression model developed for influent concentration of 30 mg/l seems compatible for rainwater harvesting sand filter performance prediction under different filtering conditions.

The model developed for vertically downward flow filter is not compatible to predict the performance of horizontal flow filter because the nature of turbidity removal by horizontal filter is entirely different from the vertically downward flow filter. Hence, the unified model (MOHEQ-30E) developed for influent concentration of 30 mg/l (run nos. 90 to 94) is again tested against rainwater samples (run nos. 100 to 104) for horizontal flow filter. The errors for effluent concentration are given in Table 7.2. From the Table 7.2, it can be seen that the errors are found as low as 10.78% (run no. 102) and as high as 14.81% (run no. 100). Figure 7.2 shows the scattering of the observed and the computed values around the line of perfect agreement using lumped data. Figure 7.3 shows the observed and the computed effluent quality for certain filter run (run no. 103).

Table 7.1: Computed APE of U and C using unified model (MOVEQ-30AL) against rainwater samples (run nos. 65 to 89)

Grain size (mm)	Flow velocity (m ³ /hr/m ²)	Computed APE	
		U	C
3.647	1.65	7.26	8.91
	3.30	5.95	6.18
	4.95	5.44	5.93
	6.60	4.57	5.57
	8.25	4.27	4.75
2.366	1.65	8.00	9.01
	3.30	5.95	6.75
	4.95	6.16	7.41
	6.60	8.95	10.13
	8.25	10.00	10.13
1.673	1.65	11.40	13.99
	3.30	7.19	7.96
	4.95	9.04	9.15
	6.60	6.29	6.85
	8.25	7.06	7.55
1.091	1.65	3.69	6.31
	3.30	8.56	12.79
	4.95	6.27	9.95
	6.60	5.92	7.57
	8.25	4.22	4.71
0.714	1.65	6.07	12.72
	3.30	5.86	11.27
	4.95	8.40	14.01
	6.60	5.52	10.89
	8.25	3.84	7.53

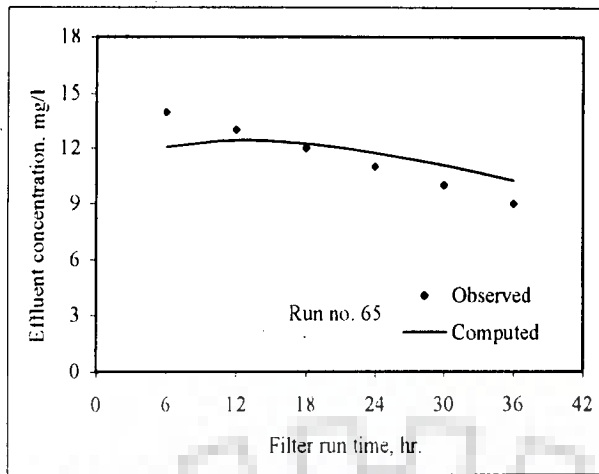


Fig. 7.1(a)

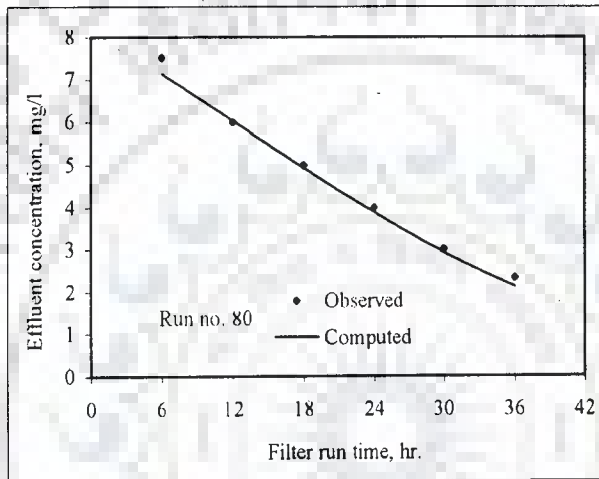


Fig. 7.1(b)

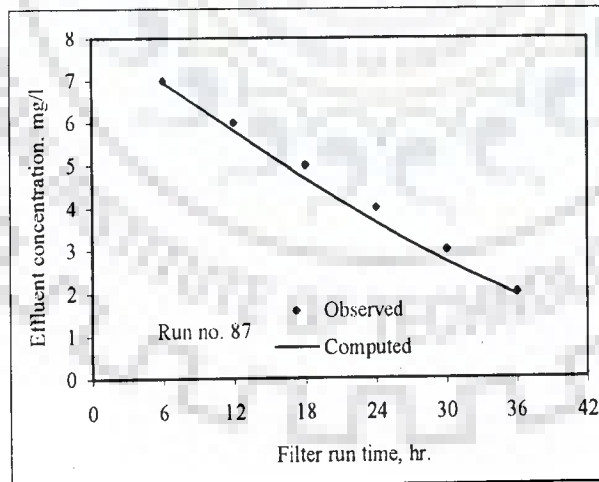


Fig. 7.1(c)

Figs. 7.1(a) -7.1(c): Plot of effluent quality observed versus computed using model (MOVEQ-30AL) for certain filter runs

Table 7.2: Computed APE of U and C using unified model (MOHEQ-30E) against rainwater samples (run nos. 100 to 104)

Grain size (mm)	Flow velocity (m ³ /hr/m ²)	Computed APE	
		U	C
0.714	1.65	9.86	14.81
	3.30	7.11	13.37
	4.95	6.76	10.78
	6.60	8.82	13.69
	8.25	7.80	14.07



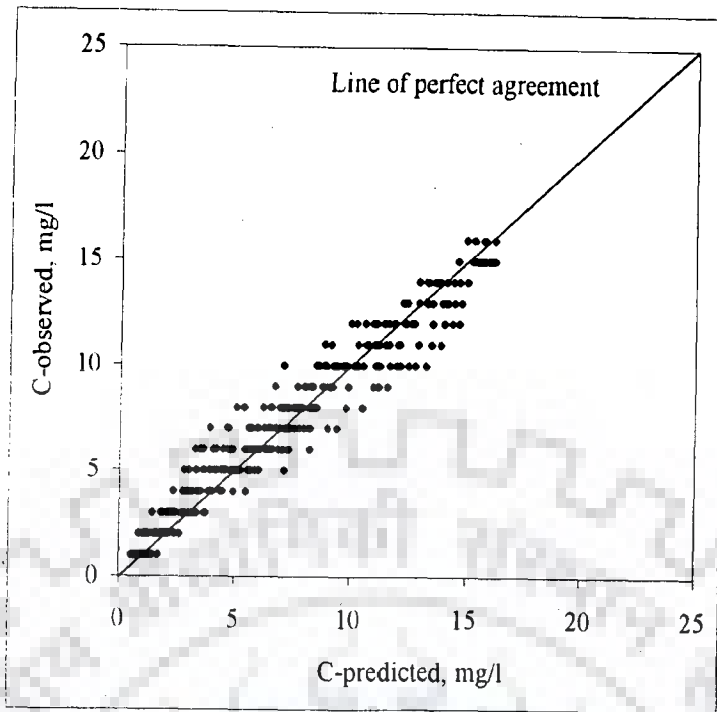


Fig. 7.2: Plot of C-observed versus C-computed using model (MOHEQ-30E) for rainwater samples (run nos. 100 to 104)

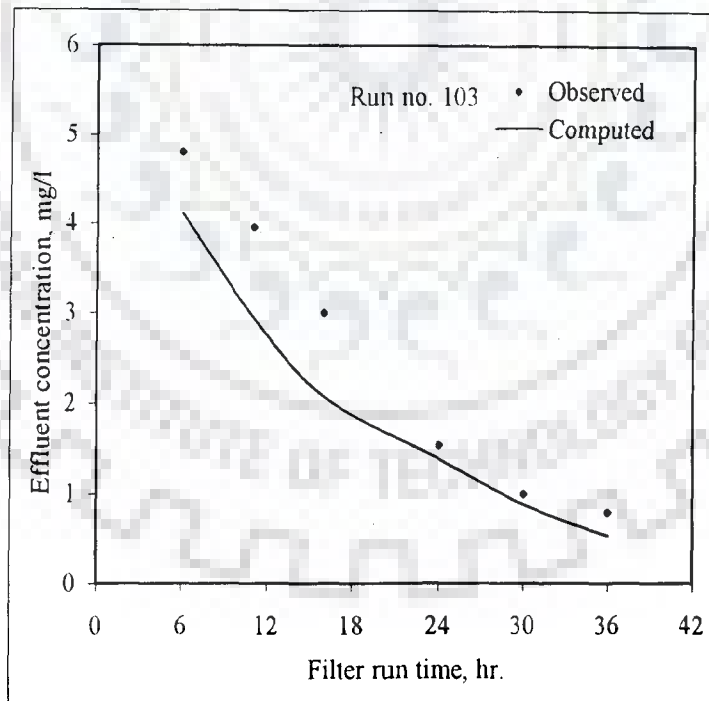


Fig. 7.3: Plot of effluent quality observed versus computed using model (MOHEQ-30E) for certain filter run

7.3 VERIFICATION OF FLOW RESISTANCE MODELS

The new unified regression models (MOVEHL-30AL and MOHOHL-30E) developed in chapter 5, are tested against rainwater fed vertically downward flow (run nos. 65 to 89) and horizontal flow (run nos. 100 to 104), respectively for prediction of sand filter head loss. The performance of the unified regression models for head loss is discussed in details in subsequent sections. The new unified model (MOVEHL-30AL) is used to predict the performance of vertically downward flow sand filters against rainwater samples having influent concentration of 17 mg/l.

The data of experimental runs (nos. 65 to 89) were used for the computation of errors and the comparison of average of errors for each of the runs using unified model (MOVEHL-30AL) is presented in Table 7.3. From the Table 7.3, it can be seen that the errors are computed as low as 22.62% (run no. 71) and as high as 75.35% (run no. 84) whereas, the errors using H-C models are computed as 739.40% and 5892.71% (Table 4.9) at the corresponding experimental runs. Figures 7.4(a)-7.4(c) show the agreement between the observed and the computed head loss values for certain filter runs.

The unified model (MOHOHL-30E) developed for influent concentration of 30 mg/l (run nos. 90 to 94) is again tested against rainwater samples for horizontal flow filter. The errors for head loss are given in Table 7.4. From the Table 7.4, it can be seen that the errors are found as high as 84.46% (run no. 100). Figure 7.5 shows the observed and the computed head loss for certain filter run (run no. 101). Hence, the new regression model seems compatible for rainwater harvesting sand filter performance prediction under different filtering conditions.

Table 7.3: Computed head loss APE using unified model (MOVEHL-30AL) against rainwater samples (run nos. 65 to 89)

Grain size (mm)	Flow velocity ($\text{m}^3/\text{hr}/\text{m}^2$)	Computed APE
3.647	1.65	36.45
	3.30	32.61
	4.95	34.64
	6.60	35.78
	8.25	30.82
2.366	1.65	23.85
	3.30	22.62
	4.95	25.64
	6.60	28.91
	8.25	30.11
1.673	1.65	28.93
	3.30	23.73
	4.95	32.40
	6.60	32.57
	8.25	36.49
1.091	1.65	46.43
	3.30	58.80
	4.95	71.56
	6.60	69.23
	8.25	75.35
0.714	1.65	40.39
	3.30	29.02
	4.95	35.50
	6.60	29.37
	8.25	30.58

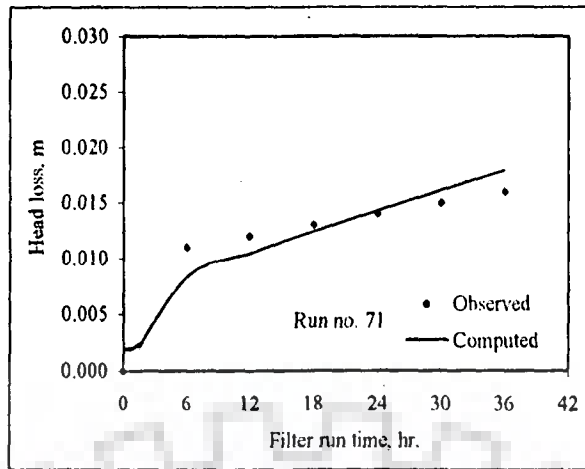


Fig. 7.4(a)

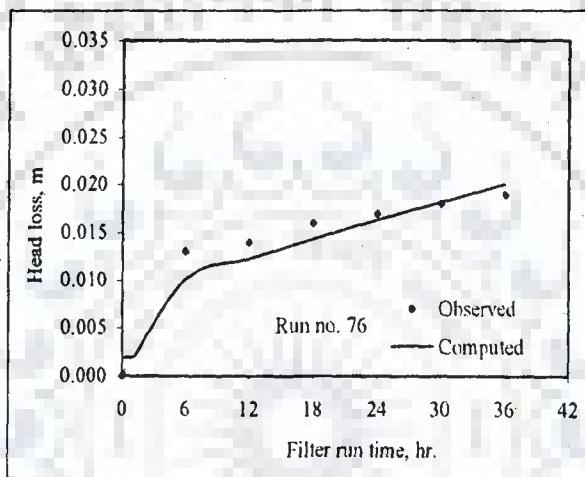


Fig. 7.4(b)

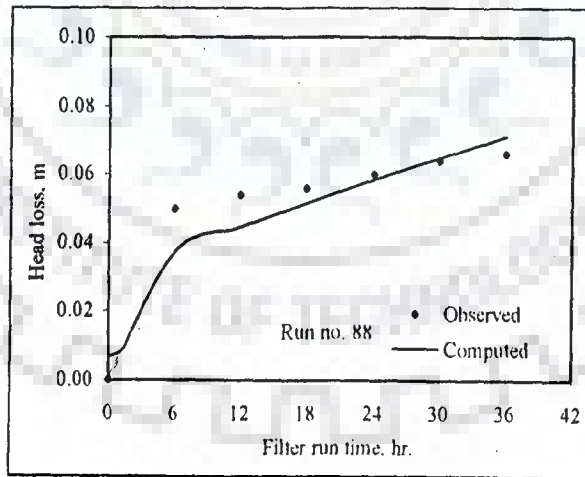
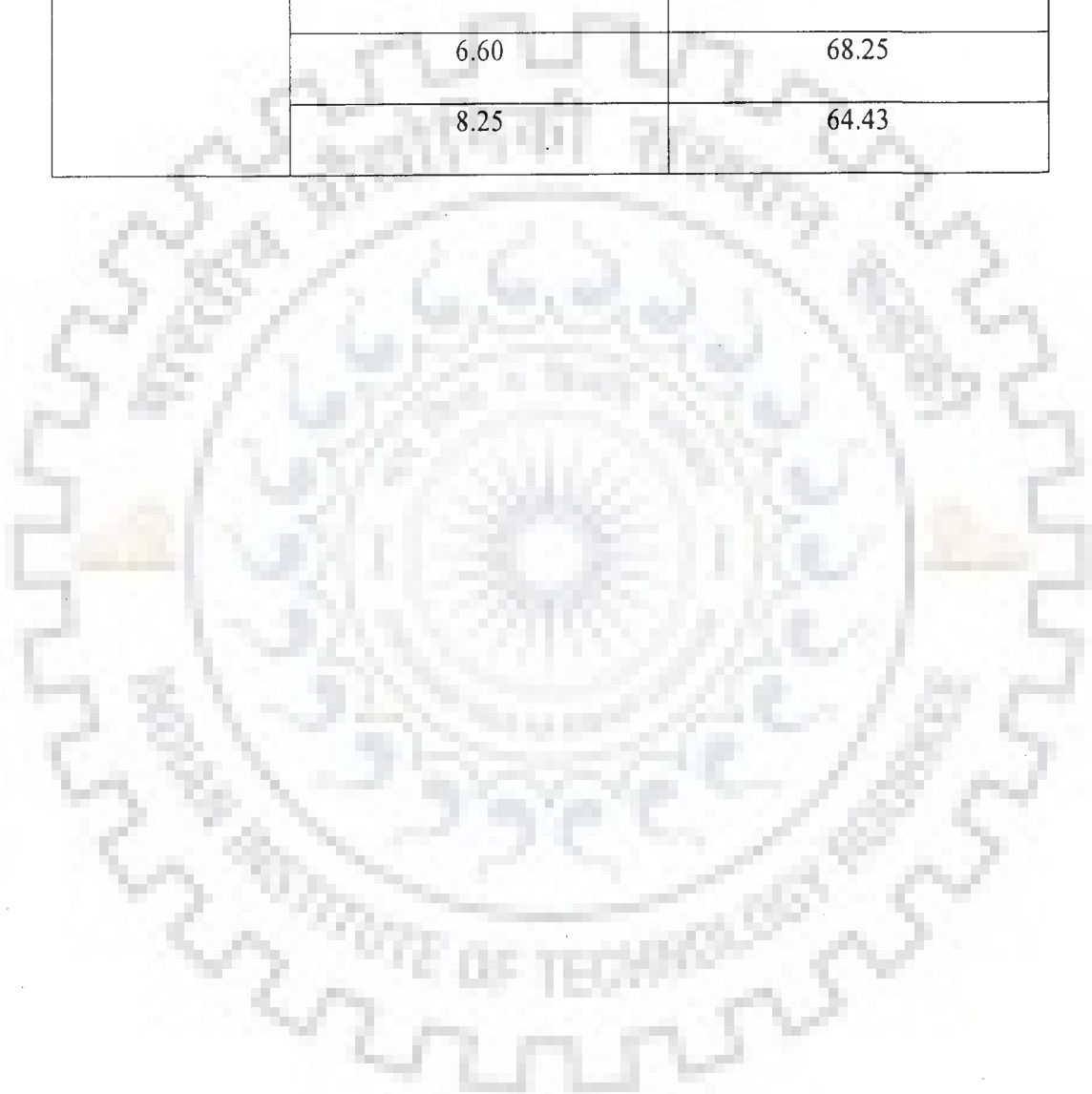


Fig. 7.4(c)

Figs. 7.4(a)-7.4(c): Plot of head loss observed versus computed using model (MOVEHL-30AL) for certain filter runs

Table 7.4: Computed head loss APE using unified model (MOHOHL-30E) against rainwater samples (run nos. 100 to 104)

Grain size (mm)	Flow velocity (m ³ /hr/m ²)	Computed APE
0.714	1.65	84.46
	3.30	75.69
	4.95	70.05
	6.60	68.25
	8.25	64.43



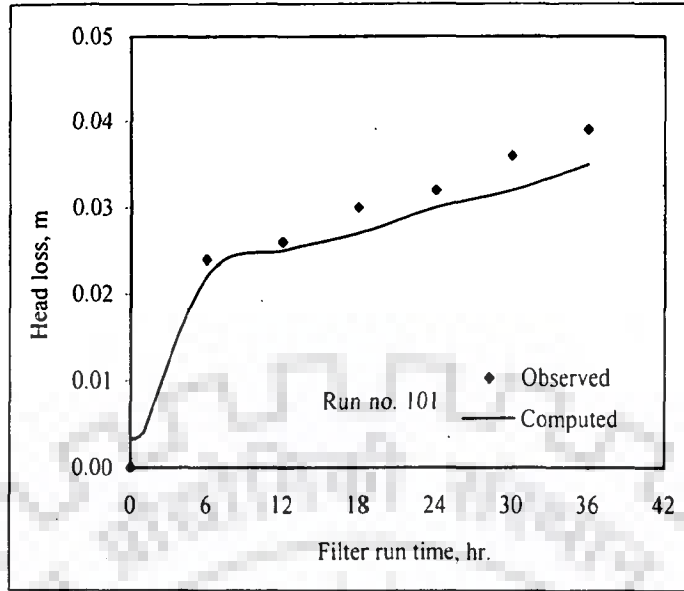


Fig. 7.5: Plot of head loss observed versus computed using model (MOHOHL-30E) for certain run

7.4 CONCLUDING REMARKS

The main aim of this chapter is to verify the new unified developed models against rainwater samples to check their compatibility for the prediction of sand filter performance under vertically downward flow and horizontal flow conditions. The unified regression models developed for effluent quality prediction seem compatible for vertically downward flow filter. But, the performance of the unified regression models for head loss prediction seems satisfactory for horizontal flow filter. Since the head losses measured in sand filters during experimentation were very low and hence one can not expect the compatibility of the models. But it is certainly better than the performance of H-C model for head loss prediction under different filtering conditions. The compatibility of the new models is assessed on average percentage error (APE) between the observed and computed values. Testing of new regression models against rainwater samples concludes that the models are much more compatible than Hsiung and Cleasby (1968) models for the prediction of sand filter performance.

RESULTS AND DISCUSSION

8.1 PREAMBLE

The design of sand filters, installed in the field for rainwater harvesting practices are on ad-hoc basis since no design specification/guidelines are available. The models for prediction of sand filter performance in terms of effluent quality and head loss are given by Hsiung and Cleasby (1968). But the application of the models shows incompatible for performance prediction of sand filters using Fuller's earth suspension samples and rooftop harvested rainwater samples. In this chapter, an overall discussion of the results observed in preceding chapters is provided to highlight the use and limitations of the present work. The presentation is reported in the following heads.

8.2 EFFLUENT QUALITY IN CASE OF VERTICALLY DOWNWARD FLOW FILTERS

The Hsiung and Cleasby (1968) model seems incompatible for sand filter performance prediction in terms of effluent quality and hence, new regression models have been developed based on the experimental data. The sand filter modules were operated with mean sand grain sizes of 3.647 mm, 2.366 mm, 1.673 mm, 1.091 mm, 0.714 mm and 0.505 mm and flow velocities between $1.65 \text{ m}^3/\text{hr}/\text{m}^2$ and $8.25 \text{ m}^3/\text{hr}/\text{m}^2$ at an equal interval of $1.65 \text{ m}^3/\text{hr}/\text{m}^2$. Two types of sand filter i.e. uniform sand filter and graded sand filter were operated using Fuller's earth suspension water solution samples and rainwater samples. Out of 110 experimental runs, 32 runs (nos. 28 to 54 and 90 to 94) were used for

development of the new regression models and 78 runs (nos. 1 to 27, 55 to 64, 65 to 89, 95 to 99, 100 to 104 and 105 to 110) were used for testing of new regression models. Each and every filter run was maintained at 36 hours, particularly for uniform sand grains filter. The models were developed under uniform sand filtering condition and tested against uniform sand and graded sand filtering conditions for harvested rainwater samples (experimental details are given in chapter 3).

Hsiung and Cleasby (H-C) model (Eq. 4.2) has been tested for effluent quality prediction at different filter runs data for influent turbidity concentrations of 25 mg/l (run nos. 1 to 27), 30 mg/l (run nos. 28 to 54), 40 mg/l (run nos. 55 to 64) and 17 mg/l (run nos. 65 to 89) (details are furnished in chapter 4). With reference to Table 4.1, it is observed that average percentage error (APE) is larger in case of experiments having lower media grain sizes. For example, corresponding to experimental run no. 26, APE reaches as high as 92.73% and certainly, this type of model is not acceptable. High values of APE are also computed for other sand grain sizes although the magnitude of such errors are low in certain cases, particularly involving larger sand grain sizes. With reference to Table 4.2, which deals with an influent turbidity of 30 mg/l, APE is not influenced by variation in flow velocity. For example, corresponding to experimental run no. 53, APE is as high as 95.20%.

The use of H-C model for influent concentration of 40 mg/l also shows APE in higher range at lower sand grain sizes (Table 4.3). From the Table 4.4, APE of 137.07% (run no. 85) for rainwater sample was observed with the use of H-C model. This reflects that even at lower sand grain sizes, variation in flow rate lead to poor performance of H-C model. H-C model at lower sand grain sizes in the running experiment should have better performance because H-C model was developed at higher sand grain size of 0.649 mm. Based on such interpretation of H-C model performance, it was inferred that the

representation of the exponents Q & d (flow velocity and sand grain diameter) in H-C model were not adequate and hence, attempts were made to redefine H-C model by tuning of exponents of Q & d .

Obviously, there were two options to achieve this. The first one relates to variation of exponents of Q & d without maintaining the dimensionless nature of the parameter G , as also evident in H-C model and secondly to make it dimensionless. In chapter 5, such numerical experiments are reported and new sets of effluent quality regression relationships at each sand grain size have been obtained. Table 5.1 contains a set of such effluent quality regression relationships. It is significant to see that APE for the same experiments has reduced significantly, as a result of numerical experiments. In these expressions, similar structure of G' is maintained as in H-C model. Although, there is no need to include d as a term, once it is being considered for individual sand grain size. For example, any expression in Table 5.1 can be recasted by substituting the appropriate values of d . However, this is intentionally not done in order to maintain consistency with H-C model.

Table 5.2 indicates another interesting feature of the modelling. Here, all the experimental runs data (nos. 28 to 54) are used to develop a unified regression model (MOVEQ-30AL) and APE has gone upto 30% in certain cases related to smaller sand grain sizes. Obviously, with such a small value of influent concentration, it is not expected that the regression models will differ from each other radically. APE for larger sand grain sizes is still very low and thus, the unified model of the effluent quality (MOVEQ-30AL) can still be a reasonable selection if one is in a position to accept such APE values. Thus, the new unified regression model (MOVEQ-30AL) can be used to get less APE.

8.3 HEAD LOSS IN CASE OF VERTICALLY DOWNWARD FLOW FILTERS

Hsiung and Cleasby (H-C) model (Eq. 4.4) has been tested for head loss prediction at different filter runs data for influent turbidity concentrations of 25 mg/l (run nos. 1 to 27), 30 mg/l (run nos. 28 to 54), 40 mg/l (run nos. 55 to 64) and 17 mg/l (run nos. 65 to 89) (details are furnished in chapter 4). With reference to Table 4.6, it is observed that the head loss APE is again larger in case of experiments having lower media grain size. For example, corresponding to experimental run no. 25, head loss APE reaches as high as 7296.88% and certainly, this type of model is not acceptable. Higher values of head loss APE are also computed for other sand grain sizes, particularly involving larger sand grain sizes.

With reference to Table 4.7, which deals with an influent concentration of 30 mg/l, APE is not influenced by variation in flow velocity. For example, corresponding to experimental run no. 52, head loss APE is as high as 6643.53%. The testing of H-C model at influent concentration of 40 mg/l for head loss prediction also shows APE in higher range at lower sand grain size (Table 4.8). An APE of 6381.62% for experimental run no. 89 was observed with the use of H-C model, as given in Table 4.9.

Thus in chapter 5, vertically downward flow filter experiments are reported and new sets of head loss regression relationships at each sand grain size have been obtained. Table 5.7 contains a set of such head loss regression models. It is significant to see that head loss APE for the same experiments has reduced significantly. In these expressions, the structure of R' is maintained similar as in H-C model. It is needless to mention that any expression in Table 5.7 can be recasted by substituting the appropriate values of d and Q .

Table 5.8 indicates another interesting feature of the modelling. Here, all the experimental runs data (run nos. 28 to 54) were used to develop an unified regression

model (MOVEHL-30AL). Obviously, head loss APE has gone upto 30% in certain cases related to higher and lower sand grain sizes. Thus, the head loss unified model can still be a reasonable solution if one is in a position to accept such APE values. Similar observations hold good when the model developed for influent concentration of 30 mg/l is tested for influent concentration of 25 mg/l and 40 mg/l, as can be seen from Tables 5.9 & 5.10. These models are very similar in form with H-C model. Obviously, with such a small values of influent concentrations, it is not expected that models will differ from each other radically. Thus, the proposed unified regression model (MOVEHL-30AL) can be used to get less APE with revised coefficients of R as R', as given in Tables 5.8.

8.4 EFFLUENT QUALITY IN CASE OF HORIZONTAL FLOW FILTER

The horizontal flow sand filter module was operated with mean sand grain size of 0.714 mm and flow velocities between 1.65 m³/hr/m² and 8.25 m³/hr/m² at an equal interval of 1.65 m³/hr/m². H-C model (Eq. 4.2) has been tested for effluent quality prediction at different filter runs data for influent turbidity concentrations of 30 mg/l (run nos. 90 to 94), 40 mg/l (run nos. 95 to 99) and 17 mg/l (run nos. 100 to 104) (details are furnished in chapter 4). With reference to Table 4.5, it is observed that APE is larger in case of experiments having different influent concentrations at same media sizes. For example, corresponding to experimental run data (run no. 95), APE reaches as high as 96.92% and certainly, this type of model is not acceptable. Higher APE are also computed for other influent concentrations. The new developed regression model (MOHEQ-30E) for horizontal flow filter shows relatively an acceptable low APE with revised coefficients of G as G'', as given in Tables 5.5 & 5.6. The model is very similar in the form with H-C model.

8.5 HEAD LOSS IN CASE OF HORIZONTAL FLOW FILTER

With reference to Table 4.10, it is observed that head loss APE is again larger in case of experiments having lower media grain sizes. For example, corresponding to experimental run no. 104, head loss APE reaches as high as 101243.04% and certainly, this type of model is not acceptable. High values of head loss APE are also computed for other influent concentrations. This reflects that even at lower sand grain sizes, variation in flow rate leads to poor performance of H-C model for head loss prediction. The new developed regression model (MOHOHL-30E) for horizontal flow filter shows relatively lower APE with revised coefficients of R as R", as given in Tables 5.11 & 5.12.

8.6 DIMENSIONLESS VERSUS DIMENSIONAL REPRESENTATIONS

The new developed regression model for effluent quality prediction was tested in dimensionless form. Here, for a given d , (Qt/L) has been used as a dimensionless term. In chapter 6, a new set of dimensionless effluent quality models at each sand grain size has been obtained. Table 6.1 contains a set of such effluent quality dimensionless regression relationships. Obviously, APE has gone upto 70% in certain cases related to smaller sand grain sizes and certainly, this type of model is not acceptable. The dimensionless model for horizontal flow filter also shows higher APE which is not acceptable, as given in Table 6.2.

The new developed regression model for head loss prediction was also tested in dimensionless form. Table 6.4 contains a set of such head loss dimensionless regression relationships. Obviously, APE has gone beyond 100% in certain cases related to higher and smaller sand grain sizes and certainly, this type of model is not acceptable. The dimensionless model for horizontal flow sand filter also shows higher APE which is not

acceptable, as given in Table 6.5. Obviously, the behaviour, in terms of APE of the dimensionless models is found similar to the behaviour with H-C model for effluent quality and head loss prediction and no advantage could be achieved by using dimensionless relationships.

8.7 USE OF GRADED SAND FILTERS

When uniform sand is used in the experiments for model development, the same model may be applied for performance prediction of a graded sand filter. Hsiung and Cleasby (1968) mentioned that the upper layer of a graded sand filter will do most of the removal during a typical length of filter run. Under the condition of present study, the above statement is not true and the penetration of turbidity has also been found in the immediate lower layer. Now, the new regression model (MOVEQ-30AL) (as discussed in section 5.2.1) is used for performance prediction of graded sand filter with Fuller's earth suspension water solution samples (run nos. 105 & 106) and rainwater samples (run nos. 107 to 110).

At the same removal efficiency by graded sand filter, an equivalent mean sand grain size is computed and the results are presented in Table 8.1. From the Table 8.1, it is clear that the contribution of upper layer of graded sand filter for turbidity removal is more significant but the contribution of immediate lower layer is also considerable since the turbidity penetrates the upper most layer of graded sand filter. The computed equivalent mean sand grain size for different layers of graded sand filter is higher than the size of upper layer sand grains.

Experimentation with graded sand filter in case of horizontal flow filter could not perform well for removal of turbidity. The turbidity removal was not significant for graded sand filter with respect to the filter operated at uniform sand grain size of 0.714 mm. Since

the maximum turbidity removal efficiency was observed for wide range of flow velocity during experimentation at 0.714 mm sand grain hence, this sand grain size has been considered for horizontal flow sand filter.

Table 8.1: Performance of graded sand filter using new regression relationship (MOVEQ-30AL) with equivalent mean sand grain size

Filter run nos.	Geometric mean size (mm)	Experimentation with	Filtration rate (m ³ /hr/m ²)	Removal (%)	C/C _o	Equivalent mean size (mm)
105	3.103	Fuller's earth (25 mg/l)	0.21	76.0	0.240	3.257
106			0.42	68.0	0.320	3.092
107	3.103	Rainwater (17 mg/l)	0.21	76.5	0.235	3.095
108			0.42	70.6	0.294	2.953
109	2.937	Rainwater (17 mg/l)	1.65	58.8	0.412	2.467
110	1.607	Rainwater (17 mg/l)	1.65	82.4	0.176	1.312

8.8 PERFORMANCE OF NEW REGRESSION MODELS USING HARVESTED RAINWATER

The new developed regression models have been tested to predict the performance of sand filter using rainwater samples (details are discussed in chapter 7). The results for effluent quality and head loss for vertically downward flow filter runs (nos. 65 to 89) are presented in Table 8.2. The results for effluent quality and head loss for horizontal flow filter runs (nos. 100 to 104) are presented in Table 8.3. A close relationship between C/C_o observed and computed and head loss observed and computed using new regression

models are observed, as given in Tables 8.2 & 8.3. From the Tables 8.2 & 8.3, it is clear that the new developed regression models are more compatible with respect to H-C model for performance prediction of sand filter in terms of effluent quality and head loss.

Table 8.2: Prediction results of typical check runs (nos. 65 to 89) using new models (MOVEQ-30AL) and (MOVEHL-30AL) at the end of filter run time

Run no.	d (mm)	Q (m ³ /hr/m ²)	C ₀ (mg/l)	L (m)	t (hrs.)	$\left(\frac{G'}{L^{1.5}}\right)$	U. computed	$\frac{R'}{L^3}$	Effluent quality		Head loss (m)	
									C/C ₀ computed	C/C ₀ observed	computed	observed
65	3.647	1.65	17	0.30	36	365.93	37.57	0.0050	0.60	0.53	0.0097	0.0120
66		3.30				397.67	40.13	0.0053	0.71	0.65	0.0117	0.0120
67		4.95				417.49	41.68	0.0054	0.76	0.71	0.0130	0.0140
68		6.60				432.16	42.81	0.0056	0.80	0.71	0.0141	0.0150
69		8.25				443.89	43.71	0.0057	0.82	0.82	0.0149	0.0140
70	2.366	1.65	17	0.30	36	314.50	33.26	0.0046	0.40	0.47	0.0150	0.0140
71		3.30				341.78	35.58	0.0048	0.51	0.71	0.0179	0.0160
72		4.95				358.82	36.99	0.0050	0.60	0.59	0.0199	0.0180
73		6.60				371.42	38.02	0.0051	0.65	0.76	0.0215	0.0190
74		8.25				381.51	38.84	0.0052	0.68	0.76	0.0228	0.0200
75	1.673	1.65	17	0.30	36	278.58	30.10	0.0040	0.26	0.41	0.0169	0.0180
76		3.30				302.74	32.24	0.0042	0.35	0.35	0.0201	0.0190
77		4.95				317.83	33.55	0.0043	0.41	0.47	0.0223	0.0280
78		6.60				329.00	34.50	0.0044	0.46	0.47	0.0240	0.0290
79		8.25				337.92	35.25	0.0045	0.50	0.53	0.0255	0.0310
80	1.091	1.65	17	0.30	36	239.86	26.55	0.0039	0.13	0.18	0.0327	0.0170
81		3.30				260.66	28.48	0.0041	0.19	0.35	0.0390	0.0180
82		4.95				273.66	29.66	0.0042	0.24	0.35	0.0432	0.0180
83		6.60				283.27	30.52	0.0043	0.27	0.35	0.0465	0.0190
84		8.25				290.96	31.21	0.0044	0.30	0.35	0.0493	0.0190
85	0.714	1.65	17	0.30	36	206.07	23.30	0.0037	0.05	0.06	0.0503	0.0640
86		3.30				223.94	25.04	0.0038	0.09	0.12	0.0599	0.0580
87		4.95				235.11	26.10	0.0039	0.11	0.12	0.0664	0.0740
88		6.60				243.37	26.88	0.0040	0.14	0.18	0.0714	0.0660
89		8.25				249.97	27.49	0.0040	0.16	0.18	0.0755	0.0710

Table 8.3: Prediction results of typical check run (nos. 100 to 104) using new models (MOHEQ-30AL) and (MOHOHL-30AL) at the end of filter run time

Run no.	d (mm)	Q (m ³ /hr/m ²)	C ₀ (mg/l)	L (m)	t (hrs.)	$\left(\frac{G^*}{L^{1/2}}\right)$	U	$\frac{R^*}{L^{1/2}}$	Effluent quality		Head loss (m)	
									C/C ₀ Computed	C/C ₀ Observed	Computed	Observed
100	0.714	1.65	17	0.60	36	88.3	17.70	0.000116	0.004	0.059	0.008	0.035
101		3.30				100.7	19.95	0.000118	0.011	0.059	0.015	0.039
102		4.95				108.8	21.37	0.000120	0.021	0.059	0.021	0.042
103		6.60				114.9	22.43	0.000121	0.032	0.059	0.027	0.048
104		8.25				119.9	23.28	0.000122	0.043	0.059	0.032	0.050

8.9 DISTRIBUTED VERSUS LUMPED MODEL ANALYSIS

To highlight the distributed versus lumped approach based on the analysis of data (run no. 28), a plot between \hat{R}_d and \hat{G} has been used for development of regression relationships by considering five cases, i.e. based on data generated at 0-100 mm filter depth from top (case 1); data generated at 0-200 mm filter depth from top (case 2); data generated at 0-300 mm filter depth from top (case 3); data generated at 0-400 mm filter depth from top (case 4); data generated at 0-500 mm filter depth from top (case 5). The developed regression relationships for all the cases are given in Table 8.4. Table 8.4 clearly highlights the influence of lumping of data for different layers with increase in APE. It can be seen that the coefficient of regression drops significantly with the inclusion of data from a large number of layers. Ojha and Graham (1992) indicated that the top layer of sand filter is not representative of the behaviour of the entire filter bed and thus results are likely to be sensitive to the depth of filter media considered in the analysis.

Table 8.4: Comparison of distributed versus lumped model analysis using new dimensionless model for certain filter run (no. 28)

Case	Filter media depth from the top (mm)	New dimensionless models	Flow velocity (m ³ /hr/m ²)	Computed head loss APE
1	100	$\hat{R}_d = -2E - 23(\hat{G})^2 + 2E - 14(\hat{G}) + 6E - 06$ $R^2 = 0.983$	1.65	4.76
2	200	$\hat{R}_d = -4E - 23(\hat{G})^2 + 2E - 14(\hat{G}) + 7E - 06$ $R^2 = 0.766$		16.52
3	300	$\hat{R}_d = -4E - 23(\hat{G})^2 + 2E - 14(\hat{G}) + 7E - 06$ $R^2 = 0.57$		26.00
4	400	$\hat{R}_d = -5E - 23(\hat{G})^2 + 2E - 14(\hat{G}) + 8E - 06$ $R^2 = 0.40$		32.68
5	500	$\hat{R}_d = -5E - 23(\hat{G})^2 + 2E - 14(\hat{G}) + 8E - 06$ $R^2 = 0.27$		37.88

8.10 CONCLUDING REMARKS

From a general discussion of several aspects of statistical modelling of filter runs, it is apparent that H-C model has limited potential for use in rainwater harvesting. Improved regression relationships developed in accordance with H-C model exhibit better performance. It is possible to model the performance of vertical as well as horizontal filters using statistical approach. Existing view that in graded filters, effective sand grain size may correspond to the sand grain size of upper layers is not well supported. Also, dimensionless approach has not yielded useful regression relationships. It is clear that Hsiung and Cleasby approach has certain potential towards the design of sand filters and only for this reason the present study has focused on the development of effluent quality and flow resistance relationships. In absence of design information for designing of rainwater harvesting sand filters, the present study is expected to fill the gap to certain extent.

CONCLUSIONS AND FUTURE SCOPE OF WORK

9.1 CONCLUSIONS

For influent concentrations likely to be encountered in rainwater harvesting, a series of filter runs have been performed. Experiments were conducted in the laboratory with sand media grain sizes of 3.647 mm, 2.366 mm, 1.673 mm, 1.091 mm, 0.714 mm and 0.505 mm and different flow rates varying between $1.65 \text{ m}^3/\text{hr}/\text{m}^2$ and $8.25 \text{ m}^3/\text{hr}/\text{m}^2$ at an equal interval of $1.65 \text{ m}^3/\text{hr}/\text{m}^2$. Largely, filters were operated in vertically downward flow conditions, although earlier runs did include horizontal mode of filter run as well as use of graded sand media. The study has focused primarily on the evaluation of existing models, development of alternate models, dimensionless model analysis and testing of new developed models against harvested rainwater. In general, following conclusions can be inferred from the present study.

1. Based on the evaluation of as many as two numbers of vertically downward flow operated filters using uniform sand grains for effluent quality, it is found that the performance of existing models is not acceptable as the associated average percentage error (APE) with the use of these models is constantly observed to be on a higher side. APE values of 50% to 100% are not acceptable by any standard. Thus, use of Hsiung and Cleasby (1968) model is not advocated for the computation of effluent quality in vertically downward flow operated filters.
2. Use of existing model for head loss prediction has been equally unsuccessful. APE values were constantly larger than 100% indicating the poor performance of the

model for vertically downward flow filters. Head loss APE for horizontal flow filter was also found much higher than the stated values for vertically downward flow sand filter. Considering that Hsiung and Cleasby (1968) model was developed for sand media grain sizes between 0.386 mm and 0.649 mm, its performance was also evaluated in these ranges. However, the model did not indicate its utility even in the range of these sand media grain sizes. It appears that the influent quality which in the present experiments did not include ferrous sulfate as additive has a marked influence on the performance of filter runs.

3. Variation in the exponents of flow rate (Q) and media grain size (d) was successful in reducing the calibration error associated with the new developed regression models. A set of regression models to describe effluent quality and head loss have been proposed for vertically as well as horizontally operated sand filters in chapter 5. It is observed that these relationships have lesser calibrated errors and thus, their use is recommended in preference to Hsiung and Cleasby (1968) models.
4. Testing of new developed regression models was made using 30 nos. of filter runs (nos. 65 to 89 and 100 to 104) with harvested rainwater. Influent concentration of harvested rainwater was found 17 mg/l, it was observed that the new developed models performed very well in representing effluent quality as well as head loss in case of vertically as well as horizontally operated filters.
5. For a given d , attempts were made to evolve dimensionless relationship. With Q , t and L , only one dimensionless variables could be defined as Qt/L . However, its use did not lead to expected improvement in either the filtrate quality or the head loss model.

6. Certain modifications were also introduced into dimensionless analysis. A generalized modelling for diameter function was attempted with not much success. Similarly, for modelling of flow resistance, the resistance parameter of H-C model was also made dimensionless. Use of this dimensionless term also did not lead to any improvement in calibration of flow resistance relationships. Subsequently, a new dimensionless relationship was also attempted with no significant improvement in calibration errors.
7. A comparative evaluation of filtrate quality coming out from vertical as well as horizontal sand filters was also made under identical conditions of flow rates, media grain sizes and filter lengths. In general, it was observed that the removal was better in case of horizontal filters and the flow resistance developed was less. This was mainly due to entrapment/settlement of impurities at the face of the filter in case of horizontal flow.
8. Finding of the Hsiung and Cleasby (1968) model that different configuration of sand filters can also be represented using statistical approach is substantial in the present work. Performance of vertically as well as horizontally operated sand filters has been modelled using similar formulated relationships and thus supports the findings of Hsiung and Cleasby (1968) work.
9. In case of filters, impurities can penetrate to different depths depending on flow rates, media grain sizes and influent concentrations. The view of Hsiung and Cleasby that top layer media grain size can be used as an effective media is not justified from the present work. In Chapter 8 (Table 8.1), it is shown that effective grain size lies somewhere in between the top two layers. The present research also supports the study made by Ojha and Graham (1992) that the topmost layer of the deep-bed filter is not representative of the behaviour of the entire media, as models

based on the top-layer performance do not simulate very well the performance of the entire media bed.

9.2 FUTURE SCOPE OF WORK

In view of investigations reported in chapter 5, and Table 8.4, it seems that the distributed approach which accounts for the contribution for the individual layer might prove a better alternative. This approach needs to be examined in subsequent study to assess the likely improvement and preferential advantages over lumped models, as developed in the present study.

In this investigation, sand filters were operated for only 36 hours. The behaviour of the filters has not been investigated for a series of rain events. In further scope of work, it may be necessary to monitor the performance of filter runs for such rainfall occurrence.



REFERENCES

1. **Agarwal, A.**, Coaxing the barren deserts back to life. *New Sci.*, 75, 1069, 674-675, 1977.
2. **Agarwal, A.**, Rainwater harvesting in a new age: when modern groundwater and river exploitation has reached its limits. Stockholm Water Symposium, Stockholm International Water Institute, Paper 2, Sweden, 1998.
3. American Water Works Association Task Group Report (AWWATGR), Progress toward a filterability index test. AWWATGR, *Am. Wat. Works Assoc.*, 51, 1539, 1959.
4. **Anonymous.**, Rainwater harvesting. Department of Rural development, Ministry of Agriculture, Government of India, India. 44, 1990.
5. **Anonymous.**, Rainwater harvesting report (unpublished). M.P. Housing Board, Khandwa, India, 2002.
6. **Appan, A.**, Water quality issues in rainwater cistern systems in some south east-Asian countries. Proc. 7th Inter. conf. on rainwater catchment systems, Beijing, China, 1995.
7. **Appan, A.**, A dual-mode system for harnessing roofwater for non-potable uses. *Ur. Wat.*, 1, 317-321, 1999.
8. **Ariyananda, T.**, Comparative review of drinking water quality from different rainwater harvesting in Sri Lanka". Proc. 9th Inter. conf. on rainwater catchment systems–rainwater catchment: an answer to the water scarcity, Petrolina, Brazil, 1999.
9. **Ariyananda, T.**, Quality of collected rainwater in relation to household water security. Rainwater harvesting conf., I.I.T. Delhi, New Delhi, D2-1-D2-4, 2001.

10. **Atkins, P.F., Tomlinson, H.D.**, Evaluation of daily carbon chloroform extracts with CAM. *Wat. Sew. Works*, 110, 281. 1963.
11. **Bo, L., Guangen, H.**, Disinfecting effects on collected rainwater and cost analysis. *Proc. 10th Inter. conf. on rainwater catchment systems, Mannheim, Germany, 2001.*
12. **Body, P.**, The contamination of rainwater tanks in Port Pirie. Report no. 8, Department of Environment and Planning, South Australia, Adelaide, 1986.
13. **Boelhouwer, W.P., Rexwinkel, G., Heesink, B.**, Rainwater treatment technology for affordable, quality drinking water. *Proc. 10th Inter. conf. on rainwater catchment system – rainwater international 2001, Mannheim, Germany, 2001.*
14. **Bowler, D.G., Turner, M.A.**, Water harvesting on a yellow grey earth. *Proc. NZ Grassl. Assoc., Department of Soil Science, Massey Univ., Palmerston North, NZ, 156-160, 1977.*
15. **Broadhead, A.N., Negrón-Alvira Baez, L.A.**, Occurrence of *Legionella* species in tropical rainwater cisterns. *Carrib. Jour. Sci.*, 24, 71-73, 1988.
16. **Brock, T.D.**, Principles of microbial ecology. Prentice-Hall, NJ, 72, 1966.
17. **Brodribb, R., Webster, P., Farrell, D.**, Recurrent campylobacter foetus subspecies bacteraemia in a febrile neutropenic patient linked to tank water. *Comm. Disease Intell.*, 19, 312-313, 1995.
18. **Burdass, W.J.**, Water harvesting for livestock in Western Australia. *Proc. of water harvesting symp., ARS-W-22, USDA, Phoenix, Arizona, 3-26, 1975.*
19. **Camp, T.R.**, Theory of water filtration. *Sanit. Engg. Div., Proc. Am. Soc. Civ. Engrs.*, SA4, 3990, 1-30, 1964.
20. **Canoy, M.J., Knudsen, A.**, Water quality of cistern water in St. Thomas, US Virgin Islands: microbial analysis and major ion composition. *Caribbean Institute, College of the Virgin Islands, USA. 1983.*

21. **Chareonsook, O.**, The entero-pathogenic bacteria and pH of rainwater from three types of containers. *Comm. Dis. Journal.*, Thailand, 12(1), 50-58, 1986.
22. **Chiarella, J.V., Beck, W.H.**, Water harvesting catchments on Indian lands in the Southwest. *Proc. of water harvesting symp.*, ARS-W-22, USDA, Phoenix, Arizona, 104-114, 1975.
23. **Coombes, P.J., Kuczera, G., Argue, J.R., Cosgrove, F., Arthur, D., Bridgeman, H.A., Enright, K.**, Design, monitoring and performance of the water sensitive urban development at Figtree Place in Newcastle. 2003.
24. **Coombes, P.J., George, K., Kalma, J.D.**, Rainwater quality from roofs, tanks and hot water systems at Figtree Place. New South Wales, *Proc. 8th Inter. conf. on urban storm drainage*, Sydney, Australia, 1319-1326, 1999.
25. **Crabtree, K., Ruskin, R., Shaw, S., Rose, J.**, The detection of *Cryptosporidium* oocysts and *Giardia* cysts in cistern water in the US Virgin Islands. *Wat. Res.*, 30, 1, 208-216, 1996.
26. **Cunliffe, D.**, Guidance on the use of rainwater tanks. National Environmental Health Forum Monographs, Water Series 3, Public and environmental health service, Department of Human Services, P.O. Box 6, Rundle Mall SA 5000, Australia, 1998.
27. **Dalal, R.C.**, Composition of Trinidad rainfall. *Wat. Resour. Res.*, 15, 5, 1217-1223, 1979.
28. **Deb, A.K.**, Theory of sand filtration. *Sanit. Engg. Div., Proc. Am. Soc. Civ. Engrs.*, SA3, 6593, 399-422, 1969.
29. **Dennis, J.M.**, 1955-56 infectious hepatitis epidemic in Delhi, India. *Am. Wat. Works Assoc.*, 51, 1288, 1959. Brock, T.D., *Principles of microbial ecology*, Prentice-Hall, NJ, 72, 1966.

30. **Diaper, E.W., Ives, K.J.**, Filtration through size-graded media. *Sanit. Engg. Div., Proc. Am. Soc. Civ. Engrs.*, SA3, 91, 89-114, 1965.
31. **Dubus, I.G., Hollis, J.M., Brown, C.D.**, Pesticides in rainfall in Europe. *Environ. Pollut.*, 110, 331-344, 2000.
32. **Durfer, C.N., Baker, E.**, Public water supplies of the 100 largest cities in the United States, 1962. US Geological Survey Water Supply Paper 1812. U.S. Geological Survey, Department of Interior, Washington D.C. USA, 1964.
33. **Eriksson, B.**, The chemical composition of Hawaiian rainfall. *Tellus.*, 9, 508-520, 1957.
34. **Evans, C.E., Woolhiser, D.A., Rauzi, F.**, Opportunity for harvesting water from and along highways in rangeland areas of Wyoming. *Proc. of water harvesting symp.*, ARS-W-22, USDA, Phoenix, Arizona, 293-301, 1975.
35. **Eveneri, M., Shanan, L., Tadmor, N.H.**, The Negev: the challenge of a desert. Harvard Univ. press, Cambridge, MA, 345, 1971.
36. **Faisst, E.W., Fujioka, R.S.**, Assessment of four rainwater catchment designs on cistern water quality, *Proc. 6th Inter. conf. on rainwater catchment systems*, Nairobi, Kenya, 399-407, 1993.
37. **Fox, D.M., Cleasby, J.L.**, Experimental evaluation of sand filtration theory. *Sanit. Engg. Div., Proc. Am. Soc. Civ. Engrs.*, SA5, 4941, 61-82, 1966.
38. **Frith, J.L.**, Design and construction of roaded catchments. *Proc. of water harvesting symp.*, ARS-W-22, USDA, Phoenix, Arizona, 122-127, 1975.
39. **Fujioka, R., Chinn, R.**, The microbiological quality of cistern waters in the Tantalus area of Honolulu, Hawaii. *Proc. 3rd Inter. conf. on rainwater cistern systems*, Khon Kaen Univ., Thailand. F3, 1-13, 1987.

40. **Fujioka, R., Inserra, S., Chinn R.,** The bacterial content of cistern waters in Hawaii. Proc. 5th Inter. conf. on rainwater cistern systems, Keelung, Taiwan. 33-45, 1991.
41. **Fujioka, R.,** Guidelines and microbial standards for cistern waters. Proc. 6th Inter. conf. on rainwater catchment systems-participation in rainwater collection for low-income communities and sustainable development, Nairobi, Kenya, 393-398, 1993.
42. **Fujioka, R., Rijal, G., Ling, B.,** A solar powered UV system to disinfect cistern waters. Proc. 7th Inter. conf. on rainwater catchment systems, Beijing, China, 48-57, 1995.
43. **Gambell, A.W.,** Chemical composition of rainfall in Eastern North Carolina and Southeastern Virginia. Geological Survey Water Supply Paper, 1535-K, 1966.
44. **Goshko, M.S., Minnigh, H.A., Pipes, W.O., Christian, R.R.,** Relationships between standard plate counts and other parameters in water distribution systems. Am. Wat. Works Assoc., 75, 568, 1983.
45. **Gould, J., McPherson, H.,** Bacteriological quality of rainwater in roof and ground catchment systems in Botswana. Wat. Inter., 12, 3, 135-138, 1987.
46. **Gould, J.,** Is rainwater safe to drink? A review of recent findings. Proc. 9th Inter. conf. on rainwater catchment systems - rainwater catchment: an answer to the water scarcity of the next millennium, Petrolina, Brazil, 1999.
47. **Gould, J., Nissen-Petersen, E.,** Rainwater catchment systems for domestic supply. TDG Publishing, London, United Kingdom. 335, 1999.
48. **Grimm, J., Bessarabov, D., Sanderson, R.,** Review of Electro-assisted methods for water purification. Desal., 115, 3, 285-294, 1998.
49. **Gumbs, A.F., Dierberg, F.G.,** Heavy metals in the drinking water from cisterns supplying single family dwellings. Wat. Inter., 10, 1, 22-28, 1984.

50. **Haas, C.N., Meyer, M.A., Paller, M.S.,** Microbial alterations in water distribution systems and their relationship to physical-chemical characteristics. *Am. Wat. Works Assoc.*, 75, 475, 1983.
51. **Haebler, R.H., Waller, D.H.,** Water of rainwater collection systems in the eastern Caribbean. *Proc. 3rd Inter. conf. on rainwater cistern systems*, Khon Kaen Univ., Thailand, F2, 1-16, 1987.
52. **Hiscock, K.M., Grischek, T.,** Attenuation of groundwater pollution by bank filtration. *J. Hydrol.*, 266, 139-144, 2002.
53. **Hofkes, E.H.,** Rainwater harvesting for drinking water supply. Draft report RWH, 81, 2, IRC, The Hague, 1981.
54. **Hsiung, K., Cleasby, J.L.,** Prediction of filter performance. *Sanit. Engg. Div., Proc. ASCE, SA6*, 1043-1069, 1968.
55. **Hu, G.P., Balasubramanian, R., Wu, C.D.,** Chemical characterization of rainwater at Singapore. *Chemos.* 51, 747-755, 2003.
56. **Hudson, H.E.,** High-quality water production and viral disease. *Am. Wat. Works Assoc.*, 54, 1265, 1962.
57. **Isaias, N.P.,** Experience in reverse osmosis pretreatment. *Desal.*, 139, 57-64, 2001.
58. **Jeyakumar, R.,** Housing builder, Chennai, India, 2001.
59. **Joklik, O.,** Potabilization of rainwater. *Proc. 7th Inter. conf. on rainwater catchment systems – rainwater utilization for the world’s people*, Beijing, China, 33-47, 1995.
60. **Kahdim, A.S., Ismail, S., Jassim, A.A.,** Modeling of reverse osmosis systems. *Desal.*, 158, 323-329, 2003.
61. **Kenny, J.F., Keeping, E.S.,** Mathematics of statistics Part 2. D. Van Nostrand Co., Inc.. New York, 2nd ed., 94-105, 1951.

62. **Kenyon, A.S.**, The Ironclad or artificial catchment. Victoria Department of Agriculture, 27, 86-91, 1929.
63. **Khare, D.**, Performance evaluation of filters and its economic analysis for rainwater harvesting (unpublished report). Indore Municipal Corporation, Indore, India, 2001.
64. **Kiran, Liang, C., Ming, W., Eldwen.**, Feasibility of collecting rainwater. Nanyang Tech. Univ. Report, Singapore, 2004.
65. **Krishna, J.**, Cistern water systems in the US Virgin Islands. Proc. 4th Inter. conf. on rainwater cistern systems, Manila, Philippines, B2, 1-11, 1989.
66. **Krishna, J.**, Water quality standards for rainwater cistern systems. Proc. 6th Inter. conf. on rainwater catchment systems—participation in rainwater collection for low-income communities and sustainable development, Nairobi, Kenya, 389-392, 1993.
67. **Kuehn, W., Mueller, U.**, Riverbank filtration: an overview. Amer. Wat. Works Assoc., 92, 12, 60-69, 2000.
68. **Lauritzen, C.W.**, Ground covers-for collecting precipitation. Farm and home science, 2, 87, 66-67, 1960.
69. **Lester, R.**, A mixed outbreak of *Cryptosporidium* and *Giardiasis*. Update, Australia, 1, 1, 14-15, 1992.
70. **Logsdon, G.S., Lippy, E.C.**, The role of filtration in preventing waterborne disease. Am. Wat. Works Assoc., 74, 649, 1982.
71. **Luksamijarulkul, P., Pumsuwan, V., Pungchitton, S.**, Microbiological quality of drinking water and using water of a Chao Phya river community, Bangkok. Southeast Asian Trop. Med. Publ. Heal., 25, 633-637, 1994.
72. **Lye, D.**, Bacterial levels in cistern water systems in Northern Kentucky. Wat. Res. Bull., 23, 1063-1068, 1987.

73. **Lye, D.**, Microbiology of rainwater cistern systems-a review. *Env. Sci. Heal.*, A27, 2123-2166, 1992a.
74. **Lye, D.**, Legionella and Amoeba found in cistern systems. *Proc. Regional Conf. of the Inter. rainwater catchment systems Assoc.*, Kyoto, Japan, 534-537, 1992b.
75. **Mackenthun, K.M., Keup, L.E.**, Biological problems encountered in water supplies. *Am. Wat. Works Assoc.*, 62, 520, 1970.
76. **Manabu, S.**, Investigation of pesticides in rainwater at Isogo Ward of Yokohama. *Heal. Sci.*, 49, 3, 221-225, 2003.
77. **Manges, H.L., Mao, L.T.**, Harvesting runoff from precipitation on irrigated lands. *ASAE paper 78-2559*, Chicago, IL. 10, 1978.
78. **Manja, K.S., Maurya, M.S., Rao, K.M.**, A simple field test for the detection of faecal pollution in drinking water. *WHO bulletin*, 60, 5, 797-801, 1982.
79. **Mansur, U.**, Quality of rainwater in storage at Badulla district, Sri Lanka. *Lanka rainwater harvesting forum* (unpublished report), Sri Lanka, 1999.
80. **Martinson, B., Thomas, T.**, Improving water quality by design. *Proc. 11th Inter. conf. on rainwater catchment systems*, Mexico City, 1-7, 2003.
81. **Mehdizadeh, P., Kowsar, A., Vaziri, E., Boersma, L.**, Water harvesting for afforestation. I. Efficiency and life span of asphalt cover. *Am. Soil Sci. Soc.*, 42, 644-649, 1978.
82. **Michealides, G.**, Investigation into the quality of roof harvested rainwater for domestic use in developing countries. *Proc. 4th Inter. conf. rainwater cistern systems*, Manila, Philippines, E2, 1-12, 1989.
83. **Mickelson, R.H.**, Performance and durability of sheet metal, butyl rubber, asphalt roofing and bentonite for harvesting precipitation. *Proc. of water harvesting symp.*, ARS-W-22, USDA, Phoenix, Arizona, 93-102, 1975.

84. **Morgan, P.**, Rural water supplies and sanitation. McMillan Education Ltd., London, 358, 1990.
85. **Movahed D.A.**, Sacredness of rainwater in Iranian culture and its harvesting for drinking and agricultural purposes. Proc. 8th Inter. conf. on rainwater catchment systems, 827-829, 1997.
86. **Myers, L.E.**, Water harvesting - 200BC - 1974AD. In: G.W. Frasier (Ed.). Proc. water harvesting symp.. ARS W-22. USDA. Phoenix, Arizona. 1-7, 1975.
87. **Myhrman, M., Cluff, C.B., Putman, F.**, Rainfall-runoff relationships for a mountain watershed in southern Arizona. In: hydrology and water resources in Arizona and the southwest. Proc. Meet. Ariz. Sect., AWRA and Hydrol. Sect. Ariz. Acad. Sci. Flagstaff, Arizona. 8, 165-170. 1978.
88. **Neefe, J.R., Baty, J.B., Reinhold, J.G., Stokes, J. Jr.**, Inactivation of the virus of infectious hepatitis in drinking water. Am. J. Publ. Heal., 37, 365, 1947.
89. National Academy of Science (NAS). More water for arid lands, NAS. Washington DC., 154, 1974.
90. National Health Medical Research Council (NHMRC), Australian drinking water guidelines, Commonwealth of Australia, Australia, 1996.
91. **Nyika, D.**, Rainwater quality during 1991-1993 and constituents of milky rain (Nov. 1992) in Bulawayo, Zimbabwe. The Sci. of the Total Env., 186, 271-281, 1996.
92. **O'Bryan, D., Colley, M.E., Winter, T.C.**, Water, population pressure and ancient Indian migrations. Bull. 10. Inter. Hydro. Decade, 438-442, 1969.
93. **Ockwell, R.**, Assisting in emergencies: a resource handbook for UNICEF field staff. UNICEF, New York. 1986.
94. **Ojha, C.S.P., Graham, N.J.D.**, Appropriate use of deep-bed filtration models. Env. Engg. Div., ASCE, 118, 6, 964-980. 1992.

95. **Ojha, C.S.P., Singh, V.P., Adrian, D.D.**, Determination of critical head in soil piping. *Hydr. Engg., ASCE*, 129, 7, 511-518, 2003.
96. **Olav, L., Ole, M.E., Borge, H., Alf, S., Asa, M.J.**, Pesticides in precipitation in Norway. *The Sci. of Total Env.*, 160/161, 421-431, 1995.
97. **Olem, H., Berthouex, P.M.**, Acidic deposition and cistern drinking water supplies. *Env. Sci. Tech.*, 23, 3, 333-340, 1989.
98. **Ostle, B.**, *Statistics in research*. 2nd ed., The Iowa State Univ. Press, Ames, Iowa, 1964.
99. **Peirson, D.H.**, Trace elements in the atmospheric environment. *Nature*, 241, 252-256, 1973.
100. Pollution Control Research Institute (PCRI), Emission from cast iron foundries and their impact on the Taj Mahal and other historical monuments in Agra (unpublished). In PCRIA-7003 (revised), BHEL, Hardwar, India, 1988.
101. **Punmia, B.C.**, *Soil mechanics and foundation*. Luxmi publication, New Delhi, India. 12th edition, 1991.
102. Rainwater Harvesting manual for urban areas (RWH manual), Centre for Science and Environment, New Delhi, India, 2003.
103. **Ram Babu, Tejwani, K.G., Agarwal, M.C., Bhushan, L.S.**, Rainfall-intensity duration-return period equations and nomographs of India. *Bulletin no. 3*, CSWCRTI, Dehradun, India, 1979.
104. **Rao, M.M.**, Bhoopal Samvardhan Mission, District collectorate office, Dewas, India, 1999.
105. **Ranatunga, N.U.K.**, First flush systems and filters in rainwater harvesting systems. (Unpublished report), Lanka RWH Forum, Sri Lanka, 1999.

106. **Ray, C., Melin, G., Linsky, R.B.**, Riverbank filtration improving source-water quality. *Wat. Sci. Tech. Lib.*, Kluwer Academic Pub., The Netherlands, 2002.
107. **Reilly, J.K. and Kippin, J.S.**, Relationship of bacterial counts with turbidity and free chlorine in two distribution systems. *Am. Wat. Works Assoc.*, 75, 309, 1983.
108. **Richards, R., Kranmer, J., Baker, D., Krieger, K.**, Pesticides in rainwater in the Northeastern United States. *Nature*, 327, 6118, 129-131, 1987.
109. **Riddle, J., Speedy, R.**, Rainwater cistern systems: the park experience. *Proc. 2nd Inter. conf. on rainwater cistern systems*, US Virgin Islands, E4, 1-7, 1984.
110. **Rott, U., Meyer, C.**, Versuche zur prüfung von regenswasser filter systemen nach DIN 1998 (Attempts to examine rainwater filter systems to DIN 1998). *Proc. Regenwassernutzung und bewirtschaftung im Internationalen kontext (Rainwater use and management in the International context)*, Mannheim, Germany, 2001.
111. **Sanderson, W.W., Kelly, S.**, Comments following a paper by Clarke et al., 1964.
112. **Satsangi, G.S., Lakhani, A., Khare, P., Singh, S.P., Kumari, K.M., Srivastava, S.S.**, Composition of rainwater at a semiarid rural site in India. *Atmos. Env.*, 32, 21, 3783-3793, 1998.
113. **Saxena, A., Kulshrestha, U.C., Kumar, N., Kumari, K.M., Srivastava, S.S.**, Characterization of precipitation at Agra. *Atmos. Env.*, 30, 20, 3405-3412, 1996.
114. **Scott, R., Waller, D.**, Water quality aspects of a rainwater cistern system in Nova Scotia, Canada. *Proc. 3rd Inter. conf. on rainwater cistern systems*, Khon Kaen Univ., Thailand, F1, 1-16, 1987.
115. **Serpien, N., Moneti, G., Pieraccrinu, G.**, Chemical and microbiological characterization of drinking water after filtration with a domestic size charcoal column and ultraviolet sterilization. *Urb. Wat.*, 2, 1, 13-20, 2000.

116. **Shaffer, P.T.B., Metcalf, T.G., Sproul, O.J.**, Chlorine resistance of poliovirus isolants recovered from drinking water. *Appl. Env. Microb.*, 40, 1115, 1980.
117. **Sharpe, W.E., Young, E.S.**, Occurrence of selected heavy metals in rural roof-catchment cistern systems. *Proc. 1st Inter. conf. on rainwater cistern systems*, Honolulu, Hawaii, 249-256, 1982.
118. **Simmons, G., Smith, J.**, Roof-water a probable source of *Salmonella* infections. *New Zealand public health report*, New Zealand, 4, 1, 5, 1997.
119. **Simmons, G., Hope, V., Lewis, G.**, Auckland roof water quality pilot study. A report, New Zealand health research council (Unpublished), 1997.
120. **Simmons, G., Heyworth, J.**, Assessing the microbial health risks of potable rainwater. *Proc. 9th Inter. conf. on rainwater catchment systems*, Science and Technology, Petrolina, Brazil, 28, 3/5, 291-299, 1999.
121. **Simmons, G., Hope, V., Lewis, G., Whitmore, J., Gao, W.**, Contamination of potable roof-collected rainwater in Auckland, New Zealand. *Wat. Res.*, 35, 6, 1518-1524, 2001.
122. **Singh, G., Venkataramanan, C., Sastry, G., Joshi, B.P.**, Manual of soil and water conservation practices. Oxford & IBH publishing Co. Pvt. Ltd., New Delhi, India, 385, 1990.
123. **Smet, J., Moriarty, P.**, Rooftop rainwater harvesting. DGIS policy support paper, IRC, Delft, 2001.
124. **Smith, G.L.**, Water harvesting technology applicable to semi arid subtropical climates. Colorado State Univ., Fort Collins, 95, 1978.
125. **Snead, M.C., Olivieri, V.P., Kruse, C.W., Kawata, K.**, Benefits of maintaining a chlorine residual in water supply systems. EPA-600/ 2-80-010, US Environmental Protection Agency (USEPA), 1980.

126. **Stotzky, G.,** Influence of clay minerals on microorganisms. III. Effect of particle size, cation exchange capacity, and surface area on bacteria. *Can. J. Microb.*, 12, 1235, 1966.
127. **Thomas, P., Greene, G.,** Rainwater quality from different roof catchments. *Wat. Sci. Tech.*, 28, 3/5, 291-299, 1993.
128. **Tzen, E., Morris, R.,** Renewable energy sources for desalination. *Sol. Energ.*, 75, 375-379, 2003.
129. **Uba, B.N., Aghogho, O.,** Rainwater quality from different roof catchments in the Port Harcourt District, Rivers State, Nigeria. *Aqua (Oxford)*. 49, 5, 281-288, 2000.
130. **UNPF,** The state of the world population: 6 billion: a time for choices. United Nations Population Fund, New York, USA, 2002.
131. **UNEP,** Rainwater harvesting and utilization, United Nations Environment Programme, Division of Technology, Industry and Economics, International Environmental Technology Centre, USA, 2002.
132. **van Maanen, J.M.S., de Vaan, M.A.J., Veldstra, A.W.F., Hendrix, W.P.A.M.,** Pesticides and nitrate in groundwater and rainwater in the Province of Limburg in the Netherlands. *Env. Monit. Assess.*, 72, 95-114, 2001.
133. **Vasudevan P., Pathak, K.,** DRWH Water quality: a literature review. Milestone 1: Report C1, Sub programme C; Health implications, Project sponsored by European Commission, Indian Institute of Technology Delhi, India, 2000.
134. **Vasudevan, P., Tandon, M., Krishnan, C., Thomas, T.,** Bacteriological quality of Water in DRWH. 10th Inter. conf. on rainwater catchment systems association - Rainwater International 2001. Mannheim, Germany, September, 2001.
135. **Vazquez, A., Costoya, M., Pena, M.R., Garcia, S., Herrero, C.,** A rainwater quality monitoring network: a preliminary study of the composition of rainwater in Galicia (NW Spain). *Chemos.*, 51, 375-386, 2003.

136. **Verma, S.**, Computer aided prediction of filter units' performance. M. Tech. Thesis submitted to Indian Institute of Technology Roorkee, Roorkee, India, 2004.
137. **Vishwanath, S.**, Member of rainwater club, Bangalore, India, 2001.
138. **Waller, D.**, Rainwater: an alternative source in developing and developed countries. *Wat. Inter.*, 14, 27-36, 1989.
139. **Waller, D., Inman, D.**, Rainwater as an alternative source on Nova Scotia. Proc. 1st Inter. conf. on rainwater cistern systems, Honolulu, Hawaii, 202-210, 1982.
140. **Waller, D.H., Sheppard, H., Paterson, B., D'Eon, W., Feldman, D.**, Quantity and quality aspects of rainwater cistern supplies in Nova Scotia. Proc. 2nd Inter. conf. rainwater cistern systems, St. Thomas, US Virgin Islands, USA, E5-1-14, 1984.
141. **Wegelin, M., Sommer, B.**, Solar water disinfection (SODIS) - destined for worldwide use. *Waterlines*, 16, 3, 30-32, 1998.
142. **Wett, B., Jarosch, H., Ingerle, K.**, Flood induced infiltration affecting a bank filtrate well at the River Enns, Austria. *J. Hydrol.*, 226, 222-234, 2002.
143. World Health Organization (WHO), Guidelines for drinking water quality. 2nd ed., Vol. 1, Geneva, 188, 1993.
144. **Wirojanagud, W., Hovichitr, V.**, Evaluation of rainwater quality: heavy metals and pathogens. IDRC, Ottawa, 103, 1989.
145. **Yaziz, M.I., Gunting, H., Sapari, N., Ghazali, A.W.**, Variation in rainwater quality from roof catchments. *Wat. Res.*, 23, 6, 761-765, 1989.
146. **Young, E.S., Sharpe, W.S.**, Atmospheric deposition and roof-catchment cistern water quality. *Environ. Qual.*, 13, 1, 38-43, 1984.
147. **Zhu, K., Zhang, L., Hart, W., Liu, M., Chen, H.**, Quality issues in harvested rainwater in arid and semi-arid Loess Plateau of northern China. *Arid Env.*, 57, 4, 487-505, 2004.

148. **Zhu, Q., Liu, C.,** Rainwater utilization as sustainable development of water resources in China. In: paper 2 Stockholm water symp., 1998, Stockholm International Water Institute, Stockholm, 1998.

WEB SITE

1. <http://www.rainwaterharvesting.org>

